Doctoral Dissertation
Doctoral Program in Chemical Engineering (36th Cycle)

Green Chemicals via Photosynthetic Microbial Factories: Integrating Metabolic and Bioprocess Engineering for 2-Phenylethanol Production and CO_2 Valorization

Giulia Usai

******

Supervisor(s):

Prof. Debora Fino

Dr. Barbara Menin

Dr. Angela Re

Politecnico di Torino 2024

Declaration

I hereby declare that, the contents and organization of this dissertation constitute my own original work and does not compromise in any way the rights of third parties, including those relating to the security of personal data.

Giulia Usai

2024

Abstract

Designing and optimizing photosynthetic microbial factories for chemicals bioproduction and CO_2 utilization is a complex, multidisciplinary endeavor merging genetics, microbiology, biochemistry, and engineering. This process includes selecting suitable photosynthetic microorganisms (e.g., cyanobacteria or microalgae), investigating metabolic pathways, enhancing carbon fixation, optimizing culture conditions (e.g., light, CO_2 supply, temperature), scaling up production, and continually refining the process to meet environmental and economic sustainability goals. The prokaryotic cyanobacteria, due to their high photosynthetic CO_2 conversion rates, minimal nutritional requirements, and genetic and bioinformatic tools, stand out as ideal candidates for these tasks.

Particularly, this thesis focused on developing a photosynthetic microbial factory combining metabolic and bioprocess engineering to produce 2-phenylethanol (2-PE) and valorize CO_2. 2-PE is a rose-scented aromatic compound and finds applications in cosmetics, pharmaceuticals, food and beverages. While plants naturally synthesize 2-PE via shikimate pathway (SKP), its extraction is costly and low-yielding, driving most production to chemical synthesis using petroleum feedstocks, and resulting in unwanted by-products and health issue. A previously published engineered strain of *Synechococcus elongatus* PCC 7942, named p120, heterologously expressed four genes to synthesize 2-PE. In the present research a combination of metabolite doping and metabolic engineering was employed to enhance 2-PE production profile in p120, resulting in a new strain, i.e. '2PE_*aroK*'. Thus, by overexpressing the native shikimate kinase (*aroK*) and subjecting it to L-phenylalanine doping, the 2-PE production significantly increased up to 285 mg L^{-1}, 2.4-fold higher than p120, and ultimately the highest reported via photoautotrophy in the literature.

To further enhance the 2-PE production, the 2PE_*aroK* mutant strain was assessed in a lab-scale flat panel photobioreactor (PBR) under several light conditions, ranging from darkness to varying photon flux levels (100-500 μmol photons m^{-2} s^{-1}). Notably, in the darkness neither biomass accumulation nor 2-PE production were observed, stressing the pivotal role of the light in driving the bioprocess. The results highlighted

150 μmol photons m^{-2} s^{-1} as the optimal setting, yielding 282 mg L^{-1} 2-PE and a productivity of 28.7 mg L^{-1} d^{-1}, which represents one of the most significant goals of this study. Conversely, the highest light condition decreased the 2-PE production by 30%. Additionally, carbon balance analysis showed that at lower light intensities, 45-50% of carbon atoms partitioned into 2-PE synthesis, while at higher light, it decreased to 28%, with the remaining carbons directed towards biomass formation. Therefore, increasing the carbon flow through the photosynthesis did not expand inevitably the target production, while the excess of carbon and energy is preferentially regulated via biomass accumulation.

Once the metabolic link between photosynthesis and 2-PE kinetics got established in 2PE_*aroK*, the study progressed to scale up the bioprocess. Four geometrically different PBRs were assessed for biomass and 2-PE productivities. Although the highest biomass productivities of the thesis were reached in this pool of tests, severe biological contaminations hindered the bioprocess, ultimately failing in 2-PE synthesis and crashing the entire cultivation. Only the stirred tank yielded 2-PE, albeit at half the titer achieved in smaller scale tests, even if no contamination appeared. This study highlighted the need for further studies to identify the optimal environmental and operative conditions in larger scale bioprocess design.

To address sustainability, the 2PE_*aroK* strain was cultivated in dairy wastewaters. Four dairy wastewaters were screened and, the liquid effluent of exhausted sludges (ES) and washing waters from milk tanks (WW) proved suitable for cyanobacterial cultivation. Thus, these waste streams were combined in several ratios and the mixture of 75% ES and 25% WW resulted in 180 mg L^{-1} 2-PE production and a productivity of 18.03 mg L^{-1} d^{-1}, overall enhancing the bioprocess sustainability.

To sum up, this thesis outlines a comprehensive approach to develop a photosynthesis-based bioprocess that has successfully achieved the production of high-value aromatic compound and CO_2 utilization. The research effectively integrated metabolic and bioprocess engineering while highlighting the strengths, applications, and challenges that bioprocess engineering faces when addressing photosynthetic microbial factory for sustainable production of green chemicals and CO_2 valorization.

Table of Contents

Chapter 1 1

1. Research Overview 1

1.1. Brief Background 2

1.2. Structure of the Thesis 3

Chapter 2 5

2. Introduction 5

2.1. CO_2 emissions and the environmental crisis 6

2.2. Environmental impact of the industrial chemical synthesis 7

2.3. Bio-based productions: Microbial Cell Factories 8

2.3.1. Exploiting metabolically different microbial cell factories: heterotrophy vs autotrophy 11

2.3.2. Photoautotrophic microbial cell factories: the case of Cyanobacteria 11

2.3.3. Some insights into the photosynthesis 12

2.4. Biotechnological production of high value molecules: the case of aromatic compounds 16

2.4.1. The Shikimate Pathway 17

2.4.2. Regulation of the Shikimate Pathway 20

2.5. A high-value aromatic compound: 2-Phenylethanol 21

2.5.1. 2-Phenylethanol production methods 22

2.5.2. Microbial cell factories for 2-Phenylethanol production 23

2.5.3. Metabolically engineered Synechococcus elongatus PCC 7942 as photosynthetic microbial factory for 2-PE production 26

2.6. How to cultivate efficiently photosynthetic microbial cell factories 27

2.6.1. The photosynthetic efficiency 27

2.6.2. Mass cultivation of photosynthetic microorganisms 28
2.6.2.1. Closed Photobioreactors 32
2.6.2.1.1. Conventional PBRs 32
2.6.2.1.2. Innovative Photobioreactors 35
2.7. Sustainability of microalgal biotechnology: wastewaters utilization 36
2.7.1. Noble wastewater for high quality microalgae 40
2.7.1.1. Dairy wastewaters 41
2.7.1.2. Dairy wastewaters valorization through microalgae 42
Results of the Thesis 46
Chapter 3 47
3. Combining Metabolite Doping And Metabolic Engineering To Improve 2-Phenylethanol Production By Engineered Cyanobacteria 47
3.0. Abstract 48
3.1. Introduction 49
3.2. Materials and Methods 53
3.2.1. Cyanobacterial strains, media and cultural conditions 53
3.2.2. Plasmid construction and transformation 55
3.2.3. qRT-PCR analysis 56
3.2.4. 2-PE and L-Phe HPLC quantification 57
3.2.5. Whole-cell protein extraction 57
3.2.6. Glycogen content determination 58
3.2.7. Bioinformatics search of class-specific enzymes 58
3.2.8. Metabolic effects of phenylalanine addition by metabolic model simulation 59
3.3. Results 61
3.3.1. Screening of several metabolite doping conditions to improve 2-phenylethanol production by p120 engineered S. elongatus PCC 7942 61

3.3.2. Improving 2-phenylethanol production through metabolic engineering of the Shikimate Pathway 63

3.3.2.1. Creation of 2-PE producing S. elongatus mutant overexpressing the endogenous shikimate kinase gene (2PE_aroK) 63

3.3.2.2. Characterization of 2-PE producing S. elongatus mutant overexpressing the endogenous shikimate kinase gene (2PE_aroK) 65

3.3.3. L-phenylalanine doping effect on mutant physiology 68

3.3.3.1. L-phenylalanine consumption analysis 68

3.3.3.2. Bioinformatics analysis about L-phenylalanine consumption in 2-PE producing S. elongatus PCC 7942 70

3.4. Discussion 71

3.5. Conclusions 76

3.6. Supplementary Materials 78

Chapter 4 86

4. Metabolic Connection Between Photosynthesis And 2-PE Production In PBR: To What Extent Does Light Intensity Affect The 2-PE Synthesis? 86

4.0. Abstract 87

4.1. Introduction 89

4.2. Materials and Methods 93

4.2.1. Cyanobacteria inoculum preparation for PBR 93

4.2.2. PBR general experimental conditions 93

4.2.2.1. PBR turbidostat experimental conditions 94

4.2.3. qRT-PCR analysis 94

4.2.4. CO_2 consumption measurement 95

4.2.5. 2-PE and L-Phe HPLC quantification 96

4.2.6. Carbon balance 96

4.2.7. Glycogen content quantification 96

4.2.8. Photosynthetic pigments quantification 97

4.3. Results 98

4.3.1. Growth of 2PE_aroK mutant strain under four photons fluxes in liquid batch mode 98

4.3.2. 2-PE production and L-Phe uptake by 2PE_aroK mutant strain under four photons fluxes in liquid batch mode 100

4.3.3. CO_2 and L-Phe uptake, and glycogen accumulation by 2PE_aroK mutant strain under four photons fluxes in liquid batch mode 103

4.3.4. Carbon Balance between biomass and 2-PE 104

4.3.5. 2PE_aroK mutant characterization in turbidostat mode 108

4.4. Discussion 109

4.5. Conclusions 115

4.6. Supplementary Materials 117

Chapter 5 119

5. Scale Up Of Photosynthetic 2-Phenylethanol Bioproduction In Photobioreactor: Opportunities And Challenges 119

5.0. Abstract 120

5.1. Introduction 121

5.2. Materials and Methods 123

5.2.5. Cyanobacteria recombinant strain for 2-PE production in large scale 123

5.2.6. Inoculum preparation for PBRs 123

5.2.7. Scale Up tests for cultivating 2PE_aroK mutant strain in pilot scale 123

5.2.7.1. Stirrer Tank 123

5.2.7.2. Airlift Flat Panel 124

5.2.7.3. Aquarium Flat Panel 124

5.2.7.4. Annular column 125

5.2.8. 2-PE and L-Phe HPLC analysis 125

5.3. Results 127

5.3.5. Setting parameters in stirrer tank PBR with external light source 127

5.3.5.1. 2-PE production by 2PE_aroK recombinant strain in 4-L stirrer tank 129

5.3.6. 2PE_aroK recombinant strain in pilot scale PBRs 130

5.3.6.1. Airlift Flat Panel – preliminary test 130

5.3.3.2. 'Aquarium', flat panel PBR 132

5.3.3.3. Annular-column PBR 133

5.3.4. Biological contaminations affect PBR cultivations 135

5.4. Discussion 137

5.5. Conclusions 140

Chapter 6 142

6. Coupling Dairy Wastewaters For Nutritional Balancing And Water Recycling: A Sustainable Heterologous 2-Phenyletanol Production By Engineered Cyanobacteria 142

6.0. Abstract 143

6.1. Introduction 144

6.2. Materials and Methods 147

6.2.1. Pre-treatment of dairy wastewaters 147

6.2.2. Hydrochemical analysis of dairy wastewaters 147

6.2.3. Cyanobacterial strain and culture maintenance 147

6.2.4. Cyanobacteria growth conditions on dairy wastewaters 148

6.2.5. Photosynthetic pigments quantification 149

6.2.6. 2-PE and L-Phe HPLC analysis 149

6.3. Results 150
6.3.1. Selection of proper dairy wastewaters for S. elongatus growth 150
6.3.1.1. Chemical characterization of dairy wastewaters 150
6.3.1.2. Nitrogen and Phosphates 150
6.3.1.3. Sodium, chloride and calcium 152
6.3.1.4. Metals 152
6.3.1.5. pH, COD and BOD 152
6.3.2. Qualitative screening of dairy wastewaters for cyanobacterial growth 152
6.3.3. Coupling dairy wastewaters for nutritional balancing and water recycling 155
6.3.3.1. pH tolerance and pH control effect on the 2PE_aroK recombinant strain 155
6.3.4. Characterization of 2PE_aroK mutant in two mixtures of ES and WW 156
6.3.4.1. Growth of 2PE_aroK mutant strain in wastewaters 156
6.3.4.2. 2-PE production and L-Phe consumption in wastewaters 159
6.3.4.3. Nutrients removal from wastewaters 161
6.3.4.4. Photosynthetic pigments accumulation by 2PE_aroK mutant strain in wastewaters 161
6.4. Discussion 163
6.5. Conclusions 170
6.6. Supplementary Materials 174
Chapter 7 176
7. Conclusions and Outlook 176
References 178

List of Figures

Figure 2.1. Diagrammatic representation of the photochemical reactions (Photosynthetic Z-scheme). PAR, photosynthetic active radiation. 14

Figure 2.2. A schematic representation of the Calvin Cycle. The enzyme ribulose-1,5-bisphosphate carboxylase (RubisCO) adds CO_2 to ribulose-1,5-bisphosphate (R-1,5-BP) and splits the product into 2 molecules of 3-phosphoglycerate (3-PG). The 3-PG is then reduced to glyceraldehyde-3-phosphate which dismutates to regenerate ribulose-5-phosphate (R-5-P). Phosphorylation of R-5-P regenerates R-1,5-BP for the next cycle. Three turns of the cycle are required for a net increase of one G-3-P..... 15

Figure 2.3. Schematic representation of the Shikimate Pathway and synthesis of AAAs in Synechococcus elongatus PCC 7942, as annotated in the Kyoto Encyclopedia of Genes and Genomes (KEGG). Green squares indicate branching points leading to the synthesis of other aromatics. Purple ovals highlight the three AAAs. Intermediates and enzymes are reported in black, and genes encoding for enzymes in blue. Full lines represent single enzymatic reactions, dashed lines represent multiple enzymatic steps. Missing proteins have not been identified yet. PEP = phosphoenol pyruvate, E4P = erythrose-4-phosphate, DAHP = 3-deoxy-D-arabino-heptulosonate-7-phosphate, EPSPS = 5-O-(1-Carboxyvinyl)-3-phosphoshikimate, PD = prephenate dehydratase, At = aminotransferase, tyrAa = arogenate dehydrogenase $NADP^+$ dependent. 19

Figure 2.4. Reactions and enzymes involved in 2-PE biosynthesis via the Ehrlich pathway...... 25

Figure 2.5. Open microalgae cultivation plants at industrial scale. **A**) Cyanotech's plant for Spirulina and Haematococcus pluvialis cultures. **B**) Earthrise Farm's plant for Spirulina. **C**) Taiwan Chlorella's plant for Chlorella sp. cultivation. **D**) Betatene® 's plant for Dunaliella salina for β-carotene production. 30

Figure 2.6. Tubular PBRs. 34

Figure 2.7. 40-L vertical-column PBR, used for Chlorella zofingiensis cultivation. 34

Figure 2.8. Flat panel PBRs. A) https://news.asu.edu/colleges-and-units/arizona-center-algae-technology-and-innovation; **B)** https://femonline.it/products/..... 35

Figure 2.9. Global wastewater production (m^3 yr^{-1} per capita). 38

Figure 3.1. Composition of genetic vectors for heterologous 2-phenylethanol synthesis in S. elongatus PCC 7942 genome. **A**) p120 vector contains: NSI (blue), homologous regions for chromosomal integration into the Neutral Site I; $lacI^q$ (purple), LacI repressor gene; kivD (violet), gene encoding phenylpyruvate decarboxylase; adhA (orange), gene for alcohol dehydrogenase A; $aroG^{fbr}$ (light blue), feedback-inhibition resistant DAHP synthase; $pheA^{fbr}$ (green), feedback-inhibition-resistant chorismate mutase/prephenate dehydratase; $Spec^R$ (pink), spectinomycin-resistance cassette. **B**) aroK overexpression vector: NSII (dark green), homologous regions for chromosomal integration into the Neutral Site II; aroK (dark pink), endogenous gene for shikimate kinase expression in S. elongatus (locus tag, SynPCC7942_0894); Kan^R (yellow), kanamycin-resistance cassette; P_{trc} (black arrow), IPTG-inducible promoter. 57

Figure 3.2. Overexpressed genes and relative protein products for 2-PE synthesis in S. elongatus PCC 7942 mutant strains p120 and 2PE_aroK. *The reactions promoted by the p120 (green boxes) and 2PE_aroK (green and red boxes) mutant strains.*..... 62

Figure 3.3. Effect of L-phenylalanine doping at three different concentrations on the p120 mutant strain. A) The bar plot shows the 2-PE yield expressed as 2-PE mg produced normalized per g of dry cell weight (mg gDW^{-1}). The control condition is represented by the p120 mutant strain grown with no L-Phe. Asterisks indicate statistical significance for both 0.1 g L^{-1} and 0.3 g L^{-1} L-Phe doping versus control condition (unpaired two-tailed t-test, p-value < 0.05) and error bars report the standard deviation. **B)** p120 mutant grown with L-Phe (0.05-0.3 g L^{-1}). As control conditions, p120 mutant (dark green) and wild type (grey) strains were both grown with no L-Phe. The L-Phe was added and gene expression was induced at the 7th day (about OD_{730} = 1, 0.26 gDW L^{-1}). The bars show the standard deviation. Each test was conducted as three biological replicates. 63

Figure 3.4. Temporal gene expression analysis. Gene expression of kivD, adhA, $pheA^{fbr}$, $aroG^{fbr}$, aroK in 2PE_aroK cells after one, five and ten days since gene expression induction. Data are expressed as log(2^-ΔΔCt) ± standard deviation. The symbol "*" indicates significant ($p < 0.05$) differences in gene expression of kivD, adhA, $pheA^{fbr}$, $aroG^{fbr}$, and aroK in 2PE_aroK cells after one, five or ten days of induction respect to wild type condition, as calculated by student t-test..... 65

Figure 3.5. Characterization of 2PE_aroK engineered strain with or without L-Phe doping. Comparison between 2-PE production (**B, D**) and biomass formation (**A,**

C) over the time since gene expression induction on 2PE_aroK under no L-Phe doping (top) or when exposed to L-Phe doping (bottom). As reference, the p120 strain was subjected to the same conditions. L-Phe was added, and the gene expression was induced at around OD_{730} = 1 (0.26 gDW L^{-1}). Bars represent standard deviation. All tests were carried out in triplicate. 67

Figure 3.6. 2-phenylethanol productivity in L-Phe-doped condition. **A**) Maximum 2-PE mg normalized by the biomass produced during the experiment for both 2PE_aroK (green) and p120 (blue) strains. **B**) 2-PE daily produced, expressed as mg per liter per day, by 2PE_aroK (green) and p120 (blue) engineered strains over the time. Bars represent standard deviation. All tests were conducted by means of three biological replicates. 68

Figure 3.7. L-phenylalanine consumption analysis. **A**) L-phenylalanine titer detected in the supernatant for 2PE_aroK (green), p120 (blue) and 7942_aroK (pink) mutant strains and the relative wild type S. elongatus PCC 7942 (grey). **B**) The L-Phe daily consumed was normalized by the biomass produced. The results were expressed as mg of L-Phe consumed by g dry cell weight every day after the gene expression induction. Bars represent standard deviation. All tests were carried out in triplicate. 69

Figure 3.8. Effects of medium supplementation with L-phenylalanine on the metabolic network of the S. elongatus PCC 7942 mutant producing 2-phenylethanol. Flux variability analysis (FVA) was carried out in the absence/presence of Phe in the medium. Each reaction was assigned a range of allowed fluxes in the two conditions. For each reaction, the fraction (in percentage value) of allowed fluxes, which do not overlap between the two conditions, was computed. Shown are the individual reactions whose flux ranges in the presence/absence of phenylalanine differ by at least 5%. Reactions on the horizontal axis marked by '*' are mentioned in the main text..... 71

Figure 4.1. Scheme of the pathway for 2-PE biosynthesis in 2PE_aroK mutant strain. All the overexpressed proteins are labelled in green. 92

Figure 4.2. 2PE_aroK growth data in batch cultures at four different light intensities and dark condition. **A**) Growth curves; **B**) Biomass accumulation during the growth phase (pink bars) and production phase (blue bars); **C**) Growth rates. Four biological replicates were carried out. Error bars represent standard deviation. 100

Figure 4.3. 2-PE-related data of the 2PE_aroK mutant strain exposed to four light conditions in batch mode. A) 2-PE kinetics production; **B**) 2-PE final concentration; **C**) 2-PE volumetric productivity; **D**) 2-PE production normalised by the biomass necessary for producing 2-PE, expressed as mg of 2-PE per gDW. All the tests were carried out as four biological replicates. Error bars represent standard deviation. The statistics was performed as one-way ANOVA ($\alpha \leq 0.05$). Asterisks refer statistical significance. *, p-value ≤ 0.05; **, p-value ≤ 0.002; ***, p-value ≤ 0.0002; ****, p-value ≤ 0.0001..... 102

Figure 4.4. Carbon consumption results of the 2PE_aroK mutant strain exposed to four light conditions in batch mode. A) Percentage of L-Phe consumed of the available one**; B**) Carbon fixed through photosynthesis, expressed as mmol of carbon atoms consumed from the supplied CO2; **C**) Total amount of carbon consumed from CO2 (pink bars) and L-Phe (violet bars). All the tests were carried out as four biological replicates. Error bars represent standard deviation. The statistics was performed as one-way ANOVA ($\alpha \leq 0.05$). Asterisks express statistical significance. *, p-value ≤ 0.05; **, p-value ≤ 0.002; ***, p-value ≤ 0.0002; ****, p-value ≤ 0.0001..... 104

Figure 4.5. Carbon distribution analysis of the 2PE_aroK mutant strain exposed to four light conditions in batch mode. A) Carbon balance indicates the percentage of the total consumed carbon atoms partitioning between 2-PE (magenta bars) and biomass (pink bars); **B**) Percentage of 2-PE producible from the L-Phe effectively consumed in every light conditions. The experiments were conducted by the means of four biological replicates. Error bars refer to standard deviation. 105

Figure 4.6. Phycocyanin profile over the time of the 2PE_aroK mutant strain exposed to four light conditions in batch mode. All the tests were carried out as four biological replicates. Error bars represent standard deviation. The statistics was performed as two-way ANOVA ($\alpha \leq 0.05$). Asterisks express statistical significance. *, p-value ≤ 0.05; **, p-value ≤ 0.002; ***, p-value ≤ 0.0002; ****, p-value ≤ 0.0001. 107

Figure 4.7. 2PE_aroK mutant strain under turbidostat cultivation mode at 150 µmol photons m^{-2} s^{-1}. A) Growth rates calculated over the time before (dotted box) and after the gene expression induction and metabolite doping (grey box). **B**) Biomass accumulation as the sum of the biomass calculated from each turbidostat cycle. **C**) 2-PE production in turbidostat mode. All the experiments were performed by the means of biological triplicates. Error bars represent standard deviation. 109

Figure 5.1. Solaris Jupiter Stirrer Tank PBR used in this study. The illustration shows the PBR at the moment of the inoculum (**A**) and at the end of the test (**B**). https://www.solarisbiotech.com/en/..... 128

Figure 5.2. Set up of the main parameters related to their effect on the biomass production. **A**) relationship between stirring force and biomass; **B**) relationship between light intensity and biomass. **C**) growth rate (grey bar) and biomass productivity (dotted bar) in the 1st and 2nd phases of the test. Error bars represent standard deviation. The test was carried out by the means of two biological replicates. 128

Figure 5.3. 2-PE production of the 2PE_aroK mutant strain in stirrer tank. **A**) biomass accumulation during the gene expression induction and metabolite doping, the box highlights the day of induction; **B**) 2-PE production (●) and L-Phe consumption (■) profiles. Error bars represent standard deviation. The test was carried out by the means of three biological replicates..... 129

Figure 5.4. Airlift Flat Panel configuration. **A**) illustration of the patented technology. **B**) Example of how the geometrical configuration allows the efficient mixing that characterizes this PBR. https://subitec.com/en/home/..... 130

Figure 5.5. Realistic picture of the Airlift flat panel used in this study. The picture illustrates the panel at the moment of the inoculum (**A**) and at the end of the study (**B**). 131

Figure 5.6. Data from the Airlift Flat Panel cultivation. **A**) Growth curve, expressed as biomass produced (g dry weight per liter); **B**) Growth rate and biomass productivity, expressed as g of dry cell weight per liter per day..... 131

Figure 5.7. Aquarium Flat panel. It represents a conventional and standard flat panel. The picture shows the vessel at the moment of the cyanobacterial inoculum (**A**) and at the end of the test (**B**). https://www.alga.cz/en/a-106-centre-algatech.html. 132

Figure 5.8. Data from the Aquarium Flat Panel cultivation. **A**) Growth curve, expressed as biomass produced (g dry weight per liter); **B**) Growth rate and biomass productivity, expressed as g of dry cell weight per liter per day. Three biological replicates were carried out. The error bars represent standard deviation. 133

Figure 5.9. Annular column PBR. The picture shows the vessel at the moment of the cyanobacterial inoculum (**A**) and at the end of the test (**B**). https://www.alga.cz/en/a-106-centre-algatech.html. 134

Figure 5.10. Data from the Annular column cultivation. **A**) Growth curve, expressed as biomass produced (g dry weight per liter) at pH 8 (blue box) and pH 10 (red box); **B**) Growth rate at pH 8 (blue bar) and pH 10 (red bar); **C**) Biomass productivity, expressed as g of dry cell weight per liter per day, at pH 8. Two biological replicates were carried out. The error bars represent standard deviation. 134

Figure 5.11. Picture about the biological contamination occurred during the scale up experiment. **A**) Realistic picture of the cyanobacterial culture during a protozoan predator contamination**. B**) Microscopic picture of the protozoan contaminant (red circled) and the bacilli represent the target cyanobacterial culture. 136

Figure 6.1. Dairy wastewaters qualitative screening. The screening has been conducted as biological triplicates for each tested condition against a control one (BG11). The study has considered the effect on the growth of the 2PE_aroK S. elongatus PCC 7942 mutant strain, ranging from no growth (red) to a growth equal to the control condition (dark green). The percentages indicate the ratio of each waste used in the single experiment..... 154

Figure 6.2. Growth rate of 2PE_arok **mutant on 75% exhausted sludge waste supplemented with 0.15 g L^{-1} NH_4^+**, which was found to be the minimum ammonium concentration able to lead a growth similar to the control condition (BG11). All tests were carried out in triplicate. Error bars represent standard deviation. 154

Figure 6.3. Study of the effect of no pH control and MOPS pH control on the growth performance of the 2PE_aroK mutant strain, on different ratios between ES and WW: i) 90:10; ii) 75:25; iii) 60:40. All tests were carried out in triplicate. Error bars represent standard deviation..... 156

Figure 6.4. Comparison between 2PE_aroK grown on three different conditions on 75 ES : 25 WW. **A**) Growth curves, expressed as biomass (gDW L^{-1}). **B**) 2-PE prodution kinetics obtained in sixteen days (mg L^{-1}). **C**) 2-PE yield, expressed as mg 2-PE normalized by the biomass produced. **D**) 2-PE daily productivity (mg L^{-1} d^{-1}). All tests were carried out in biological triplicate. Error bars represent standard deviation. The statistical tests were performed as unpaired t-test ($\alpha \leq 0.05$) versus the control

condition. *, p-value ≤ 0.05; **, p-value ≤ 0.002; ***, p-value ≤ 0.0002; ****, p-value ≤ 0.0001. 158

Figure 6.5. Comparison between 2PE_aroK grown on three different conditions on 90 ES : 10 WW. **A**) Growth curves, expressed as biomass (gDW/L). **B**) 2-PE prodution kinetics obtained in sixteen days (mg/L). **C**) 2-PE yield, expressed as mg 2-PE normalized by the biomass produced. **D**) 2-PE daily productivity (mg/L per day). All tests were carried out in biological triplicate. Error bars represent standard deviation. The statistical tests were performed as unpaired t-test (α ≤ 0.05) versus the control condition. *, p-value ≤ 0.05; **, p-value ≤ 0.002; ***, p-value ≤ 0.0002; ****, p-value ≤ 0.0001. 159

Figure 6.6. L-Phe consumption by 2PE_aroK mutant strain grown on 75:25 and 90:10 ratios between ES and WW. A) percentage of L-Phe consumed over the L-Phe available. **B**) total amount of L-Phe consumed (g L^{-1}) in all the conditions tested and control of the two wastewaters mixtures. All tests were carried out in biological triplicate. Error bars represent standard deviation. Asterisks refer to statistical significance (unpaired t-test, α ≤ 0.05). 160

Figure 6.7. **Percentage of N and P removal from the mixture 75 ES : 25 WW (patterned) and 90 ES : 10 WW (violet).** The quantification was carried out in biological triplicate**.** The error bars represent the standard deviation..... 161

Figure 6.8. Photosynthetic pigments profile of 2PE_arok mutant strain growth on 75:25 and 90:10 mixtures between ES and WW in three conditions and a control. All tests were carried out in biological triplicate. Error bars represent standard deviation. Asterisks refer to statistical significance (unpaired t-test, α ≤ 0.05)..... 162

List of Supplementary Figures

Supplementary Figure 3.1. Effect of IPTG addition for gene expression induction. The growth kinetics, expressed as g of dry cell weight per liter, of both wild-type S. elongatus and the recombinant p120 strain subjected or not to IPTG. All tests were conducted by means of three biological replicates. 78

Supplementary Figure 3.2. Response of S. elongatus p120 strain growth and 2-PE production to the supplementation in BG11 medium of two aromatic vitamins. All the results are means of three biological replicates and are relative of a reference condition (Control or 0.3 g L^{-1} L-Phe). **A**, **C** and **B**, **D** represent the p120 growth curve (gDW L^{-1}) and 2-PE yield (mg/gDW), respectively, at three different concentrations of folic acid or cyanocobalamin. **E**, **G** and **F**, **H** represent the p120 growth curve and 2-PE yield, respectively, when folic acid and cyanocobalamin were supplemented in combination with 0.3 g L^{-1} L-Phe. Statistical analyses were conducted as one-way ANOVA or unpaired two-tailed t-test (p-value < 0.05). For high resolution version see 10.3389/fbioe.2022.1005960. 79

Supplementary Figure 3.3. Response of S. elongatus p120 strain growth and 2-PE production to the supplementation in BG11 medium of aromatic amino acids. All the results are means of three biological replicates and are relative of a reference condition (0.3 g L^{-1} L-Phe). **A**, **C** and **B**, **D** represent the p120 growth curve (gDW L^{-1}) and 2-PE yield (mg gDW^{-1}), respectively, at three different concentrations of L-Tyr or L-Trp, when supplemented together with 0.3 g L^{-1} L-Phe. **E**, **F** represent the p120 growth curve and 2-PE yield, respectively, in a combination of the three aromatic amino acids condition. **G**, **H** show the 2-PE production kinetics in the presence of L-Phe and L-Trp or all the three aromatic amino acids. Statistical analyses were conducted as one-way ANOVA or Unpaired Two-tailed t-test (p-value < 0.05). Asterisk shows a statistical significance. For high resolution version see 10.3389/fbioe.2022.1005960. 80

Supplementary Figure 3.4. Genetic and Protein profile of 2PE_*aroK* mutant. **A)** Gene profile of 2PE_aroK mutant. kivD, 1647 bp; adhA, 1011 bp; $aroG^{fbr}$, 1065 bp; $pheA^{fbr}$, 1161 bp; aroK, 573 bp. **B**) Whole-cell protein profile of 2PE_aroK strain. 30 µg of proteins were loaded for both pre-induction and 5 days after induction samples.

Phenylpyruvate decarboxylase, ≈ 61 kDa, blue box; 3-deoxy-D-arabino-heptulosonate 7-phosphate (DAHP) synthase, 38.5 kDa, and alcohol dehydrogenase A, ≈ 36 kDa, could be both part of the dashed box. Shikimate kinase, ≈ 21 kDa, white dotted box. The bifunctional chorismate mutase/prephenate dehydrogenase is ≈ 43 kDa could be included into the most intense band zone, due to endogenous proteins, which make it difficult to be distinguished. All five genes are under the control of IPTG-inducible promoter, which suffers from leaky expression, so it is possible to have a slight expression of the target proteins even before the actual gene expression induction. C) Segregation evaluation. The wild type NSI (1005 bp) and NSII (168 bp) were amplified in PCR. In 2PE_aroK strain the same sites were not amplified, because occupied by p120 insert and the aroK gene, respectively, indicating a complete segregation of the inserts in each S. elongatus chromosome. 81

Supplementary Figure 3.5. Evaluation of toxicic effect of 2-phenylethanol on S. elongatus PCC 7942. Four increasing 2-PE concentration were tested, from 0.1 to 1 g L^{-1}. 2-phenylethanol was added to the medium at around OD_{730} = 1 (0.26 gDW L^{-1}). Bars represent standard deviation. All tests were carried out in biological triplicate. 82

Supplementary Figure 3.6. qRT-PCR analysis of reference genes of S. elongatus PCC 7942. A) range of cycle threshold (Ct) values of the four reference genes used in the present work (secA, ppc, prs, and 16s) across wild-type and 2PE_aroK engineered strain after one, five and ten days since gene expression induction, and the relative wild-type strain of S. elongatus PCC 7942. B) range of cycle threshold (Ct) values of the four candidate reference genes across all samples of S. elongatus PCC 7942. The box indicates the Ct value within the 25th and 75th percentiles. Whiskers include the Ct values in the 10th and 90th percentiles. The line across the box represents the median..... 82

Supplementary Figure 3.7. Glycogen content in 2PE_aroK mutant before and after the gene expression induction. The glycogen content is reported as g of glycogen per g of cell dry weight (g gDW^{-1}). Bars represent standard deviation. All tests were carried on in biological triplicate. 83

Supplementary Figure 3.8. **Reactions of the metabolic reconstruction of the 2-PE-producing strain affected by medium supplementation with phenylalanine**. L-phenylalanine supplementation affects mainly the fluxes through the reactions of the Ehrlich pathway. Shown is the simulated effect of phenylalanine addition to the medium on different functional categories. Flux variability analysis (FVA) was carried

out in the absence/presence of Phe in the medium. Each reaction is assigned a range of allowed fluxes in the two conditions. For each reaction, the fraction (in percentage value) of allowed fluxes, which do not overlap between the two conditions, is computed. Shown is the distribution of the non-overlapping flux ranges of the reactions catalyzed by the enzymes belonging to different functional categories. For high resolution version see 10.3389/fbioe.2022.1005960. 84

Supplementary Figure 4.1. Gene expression analysis by qRT-PCR. prs gene was used as reference gene and the lowest light condition was adopted as control condition. The analysis was conducted from the biomass harvested five days since the gene expression induction. Data are expressed as log(2^−ΔΔCt) ± standard deviation of the four biological replicates. 117

Supplementary Figure 4.2. Glycogen content in the biomass of 2PE_*aroK* mutant strain exposed to four light conditions. The results are reported as glycogen percentage of the dry biomass over the time since the gene expression induction. The analysis was conducted on four biological replicates and the error bars indicate standard deviation. 117

Supplementary Figure 4.3. Turbidostat pattern of the cellular density (expressed as OD_{730}), before (dotted box) and after (grey box) the gene expression induction. 118

List of Tables

Table 2.1. Comparison between open and closed PBRs. 31

Table 2.2. Prokaryotic and eukaryotic microalgae used in the treatment of wastewater. 40

Table 2.3. Eukaryotic microalgae strains used for dairy wastewater treatment. 44

Table 2.4. Cyanobacteria strains used for dairy wastewater treatment. 45

Table 3.1. **Genetic features of plasmid vectors and strains used in the present work**. *lacI^{q}, LacI repressor gene; kivD, gene encoding phenylpyruvate decarboxylase; adhA, gene for alcohol dehydrogenase A; aroG^{fbr}, feedback-inhibition resistant DAHP synthase; pheA^{fbr}, feedback-inhibition-resistant chorismate mutase/prephenate dehydratase; Spec^{R}, spectinomycin-resistance cassette; aroK, endogenous gene for Shikimate Kinase expression in S. elongatus; Kan^{R}, kanamycin-resistance cassette;* 54

Table 3.2. Genes employed for qRT-PCR analysis. For each gene, the name, acronym, and nucleotide sequences for both Forward (F) and Reverse (R) primers are reported in the table. 60

Table 3.3 Specific Growth Rate (μ) and Doubling Time (Dt) of the p120 and 2PE_aroK strains. The μ was calculated in exponential growth phase, after gene expression induction and L-phenylalanine supplementation and it is expressed as day^{-1}. SD, standard deviation..... 67

Table 4.1. Genetic features of 2PE_aroK recombinant strain of S. elongatus PCC 7942. HR, homologous recombination; NS, neutral site; DAHP, 3-deoxy-7-phosphoheptulonate; PEP, phosphoenolpyruvate; E4P, erythrose-4-phosphate 98

Table 4.2. Summary of the main results obtained from the liquid batch cultures exposed to four different light conditions. 99

Table 4.3. Summary of the carbon-related data obtained from the liquid batch cultures exposed to four different light conditions. 106

Table 5.1. Genetic features of 2PE_aroK recombinant strain of S. elongatus PCC 7942. HR, homologous recombination; NS, neutral site; DAHP, 3-deoxy-7-phosphoheptulonate; PEP, phosphoenolpyruvate; E4P, erythrose-4-phosphate. 126

Table 5.2. Main features of the photobioreactors used in this investigation..... 127

Table 5.3. Biomass-related results obtained from each PBR. μ, growth rate; Dt, doubling time (d, ln(2)/ μ); Biomass productivity, expressed as g of dry cell weight per liter per day. 136

Table 6.1. Chemical analysis of four dairy wastewaters: cheese whey, scotta, washing waters, liquid effluent of exhausted sludge. The data are expressed as mg L^{-1}. The analytical methods used for their quantification is reported in the last column. 151

Table 6.2. Sum up of the main results of the present investigation about the growth of 2PE_aroK mutant strain in 75:25 and 90:10 ratios of ES and WW. SD, standard deviation. The statistical tests were performed as unpaired t-test ($\alpha \leq 0.05$) versus the control condition. *, p-value ≤ 0.05; **, p-value ≤ 0.002; ***, p-value ≤ 0.0002; ****, p-value ≤ 0.0001. Chl α, chlorophyll α. Car, carotenoids..... 173

List of Supplementary Tables

Supplementary Table 3.1. Alignment-based analysis of the S. elongatus PCC 7942 genome for genes encoding phenylalanine transaminases. Alignment hits with statistical significance (E-value < 0.001) resulting from the alignment of known aromatic amino acid transaminases against the amino acid sequences of Synechococcus elongatus PCC 7942**.** For each retained hit, the table displays the scoring details corresponding to its top-scoring alignment. The table provides functional annotations retrieved from the UniProtKB database, both for the query and the hit proteins. 85

Supplementary Table 3.2. Effects of medium supplementation with phenylalanine on the metabolic reactions of the S. elongatus PCC 7942 mutant producing 2-phenylethanol. Flux variability analysis (FVA) was carried out in the absence/presence of phenylalanine in the medium. Each reaction is assigned a range of allowed fluxes in the two conditions. For each reaction, the fraction (in percentage value) of allowed fluxes, which do not overlap between the two conditions, is computed. Shown are the individual reactions whose flux ranges in the presence/absence of phenylalanine differ by at least 5%. …….85

Supplementary Table 3.3. Alignment-based analysis of the S. elongatus PCC 7942 genome for genes encoding L-amino acid deaminases, L-amino acid dehydrogenases and L-amino acid oxidases. Alignment hits with statistical significance (E-value < 0.001) resulting from the alignment of known L-amino acid deaminases, dehydrogenases and oxidases against the amino acid sequences of S. elongatus PCC 7942. For each retained hit, the table displays the scoring details corresponding to its top-scoring alignment. The table provides functional annotations retrieved from the UniProtKB database, both for the query and the hit proteins. (*) The query gene is a known L-amino acid dehydrogenase in Synechocystics (Schriek et al., 2009). (**) Two genes known as L-amino acid oxidase in Synechococcus elongatus (Gau et al., 2007). 85

Supplementary Table 4.1. Genes employed for qRT-PCR analysis. For each gene, the name, acronym, and nucleotide sequences for both Forward (F) and Reverse (R) primers are reported in the table. 118

Supplementary Table 6.1. Genetic features of 2PE_aroK recombinant strain of S. elongatus PCC 7942. HR, homologous recombination; DAHP, 3-deoxy-7-phosphoheptulonate; PEP, phosphoenolpyruvate; E4P, erythrose-4-phosphate. 174

Supplementary Table 6.2. Detailed results of the pH control system screening in ES:WW mixtures. SD, standard deviation. All tests were carried out in biological triplicate. Error bars represent standard deviation. 175

Chapter 1

1. *Research Overview*

1.1. Brief Background

Global carbon emissions from fossil fuels have significantly increased since 1900. Since 1970, CO_2 emissions have increased by about 90%, with emissions from fossil fuel combustion and industrial processes contributing about 78% of the total greenhouse gas emissions increase (*Inventory of U.S. Greenhouse Gas Emissions and Sinks: 1990-2021*, 2021). The worldwide consequences of this eco-systemic imbalance, which cause severe climate changes, are disastrous are disastrous and affect many aspects of our live (International Energy Agency (IEA), 2022). However, the increasing awareness about the climate issue and the attendance even more numerous at dedicated actions (from the Paris agreement in 2015 to the COP28 occurred recently), are encouraging the developments of solid and practical solutions to mitigate the atmospheric CO_2 concentration. Among those proposed, the carbon capture technologies allow to take CO_2 from the atmosphere or industrial flue gases and trap or storage it into new chemical bonds. But how?! Some of these technologies, the biology-based ones, are inspired by nature. Indeed, CO_2 is essential to support life on our planet of autotrophic organisms. Some of them are able of photosynthesis. Thus, when water and sunlight are present, they can use CO_2 to replicate themselves, releasing oxygen into the atmosphere. Terrestrial plants, microalgae and cyanobacteria possess this ability of carbon sequestration and so have attracted much attention as a cost-effective and eco-friendly strategy to mitigate CO_2 in the atmosphere. Microalgae and cyanobacteria can grow quickly and are easy to cultivate. Furthermore, from CO_2 they can generate a variety of metabolites through several metabolic pathways, producing target compounds, such as biofuels and sophisticated chemicals. Additionally, microalgae and cyanobacteria show i) great resilience at high CO_2 concentrations and extreme environmental parameters, and ii) the ability to utilize as wastewaters and flue gases as nutrient sources. For all the mentioned reasons, they are a great chassis for the development of photosynthesis-based microbial cell factories, focused on chemicals bioproduction and CO_2 utilization. This design project represents, however, a multidisciplinary effort, merging disciplines such as genetics, microbiology, biochemistry, and engineering. This intricate process starts with several biological efforts, such as finding suitable photosynthetic microorganisms (e.g. cyanobacteria or microalgae), exploration of metabolic pathways and their regulation, enhancement photosynthetic efficiency and considering genetic or metabolic engineering approaches (Chen and Wang, 2022). Once the biotechnological machinery

has been established, some extra steps are needed: optimization of culture conditions (nutrients, light exposure, CO_2 supply, and temperature), scale-up of the process for bulk cultivations (Chen and Wang, 2022), and implementation of further refinements to meet both environmental and economic sustainability goals.
Thus, microalgal biotechnology has been expanding rapidly over the past ten years (Barbosa *et al.*, 2023). However, nowadays, the clear potentialities of microalgae as green factories are hindered by the complexity to cost-effectively scale up the production, which is required to have competitive production costs. Consequently, to achieve commercial viability of microalgae-based technologies, several areas require constant innovation and improvements. Here, as scientists, it is where our pathway begins…

1.2. Structure of the Thesis

The present investigation is focused on the development and optimization of a microbial cell factory based on photosynthetic metabolism, for addressing CO_2 capture and valorization. The proposed microbial cell factory has been constructed on a model cyanobacteria through metabolic engineering to synthesize the high value compound, i.e. 2-phenylethanol (2-PE). 2-PE is a rosy-scented aromatic molecule largely required as fragrance in food and beverage, and cosmetics. The plant-extracted 2-PE can cost up to 1000 US$/kg, while the biotechnological production would cut the price down as low as 200 US$/kg. Thus, the biotechnological synthesis becomes truly competitive.

The project results have been individually structured. Therefore, each related chapter contains an abstract, introduction, materials and methods, results, discussion and conclusion sections (supplementary materials if necessary). As follow, a summary about the main objectives of the present thesis:

- **First Task (*Chapter 3*)**: *creation of a photosynthetic microbial cell factory*.
  The model cyanobacteria *Synechococcus elongatus* PCC 7942 has been adopted as chassis for metabolic engineering strategy, overexpressing five proteins involved in 2-PE synthesis pathway. The developed mutant strain was

physiologically characterized at laboratory scale, to identify the optimal cultural conditions for enhancing the 2-PE production.

- **Second Task (*Chapter 4 & 5*)**: *design of the bioprocess for 2-PE production based on the cyanobacterial mutant microbial factory*.
  The cyanobacterial mutant strain underwent comprehensive study in a laboratory scale photobioreactor, allowing better control on light exposure and CO_2 supply. The correlation between light intensity, which affects the photosynthesis, and 2-PE production was assessed, while carbon consumption and balance were calculated (***Chapter 4***). Consequently, the scale-up of the bioprocess for 2-PE production has been tested in four different photobioreactors, from four- to thirty-liter scale. This part of the project has been conducted, as visiting student period, at the *centre Algatech* (Institute of Microbiology, Třebon, Czech Republic), under the supervision of Pavel Hrouzek (Ph.D), in the group of algal biotechnology (***Chapter 5***). Understanding how to modulate process parameters is mandatory to design and optimize specific bioprocesses.
- **Third Task (*Chapter 6*)**: *towards the sustainability of cyanobacterial microbial factory***.**
  Concerns around the sustainability of microalgae mass cultivation, particularly the extensive use of freshwater, led to the exploration of alternatives, such as utilizing industrial polluting effluents as nutritional substrate for microalgae. In the present project, dairy wastewaters have been adopted to cultivate the microbial cell factory for 2-PE bioproduction. Finally, the combination of two different effluents led to successfully produce 2-PE by a metabolically engineered cyanobacterium on dairy wastewaters.

The ***Chapters 2*** and *7* include a global introduction and conclusions, respectively.
This thesis presents a comprehensive approach developing a photosynthesis-based bioprocess that successfully achieves the sustainable production of a high-value aromatic compound and utilizes CO_2. The research effectively integrates metabolic and bioprocess engineering, highlighting the strengths, applications, and challenges in addressing photosynthetic microbial factories for the sustainable production of green chemicals and CO_2 valorization.

Chapter 2

2. Introduction

2.1. CO_2 emissions and the environmental crisis

Carbon dioxide (CO_2) is a natural gas essential to support life on our planet, and it represents the primary carbon source for autotrophic organisms. In past times, atmospheric CO_2 concentration has been regulated by the natural bio-geological cycles involving photosynthetic organisms (Grace, 2013). Photosynthesis catalyzes CO_2 fixation into carbohydrates using sunlight as an energy source and releases molecular oxygen as by-product. Despite CO_2 being naturally expelled during aerobic respiration, volcanic activity, and combustion, its atmospheric concentration has registered an exponential increase since the late twentieth century. The advent of industrialization has marked the beginning of the oil-based products era that, over a few decades, has led CO_2 concentration to the highest value in recent history (~ 417 ppm in August 2023 (K.W. Thoning, A.M. Crotwell, 2023), about a 50% increase compared to the pre-industrial levels). Today, carbon dioxide is the primary greenhouse gas (GHG) emitted through human activities (*Inventory of U.S. Greenhouse Gas Emissions and Sinks: 1990-2021*, 2021). Anthropogenic activities like deforestation, industrialization, fossil fuel exploitation, and globalization, mainly contribute to this abrupt increment in CO_2 levels. The worldwide effects of this eco-systemic imbalance are disastrous and well-acknowledged: global warming, ice caps melting, soil deterioration, coastal erosion, ocean acidification, water eutrophication, desertification, species extinction, and biodiversity loss (International Energy Agency (IEA), 2022), to mention a few.

During the last decades, the world population, especially within the industrialized countries, has gained an increasing awareness about ecological issues. In this context, the World leading powers have been pushed to take appropriate measures against the environmental and climatic crisis. In response to this cultural empowerment, the Paris agreement was first adopted in 2015 with the participation of 189 world countries. The global target proposed to hold the global average temperature rise to below 2°C (Delbeke *et al.*, 2019). Noteworthily, modeled projections about GHG emissions estimated that reaching net-zero emissions by the end of the 21st century is essential to limit global warming to 2 °C (Le Quéré *et al.*, 2018). Therefore, in 2021 the European Commission approved the Green Deal, a thirty-year plan aimed at addressing Europe carbon neutral by 2050 and transforming the EU into a modern, resource-efficient economy (EC, 2019). The Green Deal program foresees the adjustment of the EU policies and economic framework to enable the transition toward a Green Economy, defined as an inclusive and non-discriminatory, while not exposing next generations to

significant environmental risks and ecological scarcities (Georgeson, Maslin and Poessinouw, 2017). In this ecological transition scenario, the establishment of a circular and bio-economy has acquired a central role (Escobar and Laibach, 2021). Inevitably, the development of industrial biotechnology for decoupling the economic growth from environmental deterioration occupies a pivotal rule (Schmidt, Padel and Levidow, 2012; Escobar and Laibach, 2021). Thus, bio-based economy can be defined as the production of renewable biological resources and the conversion of these resources as well as waste streams into value-added products, such as food, feed, bio-based products and bioenergy. Consequently, the attainment of a resource-*efficient* and *climate-neutral* world will require the implementation of innovative strategies at three different levels: (i) reduction of global CO_2 emissions; (ii) removal of the excessive atmospheric CO_2; (iii) utilization of CO_2 as a carbon source for valuable products (Gayathri *et al.*, 2021). In this panorama, the replacement of current most polluting industrial processes with sustainable technologies based on renewable sources has become an unprecedented urgency.

2.2. *Environmental impact of the industrial chemical synthesis*

The chemical and petrochemical sector represents one of the biggest and most energy-demanding industries, accounting for about 10% of the global energy consumption (International Energy Agency, 2017). Despite the effort in reducing fossil resource utilization and GHG emissions, the reliance on carbon fossil feedstocks for chemical synthesis makes this sector the first for oil and gas consumption and the third for global industrial CO_2 emissions (after the iron/steel and cement production) (Saygin and Gielen, 2021). According to the International Energy Agency (IEA), approximately 42% of the fossil sources consumption in this field is used to generate process energy, while the remaining 58% is used as carbon raw material (International Energy Agency, 2017). To align with the targets for the net-zero scenario by 2050, decoupling chemical synthesis from GHG emissions will require further efforts, such as the use of biological feedstocks (Chen and Patel, 2012), carbon capture and storage (CCS) (Bui *et al.*, 2018), and carbon capture and utilization technologies (CCU) (Kätelhön *et al.*, 2019). Carbon capture (CC) techniques enable CO_2 sequestration from the atmosphere or from industrial flue gases. Captured carbon dioxide can be addressed to different proposed fates: the long-lasting underground geological storage (CCS), or its utilization as

carbon source for chemical synthesis (CCU). The Center for Climate and Energy Solutions (C2ES, https://www.c2es.org/) estimated that carbon capture may account for 14% of the global GHG reduction needed by 2050, while CCS and CCU techniques may capture 90% of carbon dioxide emitted by power and industrial facilities (*Carbon Capture*, 2023). The carbon capture strategies can be distinguished into three main categories: (i) physical (adsorption and absorption) (Odunlami *et al.*, 2022), (ii) chemical (chemical looping, ionic liquids, amine absorption) (Rajabloo *et al.*, 2023), (iii) biological carbon capture for biomass or added-value compounds production (Gayathri *et al.*, 2021). Several physical and chemical processes have already been successfully implemented for atmospheric CO_2 removal but, so far, they are highly expensive and energy demanding. Moreover, these techniques generally lead to the production of unavoidable by-products, which makes them incompatible with the Green Transition target requirements. In this scenario, biological carbon fixation represents a promising strategy to couple CO_2 sequestration with its conversion into marketable added-value chemical compounds. On the other hand, biological carbon capture platforms exploit CO_2 from air as well as CO_2-enriched industrial flue gases as carbon source to produce biomass and/or added-value chemical compounds (Daneshvar *et al.*, 2022). Different organisms have already been used for biological CO_2 conversion, such as plants, fungi, algae, bacteria, and archaea (Kondaveeti *et al.*, 2020). Carbon fixation may occur via six pathways, both photosynthetic and non-photosynthetic (Bar-Even, Noor and Milo, 2012). Thus, biomass accumulation is an efficient and eco-friendly fashion to store atmospheric CO_2 into biomolecules, locking energy into the formation of new chemical bonds. The biomass can be used as raw material for manufacturing biofuels, foods, bio-based chemicals, and more. Alternatively, biological systems can be employed as cell factories, exploiting their natural CO_2 fixation ability for manufacturing added-value molecules extruded outside the cells.

2.3. Bio-based productions: Microbial Cell Factories

Microorganisms have been gaining increasing interest as sustainable platforms to produce high yields of both native and non-native metabolites, such as pharmaceuticals (vaccines, antibiotics, enzymes, hormones, and vitamins), chemicals, biofuels, and other bioproducts (Du, Shao and Zhao, 2011). The recent progress in system biology, metabolic engineering, and molecular biology have allowed the design and

construction of tailored biosynthetic pathways into wild-type microorganisms, thus, creating biocatalysts oriented toward the selective production of compounds. These sustainable biorefineries, defined as *Microbial Cell Factories* (MCFs), have been intensively studied and optimized to produce a variety of valuable biomolecules in a cost-effective and sustainable fashion. Here, some relevant examples of marketable compounds produced by MCFs: flavonoids, coumarins, stilbenoids, chorismate, p-hydroxybenzoic acid, 2-phenylethanol, vanillin, p-aminobenzoic acid, styrene, carotenoids (astaxanthin, lutein), bioactive peptides, small molecule organic alcohols and acids (1,3-propanediol, 1,4-butanediol, succinic acid, muconic acid), pharmaceuticals (heparin, artemisinin acid, a precursor of the antimalarial drug artemisinin), biofuels (isopropanol, n-butanol, 2-phenylethanol, alkanes, and alkenes), and more (Du, Shao and Zhao, 2011; Lee *et al.*, 2012; Huccetogullari, Luo and Lee, 2019; Zhang *et al.*, 2021). MCFs show several advantages compared to synthetic technologies. Firstly, MFCs avoid the use of polluting chemicals such as heavy metals and strong bases and acids, reducing the environmental impact of the process itself. Secondly, enzymes are usually characterized by strong substrate specificity that reduces the formation of unwanted byproducts, often unavoidable during chemical synthesis. Thirdly, the identification and implementation of chemical synthetic routes for some complex compounds can be very difficult and time-consuming, while exploiting natural biosynthetic machinery is often more convenient (Du, Shao and Zhao, 2011). Indeed, nowadays many macromolecules characterized by particularly complex structures are obtained via semi-synthesis (especially for pharmaceutical applications), i.e. employing natural metabolites as starting substrates for the chemical synthesis of target compounds (Majhi and Das, 2021). Finally, the technological improvements in molecular biology toolboxes and metabolic engineering, along with the increasing availability of genome sequencing data, are constantly improving our knowledge of metabolic networks and regulation mechanisms, allowing for sophisticated interventions at the genetic and metabolic levels. Additionally, using combinatorial biosynthesis it is possible to design novel biomolecules with altered structures, nowadays, particularly exploited for drug discovery.

Despite the multiple perks of utilizing MCFs to support the global demand for chemicals, some obstacles need to be overcome to economically outcompete chemical synthesis in the near future (Chen, 2012). First of all, rewiring natural cellular networks requires a deep understanding of the host genomic and metabolic features to avoid fatal metabolic imbalances. Microbes evolved over hundreds of thousands of years to avoid

metabolic wastes, thus their regulatory system is finely tuned to hamper compound overproduction. To this end, increasing the yield of a native compound up to industrially relevant yield requires applying metabolic engineering and synthetic biology techniques to redirect the carbon flow towards the desired compound, ideally without affecting cell growth. Clearly, implementing such manipulations requires the availability of suitable microbial hosts and specific genetic tools. Indeed, today only a very small percentage of the known microbial species can be successfully cultivated in laboratories (Hahn, Koll and Schmidt, 2019). If the target compound native producers happen to be lab-culturable, their productivity is generally too low to uphold a continuous supply chain. Thus, in addition to metabolic engineering, extensive optimization of the cultivation process is also imperative (Braga and Faria, 2020, 2022), also known as bioprocess engineering. Furthermore, when dealing with *species*- and *strain*-specific metabolic peculiarities, physiological characterization can be extremely useful to integrate and confirm the genetic interventions. Moreover, biological processes are generally more time-consuming and less yielding than chemical ones, resulting in a higher cost of bioproducts. Other limits are represented by inefficient metabolic flow, cost of downstream processes, product toxicity towards the host, and biodegradation of the target compound (Braga and Faria, 2022). However, thus far several approaches have been demonstrated advantageous to enhancing the biotechnological production of valuable chemicals. These strategies include the elimination of regulatory mechanisms and competing pathways, empowering the rate-limiting and flux-controlling enzymatic reactions, increasing the availability of precursors, and redirecting the carbon metabolism towards the target compound (Braga and Faria, 2020). The introduction of a carbon sink pathway, precisely a high-flux synthetic route that channels carbon into a selected pathway to a final molecule that cannot be consumed by the host, is another efficient way to increase the target yield (Oliver and Atsumi, 2015). Furthermore, computational tools for metabolic model simulation can be extremely helpful to predict and design genetic manipulations with the highest impact on product yield (Sveshnikova, MohammadiPeyhani and Hatzimanikatis, 2022).

2.3.1. *Exploiting metabolically different microbial cell factories: heterotrophy vs autotrophy*

So far, most advances in engineering microbial hosts for chemicals manufacturing have focused on heterotrophic microorganisms, such as the prokaryote models Escherichia coli, Corynebacterium glutamicum and, among eukaryotes, Pichia pastoris and Saccharomyces cerevisiae (Cho et al., 2022). However, a major constraint for heterotrophic chassis is their reliance on organic carbon as both energy source and raw material to produce biomass and metabolites. Today, the principal source of carbohydrate feedstocks for biotechnological purposes is represented by terrestrial crops (e.g., corn, sugarcane), even though microbial biomasses and agricultural or food-processing residues are acquiring increasing importance (Jung et al., 2013; Hays and Ducat, 2015; Lee and Wendisch, 2017). In contrast, autotrophic organisms can use gaseous carbon (e.g. CO_2) from the atmosphere as carbon source (Grogan, 2012). Specifically, photoautotrophs can harness sunlight energy to fix CO_2 into organic molecules in presence of water, which makes them ideal candidates for the design of carbon-efficient and sustainable biorefineries (Lai and Lan, 2015; Lau, Matsui and Abdullah, 2015). More recently, a synergistic approach has been proposed, where photoautotrophs and heterotrophs coexist. Therefore, photoautotrophic part, either cyanobacteria or eukaryotic algae, convert CO_2 into organic carbon necessary for the heterotrophic partners to thrive. In turn, the heterotrophs provide additional CO_2, protection from predation, and often, a diverse array of metabolites produced by secondary metabolism. Overall, the performances of both could result to be enhanced when cohabiting together (Roell et al., 2019; Zuñiga et al., 2020; Chang et al., 2023; Wang and Dai, 2023).

2.3.2. *Photoautotrophic microbial cell factories: the case of Cyanobacteria*

Cyanobacteria are widely distributed Gram-negative bacteria with a long evolutionary history, originated approximately 2.6–3.5 billion years ago (Hedges *et al.*, 2001). Cyanobacteria are only prokaryotes able of plant-like oxygenic photosynthesis. Indeed, the origin of photosynthetic organelle in eukaryotes is hypothesized to have possibly arisen by endosymbiosis between a phagotrophic host and a cyanobacterium (Löffelhardt and Bohnert, 1994). They have been found in a wide range of environments, ranging from marine, freshwater, to terrestrial habitats, including non-potable waters and non-arable lands (Sánchez-Bayo *et al.*, 2020). Cyanobacteria are

also well known for their flexible metabolism and the capacity to switch quickly from one mode to another one (STAL, 1995). Accordingly, in the darkness cyanobacteria can perform fermentations for energy generation (Stal and Moezelaar, 1997). In addition, cyanobacteria have minimal nutrients requirements for growth, eliminating the cost of complex growth synthetic media. Furthermore, the residual cyanobacteria biomasses that are left over after high-value products extraction can be used as animal feed or converted into organic fertilizer. Moreover, being prokaryotes, cyanobacteria possess relatively simple genetic background that eases to genetically manipulated (Koksharova and Wolk, 2002; Berla *et al.*, 2013). Indeed, the growing availability of genome sequences and bioinformatic tools has unraveled the outstanding potential of cyanobacteria in producing a wide plethora of biocommodities (Dhakal *et al.*, 2021) and have become attractive photosynthetic hosts for innovative metabolic engineering approaches (Bishé, Taton and Golden, 2019; Santos-Merino, Singh and Ducat, 2019; Vasudevan *et al.*, 2019). As a matter of fact, over the last decades, cyanobacterial cell factories have been studied and optimized to achieve the "green" manufacturing of valuable molecules such as ethanol (Choi and Park, 2016; Kopka *et al.*, 2017), butanol (X. Liu *et al.*, 2022), propanol (Hirokawa, Suzuki and Hanai, 2015), 2,3-butanediol (Nozzi and Atsumi, 2015), ethylene (Kallio *et al.*, 2021), polyhydroxybutyrate (P R., Das and Maiti, 2021), L-lactic acid (Andreas, Michal and J., 2012), and fatty acids (Ruffing, 2014). Among the outstanding biodiversity found within this phylum, the freshwater species *Synechococcus elongatus* PCC 7942, *Synechocystis* PCC 6803, and the marine *Synechococcus* PCC 7002, and *Anabaena* sp. PCC 7120 are considered model strains due to the availability of genetic toolkits and an increasing number of studies (Wang, Gao and Yang, 2020).

2.3.3. *Some insights into the photosynthesis*

As mentioned, cyanobacteria perform oxygenic photosynthesis. Oxygenic photosynthesis is one of the most important milestones of the evolution history as it has enabled complex life forms to emerge on the surface of the Earth (Sánchez-Baracaldo and Cardona, 2020). The first committed steps regard the so-called light-dependent cyclic reactions ('Light–Dependent Reactions of Photosynthesis', 2015; Lopez and Barclay, 2017; Cardona, Shao and Nixon, 2018). On the thylakoid membranes, pigments and associated proteins are packed together to form units called photosystems. There are two types of photosystems, designated as Photosystem I (PSI) and Photosystem II (PSII). Each photosystem has a pivotal pigment for photosynthesis

(i.e. chlorophylls) and accessory pigments. Particularly, the chlorophyll a pigment is designated P700 for PSI and P680 for PSII, indicating the light wavelength that is absorbed most efficiently by this pigment. The accessory pigments absorb light at slightly different wavelengths than chlorophyll a, and channel this energy to chlorophyll a. Particularly, light energy is trapped by PSII causing an electron from the pigment P680 to be promoted to an excited state. This excited electron is quickly transferred to a primary electron acceptor, then, the electron is transferred from one acceptor to another within PSII. In this electron transfer chain, the energy of the excited electron is utilized to move protons from the stroma to the lumen of the thylakoids. Finally, a mobile electron acceptor carries the electron to PSI where it is transferred to P700. The process is shown in **Figure 2.1** and called Z-scheme. As electrons move to PSI, the P680 (in PSII) is depleted of electrons and becomes a powerful oxidizing agent able to strip electrons from water molecule, through a process called photolysis:

$$2H_2O + 4hv \rightarrow O_2 + 4H^+ + 4e^-$$

Also, P700 (in PSI) absorbs light energy and, so, one electron (supplied by PSII) is promoted to the excited state. This electron is immediately transferred to a primary electron acceptor closely associated with PSI. From the primary electron acceptor, the excited electron moves across an electron transfer chain and is finally transferred to $NADP^+$ resulting in NADPH:

$$NADP^+ + 2e^- + H^+ \rightarrow NADPH$$

NADPH is a reducing agent, whit a strong ability to force its electrons and hydrogen on to other molecules.

All the above reactions result in the accumulation of protons (H^+) in the lumen of the thylakoids and a depletion in the stroma, which leads to a proton gradient across the thylakoid membranes. Thus, protons flow out to the stroma through specialized membrane proteins, i.e. ATP synthase, that utilize the energy resulting from this electrical flow to synthesize ATP from adenosine diphosphate (ADP) and inorganic phosphate (Pi):

$$ADP + Pi + energy \rightarrow ATP$$

The following stage, known as light-independent, take place in chloroplasts and are fed by the ATPs and NADPHs produced by the light-dependent partners (Lopez and Barclay, 2017). Here the actual carbon fixation occurs. Therefore, the three main stages

are carboxylation, reduction and regeneration in a cyclic fashion and notoriously know as Calvin cycle (**Figure 2.2**) (Tamoi *et al.*, 2005; Wilson and Matschinsky, 2021). Rubisco (ribulose bisphosphate carboxylase-oxygenase) catches CO_2 and combines it with a C5-compound (ribulose bisphosphate; RuBP), resulting in an unstable product that immediately breaks down in two C3-molecules (phosphoglyceric acid or PGA). The carbon atoms entered through photosynthesis are used then to build biomass, while the excess is stored in starch or glycogen molecules.

Figure 2.1. Diagrammatic representation of the photochemical reactions *(Photosynthetic Z-scheme). PAR, photosynthetic active radiation.*

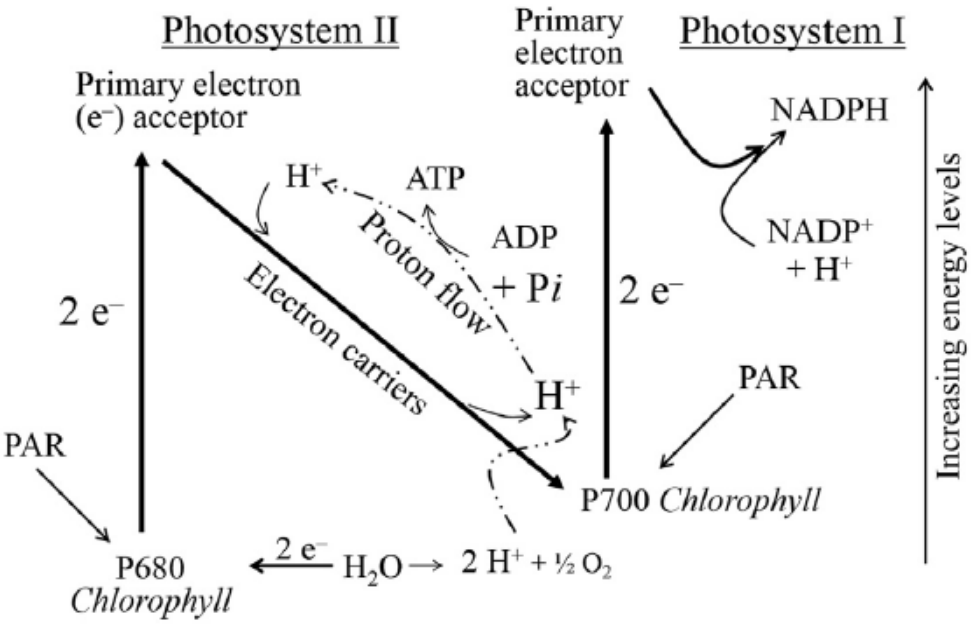
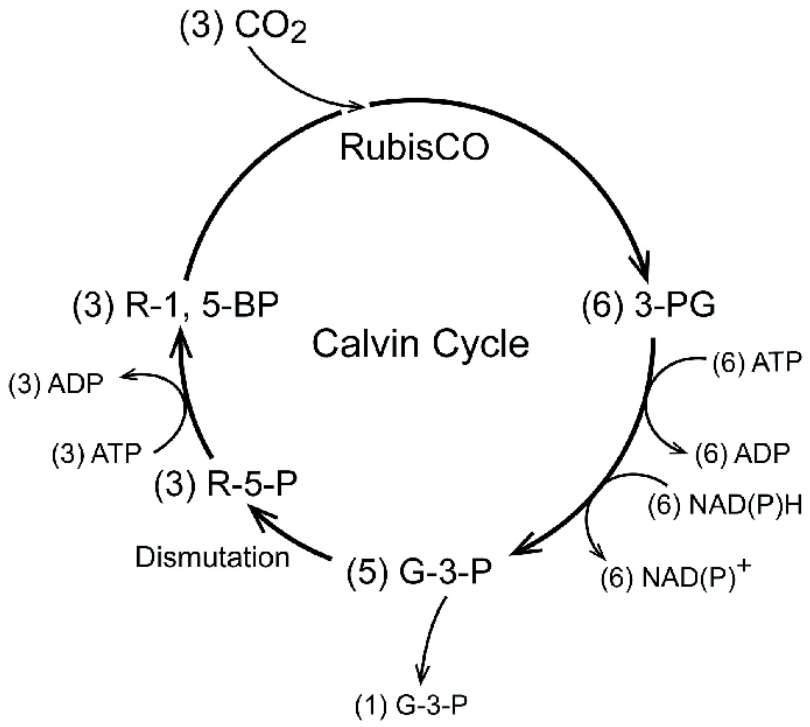


Figure 2.2. A schematic representation of the Calvin Cycle*. The enzyme ribulose-1,5-bisphosphate carboxylase (RubisCO) adds CO_2 to ribulose-1,5-bisphosphate (R-1,5-BP) and splits the product into 2 molecules of 3-phosphoglycerate (3-PG). The 3-PG is then reduced to glyceraldehyde-3-phosphate which dismutates to regenerate ribulose-5-phosphate (R-5-P). Phosphorylation of R-5-P regenerates R-1,5-BP for the next cycle. Three turns of the cycle are required for a net increase of one G-3-P.*



2.4. Biotechnological production of high value molecules: the case of aromatic compounds

An important class of petrochemical-derived compounds valued as promising targets for biotechnological production is represented by aromatics. Aromatic compounds are characterized by the presence of at least one aromatic ring (conjugated cyclic C6-ring) which can be variously substituted, but their chemical structure ranges from basilar (i.e. benzene) to more elaborated ones (e.g. Polycyclic Aromatic Hydrocarbons or PCAs). These molecules are naturally synthesized by several bacteria, archaea, algae, plants, and fungi via the Shikimate Pathway (SKP). SKP is a secondary metabolic route necessary for producing mainly the Aromatic Amino Acids (AAAs). Aromatics include many commercially viable molecules requested for diverse applications (Braga and Faria, 2022), such as chemicals, pharmaceuticals (e.g., salicylic acid (Ahmadi *et al.*, 2016)), flavours (e.g., vanillin (Hansen *et al.*, 2009), 2-phenylethanol (Qian *et al.*, 2019)), food additives (e.g., L-tryptophan (Niu *et al.*, 2019), L-phenylalanine (Y. Liu, Xu, Ding, *et al.*, 2018)), and for the synthesis of polymers (e.g., styrene (C. Liu, Men, *et al.*, 2018)). The global demand for these chemicals is additionally enhanced by the booming public recognition of their natural bioactive properties as antioxidant, anti-inflammatory, antimicrobial, and antifungal (Dickey, Forti and Kunjapur, 2021). While some molecules serve as end products, other aromatics are widely used as building blocks in the chemical industry. Accordingly, more than 40% of bulk chemicals are aromatic compounds (Haveren, Scott and Sanders, 2008). Many aromatics are highly produced by higher plants and, consequently, can be extracted from raw plant material (Ravikant Singh *et al.*, 2022). This process is generally low-yielding and time-consuming, resulting in a higher cost of bio-produced aromatics (Qian *et al.*, 2019). Historically, the majority of aromatic molecules are chemically produced from petroleum-based feedstocks (such as benzene, xylene, and toluene) via different methodologies that require severe conditions (elevated pressures and temperatures, and toxic catalysts, among others) (Lee and Wendisch, 2017). As already mentioned, the chemical synthetic branch detains the world's primate for oil and gas utilization and the third place for global industrial CO_2 emissions (Saygin and Gielen, 2021). With the current trend of oil consumption and progressive environmental deterioration, the development of biorefineries for aromatics sustainable synthesis has gathered great scientific and industrial interest. The replacement of chemically synthesized aromatics with bioproduced ones would provide high-quality natural molecules with reduced

environmental impact, thus contributing to the mitigation of CO_2 emissions (Braga and Faria, 2022). Recent estimates of the OECD (Organization for Economic Co-operation and Development, https://www.oecd.org) valued the global opportunities for the biobased economy at 80 trillion USD by 2050, with biosythetized aromatics accounting for a significant share (Sabina Asanova (CARSA), Demetrius Klitou (CARSA) and (PwC), 2017).

2.4.1. *The Shikimate Pathway*

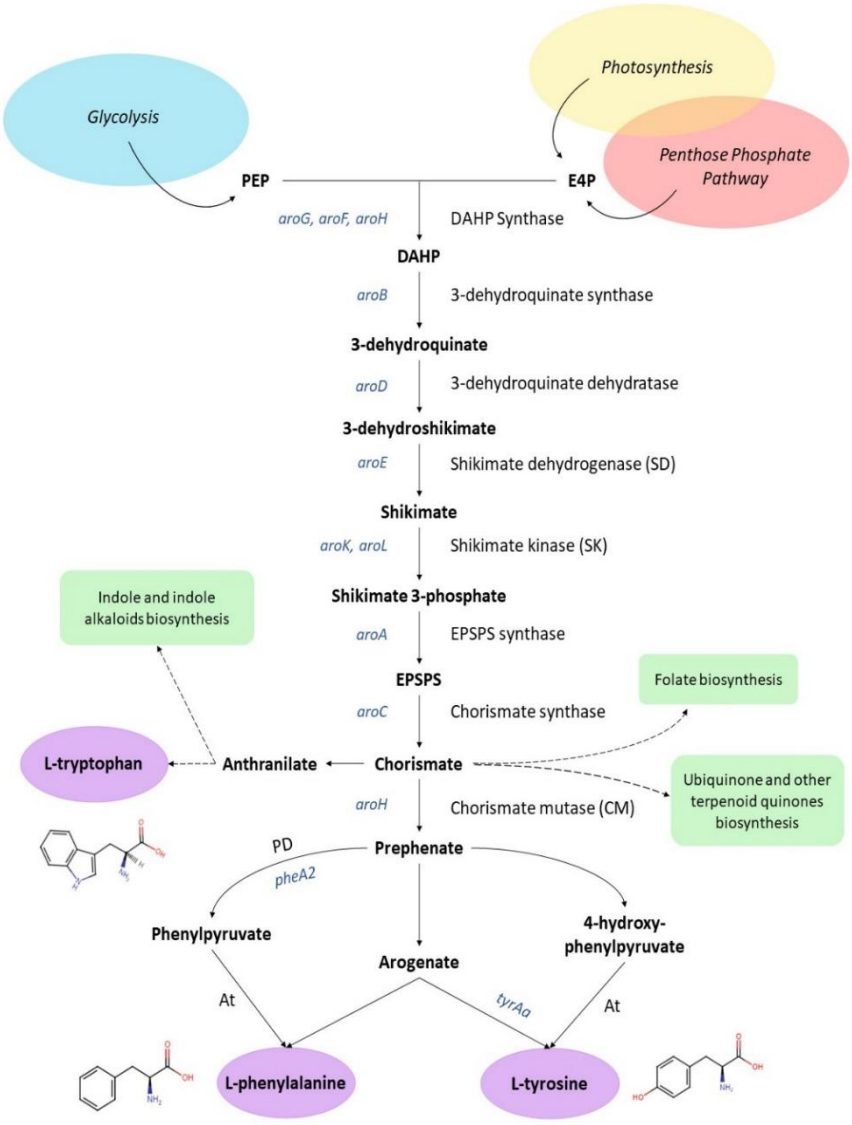
Despite the wide structural diversity found within aromatic compounds, their biosynthesis in all plants and microorganisms is branched from the Shikimate Pathway (SKP) (Herrmann, 1995). This secondary metabolic route includes seven enzymatic steps, provides precursors for the synthesis of most aromatic compounds, e.g. the three Aromatic Amino Acids (AAAs) – L-phenylalanine (L-Phe), L-tyrosine (L-Tyr), and L-tryptophan (L-Trp) – and folates (Weaver and Herrmann, 1997). In many photosynthetic organisms, such as cyanobacteria, this pathway is also essential for the production of electron chain transporters involved in both oxygenic photosynthesis and aerobic respiration, like ubiquinone and other isoprenoid quinones (Nowicka and Kruk, 2016). The lack of this route in mammalian cells forces them to introduce AAAs from their diet, reason why they are considered "essential". Enzymes and intermediates of the Shikimate Pathway are schematized in **Figure 2.3**.

The SKP starts condensating erythrose-4-phosphate (E4P) and phosphoenolpyruvate (PEP) into 3-deoxy-D-arabino-heptulosonate-7-phosphate (DAHP), linking the central carbohydrates metabolism to the biosynthesis of aromatics. In fact, E4P derives primarily from the pentose phosphate pathway while PEP is from glycolysis. A subsequent series of condensations, phosphorylations, and redox reactions convert DAHP into chorismate (CHA), passing through the formation of 3-dehydroquinate (DHQ), 3-dehydroshikimate (DHS), shikimate (SHK), 3-phosphoshikimate (3PS) and 5-O-(1-carboxyvinyl)-3-phosphoshikimate (EPSP) (Mir, Jallu and Singh, 2015). These intermediates can be directed to different routes, determining the accumulation of various aromatic and even non-aromatic molecules (Mir, Jallu and Singh, 2015). The genetic organization of the enzymes occurring after DAHPS can vary among different organisms: lower eukaryotes (i.e., yeasts) possess a pentafunctional enzyme with five catalytic domains fused together (encoded by *aroM*), while in bacteria each reaction is performed by a separately encoded protein (Pittard and Yang, 2008). The pathway

terminal metabolite , i.e. CHA, is the key precursor of all AAAs and many valuable aromatic secondary metabolites, i.e., phenolic acids, flavonoids, stilbenoids, folates, quinones, and coumarins (Tzin and Galili, 2010). Two distinct routes starting from CHA lead to the biosynthesis of L-Trp via the precursor anthranilate, or to L-Phe and L-Tyr via prephenate.

Despite the intricated network of regulations limiting the carbon flow through the SKP (Jossek, Bongaerts and Sprenger, 2001; Darmawi *et al.*, 2012), many the engineering strategies were adopted for aromatic compounds overproduction in several model microorganisms and cyanobacteria, here some reports: (Jiang and Zhang, 2016; Averesch and Krömer, 2018; Ni *et al.*, 2018; Brey *et al.*, 2020; Deshpande, Vue and Morgan, 2020; Fujiwara *et al.*, 2020; Z. Li *et al.*, 2020; Wu *et al.*, 2022; Goldfinger *et al.*, 2023; Kukil *et al.*, 2023). Indeed, along with the advances in metabolic engineering, and with the increasing availability of *-omics* data, many studies have investigated the microbic peculiarities of this promising route, opening the way for its biotechnological exploitation.

Figure 2.3. Schematic representation of the Shikimate Pathway and synthesis of AAAs *in Synechococcus elongatus PCC 7942, as annotated in the Kyoto Encyclopedia of Genes and Genomes (KEGG). Green squares indicate branching points leading to the synthesis of other aromatics. Purple ovals highlight the three AAAs. Intermediates and enzymes are reported in black, and genes encoding for enzymes in blue. Full lines represent single enzymatic reactions, dashed lines represent multiple enzymatic steps. Missing proteins have not been identified yet. PEP = phosphoenol pyruvate, E4P = erythrose-4-phosphate, DAHP = 3-deoxy-D-arabino-heptulosonate-7-phosphate, EPSPS = 5-O-(1-Carboxyvinyl)-3-phosphoshikimate, PD = prephenate dehydratase, At = aminotransferase, tyrAa = arogenate dehydrogenase NADP+ dependent.*



2.4.2. *Regulation of the Shikimate Pathway*

The SKP is subjected to a sophisticated regulation system aimed at preserving cell homeostasis and limiting energetic consumption. This involves mainly allosteric or transcriptional mechanisms that act by limiting the carbon flow directed to the SKP, thus hampering the metabolic manipulations targeted at compounds overproduction. One of the major flux-controlling nodes of the SKP is the initial condensation of PEP and E4P, catalyzed by DAHP synthase (Herrmann, 1995; Weaver and Herrmann, 1997; Chen *et al.*, 2012; Jiang and Zhang, 2016). Thus, its regulation mechanism is one of the most studied (Bongaerts *et al.*, 2001). *Escherichia coli* expresses three isomers of DAHP synthase, encoded by the genes *aroF, aroG,* and *aroH,* which are selectively feedback-inhibited by tyrosine, phenylalanine, or tryptophan, respectively (Jossek, Bongaerts and Sprenger, 2001; Chávez-Béjar *et al.*, 2012; Noda and Kondo, 2017). Additionally, in *E. coli* two transcriptional repressors are also known to regulate the expression of *aroG* and *aroF* (mediated by TyrR), and of *aroH* (mediated by TrpR) (Pittard and Yang, 2008; Braga and Faria, 2020). In *Saccharomyces cerevisiae,* DAHPS is encoded by the genes *aro3* and *aro4,* inhibited by Tyr and Phe respectively (Hartmann *et al.*, 2003).

Another important regulation step regards the release of chorismate from the SKP, which is the principal branching point for the synthesis of aromatics. Here, Chorismate Mutase (CM) isomerizes chorismate to prephenate, the common precursor for both L-Phe and L-Tyr. From prephenate, the activity of prephenate dehydratase (PD) leads to the synthesis of L-Phe via the intermediate phenylpyruvate, or alternatively, prephenate dehydrogenase (PDH) leads to L-Tyr via 4-hydroxyphenylpyruvate. In *S. cerevisiae,* as in most yeasts, each reaction is performed by a separate enzyme, and CM (encoded by *aro7*) is allosterically inhibited by L-Tyr and stimulated by L-Trp (Luttik *et al.*, 2008). Differently, in *E. coli*, L-Phe and L-Tyr are synthesized via two bifunctional enzymes with respectively CM/PD (gene *pheA*) or CM/PDH activity (gene *tyrA*), which are feedback inhibited by their functional products. Indeed, the co-overexpression of feedback-inhibition resistant DAHPS and CM/PD-PDH mutants from *E. coli* is one of the most common and efficient ways to increase the carbon flux through the SKP, as demonstrated by many engineering attempts in yeasts (Luttik *et al.*, 2008; Rodriguez *et al.*, 2015; Zhu, Wang, *et al.*, 2021) and *E. coli* (Lütke-Eversloh and Stephanopoulos, 2005, 2008; Zhou *et al.*, 2010; Darmawi *et al.*, 2012; Cao *et al.*, 2016; Noda and Kondo, 2017), but even in cyanobacteria (Ni *et al.*, 2018; Brey *et al.*,

2020).

Besides the widely studied DAHPS and CM/PD-PDH, additional potential bottleneck effect has been suggested in *E. coli* and *S. cerevisiae*, i.e. Shikimate Kinase (SK) (Luttik *et al.*, 2008; Takai A, Nishi R, Joe Y, 2009; Darmawi *et al.*, 2012; Rodriguez *et al.*, 2015; Xu *et al.*, 2019; Zhu, Wang, *et al.*, 2021). The SK enzyme catalyzes the phosphorylation of shikimate to shikimate-3-phosphate. By applying targeted proteomics and metabolite profiling at *E. coli* SKP, Juminaga and colleagues (Darmawi *et al.*, 2012) identified two bottlenecks attributed to the low activity of SK (*aroK, aroL*). By replacing these enzymes with higher efficiency ones, through a modular engineering approach, they significantly increased L-Tyr production in glucose-fed *E. coli.* Similar results were obtained by Rodriguez *et al.*, (Rodriguez *et al.*, 2015) in an engineered strain of *S. cerevisiae* for p-coumaric acid overproduction from glucose. Here, by evaluating the effect of single heterologous gene overexpression from *E. coli* on p-coumaric production, they found that the Shikimate Kinase (*aroL*) had the highest flux control.

2.5. A high-value aromatic compound: 2-Phenylethanol

Owing to the wide range of high value compounds obtainable from the Shikimate Pathway, several research efforts have been targeted at realizing sustainable biocatalysts with both wild-type and genetically modified microorganisms. Among the aromatic compounds, 2-phenylethanol (2-PE, also called phenylethyl alcohol) is emerging as one of the most valuable for biotechnological production. This higher aromatic alcohol, characterized by a pleasant rose-like scent, is highly demanded for several applications in the food and beverage, cosmetics, pharmaceuticals, and chemical industries. More in detail, thanks to its rosy aroma and chemical stability, 2-PE is commonly used as fragrance in diverse foods and wines, as well as in cosmetics and perfumes. Being rose one of the most popular and appreciated fragrances guarantees 2-PE a huge market demand, which is additionally enhanced by its approval as a GRAS molecule (Generally Recognized As Safe, 2858) by many international organizations, including the Food and Drug Administration (FDA), Flavour and Extract Manufacturers Association (FEMA), the Joint Expert Committee on Food Additives (JECFA), and the Council of Europe (COE) (Adams *et al.*, 2005; Scognamiglio *et al.*, 2012). Additionally, 2-PE has been proven to inhibit the growth of some bacteria (ZAHN *et al.*, 1966; Corre *et al.*, 1990; Fraud *et al.*, 2003;

Kleinwächter *et al.*, 2021; Yangyang *et al.*, 2023), but mostly it is active on many fungal species (i.e. *Phytophthora infestans*, *Candida albicans, Candida dubliniensis, S. cerevisiae, Kluyveromyces marxianus*) (Wang *et al.*, 2011; Hua *et al.*, 2014; Huang *et al.*, 2020; Lu *et al.*, 2023). These properties have made 2-PE an appealing antimicrobial and antifungal additive used in antiseptics, preservatives, cleaning, and personal care products (Majdabadi *et al.*, 2018; Martínez-Avila *et al.*, 2018). Moreover, 2-PE is employed as a precursor for the chemical synthesis of other valuable flavours or pharmaceutical compounds such as 2-phenethyl acetate, a volatile ester with a similar rosy scent (Etschmann *et al.*, 2002). Alongside its traditional use as a specialty chemical, more recently this alcohol has gathered interest as a potential biofuel or fuel additive, specifically thanks to its low volatility, high energy density, non-hygroscopic properties, and high octane number (Keasling and Chou, 2008; Shankar *et al.*, 2017; Fang and Sung, 2021). Finally, 2-PE is also used in aromatherapy since the flowery scent has been proven to have beneficial effects on the human sympathetic system (Ueno *et al.*, 2019). Due to the comprehensive applications of this valuable aromatic, its market demand is hardly fulfilled by the actual global production, estimated at approximately 11,000 tons per year in 2018 (*2-Phenylethanol Market - By Product (Synthetic, Natural), By Application (Cosmetics & Personal Care, Laundry & Home Care, Food & Beverages, Pharmaceuticals) & Forecast, 2022-2028*, 2022). Indeed, its market value surpassed USD 255 million in 2021, and is estimated to grow at over 370 million USD by 2028 (*2-Phenylethanol Market - By Product (Synthetic, Natural), By Application (Cosmetics & Personal Care, Laundry & Home Care, Food & Beverages, Pharmaceuticals) & Forecast, 2022-2028*, 2022).

2.5.1. *2-Phenylethanol production methods*

Today, the majority of 2-PE is chemically synthesized using petroleum-derived feedstocks, costing 3.5 - 5 US$/kg (Etschmann *et al.*, 2002; Hua and Xu, 2011). Large-scale industrial processes exploit three main chemical paths: (I) the Friedel-Craft reaction of ethylene oxide with benzene in the presence of aluminum chloride; (II) the catalytic reduction of styrene oxide with Raney nickel as a catalyst and a small amount of sodium hydroxide; and (III) the oxidation of propylene with 2-phenylethyl hydroperoxide (Etschmann *et al.*, 2002). All these methods involve the use of hazardous chemicals such as benzene, methylbenzene, and styrene oxide, which are known as carcinogenic and toxic to human and environmental health (Etschmann *et*

al., 2002; Zhu, Xu, *et al.*, 2021). Even the organic reagents used for 2-PE purification are harmful to the environment and often generate unwanted by-products, which negatively affect the final product quality. Additionally, chemical synthesis processes are based on harsh conditions such as high temperature, high pressure, and extreme pH, accounting for a significant energy demand with all the related implications on GHGs emissions.

Alternatively, 2-PE can be extracted from various flowers, including roses, jasmine, hyacinth, lilies, and daffodils (Hua and Xu, 2011). However, 2-PE concentration in the relative essential oils is generally too low, requiring complicated and costly downstream processes (Etschmann *et al.*, 2002). The only exception is represented by rose oil, which can contain up to 60% of 2-PE (particularly *Rosa damascena*, commonly known as damask rose, in which 2-PE is the dominant aromatic molecule) (SAKAI *et al.*, 2007). Nevertheless, due to the poor scalability and high cost of the botanical extraction process (around 1000 US$/kg) (Etschmann *et al.*, 2002), this route cannot fulfil the huge market demand for 2-PE (Mitri, Koubaa, Maroun, Rossignol, J.-M. Nicaud, *et al.*, 2022).

2.5.2. *Microbial cell factories for 2-Phenylethanol production*

The restrictive European and US policy regarding the use of chemically synthesized fragrances in food, beverages, and cosmetics, has been one of the main drivers of the increased demand for natural aromas (America and Europe, 2020), thus boosting research to find alternatives to the disadvantageous plant extraction. Several bacteria and yeast species have been studied for 2-PE production through bioconversion or *de novo* biosynthesis. These microbial biocatalysts claim different advantages, such as mild reaction conditions, enhanced environmental compatibility, reduced energetic requirements, higher substrate selectivity and higher stereoselectivity of the target product. According to Martinez-Avila *et al.*, microbial production of 2-PE would cost around 220 US$/kg (Martínez-Avila *et al.*, 2018).

So far, numerous studies have investigated the potential of yeast fermentation to naturally produce 2-PE, with particular emphasis on the model *S. cerevisiae*. Actually, many yeasts can naturally produce small quantities of fusel alcohols (including 2-PE) via the Ehrlich pathway, the biological route designated to branched-chain and aromatic amino acids catabolism (**Figure 2.4**) (Etschmann *et al.*, 2002; Hazelwood *et al.*, 2008; Gu *et al.*, 2020). These species include *S. cerevisiae, Kluyveromyces*

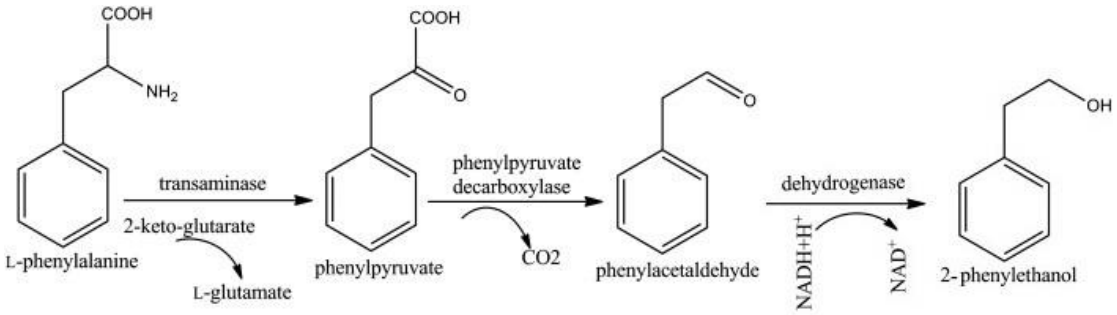
marxianus, Kluyveromyces lactis, Pichia fermentans, Pichia anomala, Schizosaccharomyces pombe, and *Hansenula anomala* (Hua and Xu, 2011; Chreptowicz *et al.*, 2018; Martínez-Avila *et al.*, 2018; Adame-Soto *et al.*, 2019; Rodríguez-Romero *et al.*, 2020; Dai *et al.*, 2021; Zhu, Xu, *et al.*, 2021). Specifically, 2-PE production via this path consists of three steps: i) transamination of L-Phe to phenylpyruvate (PPY) by an aminotransferase, ii) decarboxylation of PPY to phenylacetaldehyde (PAA) by a decarboxylase, and iii) reduction of PAA to 2-PE catalyzed by a dehydrogenase (**Figure 2.4**).

However, the reversibility of the transamination step makes this reaction sensitive to L-Phe concentration: when it is available in great quantity it is used as the sole nitrogen source to synthesize 2-PE. On the other hand, a lack of the amino acid causes ammonium to be utilized as a nitrogen source, with L-Phe being generated for protein synthesis from PPY by an aminotransferase, thus decreasing the flux of PPY to 2-PE (Y. Wang *et al.*, 2019). Alternatively, *de novo* 2-PE biosynthesis in yeast can occur via the shikimate pathway using glucose as carbon source, which enters the route after being converted into PEP and E4P by the glycolysis and the pentose phosphate pathway, respectively. The SKP eventually leads to the production of PPY, which can enter the Ehrlich pathway as described hereabove. The combination of the shikimate and the Ehrlich pathways has been named the phenylpyruvate pathway (Etschmann *et al.*, 2002; Y. Wang *et al.*, 2019). However, as previously discussed in the section 2.4.2. ("*Regulation of the Shikimate pathway*"), this route suffers from tight feedback inhibition and sophisticated regulation mechanisms which require efficient coping strategies. These usually include the removal of allosteric inhibition on the main flux-controlling enzymes, such as DAHP synthase, chorismate mutase/prephenate dehydratase (Kim, Lee and Oh, 2014; Romagnoli *et al.*, 2015), engineering of transcription factors (Chen *et al.*, 2017), and product removal (Kim, Cho and Hahn, 2014). As expected, most biotechnological advances made on yeasts have focused on the engineering of the Ehrlich pathway, which is considered more industrially relevant thanks to its higher yield and easier metabolic regulation than the SKP. Furthermore, by providing high concentrations of L-Phe to the media, the natural cell metabolism shifts to the Ehrlich pathway, thus significantly improving 2-PE accumulation. This technique, known as substrate co-feeding or metabolite doping, has been successfully applied in many studies resulting in a considerable increase in 2-PE yield (J. O. Park *et al.*, 2019; Q. Liu *et al.*, 2019; Gu *et al.*, 2020; Dai *et al.*, 2021; Mitri, Koubaa, Maroun, Rossignol, J.-M. Nicaud, *et al.*, 2022). Indeed, despite single substrate feeding being

generally (and traditionally) preferred, it often imposes stoichiometric constraints on available carbon atoms, energy, and redox state, leading to metabolic imbalances (J. O. Park *et al.*, 2019). Especially, when dealing with pathways engineered for chemicals overproduction, providing an alternative substrate can alleviate the metabolic burden by entering the pathway at a different node, and potentially rewiring the carbon flow (J. O. Park *et al.*, 2019; Liu, Santala and Stephanopoulos, 2020). Indeed, co-substrate feeding or nutrient modulation strategies have been applied also in other microorganisms, cyanobacteria and microalgae included (Papazi *et al.*, 2012; Anfelt *et al.*, 2015; Ndayisenga *et al.*, 2021).

Conversely to yeast chassis, which requires expensive fermentable sugars as carbon feedstocks, photoautotrophs possess the invaluable feature of entangling one of the most problematic GHGs into added-value compounds utilizing only sunlight, water, and releasing molecular oxygen. Accordingly, easily culturable photoautotrophs, i.e. cyanobacteria and microalgae, are considered more sustainable biorefineries than heterotrophic ones in terms of carbon usage and energetic efficiency (Srisawat, Higuchi-Takeuchi and Numata, 2022). Furthermore, thanks to their natural ease to be genetic manipulated, high CO_2 fixation rates, and fast cell growth compared to higher plants, cyanobacteria and microalgae have been becoming one of the most attractive hosts for eco-sustainable chemical production. Furthermore, cyanobacteria have been already proved to be suitable hosts for 2-PE production (Ni *et al.*, 2018).

Figure 2.4. Reactions and enzymes involved in 2-PE biosynthesis via the Ehrlich pathway.



2.5.3. *Metabolically engineered Synechococcus elongatus PCC 7942 as photosynthetic microbial factory for 2-PE production*

In a previous work, Ni and colleagues applied a synthetic biology approach aimed at redirecting the carbon flux toward the shikimate pathway for 2-PE synthesis in *Synechococcus elongatus* PCC 7942 (hereafter *S. elongatus*) (Ni *et al.*, 2018). By introducing a heterologous route for 2-PE biosynthesis, and an artificial feedback-inhibition-resistant cassette into the SKP, they successfully created a mutant strain capable of producing 119.5 mg L^{-1} of 2-PE in ten days. The so-called p120 mutant contains four heterologous genes necessary for 2-PE biosynthesis, *kivD*, *adhA, aroG*^{fbr}, and *pheA*^{fbr}, each one under the control of its own IPTG-inducible promoter, P_{trc}. *aroG*^{fbr} taken from *E. coli*, encodes for a feedback-resistant DAHP synthase (3-deoxy-D-arabino-heptulosonate 7-phosphate), which initiates the SKP by catalyzing the condensation of PEP and E4P into 3-deoxy-D-arabino-heptulosonate 7-phosphate (DAHP). *pheA*^{fbr} (from *E.* coli) encodes for a bifunctional chorismate mutase/prephenate dehydrogenase (CM/PD), which catalyzes the release of chorismate from the shikimate pathway, the major branch point for many aromatic biosynthetic routes. Being DAHPS and CM/PD the key flux-controlling nodes for aromatic biosynthesis in most photosynthetic microorganisms (Hall and Jensen, 1980), the introduction of a feedback-inhibition-resistant (fbr) cassette at these nodes effectively improved the carbon flux into SKP. A phenylpyruvate decarboxylase, the protein product of *kivD* gene (from *Lactobacillus lactis* and codon optimized for *S. elongatus* PCC 7942), converts phenylpyruvate (PPY) into phenylacetaldehyde (PAA). Finally, PAA is reduced to 2-PE by the alcohol dehydrogenase A encoded by the *adhA* gene (from *Synechocystis* sp. PCC 6803). However, despite progress in metabolic analysis and engineering, titers and productivities in cyanobacteria are still far below their heterotrophic counterparts and will need further research efforts to achieve industrial feasibility.

2.6. *How to cultivate efficiently photosynthetic microbial cell factories*

2.6.1. *The photosynthetic efficiency*

Once the photosynthetic microbial factory has been designed for a target product synthesis, many efforts are necessary prior to release the target product into the market. Let's into them! Those steps include: best strain selection, optimization of cultivation conditions and process scale-up for actual industrial applications (Kamravamanesh, Lackner and Herwig, 2018). Since light provides all the energy required for metabolism, illumination plays a pivotal role in photosynthesis-based biorefineries. Indeed, the light influence on photosynthesis has been largely studied (Muhetaer *et al.*, 2020; Kwan *et al.*, 2021; Lisondro *et al.*, 2022; Rahman *et al.*, 2023) and many approaches for improving it have been proposed. Indeed, despite the versatility of microalgae (prokaryotic and eukaryotic) and their several commercial applications, large-scale cultivation sometimes still represents a limit in the industrial production. Limited biomass yields are mostly due to insufficient photosynthetic efficiency, which has been proved to be much lower than its theoretical maximum (Wobbe and Remacle, 2015). This is mainly caused by imbalances between the light capture rate and the photosynthetic electron transfer and the subsequent carbon fixation, which trigger energy dissipation through heat or chlorophyll fluorescence. Moreover, non-homogenous distribution of light and insufficient culture mixing in photobioreactors can determine poor exposure of inner cells layers because of mutual shading (de Mooij *et al.*, 2015). To overcome all these issues and enhance photosynthesis efficiency, different approaches have been proposed. Some of them are focused on the optimization of the external parameters, such as light intensity or absorption wavelengths, CO_2 availability, and photobioreactor design, while others are genetic-engineering-oriented (de Mooij *et al.*, 2015; Fu *et al.*, 2017; Ramanna, Rawat and Bux, 2017; Leone *et al.*, 2021). Thus, to tackle the low photosynthetic efficiency at high cell density, the research has created mutant strains overexpressing photosynthesis-related proteins or acting on the light-harvesting antennae size, through different genetic modification approaches (Shin *et al.*, 2016; Fu *et al.*, 2017; Sharwood, 2017; Meyer *et al.*, 2020; Guardini *et al.*, 2021; Chen *et al.*, 2022). The regulation of the key enzymes involved in the Calvin cycle (light-independent stage) was extensively studied as well, as main role in the rate-limiting steps of photosynthesis (Ogawa *et al.*, 2015; Ng *et al.*,

2017; Yang *et al.*, 2017; Sriram, A. and Robert, 2019). Additionally, the photosynthetic efficiency can also be enhanced by optimizing the light-harvesting antennae size (Melis, 2009). Microalgae with a reduced antenna system could prevent the oversaturation of the photosystems that causes light energy dissipation and photoinhibition (de Mooij *et al.*, 2015). The pigments content of the photosynthetic complexes of several microalgae has been reduced through genetic modification techniques, e.g. RNAi technology, chemical and UV mediated mutagenesis (Dall'Osto *et al.*, 2019; Guardini *et al.*, 2021), resulting in pale green mutant strains and allowing the light radiation to penetrate deeper in high density cultures (Melis, 2009; Cazzaniga *et al.*, 2014).

To alternatively improve the microalgae growth, photon management optimization through pulsed light illumination or spectral matching (between the incident light and the absorption of light-harvesting complexes) is a promising approach (Shen and Yin, 2022). Recent studies (Zarmi *et al.*, 2020; Diotto *et al.*, 2022; Eilertsen *et al.*, 2023) investigated the effect of high frequency pulsed light (> 1 kHz) in microalgae cultures growth, as previously proposed (Terry, 1986). This strategy allows deeper light penetration in high density cultures and reduced self-shading effect, leading to the "flashing light effect", which determines higher biomass concentration (Park and Lee, 2000; Martín-Girela, Curt and Fernández, 2017). Additionally, the direct or indirect supplementation of fluorescent dyes, e.g. cyanine or rhodamine, to microalgae cultures has been adopted for spectral shifting. Indeed, they are able to catch light in the ranges non-photosynthetically absorb by microalgae and then emit fluorescence at specific wavelengths that can eventually excite the photosynthetic pigments (Prokop *et al.*, 1984; Milano *et al.*, 2012; Mohsenpour, Richards and Willoughby, 2012; Wondraczek *et al.*, 2013; Seo *et al.*, 2014; Burak, Dunbar and Gilmour, 2019; la Gatta *et al.*, 2019; Leone *et al.*, 2021).

From a more engineering point of view, the light supply efficiency can be enhanced as well, by purposefully selecting devices for microalgae cultivation, i.e. photobioreactors (PBRs), which will be better discussed in the following section.

2.6.2. *Mass cultivation of photosynthetic microorganisms*

The large-scale microalgal cultivation has been studied for years (Lee, 2001). The first mono-cultivation was conducted with the microalga *Chlorella vulgaris* by Martinus Willem Beijerinck in 1890 (Borowitzka, 1999). During the World War II, Germany

adopted microalgal cultivation for use as a food supplement. Later on, in the 1951, Arthur D. Little of the Carnegie Institute in Washington, D.C., implemented algae cultures for CO_2 biofixation (Myerson, 1954; Krauss, 1962). In 1970 Eastern Europe, Israel, and Japan began commercial productions of microalgae as healthy foods (Ugwu, Aoyagi and Uchiyama, 2008). Today, the global market of microalgae accounts for about 75 000 tons of biomass (Olaizola and Grewe, 2019), which is still small despite the increasing public interest in microalgae.

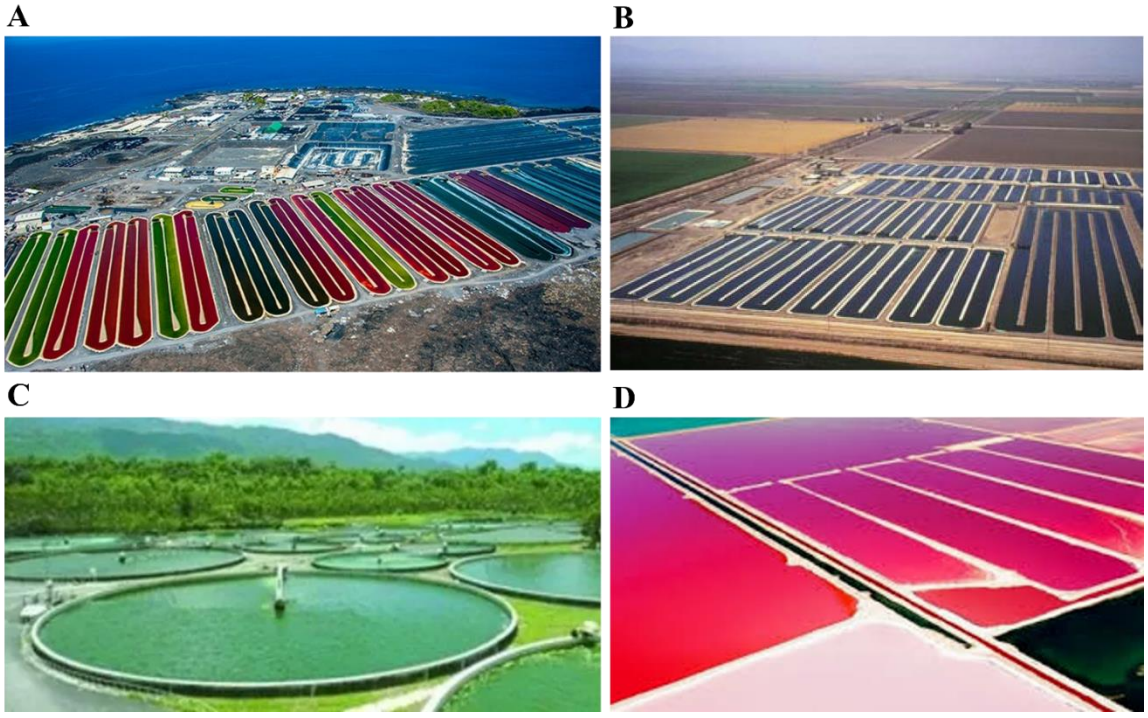
The massive cultivation of microalgae occurs prevalently in open, e.g. ponds and tanks, or closed systems. The open systems are considered more energy-efficient and require less capital investment for construction and operation than closed bioreactors, and, so, became more popular. However, the high risks of biological contamination by bacteria and protozoa, the low photosynthetic efficiency and biomass productivity, high water evaporation make them disadvantage. Indeed, they massively depend on environmental conditions, such as location, whether and habitat, resulting in a very uneven controllability of the growth conditions. Nevertheless, open ponds are the microalgal cultivation systems that have been studied for the longest time, from lagoon to raceway, shallow big, or circular tanks (Chisti, 2008; Ugwu, Aoyagi and Uchiyama, 2008; Masojídek and Torzillo, 2014). Over the years, many upgrades have been studied to improve the performances of open cultivation systems at high cell density, such as the inclined surface system (Masojídek and Prášil, 2010). Overall, several open system configurations are currently used on an industrial scale (**Figure 2.5**) by companies, such as Sosa Texcoco, Cyanotech, Earthrise Farm, Parry Nutraceuticals, Japan Spirulina, Far East Microalga, Taiwan Chlorella, Betatene®, and Western Biotechnology (Spoalore *et al.*, 2006; Costa and de Morais, 2013). As example, more than 70 companies cultivate worldwide *Chlorella* in open pond systems, with the largest efforts located in Taiwan (Tan *et al.*, 2020).

On the other hand, closed bioreactors offer many advantages, such as controllability of several parameters affecting the microalgae (e.g. temperature, pH, salinity, agitation), lower susceptibility to contamination (although existing), and, in addition, by modulating the geometry of the vessel, light and gas/liquid transfer can be really improved. The closed photobioreactors for microalgae cultivation will be deeply discussed in the following section, with some examples. **Table 2.1** resumes the main differences characterizing open and closed cultivation systems (Xu *et al.*, 2009).

Not insignificantly, the magnitude of the light supply has been considered while discussing mass microalgae cultivation techniques. Actually, prokaryotic and

eukaryotic microalgae can be industrially cultivated by exposing the culture to sunlight or artificial light. Obviously, sunshine lighting is cheaper than artificial one, but its quality and intensity strictly depend on weather, geography, season and day-night cycle. On the other hand, artificial exposure by LEDs (light-emitting diodes) can be *ad-hoc* modulated accordingly to the requirements. Despite LEDs illumination systems represent an economic burden, estimated to be on average 15 US$ per kg of microalgae biomass (Blanken *et al.*, 2013; Singh and Mishra, 2023), non-stop operating mode through year-round makes artificial lighting strongly demanded (Kratky, Jirout and Belohlav, 2023). Finally, to even improve the energy efficiency, new and old types of PBR should be coupled to photovoltaic cells, and some are currently under development (Sforza, Barbera and Bertucco, 2015; Cho *et al.*, 2019; Morales, Hélias and Bernard, 2019; Nwoba *et al.*, 2019, 2020).

***Figure 2.5. Open microalgae cultivation plants at industrial scale**. **A)** Cyanotech's plant for Spirulina and Haematococcus pluvialis cultures. **B)** Earthrise Farm's plant for Spirulina. **C)** Taiwan Chlorella's plant for Chlorella sp. cultivation. **D)** Betatene® 's plant for Dunaliella salina for β-carotene production.*



Feature	*Open*	*Closed*
Contamination risk	High	Low
CO2 losses	High	Low
Evaporative losses	High	Low
Light efficiency	Poor	Excellent
Surface/volume ratio	Low	High
Area required	High	Low
Process control	Difficult	Easy
Biomass productivities	Low	High
Investment costs	Low	High
Operation costs	Low	High
Harvesting costs	High	Relatively low
Scale-up	Easy	Difficult

Table 2.1. Comparison between open and closed PBRs.

2.6.2.1. Closed Photobioreactors

While open systems are commonly diffused for large-scale industrial applications, closed PBRs represent sophisticated and flexible systems suitable for both outdoor and indoor purposes (Qin *et al.*, 2023). Additionally, PBRs are useful for axenic cultivation and to keep a clean culture operation. A PBR is usually equipped with light support, stirring, CO_2 supply, and temperature control, and it can be properly settled according to the biological requirements of the microalgal species. Several advantages are associated to PBRs over open culture systems (Tan *et al.*, 2018): (i) larger surface-to-volume ratio, (ii) low CO_2 losses, (iii) reduced susceptibility of contamination, (iv) smaller area requirements, (v) prevention of evaporation, and (vi) higher biomass yields. So far, several PBRs made of glass or transparent plastics, as columns, panels or tubes, have been configured and studied adopting either natural or artificial lighting. While extensive efforts have been spent for optimizing either medium or cultivation conditions (Li, Horsman, Wang, *et al.*, 2008; Han *et al.*, 2015; Parichehreh *et al.*, 2019), development of highly-efficient cultivation systems is expected to make significant progresses to the cost-effectiveness of microalgae production. Nowadays, fortunately, the high costs associated with closed systems are compensated by the high homogeneity and productivity of biomass (Blanken *et al.*, 2013). For this reason, the use of closed systems on a larger scale has been becoming popular, especially for high added-value products, e.g. biopharmaceuticals, top-quality cosmetics or healthy/super foods (Ting *et al.*, 2017; Terezinha Schneider *et al.*, 2023).

2.6.2.1.1. Conventional PBRs

The most commonly diffused closed PBRs are vertical-column and tubular. Vertical-column reactors were the first real closed systems for microalgae culture developed by Cook in 1950 (Chaumont, 1993). This system is a relatively simple, where stirring is achieved by gas bubbling from the bottom (**Figure 2.6** (Huo *et al.*, 2018)). Over the decades, several upgrades have been made to increase the applicability of the vertical-column, such as bubble column or air lift (Huang *et al.*, 2016; Muharam, Putri and Hamzah, 2019; Eilertsen *et al.*, 2022). Nevertheless, vertical-column PBRs are commonly used as seed culture in microalgae factories, because their scale-up resulted to be difficult to realize (Qin *et al.*, 2023). On the other hand, the reactors used industrially the most for biomass production are tubular. The tubes are usually made of glass, plastic, or acrylic, arranged as a serpentine loop or as manifold rows (**Figure 2.7**

(Fernández *et al.*, 2014)). Recirculation of the culture suspension are obtained through peristaltic or centrifuge pumps or by air-lifting (Acién Fernández *et al.*, 2001; Bahadur, Zubair and Khan, 2013). Furthermore, tubular PBRs for commercial application are usually modular, which allows to be easily installed in any space (Arad and Cohen, 1991; Torzillo *et al.*, 1993).

Due to the extensive lighted surface area, flat panel PBRs (**Figure 2.8**) have found popularity among the microalgal biotechnology. In fact, they consist of thin layers made of glass or plastics, resulting in a relatively short light pathway, a minimal required site area, and reduced energy utilization. For being industrially implemented, flat panel PBRs can be modulable and illuminated by both artificial and natural light and, so, suitable for outdoor as well as indoor cultivation. Theoretically, these systems could achieve the highest photosynthetic efficiency of the cultivated microalgal species, mainly at high cell density and avoiding the mutual shading effect. Thus, overall, flat panel PBRs are considered the most effective microalgal cultivation systems (Norsker *et al.*, 2011, 2019; Slegers *et al.*, 2011; Tredici *et al.*, 2015; Romero-Villegas *et al.*, 2018). Currently, the main issue associated regards the low mixing efficiency, often, relied on only gas bubbling and causing biofouling and low gas mass transfer (Sierra *et al.*, 2008; Tredici *et al.*, 2015). Indeed, most of the scientific efforts have been focusing to solve the mixing efficiency inside a PBR.

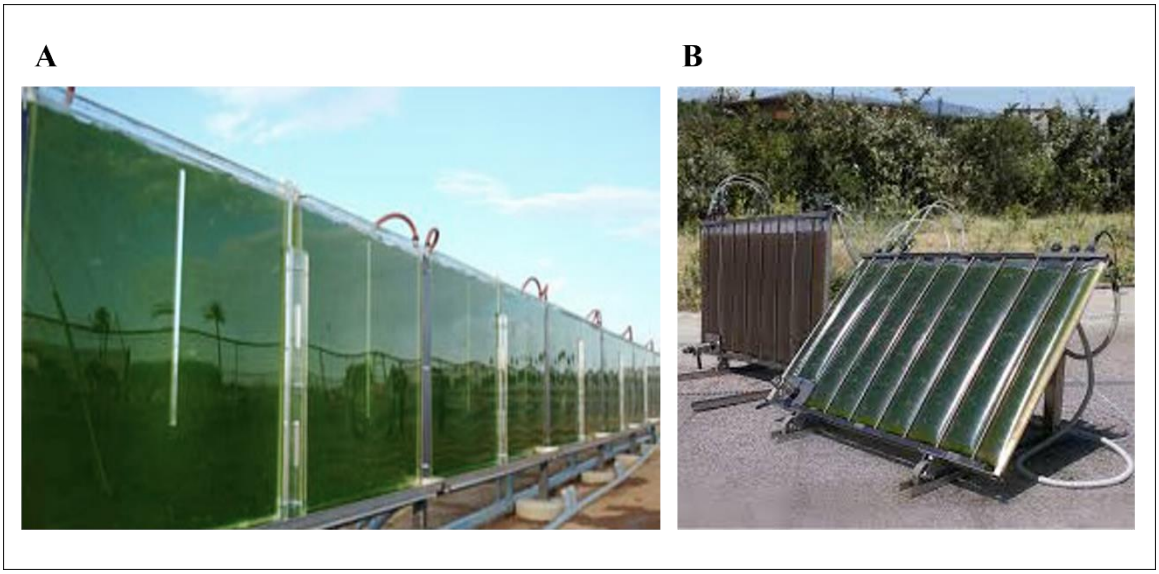
Figure 2.7. 40-L vertical-column PBR, used for Chlorella zofingiensis cultivation.



Figure 2.6. Tubular PBRs.



Figure 2.8. Flat panel PBRs. A) *https://news.asu.edu/colleges-and-units/arizona-center-algae-technology-and-innovation;* ***B)*** *https://femonline.it/products/.*



2.6.2.1.2. Innovative Photobioreactors

The demand for efficient microalgal cultivation (and drastically cut the costs associated to this biotechnology) has pushed the design of new PBRs configurations. Unsurprisingly, most of these new designs propose an evolution of flat panels, where the mixing efficiency is definitely a target to address.

Carone and colleagues (Carone *et al.*, 2022) developed a 1.3cm-tick alveolar flat panel, which enhances the global CO_2 gas-liquid mass transfer, resulting in an improved CO_2 fixation. Particularly, the system is equipped with a hydraulic pump, pushing the cells to flow inside a positive-pressurized serpentine directly exposed to the light source (Carone *et al.*, 2022).

An ultra-thin vertical flat panel (3 mm) has been developed by Gifuni *et al.*, for *Chlorella sorokianiana* (Gifuni *et al.*, 2018). They reached a volumetric biomass productivity of $1.34\,g\,m^{-2}\,h^{-1}$ and growth rate of $0.1\,h^{-1}$ at 1000 µmol photons $m^{-2}\,s^{-1}$.

In 2019, a very interesting Fibonacci-type tubular PBR was developed, from laboratory to pilot scale (Díaz, Inostroza and Acién Fernández, 2019). It is designed

to mimic higher plants, which have varied leaf distribution geometries to optimize light absorption. The configuration of this PBR allows up to 1.4-fold increase in absorbed solar radiation with respect to that received on a horizontal surface (Díaz, Inostroza and Acién Fernández, 2019).

A 'hybrid' PBR consisting of a bubble column reactor equipped with an illumination platform allowed to have high hydrodynamic performances (Deprá *et al.*, 2019). They obtained a biomass yield of 2.8 g L^{-1} with *Scenedesmus obliquus* CPCC05 (Deprá *et al.*, 2019).

Finally, to reduce consumption (focusing mainly on water consumption) and increase the efficiency of photosynthesis in PBRs, all these newly designed cultivation technologies, despite under development, may become conventional tomorrow, as the case of Algofilm© (Pruvost *et al.*, 2017; Mangi *et al.*, 2021).

2.7. ***Sustainability of microalgal biotechnology: wastewaters utilization***

Mass microalgae cultivation requires large volumes of water. For instance, microalgae have the largest water footprint among biofuel feedstocks (Zhang, Xie and Huang, 2014). Yang *et al.*, calculated that for microalgae production reusing the cultural water could reduce freshwater demand by 84% and nutrient usage by 55% (Yang *et al.*, 2011). Therefore, recycling water is considered a key step for long-term development of the microalgae biotechnology (Borowitzka and Vonshak, 2017). However, reused water may contain accumulated cell exudates, salts, bacteria, viruses, cell debris, which can potentially inhibit the performances of microalgae (Farooq *et al.*, 2015). Noteworthy, water is an essential resource in numerous industries, including pharmaceutics, electronics, food and beverage, textile, petrochemicals, agrochemicals, oil and gas industries, and domestic purposes (Wollmann *et al.*, 2019; Abdelfattah *et al.*, 2023). Thus, these factories produce worldwide large volumes of wastewater (**Figure 2.9** (Jones *et al.*, 2021)), which need to be properly disposal. They differ in the composition among organic carbon (Venkata Mohan, Lalit Babu and Sarma, 2008), heavy metals (Barakat, 2011), Nitrogen (N) (Carrera *et al.*, 2003), Phosphorous (P) (Bunce *et al.*, 2018), salts (Zhao *et al.*, 2020) and solid organic matter. Chemical methods, i.e. chlorination, coagulation/flocculation, chloramination, UV, and ozonation (Al-

Tohamy *et al.*, 2022; Abdelfattah *et al.*, 2023), are conventionally used for most of the wastewaters. However, these techniques have some shortfalls, such as high operational costs and unavoidable secondary pollution (El-sheekh *et al.*, 2021). Additionally, the conventional biological treatments, i.e. activated sludge and anaerobic digestion, concern high energy consumption, costs of the gas bubbling process (47–70% of total energy), and management of sludge from the treatments (Daverey *et al.*, 2019; L. Li *et al.*, 2020; Yadav *et al.*, 2021). Moreover, it has been estimated that wastewater treatment plants account for 3% of the global greenhouse gas emissions (BOBBY MAGILL & CLIMATE CENTRAL, 2016). Alternatively, prokaryotic and eukaryotic microalgae have been extensively proven to treat both domestic and industrial wastewaters while fixating atmospheric CO_2. Furthermore, (Craggs, Lundquist and Benemann, 2013) have reported an energy reduction by 50% if using microalgae than conventional wastewater treatments. Indeed, microalgae and cyanobacteria are very flexible and adaptative microorganisms, evolved in fluctuating environments and able to tolerate a plethora of different pollutants (Palmer, 1969). According to the published literature, species as *Chlorella*, *Chlamydomonas*, *Scenedesmus, Botryococcus sp, Spirulina, Nostoc and Anabaena* are ideally suited for phycoremediation (*phyco* means "*algae*" in Greek) (Dayana Priyadharshini *et al.*, 2021; Ahmad, 2022a). Particularly, microalgae can efficiently remove P and N components (Dayana Priyadharshini *et al.*, 2021), minimizing the risk of eutrophication in natural water bodies associated with several types of wastewaters. Municipal, sewage plants, agriculture, food, and livestock wastewaters show the highest risk as eutrophication anthropogenic factors (Kakade *et al.*, 2021). Furthermore, some microalgae utilize both organic carbon and nutrients from wastewater to thrive, and, so, they can shift from phototrophy to mixotrophy or even heterotrophy (with no light needs). In fact, microalgae have the ability to reduce by 45–65% of (biochemical oxygen demand) BOD and COD (chemical oxygen demand) (Al-Jabri *et al.*, 2021; Geremia *et al.*, 2021), even higher for N and P content (80-100% and 90-100%, respectively) (Dayana Priyadharshini *et al.*, 2021). Microalgae-based treatment of wastewaters has also natural disinfection properties against some pathogens (Espinosa *et al.*, 2021). **Table 2.2.** reports some examples of recent wastewater treatment studies conducted using both prokaryotic and eukaryotic microalgae.

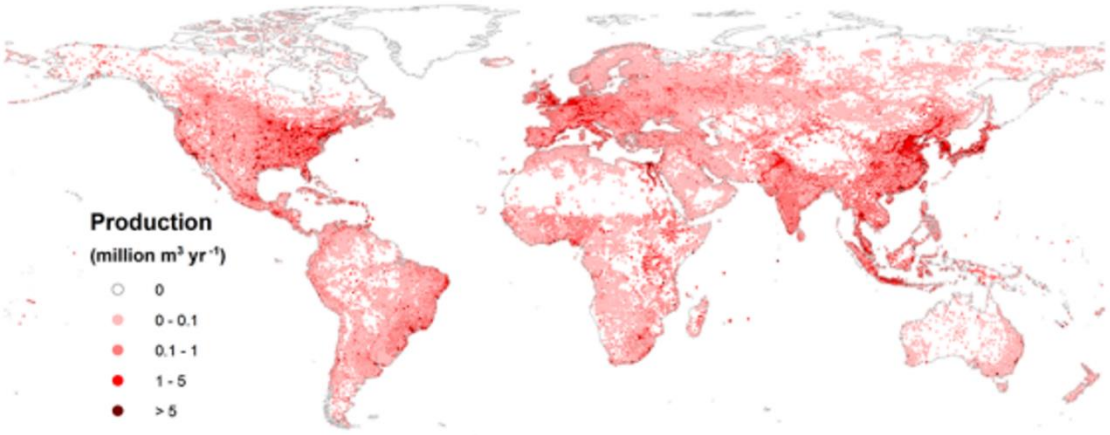
The reactor systems mainly employed for algal treatment of wastewaters are open ponds. They are shallow (0.3 m–0.5 m) loop pools, equipped with a paddle wheel

that circulates wastewater, with the same configuration previously described. These systems are primarily employed for combining organic matter breakdown and disinfection from pathogenic bacteria (Wollmann *et al.*, 2019). Recently, new high rate fluid flow reactors were created to increase the efficiency of these ponds (Ding *et al.*, 2020; Sutherland *et al.*, 2020).

Biofilm reactors have attracted interests because the ease of selectively harvesting biomass among the solid particulate contained in wastewaters. Prokaryotic microalgal biofilm reactors has been recently studied as well (Al Azad *et al.*, 2017; Garbowski *et al.*, 2020). Furthermore, algal immobilization has been already effectively adopted for nutrients elimination from industrial wastewaters (de Assis *et al.*, 2019).

Despite closed photobioreactors are not diffused for wastewater treatments, they allow a fully controlled process, which lead to obtain a high-quality biomass for diverse downstream applications. Indeed, micro and macroalgae biomasses are cultivated as supplements in food and feed, biologically active compounds in cosmetics and personal care, chemical and pharmaceutical industry. For those applications, microalgae can be marketed commercially in many countries as long as do not contain any toxic compounds and then, should be well marked accordingly with Good Manufacturing Practice (GMP guidelines).

Figure 2.9. Global wastewater production (m^3 yr^{-1} per capita).



Microalgae Strain	Wastewater	Ref.
***Chlorella* sp.**	Domestic	(Kumar *et al.*, 2018)
Chlorella sorokiniana/vulgaris; Scenedesmus sp.	Tannery	(Nagi *et al.*, 2020)
Chlorella vulgaris	Piggery	(Wang *et al.*, 2020)
Chlorella vulgaris	Sewage effluent treatment plant	(Moreno Osorio *et al.*, 2019)
Chlorella pyrenoidosa	Coal gasification plant	(S. and A.K., 2019)
Scenedesmus quadricauda*; *Tetraselmis suecica	Dairy	(Daneshvar *et al.*, 2019)
Microalgae consortia	Textile and urban	(Huy *et al.*, 2018; Marella, Parine and Tiwari, 2018)
Neochloris oleoabundans, Chlorella vulgaris* and *Scenedesmus obliquus	Agro-zootechnical digestate	(Franchino *et al.*, 2013)
Microalgae-bacteria consortium	Municipal	(Toyama *et al.*, 2018)
Spirulina sp.	Aquaculture	(Cardoso *et al.*, 2021)

Spirulina maxima	Sugarcane vinasse	(dos Santos *et al.*, 2016)
Phormidium fragile	Pharmaceuticals	(Shabana, Senousy and Khourshid, 2019)
Microcystis aeruginosa	Pharmaceuticals and personal care products	(Pan *et al.*, 2021)
Marine Cyanobacteria mixture	Heavy metals	(M. Ciani;G. Daly;R. De Philippis;A. Adessi, 2023)
Cyanobacteria-bacteria consortium	Brewery	(Papadopoulos *et al.*, 2020)

Table 2.2. Prokaryotic and eukaryotic microalgae used in the treatment of wastewater.

2.7.1. *Noble wastewater for high quality microalgae*

As mentioned earlier, microalgae applications for human food or cosmetic purposes are really limited. Indeed, often the usage of wastewater to grow microalgae does not align with the top-quality targets for those purposes (Lafarga and Acién, 2022). Therefore, several steps that should be evaluated to use industrial wastewater for biomass production. First, wastewater must be treated to remove pollutants and contaminants: filtration, sedimentation, and biological processes. Finally, microalgae are cultivated using the nutrient-rich wastewater as a growth medium. As a result, biomass can be harvested, processed, and converted into food-grade products (Ahmad and Ashraf, 2023; Fal, Smouni and Arroussi, 2023). Among those products we can have omega-3, PUFAs (poly unsaturated fatty acids), proteins, carbohydrates, vitamins and pigments. Therefore, for achieving sophisticated marketable products from microalgae, the suitable wastewater should be properly selected. Unsurprisingly,

wastes from the food industry itself are ideal, resulting in a less toxic substrates for microalgae (Ummalyma *et al.*, 2023).
Additionally, to drive microalgae-based processes gas bubbling, specifically enriched by CO_2, is necessary either to provide carbon source or to improve the mixing. Therefore, to increase the sustainability of microalgae cultivation, the adoption of industrial flue gasses rich in CO_2 are considered as the most impactful input in microalgae biotechnology development (Magalhães *et al.*, 2021). Some interesting studies concerning the actual usage of flue gas over the years are reported here (Doucha, Straka and Lívanský, 2005; Crofcheck *et al.*, 2013; He *et al.*, 2013; Nayak, Karemore and Sen, 2016; S. Park *et al.*, 2019; Molitor and Schnoor, 2020). This win-win strategy allows to combine the recovery of CO_2 from industrial waste streams (otherwise released into the atmosphere) with the production of valuable microalgae biomass.

2.7.1.1. Dairy wastewaters

For a high-quality microalgae production, employable for food or cosmetic, dairy wastes suit the best. The inherent composition of these waste streams, i.e. high nutrients content, such as organic acids, carbohydrates, phosphates and nitrogen, make them extremely dangerous for the environment, responsible for eutrophication of the water bodies (Das and Karar Paul, 2022). Additionally, the dairy industry utilizes large water amount for its activities (e.g. cleaning equipment, milk processes, pasteurization and sterilization), ranging from 1 to 10 m^3 of water per m^3 of processed milk (Boguniewicz-Zablocka, Klosok-Bazan and Naddeo, 2019). In 2019, Europe has been the second largest producer of milk with 167.4 million tons (FAO, 2019) (UN-Food & Agriculture Organization (FAO), 2020). Consequently, the relative production of wastewater accounted for 192.5 x 10^6 m^3 per year among the European countries (Stasinakis, Charalambous and Vyrides, 2022). For instance, Italy is the third European country, contributing, only in 2019, for 18.9 x 10^6 m^3 of dairy wastewaters (Stasinakis, Charalambous and Vyrides, 2022). The most abundant components are fats, organic compounds, proteins and minerals, with a chemical oxygen demand (COD) ranging 80-95 g L^{-1} and a biological oxygen demand (BOD) of 40-48 g L^{-1} (Qasim and Mane, 2013). Furthermore, dairy wastewaters contain large amounts of total nitrogen (14–830 mg L^{-1}) and total phosphorus (9–280 mg L^{-1}), while the pH ranges from 3 to 8 (Chokshi *et al.*, 2016). As a consequence of both production line and activity, different kinds of

liquid wastes are generated. Among them, the cheese-whey (CW) is the primary waste of the dairy sector, as a derivative of the milk coagulation and the subsequent separation of the curd. It is estimated that about 8-9 kg of CW are produced every 1-2 kg of cheese product (Baldasso, Barros and Tessaro, 2011). CW contains large quantity of suspended solids, proteins, lactose and water-soluble minerals and vitamins (Atra *et al.*, 2005). Moreover, the content of phosphorus (0.124 - 0.54 kg m^{-3}) and nitrogen (0.2 - 1.76 kg m^{-3}) (Prazeres, Carvalho and Rivas, 2012) is impressively high, making CW toxic for the receiving environments but even biotechnologically appealing (Carvalho, Prazeres and Rivas, 2013). For all these reasons, CW has been attracting attention in the biotechnological scenario and, thus, CW is the most investigated dairy waste for its recovery and valorisation (Zandona, Blažić and Režek Jambrak, 2021; Sar *et al.*, 2022). However, in Italy CW itself is employed to produce 'Ricotta' cheese, whose relative waste is called 'Scotta' (Maragkoudakis *et al.*, 2016). Scotta is on average characterized by 80 and 50 g L^{-1} of COD and BOD, respectively (Sansonetti *et al.*, 2009). This waste has a lower level of fats and proteins but it is richer in carbohydrates, such as lactose, and minerals (Bergamaschi *et al.*, 2016; Monti *et al.*, 2018).
In addition, the cleaning of tanks and pipelines generates large volume of effluents. Importantly, the washing procedures account for 75% of the total water used by the dairy industry (Buabeng-Baidoo *et al.*, 2017). These washing waters (WW), depending on the process or the cleaning step, retain significant quantities of dissolved nutrients, proteins, fats and lactose (Brião *et al.*, 2019). Finally, the secondary wastewaters of dairy industry derive from biological treatments of raw or primary dairy effluents, e.g. activated sludge treatment is currently applied as main step for the removal of organic compounds and nitrogen from the dairy effluents (Lateef, Chaudhry and Ilyas, 2013). The resulted exhausted sludge still contains contaminants, mainly as nitrogen and phosphorus as well as metals (Kaur, 2021) and so worth of further treatment.

2.7.1.2. Dairy wastewaters valorization through microalgae

So far, a plethora of eukaryotic microalgal species have been cultivated on dairy wastewaters and some examples are reported in **Table 2.3**. Microalgae serve as a compelling illustration of efficient dairy effluent treatment, significantly mitigating its environmental impact. They exhibit the ability to decrease COD and BOD levels by as much as 90%, while also reducing nitrogen and phosphates by 70-90% and 80-100%, respectively. Furthermore, the biomass generated from these treatments can boast lipid content ranging from 40 to 70%, making it a valuable resource for the production of

biofuels (Kothari *et al.*, 2013; Chokshi *et al.*, 2016; Khalaji *et al.*, 2023; Paulenco *et al.*, 2023).

However, while cyanobacteria have demonstrated effectiveness in removing nitrogen and phosphate from wastewater (Lincoln, Wilkie and French, 1996; Dubey *et al.*, 2011; El-Sheekh, El-Otify and Saber, 2011; G and G, 2016; Of and Microbiology, 2016; Álvarez *et al.*, 2020; Ouhsassi *et al.*, 2020; Ahmad, 2022a), the predominant focus of research has been on their potential for producing high-value compounds. These compounds can be extruded or derivatives of the biomass, such as pigments (H. Kabariya and M. Ramani, 2018; Menin *et al.*, 2019; Arashiro *et al.*, 2020; Thevarajah *et al.*, 2023). Alternatively, cyanobacteria have been exploited in disinfecting waste effluents (Samiotis, Ziagova and Amanatidou, 2023) and their biomass have been utilized as a substrate for fermentation processes (Möllers *et al.*, 2014; Álvarez *et al.*, 2020; Comer *et al.*, 2020; De Oliveira, Bassin and Cammarota, 2022). If compared to eukaryotic counterpart, fewer studies have been published in literature about the adoption of cyanobacteria for dairy wastewater treatment and many of them focused on the well-known cyanobacterium: *Spirulina platensis*. **Table 2.4** outlines some of cyanobacterial applications on dairy effluents, centered mainly around water purification or biomass accumulation.

STRAIN	EFFLUENT TYPE	REFERENCE
Chlamydomonas polypyrenoideum	Dairy wastewater	(Kothari *et al.*, 2013)
Chlorella vulgaris	Dairy wastewater	(Qin *et al.*, 2014; Choi, 2016; Handayani *et al.*, 2020; Khalaji *et al.*, 2023)

Acutodesmus dimorphus	Dairy wastewater	(Chokshi *et al.*, 2016)
Chlorella pyrenoidosa, Anabaena ambigua, Scenedesmus abundans	Dairy wastewater	(Brar, Kumar and Pareek, 2019)
***Chlorella sorokiniana* SU-1**	Dairy wastewater	(Kusmayadi *et al.*, 2022)
Nannochloris sp.	Cheese Whey	(Paulenco *et al.*, 2023)
Scenedesmus quadricauda, Tetraselmis suecica	Dairy wastewater	(Daneshvar *et al.*, 2019)
Chlorella vulgaris, Chlorella sorokiniana, Chlorella saccharophila, Auxenochlorella protothecoides and Chlamydomonas reinhardtii.	Cheese Whey and Scotta	(Gramegna *et al.*, 2020)

Table 2.3. Eukaryotic microalgae strains used for dairy wastewater treatment.

STRAIN	EFFLUENT TYPE	REFERENCE
Spirulina platensis	Dairy wastewater/cheese whey	(Pereira *et al.*, 2019; Álvarez *et al.*, 2020; Zapata *et al.*, 2021; Escolà Oliva *et al.*, 2022)
Pseudanabaena galeata	Dairy wastewater	(Ouhsassi *et al.*, 2020)
***Oscillatoria*, *Phormidium* species**	Dairy wastewater	(H. Kabariya and M. Ramani, 2018)
Desertifilum tharense	Dairy wastewater	(Khemka and Saraf, 2017)
Aphanothece microscopica Nägeli	Dairy wastewater	(Vieira *et al.*, 2012)

Table 2.4. Cyanobacteria strains used for dairy wastewater treatment.

Results of the Thesis

- ***Chapter 3:*** Combining Metabolite Doping And Metabolic Engineering To Improve 2-Phenylethanol Production By Engineered Cyanobacteria (doi: 10.3389/fbioe.2022.1005960)

- ***Chapter 4:*** Metabolic Connection Between Photosynthesis And 2-PE Production In PBR: To What Extent Does Light Intensity Affect The 2-PE Synthesis?

- ***Chapter 5***: Scale Up Of Photosynthetic 2-Phenylethanol Bioproduction In Photobioreactor: Opportunities And Challenges

- ***Chapter 6***: Coupling Dairy Wastewaters For Nutritional Balancing And Water Recycling: A Sustainable Heterologous 2-Phenyletanol Production By Engineered Cyanobacteria (doi: 10.3389/fbioe.2024.1359032)

Chapter 3

3. Combining Metabolite Doping And Metabolic Engineering To Improve 2-Phenylethanol Production By Engineered Cyanobacteria

This chapter was published as:

Usai G, Cordara A, Re A, Polli MF, Mannino G, Bertea CM, Fino D, Pirri CF and Menin B (2022) **Combining metabolite doping and metabolic engineering to improve 2-phenylethanol production by engineered cyanobacteria**. *Front. Bioeng. Biotechnol.* 10:1005960. doi: 10.3389/fbioe.2022.1005960.

3.0. Abstract

2-Phenylethanol (2-PE) is a rose-scented aromatic compound, with broad application in cosmetic, pharmaceutical, food and beverage industries. Many plants naturally synthesize 2-PE via Shikimate Pathway, but its extraction is expensive and low-yielding. Consequently, most 2-PE derives from chemical synthesis, which employs petroleum as feedstock and generates unwanted by products and health issues. The need for 'green' processes and the increasing public demand for natural products are pushing biotechnological production systems as promising alternatives. So far, several microorganisms have been investigated and engineered for 2-PE biosynthesis, but a few studies have focused on autotrophic microorganisms. Among them, the prokaryotic cyanobacteria can represent ideal microbial factories thanks to their ability to photosynthetically convert CO_2 into valuable compounds, their minimal nutritional requirements, high photosynthetic rate and the availability of genetic and bioinformatics tools. An engineered strain of *Synechococcus elongatus* PCC 7942 for 2-PE production, i.e. p120, was previously published elsewhere. The strain p120 expresses four heterologous genes for the complete 2-PE synthesis pathway.

Here, we developed a combined approach of metabolite doping and metabolic engineering to improve the 2-PE production kinetics of the *Synechococcus elongatus* PCC 7942 p120 strain. Firstly, the growth and 2-PE productivity performances of the p120 recombinant strain were analyzed to highlight potential metabolic constraints. By implementing a BG11 medium doped with L-phenylalanine, we covered the metabolic burden to which the p120 strain is strongly subjected, when the 2-PE pathway expression is induced. Additionally, we further boosted the carbon flow into the Shikimate Pathway by overexpressing the native Shikimate Kinase in the *Synechococcus elongatus* PCC 7942 p120 strain (i.e. 2PE_*aroK*). The combination of these different approaches led to a 2-PE yield of 300 mg/gDW and a maximum 2-PE titer of 285 mg/L, 2.4-fold higher than that reported in literature for the p120 recombinant strain and, to our knowledge, the highest recorded for photosynthetic microorganisms, in photoautotrophic growth condition.

Finally, this work provides the basis for further optimization of the process aimed at increasing 2-PE productivity and concentration, and could offer new insights about the use of cyanobacteria as appealing microbial cell factories for the synthesis of aromatic compounds.

3.1. Introduction

The global emergency to reduce greenhouse gas emissions to net-zero is currently a burning issue. As part of the Paris Agreement and the European Green Deal, the transition to a climate-neutral society should be gained by investigating realistic technological solutions, by aligning action in key areas such as industrial policy, finance and research (Delbeke *et al.*, 2019; EC, 2019). In this panorama, biorefineries can help decarbonization by fostering greener solutions. Among these, the photosynthetic activity of some organisms can be outstandingly fitting. Indeed, plants, algae and cyanobacteria can naturally convert CO_2, when sunlight and water are both present, to organic molecules, useful as fuels or other add-value commodities (Daneshvar *et al.*, 2022). The prokaryotic cyanobacteria, which fix CO_2 more efficiently than higher plants and grow faster (Li, Horsman, Wu, *et al.*, 2008), are one of the most promising actors that can deal with this time in history. Indeed, cyanobacteria can grow in non-arable lands and in nutritionally poor conditions (Jenkins, 1991; Ducat, Way and Silver, 2011) or non-potable water (Nozzi, Oliver and Atsumi, 2013; Sánchez-Bayo *et al.*, 2020). Additionally, in comparison with eukaryotic algae and plants, cyanobacteria are more genetically amenable (Berla *et al.*, 2013; Lau, Matsui and Abdullah, 2015; Sengupta *et al.*, 2019; Wang, Gao and Yang, 2020) and so attractive hosts for challenging metabolic engineering strategies (Bishé, Taton and Golden, 2019; Santos-Merino, Singh and Ducat, 2019; Vasudevan *et al.*, 2019). Indeed, they have been largely metabolically engineered to produce a huge array of valuable products (Zhou and Li, 2010; Lai and Lan, 2015; Santos-Merino, Singh and Ducat, 2019).

Recently, some efforts have been targeted to produce aromatic compounds by cyanobacteria (Ni *et al.*, 2018; Xue and He, 2018; Huccetogullari, Luo and Lee, 2019; Brey *et al.*, 2020; Jin *et al.*, 2021). Aromatics, characterized by a benzene ring or derivatives, are mainly adopted as organic solvents, dyes and precursors for the synthesis of many products employed in the food, pharmaceutical and chemical fields. Currently, the majority of aromatic chemicals are manufactured using petroleum as the raw source, which makes them undesirable for environmental, safety and health issues (Gosset, 2009; Qian *et al.*, 2019).

In all microorganisms and plants, the aromatics synthesis takes place via the Shikimate Pathway (SKP), a sequence of seven enzymatic steps in which phosphoenolpyruvate and erythrose 4-phosphate are converted to chorismate, the precursor of the three

aromatic amino acids (AAA) - tryptophan (Trp), phenylalanine (Phe), and tyrosine (Tyr) - and most of the aromatic metabolites. Several intermediates can serve for the subsequent synthesis of both aromatic and non-aromatic molecules commercially valuable (Herrmann, 1995; Mir, Jallu and Singh, 2015).

De novo synthesis of aromatic compounds has been already achieved through different organisms by exploiting the SKP (Dickey, Forti and Kunjapur, 2021). However, the enzymes involved in some steps of the SKP are tightly regulated by feedback inhibition and transcriptional mechanisms, which hamper their use for target compounds oversynthesis. In bacteria and yeast, one of the most studied regulatory mechanisms is the 3-Deoxy-D-arabinoheptulosonate 7-phosphate (DAHP) synthase (EC 2.5.1.54), the first committed enzyme of the SKP. *E. coli* expresses three genes encoding DAHP synthases, which are respectively sensitive to a specific AAA (Jossek, Bongaerts and Sprenger, 2001; Chávez-Béjar *et al.*, 2012; Noda and Kondo, 2017). Furthermore, as already reported in some bacteria and yeast, the shikimate kinase (EC 2.7.1.71), which catalyzes the conversion of shikimate in shikimate-3-phosphate (the fifth step in SKP), can relevantly affect the carbon flow by acting as bottleneck in the SKP (Luttik *et al.*, 2008; Takai A, Nishi R, Joe Y, 2009; Rodriguez *et al.*, 2015; Xu *et al.*, 2019).

So far, numerous efforts have been already pursued to yield aromatic chemicals by genetically and non-genetically modified microorganisms. 2-phenylethanol (2-PE) is one of the most valuable aromatic compounds, with a global market value estimated to reach 351 Million USD by 2027 (Kang *et al.*, 2014; Kim, Lee and Oh, 2014; Romagnoli *et al.*, 2015; Averesch and Krömer, 2018). 2-PE is an aromatic alcohol with pleasant rose-like scent, which makes it exploitable mostly in the food, fragrance, and flavor industries, but still employable as antifungal or fuel additive (Etschmann *et al.*, 2002; Majdabadi *et al.*, 2018; Nielson, Machas and Mckenna, 2018; Fang and Sung, 2021). Plant-extracted 2-PE costs 1,000 US$/kg and suffers from economics and scalability for a sustainable industrial production (C. Liu, Zhang, *et al.*, 2018; Qian *et al.*, 2019). On the other hand, biotechnologically synthesized 2-PE has a value of around 220 US$/kg (Mitri, Koubaa, Maroun, Rossignol, J. Nicaud, *et al.*, 2022), so the 2-PE synthesis by microorganisms has been emerging as appealing bioproduction system, alternatively to plant extraction (Gu *et al.*, 2020; Kong *et al.*, 2020; Dai *et al.*, 2021; Zhu, Xu, *et al.*, 2021).

While a few bacteria are known to naturally synthesize 2-PE (H. Zhang *et al.*, 2014; C. Liu, Zhang, *et al.*, 2018; J. Liu, Jiang, Bai, *et al.*, 2018), the microbiological 2-PE biosynthesis has been intensively investigated mainly in yeast. Particularly, yeast

preferentially use the three-stepped Ehrlich pathway for 2-PE production, by starting from phenylalanine. Thus, to sustain 2-PE production, the yeast-based microbial platform needs to be fed with both sugar substrate and aromatic amino acid (Q. Liu *et al.*, 2019; Gu *et al.*, 2020; Dai *et al.*, 2021). Generally, this strategy is known as co-substrate feeding or metabolite doping (H. Liu *et al.*, 2019; Hong *et al.*, 2019; J. O. Park *et al.*, 2019; Gu *et al.*, 2020; Liu, Santala and Stephanopoulos, 2020; Chang *et al.*, 2021). However, single substrate feeding is conventionally preferred but naturally elicits stoichiometric constraints on available carbon atoms, energy and redox state, leading to metabolic imbalance, when a specific route has to be exploited. Also, in cyanobacterial and microalgal cultivations, co-substrate feeding or nutrient modulation strategies have been adopted (Papazi *et al.*, 2012; Anfelt *et al.*, 2015; Ndayisenga *et al.*, 2021). In comparison to carbohydrate-using microorganisms, cyanobacteria may represent a more sustainable alternative because, drawing energy from photosynthesis, they avoid expensive fermentable sugars as carbon feedstock and can be exploited for CO_2 capture and conversion. Furthermore, cyanobacteria have been already proved to be suitable hosts for 2-PE production (Ni *et al.*, 2018). In a previous work, Ni and co-workers applied a synthetic biology approach aimed at redirecting the carbon flux toward the SKP for 2-PE synthesis in *Synechococcus elongatus* PCC 7942 (*S. elongatus* PCC 7942) (Ni *et al.*, 2018). They have successfully obtained a mutant strain (p120), which heterologously overexpresses four genes necessary for 2-PE biosynthesis: $aroG^{fbr}$ and $pheA^{fbr}$, related to the SKP, and *kivD* and *adhA* to effectively synthetize 2-PE. Both the protein products of *aroG* and *pheA* are known bottlenecks afflicting the SKP, and therefore these gene sequences have been genetically modified not to be sensitive to the feedback inhibition by phenylalanine (feedback inhibition resistant, *fbr*). Phenylpyruvate decarboxylase is the protein product of *kivD* and catalyzes the conversion of phenylpyruvate in phenylacetaldehyde. Finally, the alcohol dehydrogenase A, the protein encoded by *adhA* gene, converts phenylacetaldehyde in 2-PE. Particularly, in Ni *et al*., 2018 the p120 mutant strain produced 119.5 mg L^{-1} 2-PE in ten days (Ni *et al.*, 2018). However, we were not able to replicate this outcome in our laboratory.

In the present work, we optimized the 2-PE production process in the recombinant *S. elongatus* PCC 7942 p120 strain (Ni *et al.*, 2018) by combining two strategies of metabolite doping and metabolic engineering: i) we implemented a phenylalanine-doped growth medium to overcome metabolic load and the competition between 2-PE synthetic pathway and endogenous routes for Phe usage; ii) we metabolically

engineered the p120 mutant strain to increase the carbon flow into the SKP by means of the endogenous Shikimate Kinase overexpression, obtaining a new engineered strain (2PE_*aroK*). The resulting mutant strain and the related biosystem could effectively increase 2-PE production and offer new insights about the aromatic metabolism in cyanobacteria.

3.2. Materials and Methods

3.2.1. Cyanobacterial strains, media and cultural conditions

All strains used in the present study are listed in **Table 3.1**. *Synechococcus elongatus* PCC 7942 was obtained from the Pasteur Culture Collection of Cyanobacteria and was cultivated in sterilized BG11 medium (Stanier *et al.*, 1971) with an optimized recipe and some modifications (Cordara *et al.*, 2018; Vasile *et al.*, 2021). Briefly, the final BG11 medium composition is: 1.5 g L^{-1} $NaNO_3$, 0.075 g L^{-1} $MgSO_4 \cdot 7H_2O$, 0.004 g L^{-1} $FeCl_3 \cdot 6H_2O$, 0.04 g L^{-1} K_2HPO_4, 0.036 g L^{-1} $CaCl_2$, 0.024 g L^{-1} $Na_2EDTA \cdot 2H_2O$, 2.86 mg L^{-1} H_3BO_3, 1.81 mg L^{-1} $MnCl_2 \cdot 4H_2O$, 0.39 mg L^{-1} $Na_2MoO_4 \cdot 2H_2O$, 0.22 mg L^{-1} $ZnSO_4 \cdot 7H_2O$, 0.05 mg L^{-1} $CuSO_4 \cdot 5H_2O$, 0.03 mg L^{-1} $Co(NO_3)_2 \cdot 6H_2O$. The BG11 medium was buffered with 6.05 g L^{-1} TES (2-([Tris(hydroxymethyl)methyl]amino)ethane-1-sulfonic acid sodium salt) to pH = 8. For the *S. elongatus* recombinant strains (*S. elongatus* p120, *S. elongatus* 7942_*aroK* and *S. elongatus* 2PE_*aroK*), the BG11 medium was supplemented with the appropriate antibiotic (20 µg mL^{-1} spectinomycin and/or 10 µg mL^{-1} kanamycin). Cells were grown either in shaking flasks at 30°C under continuous lighting (30 µmol photons m^{-2} s^{-1}) 130 rpm or on solid BG11 1.5% agar plates. For the study of the physiological effect of aromatic compounds on the p120 mutant strain metabolism, the three aromatic amino acid (L-Phe, L-Tyr and L-Trp) and two aromatic vitamins (folic acid and cyanocobalamin) were supplemented into the BG11 medium individually or in combination. The toxicity assay was conducted by exposing the wild type strain to 0.1, 0.3, 0.5 and 1 g L^{-1} 2-PE. The growth of all strains of *S. elongatus* used in this work were daily monitored by measuring optical density at 730 nm (OD_{730}) and subsequently converted into biomass as gram of dry cell weight per liter (gDW L^{-1}), by using a conversion factor of 0.26 (previously achieved in our laboratory). Specific growth rate (µ, d^{-1}) was obtained from the slope of the logarithmic plot of OD_{730} versus time, for the growth curve points enclosed into the exponential phase. Gene expression in mutant strains was inducted by adding 1mM IPTG (Isopropyl β-d-1-thiogalactopyranoside) into the BG11 medium when the cell cultures reached OD_{730} = 1. One-way ANOVA or unpaired two-tailed t-test were used to assess the statistical significance of the cultural conditions screened in the present study (p-value < 0.05).

Plasmid or Strain	Genetic features	Source
p120	lacI^{q}; P_{trc}::*kivD*, P_{trc}::*aroG^{fbr}*, P_{trc}::*pheA^{fbr}*, P_{trc}::*adhA*, Spec^{R}, NSI homologous sites	(Ni *et al.*, 2018)
pAM2991	lacI^{q}, P_{trc}, Spec^{R}, NSI homologous sites	addgene, https://www.addgene.org/40248/
pAM1579	Kan^{R}, NSII homologous sites	addgene, https://www.addgene.org/40240/
pAM1579_LacI	lacI^{q}, P_{trc}, Kan^{R}, NSII homologous sites	This work
pAM1579_LacI_*aroK*	lacI^{q}, P_{trc},::*aroK*, Kan^{R}, NSII homologous sites	This work
***S. elongatus* PCC 7942**	wild type	Pasteur Culture Collection
***S. elongatus* p120**	*S. elongatus* overexpressing 2-PE biosynthetic pathway enzymes (p120)	(Ni *et al.*, 2018)
S. elongatus* *7942_aroK	*S. elongatus* overexpressing the native shikimate kinase gene	This work
S. elongatus* 2PE_*aroK	*S. elongatus* overexpressing both 2-PE biosynthetic pathway enzymes (p120) and the native shikimate kinase gene	This work

***Table 3.1*. Genetic features of plasmid vectors and strains used in the present work**. *lacI^{q}, LacI repressor gene; kivD, gene encoding phenylpyruvate decarboxylase; adhA, gene for alcohol dehydrogenase A; aroG^{fbr}, feedback-inhibition resistant DAHP synthase; pheA^{fbr}, feedback-inhibition-resistant chorismate mutase/prephenate dehydratase; Spec^{R}, spectinomycin-resistance cassette; aroK, endogenous gene for Shikimate Kinase expression in S. elongatus; Kan^{R}, kanamycin-resistance cassette; P_{trc}, IPTG-inducible promoter; NSI, homologous regions for Neutral Site I insertion; NSII, homologous regions for Neutral Site II insertion.*

3.2.2. ***Plasmid construction and transformation***

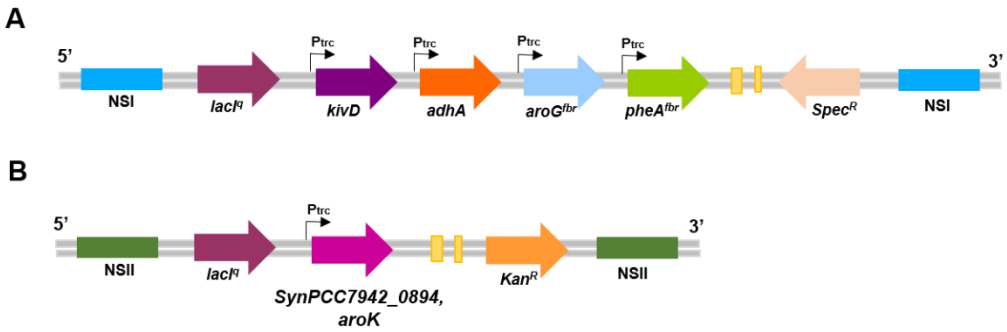
Chemically competent *Escherichia coli* DH5α strain was used for gene cloning and was grown in LB (Luria-Bertani) broth at 37°C, either in liquid cultures with continuous shaking (130 rpm) or on solid 1.5% (w/v) agar plates with the proper selection antibiotic (100 μg mL^{-1} spectinomycin or 50 μg mL^{-1} kanamycin). The plasmid p120 (kindly provided by Prof. Ping Xu at the State Key Laboratory of Microbial Metabolism of the Shanghai Jiao Tong University (Ni *et al.*, 2018); **Figure 3.1A**, **Table 3.1**) is responsible for the heterologous expression of the pathway for 2-PE biosynthesis in *S. elongatus*. It contains two flanking sequences for targeted multigene insertion by homologous recombination in *S. elongatus* Neutral Site I (NSI). Also, the IPTG-inducible gene expression platform (*LacI*^{q} repressor gene, LacI operator), spectinomycin-resistance cassette (aminoglycoside adenylyltransferase) and the four genes involved in 2-PE synthesis: feedback-inhibition resistant DAHP synthase (*aroG*^{fbr}, from *E. coli*), feedback-inhibition resistant chorismate mutase/prephenate dehydratase (*pheA*^{fbr}, from *E. coli*), phenylpyruvate decarboxylase (*kivD*, from *L. lactis* codon optimized for *S. elongatus*), and alcohol dehydrogenase A (*adhA*, from *Synechocystis* sp. PCC 6803) (**Figure 3.1A**). Each gene is preceded by trc promoter, lacI operator and RBS. Additionally, the pAM1579-LacI was created by standard cloning LacI repressor gene, LacI operator, trc promoter and RBS from pAM2991 into pAM1579 (Ptrc start-NheI-FW CATGGCTAGCGTACCGAGCTCGAATTCCATGGTC and LacI start-XbaI-RV CGTCTAGAGACACCATCGAATGGTGCAAAACC). For the native shikimate kinase gene (Synpcc7942_0894, *aroK*) overexpression strategy, the gene was amplified from the purified *S. elongatus* PCC 7942 genome by touchdown PCR with the following primers: SK start-EcoRI-rv (CATGGAATTCGTGTCATTGGTGACAGCTCTGAACGGC) and SK stop-NheI-fw (CATGGCTAGCTTAAGTCTCTATCTCTGCAGGAGAGCTATCAGC). The amplified gene was cloned into pAM1579-LacI, containing the IPTG-inducible gene expression platform, kanamycin resistance and the homologous regions for the Neutral Site II insertion in *S. elongatus* genome (pAM1579-LacI-*aroK*, **Figure 3.1B**, **Table 3.1**). Any transformation was conducted by incubating *S. elongatus* with 0.5 μg DNA for 5h in the darkness at 30°C. Then, bacteria were plated on the proper selection antibiotic (spectinomycin and/or kanamycin). To promote chromosomal segregation, the new colonies were periodically streaked on increasing concentration of selection

antibiotic (until 100 µg L^{-1} spectinomycin and/or 50 µg L^{-1} kanamycin). The strains were confirmed by PCR and the full segregation was verified by using the following primers for Neutral Site I, NSI-fw AAGCGCTCCGCATGGATCTGAC and NSI-rv GTAGGGATTTCGCCAGATCAATGCC, and Neutral Site II, NSII-fw CGATCGCTGACTGAGTTGC and NSII-rv GAAGCGGGTCACTACTTGG.

3.2.3. ***qRT-PCR analysis***

In order to validate the RNA-seq data, qRT-PCR analysis was performed. Briefly, pellets of 2PE_*aroK* mutant strain of *S. elongatus* PCC 7942 and the relative wild type strain grown under the different experimental conditions were obtained after centrifugation (4,000 *g*, 4°C, 20 min) of the respective liquid culture. Then, the pellets were freeze-dried and stored at -80 °C until total RNA extraction was performed. Before performing nucleic acid extraction from the lyophilized pellets, they were washed twice with a 0.9% (w/v) NaCl solution and, in order to prevent bacterial RNA degrading, incubated with 1 mL of RNAprotect R Bacterial Reagent (Qiagen, Hilden, Germany) for 5 min and at room temperature. After centrifugation (5,000 *g*, 10 min, 4°C), total RNA extraction was performed by using RNeasy Mini Kit R (Qiagen, Hilden, Germany) as previously described (Campobenedetto *et al.*, 2020). The amount of total RNA was measured with a UV/visible nano-spectrophotometer (BioSpec-nano, Shimadzu, Japan), and the quality was checked by 1% (w/v) agarose gel electrophoresis. The isolated RNA was then used as template for retro-transcription (cDNA Maxima H Minus First Strand, Thermo Fisher Scientific, United States), following the manufacturer's instructions. The obtained cDNA was consequently used for quantitative real-time PCR using QuantStudio 3 (Thermo Fisher Scientific, United States), Maxima SYBR Green qPCR Master Mix (Thermo Fisher Scientific, United States), and the primers reported in **Table 3.2**. After evaluating the stability of each reference gene (*secA, ppc, prs,* and *16s*) under the different experimental conditions, the expression levels of the target genes (*kivD, adhA, aroG^{fbr}, pheA^{fbr}, aroK*) were calculated using the Pfaffl method (Mannino *et al.*, 2021). Primers for both target and reference genes listed in **Table 3.2** were designed with Primer3 software (Untergasser *et al.*, 2012).

***Figure 3.1. Composition of genetic vectors for heterologous 2-phenylethanol synthesis in S. elongatus PCC 7942 genome**. **A)** p120 vector contains: NSI (blue), homologous regions for chromosomal integration into the Neutral Site I; $lacI^q$ (purple), LacI repressor gene; kivD (violet), gene encoding phenylpyruvate decarboxylase; adhA (orange), gene for alcohol dehydrogenase A; $aroG^{fbr}$ (light blue), feedback-inhibition resistant DAHP synthase; $pheA^{fbr}$ (green), feedback-inhibition-resistant chorismate mutase/prephenate dehydratase; $Spec^R$ (pink), spectinomycin-resistance cassette. **B)** aroK overexpression vector: NSII (dark green), homologous regions for chromosomal integration into the Neutral Site II; aroK (dark pink), endogenous gene for shikimate kinase expression in S. elongatus (locus tag, SynPCC7942_0894); Kan^R (yellow), kanamycin-resistance cassette; P_{trc} (black arrow), IPTG-inducible promoter.*



3.2.4. 2-PE and L-Phe HPLC quantification

2-PE production by mutant strains was assessed by ultra-high-performance liquid chromatography (UHPLC UltiMate 3000, Thermo Fisher, Waltham, Massachusetts, USA) equipped with a Hypersil GOLD™ C18 reversed phase column (250 × 4.6 mm, 5 µm; Thermo Fisher Scientific) and UV detector set at 205 nm. As mobile phase, acetonitrile and H_2O (50:50) was used with 1 mL/min flow rate, 40 °C. L-phenylalanine was quantified through the Hypersil GOLD™ Amino column (120 x 4.6 mm, 5 µm; Thermo Fisher Scientific) at 210 nm. 9 mM sulfuric acid was pumped as mobile phase at 0.8 mL/min, column oven was set at 50 °C. For sample preparation, 1 mL of bacterial culture was collected and centrifuged at 12,000 *g* for 10 minutes, and 20 µL of the supernatant was injected for HPLC analysis.

3.2.5. Whole-cell protein extraction

Ten mL cell cultures were collected before the gene expression induction and five days since IPTG supplementation. The cell culture was centrifuged at 4,000 g for 10 min

and the cell pellet was twice washed with 0.9% (w/v) NaCl. Then, the cell pellet was depigmented from the chlorophyll a by washing it twice in 10 mL cold acetone and centrifuged at 4,000 *g* for 10 min. Next, the cell pellet was lyzed in 2 mM Tris-HCl, 0.4% (w/v) SDS, pH 7.6 and 100 mM DTT, incubated 30 min at 95°C and centrifuged at 15,000 g for 10 min. From the supernatant, whole-cell proteins were purified by following methanol-chloroform method (Wessel and Flügge, 1984). The protein pellet was resuspended in 10 mM Tris-HCl pH = 7 and 1% (w/v) SDS and the protein content was assessed by BCA method with Quantum Protein kit (Euroclone, Milan, Italy), following the manufacturer's instructions. Proteins were resolved on 12% SDS-PAGE gel, by running at 80 V for 3 h.

3.2.6. ***Glycogen content determination***

One mL of cell culture was collected before induction of the gene expression and at 1 d, 3 d and 6 d since supplementation of IPTG. The cell culture was centrifuged at 13,000 *g* for 10 min and processed as previously reported in (Osanai *et al.*, 2011) with some modifications. Briefly, the cell pellet was lysed in 100 µL of 3.5% sulfuric acid and boiled for 40 min. Then, a centrifugation of 13,000 *g* for 2 min was followed by addition of 350 µL of 10% (w/v) trichloroacetic acid and incubated for 10 min at room temperature. The quantification was conducted from 150 µL of supernatant, by adding 750 µL of 6% (v/v) 2-aminotoluene (diluted in glacial acetic acid) and boiled for 10 min. The absorbance was measured at 635 nm. The standard curve was performed with D-glucose (0-3 mg mL^{-1}).

3.2.7. ***Bioinformatics search of class-specific enzymes***

An alignment-based approach was employed to mine the *S. elongatus* PCC 7942 genome for genes encoding phenylalanine transaminases and enzymes able to catalyze the conversion of L-amino acids into α-keto-acids. The Enzyme Commission (EC) numbers EC 2.6.1.57, EC 1.4.99.B3, EC 1.4.1.5, and EC 1.4.3.2 were used to gather the amino acid sequences of, respectively, known aromatic amino acid transaminases, L-amino acid deaminases, L-amino acid dehydrogenases and L-amino acid oxidases from the UniProtKB database. Among the UniProtKB entries fulfilling the assignment to the EC numbers of interest, only reviewed records were selected with information extracted from literature and curator-evaluated computational analysis. Exception only for L-amino acid deaminases since no reviewed record was available in UniprotKB.

For each functional category, an alignment of the protein sequences of known functional annotation was made against the protein sequences of *Synechococcus elongatus* PCC 7942 (taxid:1140) by using the blastp tool (default parameters). Alignment hits were ordered based on E-value and sequence percent identity. The unique hits in *Synechococcus elongatus* with at least an alignment with E-value < 0.001 were shortlisted. For each of the retained hits, the details of the top-scoring alignment were reported.

3.2.8. ***Metabolic effects of phenylalanine addition by metabolic model simulation***

We used the GEnome-scale Metabolic model (GEM) iJB785 (Broddrick *et al.*, 2016) publicly available for *Synechococcus elongatus* PCC 7942 in the BIGG database (King *et al.*, 2016). The *S. elongatus* GEM iJB785 contains 768 metabolites, 849 reactions and 785 genes. The GEM was constrained with CO_2 uptake rate and photon uptake rates derived from (Broddrick *et al.*, 2019). The metabolic reconstruction was enriched with the reactions catalyzed by the heterologously expressed protein products of *kivD* and *adhA* genes as well as the exchange reaction corresponding to the 2-phenylethanol target product. To simulate the effects of medium supplementation with phenylalanine on the metabolic network, the corresponding exchange reaction was added to the metabolic reconstruction and Flux Variability Analysis (FVA) was carried out by maximizing biomass and comparing model predictions in the cases of zero or non-zero flux through the phenylalanine exchange reaction. By effect of FVA, each reaction was assigned a range of allowed fluxes in the two conditions. To gauge the effect of phenylalanine doping on the metabolic fluxes, for each reaction, the fraction (in percentage value) of allowed fluxes (not shared between the two conditions) was computed.

Gene	Definition	Typology	Primer Sequence (5'-3')		Size
			Forward	Reverse	
secA	preprotein translocase, SecA subunit	Reference Gene	ACGACGGTCAGATTGCCGAGAT	GCGACATTCCCTGCTGGATTAG	204
ppc	phosphoenolpyruvate carboxylase	Reference Gene	CCCTTGCCAGGACCAGATGA	CGTCGGGTGAGCGGTGAAAA	146
prs	ribose-phosphate pyrophosphokinase	Reference Gene	TCTTGCCCTACTACGGTTACGC	TCGCTCCAGCCTGAGTGATTAG	247
16s	16s ribosomal RNA	Reference Gene	GCAAGCCTGACGGAGCAAC	CGGACGCTTTACGCCCAAT	160
kivD	phenylpyruvate decarboxylase	Target Gene	TCATCATCAACAACGACGGC	GCTGGCTAAAGAAGACGCTC	240
adhA	alcohol dehydrogenase A	Target Gene	ACTTTGTTGGGGTGGTGTTG	ACTATGGCTGAGCACTACCC	239
aroG^{fbr}	DAHP synthase, feedback-inhibition-resistant	Target Gene	CTGACGTTTGCCAGCAGATT	GCATTCGCCAGTTGACGTAA	184
pheA^{fbr}	chorismate mutase/prephenate dehydratase, feedback-inhibition-resistant	Target Gene	GCGACAAAACTTCACCCGAT	CCAGACGGGGCATAATCAGA	167
aroK	shikimate kinase	Target Gene	GCAAATCGAAACGCAGGTCT	CCGGAGCCTCAGTTTGTAGA	203

Table 3.2. Genes employed for qRT-PCR analysis. *For each gene, the name, acronym, and nucleotide sequences for both Forward (F) and Reverse (R) primers are reported in the table.*

3.3. Results

3.3.1. Screening of several metabolite doping conditions to improve 2-phenylethanol production by p120 engineered S. elongatus PCC 7942

The non-native 2-PE synthesis pathway exploits some intermediates of the shikimate pathway, which is the biosynthetic route dedicated to the aromatics synthesis, such as aromatic amino acids and some vitamins (Braga and Faria, 2020). To understand whether the 2-PE synthetic pathway competes with other natural ones, we investigated the influence of some physiological aromatic molecules on the p120 *S. elongatus* PCC 7942 mutant strain metabolism. The p120 recombinant strain overexpressed four genes involved in 2-PE biosynthesis: *kivD*, *adhA*, *aroG*^{fbr} and *pheA*^{fbr} (**Figure 3.1A**). Their relative enzymatic role in 2-PE production was contextualized in **Figure 3.2**.

First of all, the effect of IPTG addition was assessed for both wild type and p120 engineered strains. The wild type metabolism seemed not to be affected by the IPTG addition, indeed, no significant difference was noted from the relative growth curves (**Supplementary Figure 3.1**). By contrast, the addition of IPTG, which induces the gene expression of the heterologous pathway, to the p120 strongly influenced the mutant growth, causing a decrement in the growth rate with respect of the non-induced p120 strain (**Supplementary Figure 3.1**). Then, the three aromatic amino acids L-Phe, L-Tyr and L-Trp, and two aromatic-derived vitamins (folic acid and cyanocobalamin) were supplemented to the growth medium, either individually or in combination, at different concentrations. Each test was conducted in biological triplicate on the p120 mutant in shake flasks. Control condition represented the p120 recombinant strain grown with no L-Phe and all the results are shown in the **Figure 3.3 and Supplementary Figure 3.2 and 3.3**. The best performing conditions were the L-Phe supplementation out of all tested compounds. Moreover, when assessing different L-Phe concentrations, we found that 0.3 g L^{-1} L-Phe almost doubled 2-PE yield (222 ± 42 2-PE mg normalized by g of dry cell weight capable of producing 2-PE, mg gDW^{-1}), in comparison with the yield of the reference condition (124 ± 15 mg/gDW, **Figure 3.3A**). However, the 2-PE final titer was not significantly increased (82 ± 11 mg L^{-1} at 12 days after the gene expression induction). Furthermore, L-Phe supplementation did not affect the bacterial growth, which appeared suffer the most from the gene expression induction, if compared with the growth kinetics of the wild type strain (**Figure 3.3B**). Further increasing L-Phe concentration in the medium beyond 0.3 g/L was ineffective, instead inhibited cell growth and led to chlorosis. The tested aromatic

vitamins, i.e. folic acid and cyanocobalamin, did not affect neither bacterial growth nor 2-PE production, when supplemented into the medium singularly or in combination with L-Phe (**Supplementary Figure 3.2**). Also, L-Tyr and L-Trp showed no influence on the physiology of the p120 strain, when used individually as metabolite supplementation (data not shown). However, in combination with L-Phe, L-Tyr showed interference by negatively affecting 2-PE yield (**Supplementary Figure 3.3B, F**) and slightly increasing the growth rate (**Supplementary Figure 3.3A**). L-Trp only influenced the 2-PE production kinetics (**Supplementary Figure 3.3G, H**), by extending the production time, but had no significant effect on the 2-PE maximum yield (**Supplementary Figure 3.3D**). Due to these aromatics screening results, we chose to further explore the L-Phe supplementation as the only metabolite doping strategy in the present work. A deeper analysis about the fate of phenylalanine in *S. elongatus* mutant strains was performed and will be discussed in the next section.

Figure 3.2. Overexpressed genes and relative protein products for 2-PE synthesis in S. elongatus PCC 7942 mutant strains p120 and 2PE_aroK*. The reactions promoted by the p120 (green boxes) and 2PE_aroK (green and red boxes) mutant strains.*

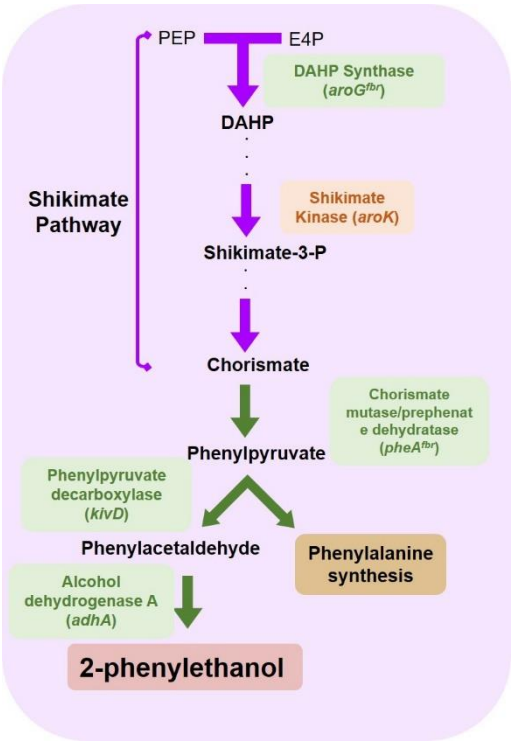
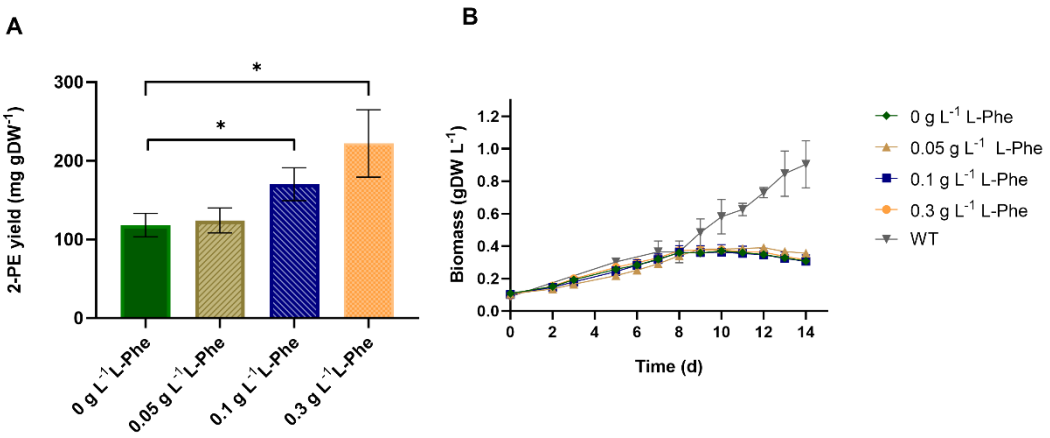


Figure 3.3. Effect of L-phenylalanine doping at three different concentrations on the p120 mutant strain. A) *The bar plot shows the 2-PE yield expressed as 2-PE mg produced normalized per g of dry cell weight (mg gDW^{-1}). The control condition is represented by the p120 mutant strain grown with no L-Phe. Asterisks indicate statistical significance for both 0.1 g L^{-1} and 0.3 g L^{-1} L-Phe doping versus control condition (unpaired two-tailed t-test, p-value < 0.05) and error bars report the standard deviation.* ***B)*** *p120 mutant grown with L-Phe (0.05-0.3 g L^{-1}). As control conditions, p120 mutant (dark green) and wild type (grey) strains were both grown with no L-Phe. The L-Phe was added and gene expression was induced at the 7th day (about OD_{730} = 1, 0.26 gDW L^{-1}). The bars show the standard deviation. Each test was conducted as three biological replicates.*



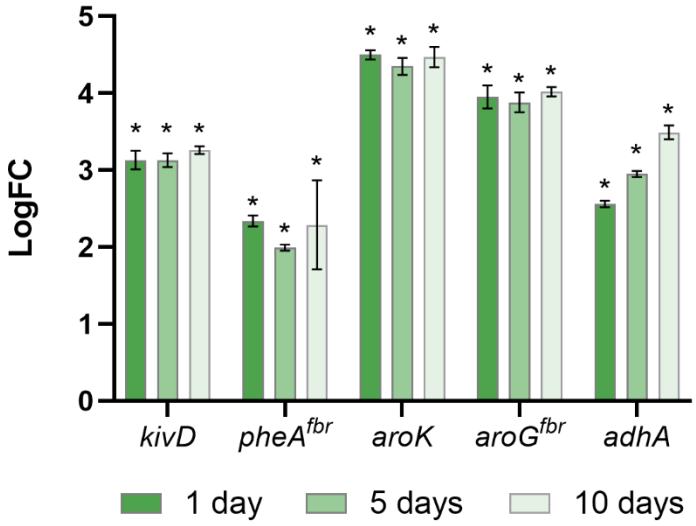
3.3.2. Improving 2-phenylethanol production through metabolic engineering of the Shikimate Pathway

3.3.2.1. Creation of 2-PE producing S. elongatus mutant overexpressing the endogenous shikimate kinase gene (2PE_aroK)

To boost the carbon flow into SKP and to overcome some bottlenecks of this pathway, we co-expressed *aroG^{fbr}*, *pheA^{fbr}* (from the p120 mutant strain) and the native Shikimate Kinase (as double gene copy of *SynPCC7942_0894*, aka *aroK*, into the Neutral Site II, under the control of IPTG-inducible promoter, **Figure 3.1B**), together with *kivD* and *adhA* to effectively produce 2-PE (**Figure 3.2**). Hence, the obtained mutant strain contains both p120 and *aroK* inserts, so, hereinafter, it is called 2PE_*aroK*. The successful obtainment of the mutant strain was first demonstrated by PCR screening (**Supplementary Figure 3.4 A, C**) and subsequently the accumulation of the protein corresponding to shikimate kinase following induction with IPTG was

analyzed by SDS-PAGE analysis, where the band corresponding to the gene product of approximately 21 KDa was detected (**Supplementary Figure 3.4B**). Furthermore, an analysis about the expression related to all the five genes involved in 2-PE biosynthesis (*kivD*, *adhA*, *aroG*, *pheA* and *aroK)* was performed. The expression of all of the involved genes was confirmed by qRT-PCR at one, five and ten days since the gene expression induction, keeping a stable expression level (**Figure 3.4**). Expression analysis on target genes was performed by first assessing the stability of reference genes under the different experimental conditions. Specifically, the expression of *secA, ppc, prs*, and *16s* genes was evaluated across both wild type strain and 2PE_*aroK* engineered strain after one, five and ten days since gene expression induction (**Supplementary Figure 3.5A**). All the analyzed candidate reference genes were quite stable under the different experimental conditions. Among them, *secA* and *16s* genes had percentage coefficients of variation much less than 1%. Since *16s* gene encodes the most abundant transcripts in cyanobacteria, its expression had the lowest median Ct values (15.30 ± 0.08) compared with the other three candidates during qPCR amplification, despite the same amounts of total RNA and cDNA were used for qRT-PCR analysis On the other hand, the other candidates recorded very similar median Ct *(secA*: 19.00 ± 0.10; *ppc:* 19.56 ± 0.61; *prs:* 19.11 ± 0.52) (**Supplementary Figure 3.5 B**). Consequently, also based on the percentage coefficient of variation, *secA* was chosen as the reference gene. This result is in agreement with the study of Xiao Luo (2019) (Luo *et al.*, 2019). By performing the statistical analysis with geNorm, NormFinder and BestKeeper softwares, *secA* and *prs* were found to be the most stable under all analyzed conditions, while *16s* could not be selected as a reference gene due to a significant imbalance in abundance between rRNA and mRNA molecules (Luo *et al.*, 2019). Concerning target genes, the expression of 2PE_*aroK* engineered strain was assessed against the wild type, which, except for *aroK*, does not naturally express those heterologous genes (*kivD, adhA, pheA*^{fbr} and *aroG*^{fbr}). Although a time-dependent change of target gene expression was not observed for most investigated genes, all the studied target genes were strongly up-regulated in comparison with wild type condition (Figure 4). The double gene copy expression of *aroK* contributed to almost increase the *aroK* expression by 4.5-fold, over all the time tested, followed by *aroG*^{fbr} (4-fold) and *kivD* (3.2-fold) (**Figure 3.4**). On the other hand, *pheA*^{fbr} and *adhA* showed different profiles. Interestingly, *adhA* gene boosted its expression over the time, reaching a 3.5-fold increment at ten days since the gene expression induction (**Figure 3.4**). *pheA*^{fbr} resulted to be the less expressed gene, in all the tested conditions.

***Figure 3.4. Temporal gene expression analysis**. Gene expression of kivD, adhA, pheA^{fbr}, aroG^{fbr}, aroK in 2PE_aroK cells after one, five and ten days since gene expression induction. Data are expressed as log(2^-ΔΔCt) ± standard deviation. The symbol "*" indicates significant ($p < 0.05$) differences in gene expression of kivD, adhA, pheA^{fbr}, aroG^{fbr}, and aroK in 2PE_aroK cells after one, five or ten days of induction respect to wild type condition, as calculated by student t-test.*



3.3.2.2. ***Characterization of 2-PE producing S. elongatus mutant overexpressing the endogenous shikimate kinase gene (2PE_aroK)***

2PE_*aroK* mutant strain was analyzed for its 2-PE production ability without L-Phe, as metabolite doping in growth medium. The abovementioned mutant strain reached a maximum production of 94.05 ± 12.6 mg L^{-1} after eight days since gene expression induction (**Figure 3.5B**). **Figure 3.5C, D** shows the characterization of 2PE_*aroK* mutant with supplementation of 0.3 g/L L-Phe, which has been previously shown to be the best metabolic doping condition, among those assayed. Thus, *aroK* overexpression combined with L-Phe doping strongly influenced the 2-PE production kinetics (**Figure 3.5D**). Specifically, the 2-PE production kinetics of 2PE_*aroK* strongly diverged from that of non-L-Phe-doped engineered strain and p120 mutant strain exposed to L-Phe doping, accordingly with our study (**Figure 3.5**), since four and five days after gene expression induction, respectively. Indeed, 2PE_*aroK* mutant reached a maximum titer

of 285 ± 15 mg L^{-1} at the end of the experiment. However, 2PE_*aroK* reached the highest 2-PE yield at 15 days since induction, amounting to about 323 mg gDW^{-1} (**Figure 3.6A**) and corresponding to 263 ± 3 mg L^{-1}. Consequently, the daily 2-PE productivity was influenced (**Figure 3.6B**). Indeed, the 2PE_*aroK* produced on average 19.3 ± 4.86 mg/L per day, until thirteen days since gene expression induction and then gradually decreased. Meanwhile, the reference p120 strain showed a significant 2-PE productivity until five days since induction (**Figure 3.6B**), reaching a maximum 2-PE yield of 133.65 ± 14.53 mg gDW^{-1} (**Figure 3.6A**). Also, the growth kinetics resulted to be affected, with a reduction in the specific growth rate (**μ**), equal to 0.09 d^{-1} and 0.12 d^{-1} for 2PE_*aroK* and p120 mutant strains, respectively. **Table 3.3** precisely reports μ and the relative doubling time (D_t) about 2PE_*aroK* and p120, with respect of our study. Additionally, the toxicity of 2-PE on *S. elongatus* PCC 7942 was assessed from 0.1 to 1 g L^{-1}, supplemented to the bacteria culture at OD_{730} = 1, mimicking the usual 2-PE production condition, to which the recombinant strain 2PE_*aroK* was subjected. However, no significant reduction in bacterial growth kinetics was observed at the 2-PE concentration obtained in the present investigation (about 0.3 g L^{-1}). However, higher 2-PE concentrations caused the bacterial growth reduced but not totally inhibited (**Supplementary Figure 3.6**).

Furthermore, it is known that shikimate kinase uses ATP as co-substrate. To understand if the ATP pool necessary to sustain SK overexpression could come from the glycogen catabolism, beside photosynthesis, we quantified glycogen content from the biomass before and after one, three and six days gene expression induction. Glycogen quantification from 2PE_*aroK* biomass did not show any consumption after the gene expression induction, while the glycogen content steadily increased as the biomass grew (**Supplementary Figure 3.7**).

Recombinant Strain	*Specific growth rate (d^{-1})*	*SD*	*Doubling time (d)*	*SD*
p120	0.125	0.005	5.6	0.21
2PE_aroK	0.092	0.004	7.6	0.34

Table 3.3 Specific Growth Rate (μ) and Doubling Time (Dt) of the p120 and 2PE_aroK strains. *The μ was calculated in exponential growth phase, after gene expression induction and L-phenylalanine supplementation and it is expressed as day^{-1}. SD, standard deviation.*

Figure 3.5. Characterization of 2PE_aroK engineered strain with or without L-Phe doping. *Comparison between 2-PE production (**B, D**) and biomass formation (**A, C**) over the time since gene expression induction on 2PE_aroK under no L-Phe doping (top) or when exposed to L-Phe doping (bottom). As reference, the p120 strain was subjected to the same conditions. L-Phe was added, and the gene expression was induced at around OD_{730} = 1 (0.26 gDW L^{-1}). Bars represent standard deviation. All tests were carried out in triplicate.*

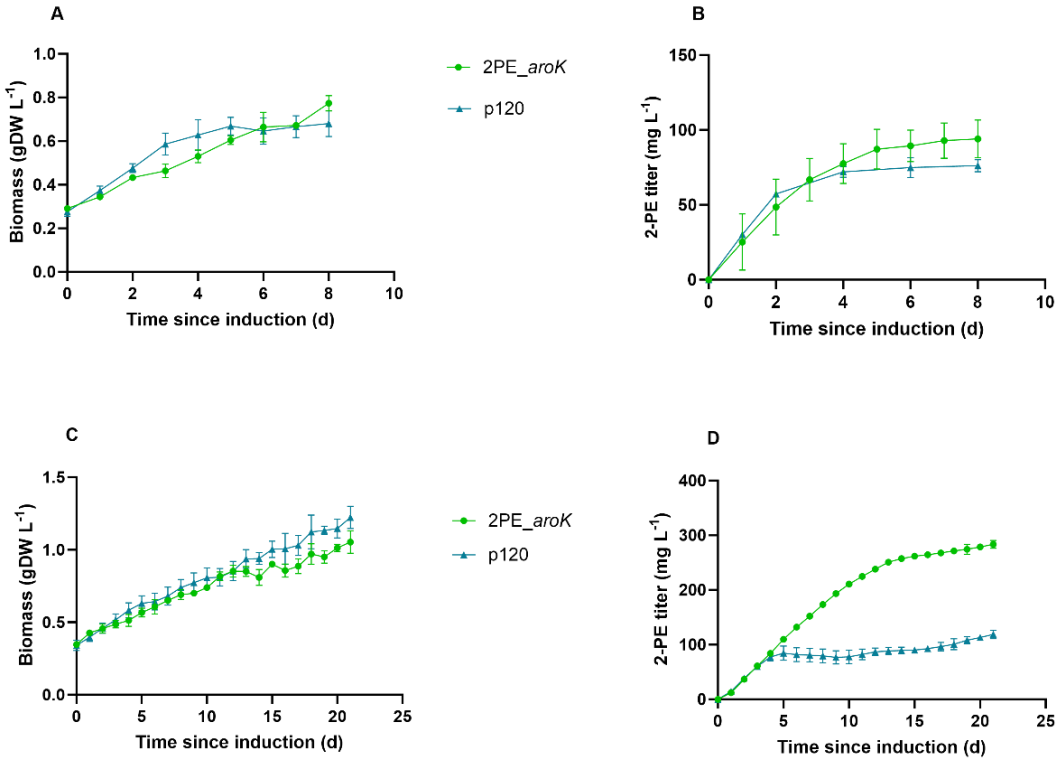
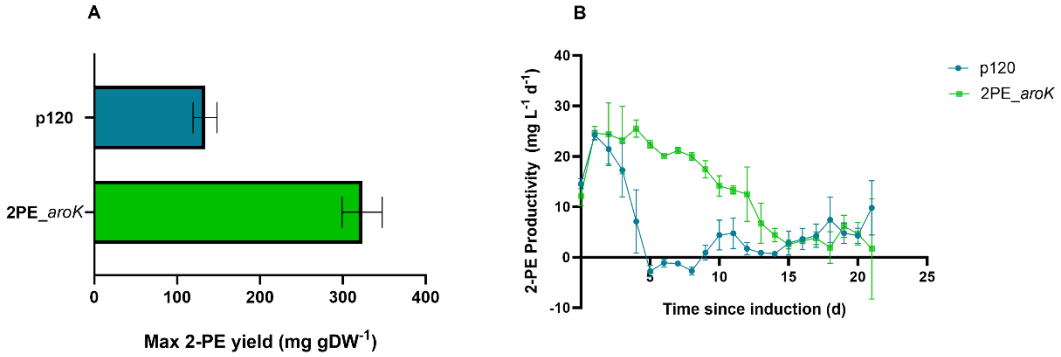


***Figure 3.6. 2-phenylethanol productivity in L-Phe-doped condition**. A) Maximum 2-PE mg normalized by the biomass produced during the experiment for both 2PE_aroK (green) and p120 (blue) strains. **B**) 2-PE daily produced, expressed as mg per liter per day, by 2PE_aroK (green) and p120 (blue) engineered strains over the time. Bars represent standard deviation. All tests were conducted by means of three biological replicates.*

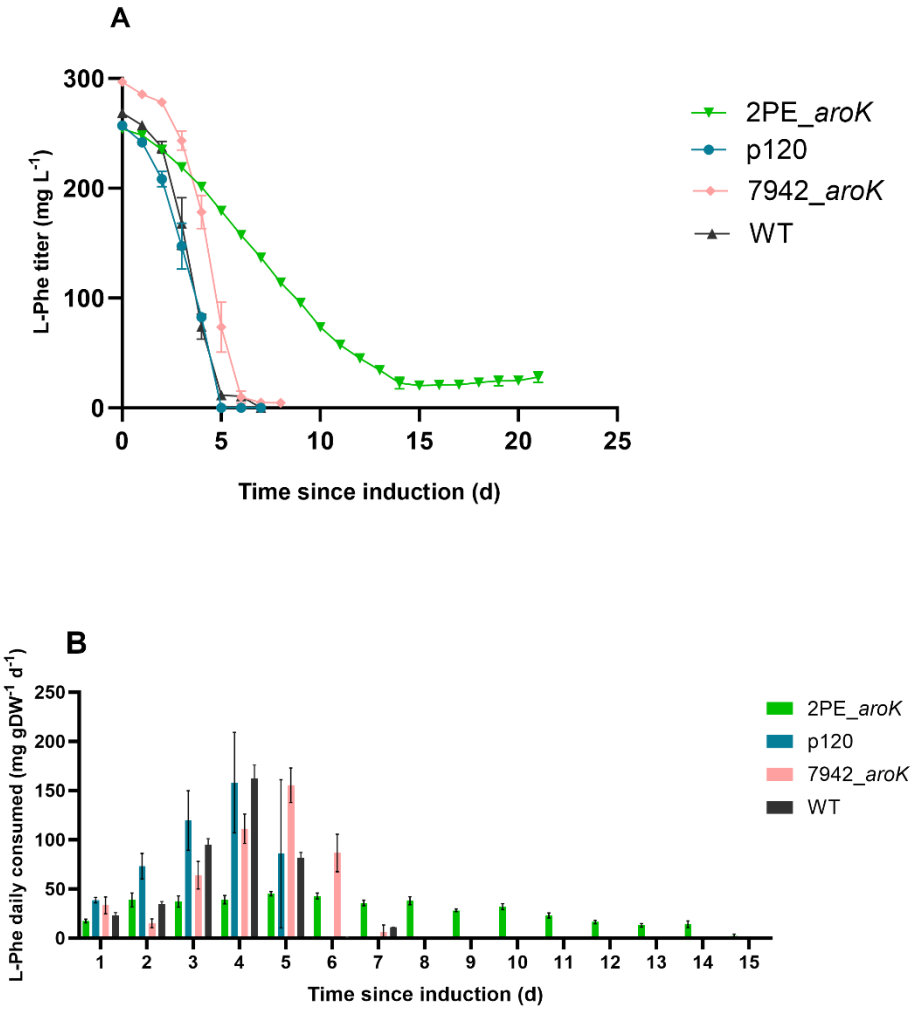


3.3.3. L-phenylalanine doping effect on mutant physiology

3.3.3.1. L-phenylalanine consumption analysis

The daily consumption of the supplemented L-phenylalanine in the growth medium was investigated for 2PE_*aroK* and p120 mutant strains, *S. elongatus* overexpressing only *aroK* gene (i.e. 7942_*aroK*) and the wild type *S. elongatus* as well (**Figure 3.7A, B**). The 2PE_*aroK* mutant gradually consumed L-Phe up to 14 days since induction, with a steady average consumption rate of 30 mg L-Phe gDW^{-1} d^{-1} (**Figure 3.7B**). In contrast, the p120 reference mutant and 7942_*aroK* consumed all available L-Phe within the first five and six days since induction, respectively. However, a basal L-Phe uptake by the wild type *S. elongatus* PCC 7942 exists. Although *S. elongatus* PCC 7942 can produce L-Phe by itself, it consumed all the available L-Phe in seven days (**Figure 3.7A, B**) and drastically increased its consumption three days after the L-Phe addition into the growth medium, which is a comparable trend detected with the p120 and 7942_*aroK* mutants.

***Figure 3.7. L-phenylalanine consumption analysis**. **A)** L-phenylalanine titer detected in the supernatant for 2PE_aroK (green), p120 (blue) and 7942_aroK (pink) mutant strains and the relative wild type S. elongatus PCC 7942 (grey). **B)** The L-Phe daily consumed was normalized by the biomass produced. The results were expressed as mg of L-Phe consumed by g dry cell weight every day after the gene expression induction. Bars represent standard deviation. All tests were carried out in triplicate.*

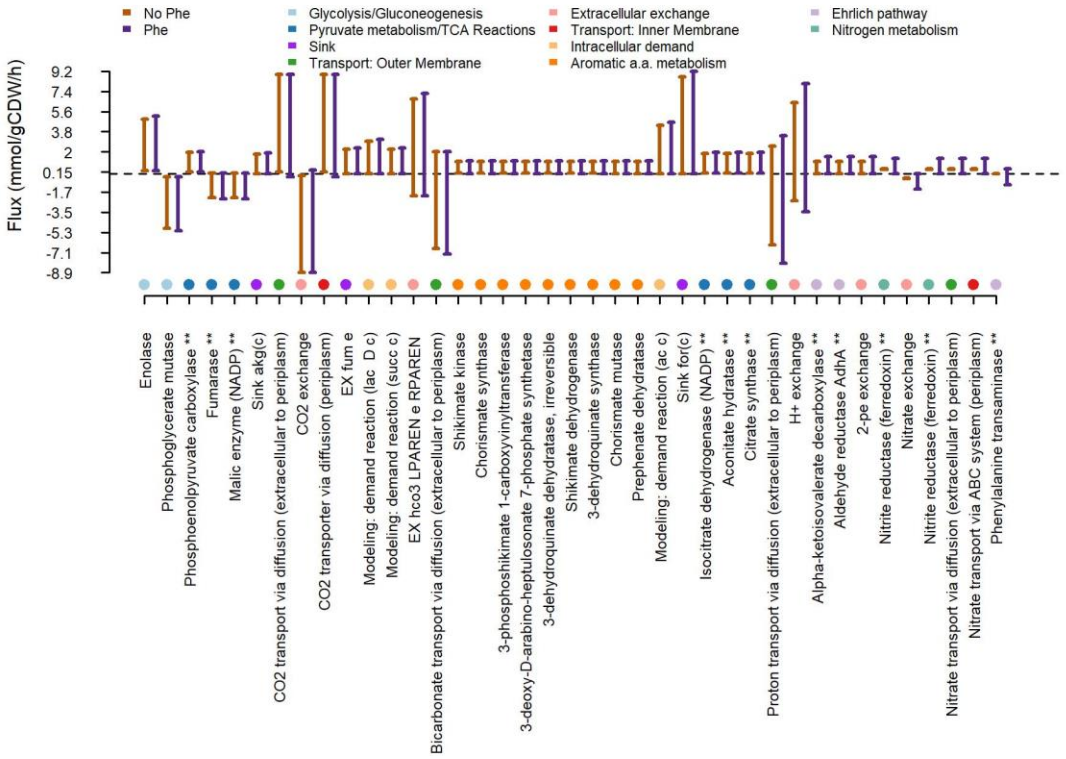


3.3.3.2. Bioinformatics analysis about L-phenylalanine consumption in 2-PE producing S. elongatus PCC 7942

The natural use of L-Phe for 2-PE biosynthesis has been widely investigated mainly in plants and yeast, while a few bacteria are known to naturally synthetize 2-PE (H. Zhang *et al.*, 2014; C. Liu, Zhang, *et al.*, 2018; J. Liu, Jiang, Bai, *et al.*, 2018). In yeast the 2-PE production is based on the Ehrlich pathway (Q. Liu *et al.*, 2019; Gu *et al.*, 2020; Dai *et al.*, 2021). According to this pathway, L-Phe is transaminated to phenylpyruvate, where α-ketoglutarate is the acceptor of the amino group and converted into glutamate. Subsequently, phenylpyruvate is transformed into 2-PE, through sequential decarboxylation and reduction reactions (Hazelwood *et al.*, 2008). Here, through bioinformatics analysis, we investigated the fate of the L-Phe into the mutant *S. elongatus* p120 and we verified the completeness of the enzyme set carrying out the Ehrlich pathway. Since, the mutant producing 2-PE heterologously overexpresses both the phenylpyruvate decarboxylase (*kivD* gene) and the alcohol dehydrogenase A (*adhA* gene), it could be capable of putatively processing the last two steps of the Ehrlich pathway. Thus, we searched in UniProtKB database the protein sequences of *S. elongatus* PCC 7942 for putative phenylalanine transaminases encoding genes, which could transaminate L-Phe in phenylpyruvate (Gu *et al.*, 2020). We identified several hypothetical phenylalanine transaminase proteins based on amino acid sequence similarity with proteins known to carry out aromatic aminotransferase activity either in *Thermococcus litorali* (Andreotti *et al.*, 1994) or in *Saccharomyces cerevisiae* (Iraqui *et al.*, 1998), as reported in **Supplementary Table 3.1**. Furthermore, we carried out a genome-scale metabolic Flux Variability Analysis (FVA) on the GEnome-scale Metabolic model (GEM) iJB785 (Broddrick *et al.*, 2016, 2019), customized to account for the heterologous expression of the *kivD* and *adhA* protein products in *S. elongatus*. We could confirm that the addition of phenylalanine led to increased flux through the reactions involved in the putative Ehrlich pathway, as shown in **Supplementary Figure 3.8**. Besides, additional reactions mainly related to nitrogen metabolism, aromatic amino acid biosynthesis and to the tricarboxylic acid (TCA) cycle were affected by phenylalanine doping (**Figure 3.8**, **Supplementary Table 3.2**). Alternatively, some bacteria, such as *Proteus* sp., can produce 2-PE by expressing an oxidative deaminase (J. Liu, Jiang, Bai, *et al.*, 2018), which converts L-Phe in phenylpyruvate. We then verified the presence of enzymes converting amino acids into α-keto-acids by sequence alignment against proteins assigned to relevant functional categories, namely L-amino acid deaminases, L-amino acid oxidases, and L-amino

acid dehydrogenases (Nshimiyimana, Liu and Du, 2019). We could not detect any statistically significant hit of L-amino acid deaminase enzymes in *S. elongatus* PCC 7942, whereas we could detect several candidates for L-amino acid dehydrogenases and L-amino acid oxidases (**Supplementary Table 3.3**). In particular, the FAD-dependent oxidoreductase Synpcc7942_0369 was detected by sequence homology with the known L-amino acid dehydrogenase slr0782 in *Synechocystis* sp. PCC 6803 (Schriek *et al.*, 2009). As to L-amino acid oxidases, our alignment-based search highlighted the FAD-dependent oxidoreductases Synpcc7942_0946 and Synpcc7942_0369, as previously recorded in the literature (Gau *et al.*, 2007).

Figure 3.8. Effects of medium supplementation with L-phenylalanine on the metabolic network of the S. elongatus PCC 7942 mutant producing 2-phenylethanol*. Flux variability analysis (FVA) was carried out in the absence/presence of Phe in the medium. Each reaction was assigned a range of allowed fluxes in the two conditions. For each reaction, the fraction (in percentage value) of allowed fluxes, which do not overlap between the two conditions, was computed. Shown are the individual reactions whose flux ranges in the presence/absence of phenylalanine differ by at least 5%. Reactions on the horizontal axis marked by '*' are mentioned in the main text.*



3.4. Discussion

Engineering cyanobacteria into cyano-factories for producing chemicals from solar energy, CO_2 and water is an appealing chassis to address either environment issues or economical and sustainable bioproduction platforms. Furthermore, cyanobacteria are notorious for their genetic malleability and today many powerful genetic tools are available (Santos-Merino, Singh and Ducat, 2019; Sengupta *et al.*, 2019; Wang, Gao and Yang, 2020; Zhou *et al.*, 2022). Indeed, cyanobacteria have been widely metabolically engineered to produce a huge range of valuable molecules (Zhou and Li, 2010; Lai and Lan, 2015; Santos-Merino, Singh and Ducat, 2019). However, in engineered strains often the expression of heterologous pathways can compete with the native ones for precursors, intermediates, reducing agents and energy charge, by altering the natural metabolic flux. As a common consequence, the metabolic burden for the heterologous expression leads to imbalance the cellular activities due to the redirection of cellular resources to biomass formation and growth, as well as target products synthesis (Su *et al.*, 2020; Kulagina *et al.*, 2021; Kastberg *et al.*, 2022). Here, to deeper investigate the impact of 2-phenylethanol heterologous pathway expression on *S. elongatus* p120 mutant strain (already published elsewhere (Ni *et al.*, 2018)), we screened the effect of several native aromatic molecules (three AAAs, folic acid and cyanocobalamin) on mutant physiology related to aromatics biosynthesis (**Figure 3.3** and **Supplementary Figure 3.2 and 3.3**), by assessing bacterial growth and 2-PE production. Indeed, the 2-PE synthetic pathway steals precursors and intermediates from the shikimate pathway, the common route for aromatics biosynthesis, and AAAs synthesis. Unsurprisingly, the major influence was recorded for the L-phenylalanine supplementation, at 0.3 g L^{-1} (**Figure 3.3**). Thus, we almost doubled 2-PE yield, up to 222 mg gDW^{-1}, when we supplemented L-Phe to the induced cyanobacteria for the heterologous expression of the 2-PE synthetic pathway, but any particular increase in 2-PE concentration was recorded. The Phe addition is a consolidated strategy adopted to push 2-PE production by yeast, where the Ehrlich pathway is exploited (Q. Liu *et al.*, 2019; Gu *et al.*, 2020; Dai *et al.*, 2021). The Ehrlich pathway is composed of three enzymatic steps, where L-Phe is firstly transaminated, in the presence of α-ketoglutarate, as amino group acceptor, to produce phenylpyruvate. Next, phenylpyruvate is decarboxylated in phenylacetaldehyde, then, is reduced in 2-PE, by a dehydrogenase (Hazelwood *et al.*, 2008). In cyanobacteria, the ability of 2-PE biosynthesis has not been reported, as well as, the existence of the Ehrlich pathway.

Nevertheless, the p120 mutant heterologously expresses a decarboxylase (*kivD* gene) and an alcohol dehydrogenase (*adhA* gene) (**Figure 3.4**), which could be responsible for the 2-PE production via non-shikimate-pathway-based route. It still has to be understood if *S. elongatus* PCC 7942 can express itself a specific enzyme capable of processing L-Phe in phenylpyruvate, i.e. the first reaction in the Ehrlich pathway. However, through bioinformatic analysis, we identified several putative phenylalanine transaminases, which requires α-ketoglutarate as co-substrate, in a 1:1 ratio with L-Phe. Interestingly, by genome-scale metabolic Flux Variability Analysis (FVA), we found several reactions affected by L-Phe addition (**Figure 3.8**, **Supplementary Table 3.2**), including the Tricarboxylic acid Cycle (TCA). Among the several steps of this pathway, the reaction mediated by the isocitrate dehydrogenase, which catalyzes the production of α-ketoglutarate, is influenced by L-Phe doping. Accordingly, it could be possible that this increased flow through the TCA cycle effectively feeds the 2-PE production from L-Phe. Additionally, we pointed out an alternative pathway, previously highlighted in 2-PE producing bacteria (Hazelwood *et al.*, 2008), which is equally noteworthy. In particular, by *in silico* homology search of protein sequences, we could gather preliminary evidence of hypothetical oxidative deaminases that can convert L-Phe in phenylpyruvate. Here, we identified in the FAD-dependent oxidoreductases Synpcc7942_0946 and Synpcc7942_0369 (Gau *et al.*, 2007) two possible protein candidates to carry out L-amino acid oxidase activity. Noteworthy, the wild type strain of *S. elongatus* PCC 7942 showed itself a basal L-Phe uptake (**Figure 3.7**). In some cyanobacteria, a Phenylalanine ammonia lyase (PAL) activity has been detected (Moffitt *et al.*, 2007; Babaoğlu Aydaş, Ozturk and Aslım, 2013). PAL catalyzes the non-oxidative deamination of phenylalanine to trans-cinnamate, the main branch for phenylpropanoid metabolism. Although, in *S. elongatus* PCC 7942 a PAL activity has not been reported so far, it could be presumable a similar trend, where the supplemented L-Phe could be directed towards this secondary metabolism. However, our findings suggest an important, although not pivotal, role of Phe in *S. elongatus* PCC 7942 physiology and could help to formulate hypothesis about the fate into the aromatics metabolism in cyanobacteria, but further studies are needed.

Additionally, we looked at some possible carbon flux limiting steps for the shikimate pathway. Besides cyanobacteria, several metabolic engineering attempts have already been conducted to enhance the carbon flow into the SKP. Commonly, the main strategies include: i) the engineering of transport systems (mainly for carbohydrate-using microorganisms) (Báez-Viveros *et al.*, 2004; Ahn *et al.*, 2011; Gottlieb,

Albermann and Sprenger, 2014; Gu *et al.*, 2017), ii) the deletion of competing pathways (Báez-Viveros *et al.*, 2004; Xu *et al.*, 2017) or iii) optimization of the critical enzymes activity (Báez-Viveros *et al.*, 2004). One of the most consolidated approaches concerns the very first step of the SKP, i.e. the condensation of intermediates from glycolysis and pentosephosphate-pathway, phosphoenolpyruvate (PEP), and erythrose-4-phosphate (E4P), respectively. This reaction is catalyzed by 3-deoxy-D-arabino-heptulosonate 7-phosphate (DAHP) synthase. *E. coli* encodes three DAHP synthase isoenzymes, which are inhibited by phenylalanine, tyrosine or tryptophan, respectively. Several mutational analyses highlighted different genetic approaches to overcome this feedback inhibition (Kikuchi, Tsujimoto and Kurahashi, 1997; Jiang *et al.*, 2000; Jossek, Bongaerts and Sprenger, 2001; Liao *et al.*, 2001; Hu *et al.*, 2003; Chávez-Béjar *et al.*, 2012) in order to increase the precursors input towards the SKP. Along with this, in *E. coli* another carbon flow-controlling step is related to the enzyme chorismate mutase, which catalyzes the release of chorismate from the SKP, the main branch point for the synthesis of aromatics. Also, the chorismate mutase is affected by a feedback inhibition by Phe or Tyr and, accordingly, $tyrA^{fbr}$ and $pheA^{fbr}$ mutated proteins have been created (Turnbull and Morrison, 1990; Vincent *et al.*, 2002; Lütke-Eversloh and Stephanopoulos, 2005; Zhou *et al.*, 2010; Cao *et al.*, 2016). Nowadays, the co-overexpression of both feedback-inhibition resistant *E. coli* enzymes is common to gain aromatics production, mostly in *E. coli* and yeast (Báez-Viveros *et al.*, 2004; C. Zhang *et al.*, 2014; Rodriguez *et al.*, 2014, 2015; T. Wang *et al.*, 2019; Koma *et al.*, 2020), as well as in cyanobacteria (Ni *et al.*, 2018; Brey *et al.*, 2020; Deshpande, Vue and Morgan, 2020). Additionally, in the literature another reaction has been reported as high flux controlling step (Luttik *et al.*, 2008; Takai A, Nishi R, Joe Y, 2009; Darmawi *et al.*, 2012; Rodriguez *et al.*, 2015; Xu *et al.*, 2019), i.e. shikimate kinase-mediated reaction, the conversion of shikimate and ATP in shikimate-3-phosphate and ADP. For all the above reasons, we co-overexpressed $aroG^{fbr}$, $pheA^{fbr}$, from *E. coli*, and the native shikimate kinase (*SynPCC7942_0894*, *aroK*), to overcome the abovementioned bottlenecks of this pathway, together with *kivD* and *adhA* to synthesize 2-PE through *S. elongatus* PCC 7942 (**Figure 3.2**). The resulted 2PE_*aroK* mutant was able to express all the genes involved in 2-PE biosynthesis, keeping their expression stable (**Figure 3.4**). In particular, *aroK* resulted to be the most expressed gene, among the other ones, up to 4.5-fold higher than the wild type strain. The resulting mutant strain effectively increased 2-PE production in L-Phe doping condition (**Figure 3.5**). It is interesting to remind that SK overexpression in the absence of L-Phe supplementation

was not significantly effective on the 2-PE production kinetics (**Figure 3.5**). Under phenylalanine doping condition, with respect of our study (**Figure 3.5**) on p120 engineered strain (Ni *et al.*, 2018), the 2PE_*aroK* mutant rose (by 2.2-fold) 2-PE production up to 285 mg L^{-1}, keeping a steady daily productivity of 19 mg L^{-1} d^{-1} for the first two weeks (**Figure 3.6B**). Interestingly, the 2-PE productivity was higher within nine days since gene expression induction, although the genes expression resulted quite stable over the time (**Figure 3.4**). Probably, different mechanisms rule the 2-PE production, maybe at the proteins level or turn over events.

Moreover, the 2PE_*aroK* decreased its growth kinetics, by 1.4-fold. This detrimental effect on the growth kinetics could be more likely due to the metabolic focus on the target compound overproduction. Indeed, the toxicity assay carried out on *S. elongatus* PCC 7942 exposed to several 2-PE concentrations (0.1-1 g L^{-1}), confirmed that no negative effects are caused by 2-PE at the concentration produced by 2PE_*aroK* recombinant strain, equal to about 0.3 g/L (**Supplementary Figure 3.6**). An inherent link between SK overexpression and L-Phe supplementation was further supported by the different L-Phe consumption profile between p120, 7942_*aroK* and the wild type strains when compared to 2PE_*aroK* (**Figure 3.7**). Indeed, the 2-PE producing mutant overexpressing *aroK* gene reduced the bacterial L-Phe consumption rate, which remained steady for almost two weeks, and simultaneously improved the 2-PE production, compared to the p120 engineered strain.

Interestingly, shikimate kinase uses ATP as co-substrate and its functional overexpression in a biological system is not obvious, due to the fine energy and ATP homeostasis through the metabolic network. Besides the photosynthesis, another ATP source in cyanobacteria comes from the catabolism of glycogen, the major carbon storage compound in many cyanobacteria species. Nevertheless, our glycogen quantification from 2PE_*aroK* biomass did not show any consumption after the gene expression induction, where the glycogen content steadily increased as the biomass grew (**Supplementary Figure 3.7**), up to 12% of cell biomass, as previously reported (Hasunuma *et al.*, 2013; De Porcellinis, Frigaard and Sakuragi, 2017).

Additionally, the maximum theoretical yield for the 2-PE (C8) producible from Phe (C9) is roughly 0.89 mol/mol. Here, for 2PE_*aroK* mutant, the maximum yield would be higher than the theoretical one (≈ 150%), which further suggests that the 2-PE cannot be produced only from the Phe, but from photosynthesis as well. Moreover, the SK enzyme is placed upstream the putative pathway processing Phe into 2-PE, therefore it is reasonable to speculate that a combinatorial and synergistic effect of

multiple phenomena on the 2PE_*aroK* mutant aromatics metabolism could exist, whose relative interconnections are still unclear but worthy of further investigation. Nevertheless, our approach demonstrates how the complex microbial response to metabolic perturbations, could be fixed by setting up *ad-hoc* cultivation processes for any specific metabolic engineering applications.

3.5. Conclusions

In this study, a recombinant photosynthetic cell factory producing 2-phenylethanol was successfully improved. Overall, this investigation highlighted the potentiality of a combinatorial strategy, which can be able to overcome synergistically different metabolism-related issues, by combing metabolic engineering and process engineering. Hence, we firstly explored the metabolite doping strategy, by adopting a phenylalanine-supplemented BG11 medium. Here, we supplied the main C source (CO_2) and L-phenylalanine at different times during the bacterial phototrophic cultivation. As a result, we led to segregate growth and 2-PE production phases and increase the final 2-PE concentration and yield. Secondly, the implementation of the native shikimate kinase overexpressed, in addition to the 2-PE synthetic pathway, modified the cell kinetics by both increasing the 2-PE amount and reducing the phenylalanine consumption rate during the mutant strain growth. Finally, the L-Phe doping growth condition with this new mutant strain led to a maximum 2-PE titer of 285 mg L^{-1}, about 2.4-fold higher than previously reported in the literature (Ni *et al.*, 2018) and, to the best of our knowledge, the highest 2-PE production reported so far in photoautotrophic growth condition for photosynthetic microorganisms. Here, the overexpression of the native shikimate kinase firmly suggests a bottleneck in the SKP of cyanobacteria, indicating this enzyme as suitable target gene for many other aromatics and derived compounds production strategies.

From an application-oriented point of view, the impressive increment in 2-PE production and yield achieved in the present work could support the implementation of L-Phe-doped BG11 medium, also for a large-scale production. Although, single substrate feeding is often conventionally favored in biotechnological applications, it could lead to multiple metabolic constraints, mainly due to the fine coordination required to simultaneously balance global cell metabolism, growth and overproduction of target compounds (Babel, 2009; Liu, Santala and Stephanopoulos, 2020; Hartline *et*

al., 2021). On the other hand, several experimental efforts have already demonstrated that is possible overcome these limitations by adopting metabolite doping or co-substrate feeding, accordingly with particular metabolic engineering applications (Papazi *et al.*, 2012; Anfelt *et al.*, 2015; H. Liu *et al.*, 2019; J. O. Park *et al.*, 2019; Gu *et al.*, 2020; Ndayisenga *et al.*, 2021), in agreement with the present work. Additionally, thanks to the very poor nutritional requirements of cyanobacteria, the BG11 growth medium is still suitable for further supplementation, in the light of large-scale application. Furthermore, the adoption of phenylalanine-rich waste waters, such as dairy wastes, has the potential to further reduce the process costs, making this 2-PE production cyano-based system sustainable and feasible.

In conclusion, although this photosynthetic cyanobacterial factory is still at lab-scale, our study provides the basis to further optimize this biotechnological process for 2-PE production. Hence, by finely regulating the CO_2 and L-Phe supply and light intensity, it could be possible to simultaneously increase both the growth and biosynthetic kinetics and productivity for 2-PE. Furthermore, by exploring how this mutant strain processes phenylalanine could help not only the optimization of 2-PE biosynthesis, but also the whole aromatics production, and stimulate in-depth studies about the still poorly characterized aromatic-related pathways in cyanobacteria and their interconnection.

List of abbreviations:

2-PE: 2-phenylethanol

SKP: shikimate pathway

AAA: aromatic amino acid

DAHP: 3-deoxy-D-arabino-heptulosonate 7-phosphate

fbr: feedback-inhibition resistant

Phe: phenylalanine

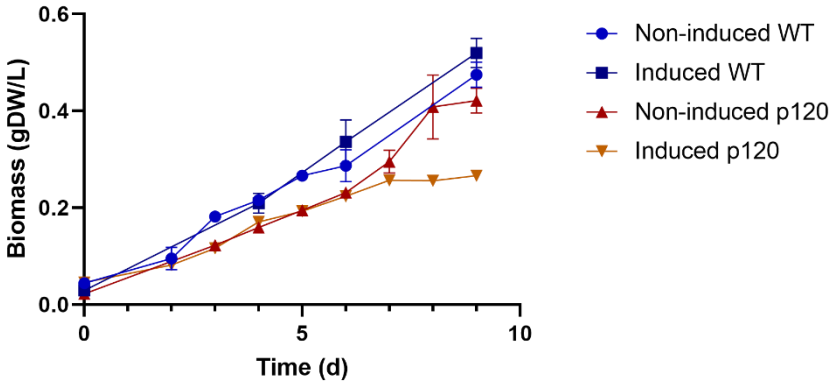
***aroK*:** gene encoding for Shikimate Kinase

SK: Shikimate Kinase

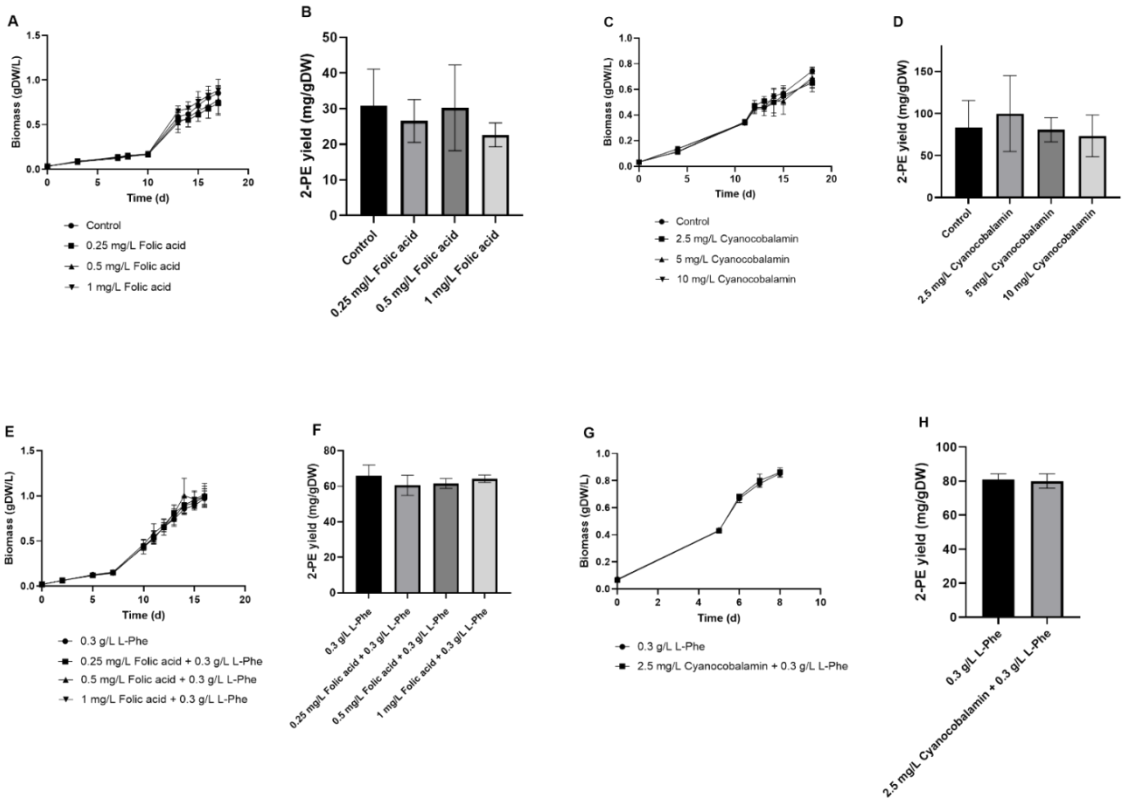
IPTG: Isopropyl β-D-1-thiogalactopyranoside

3.6. Supplementary Materials

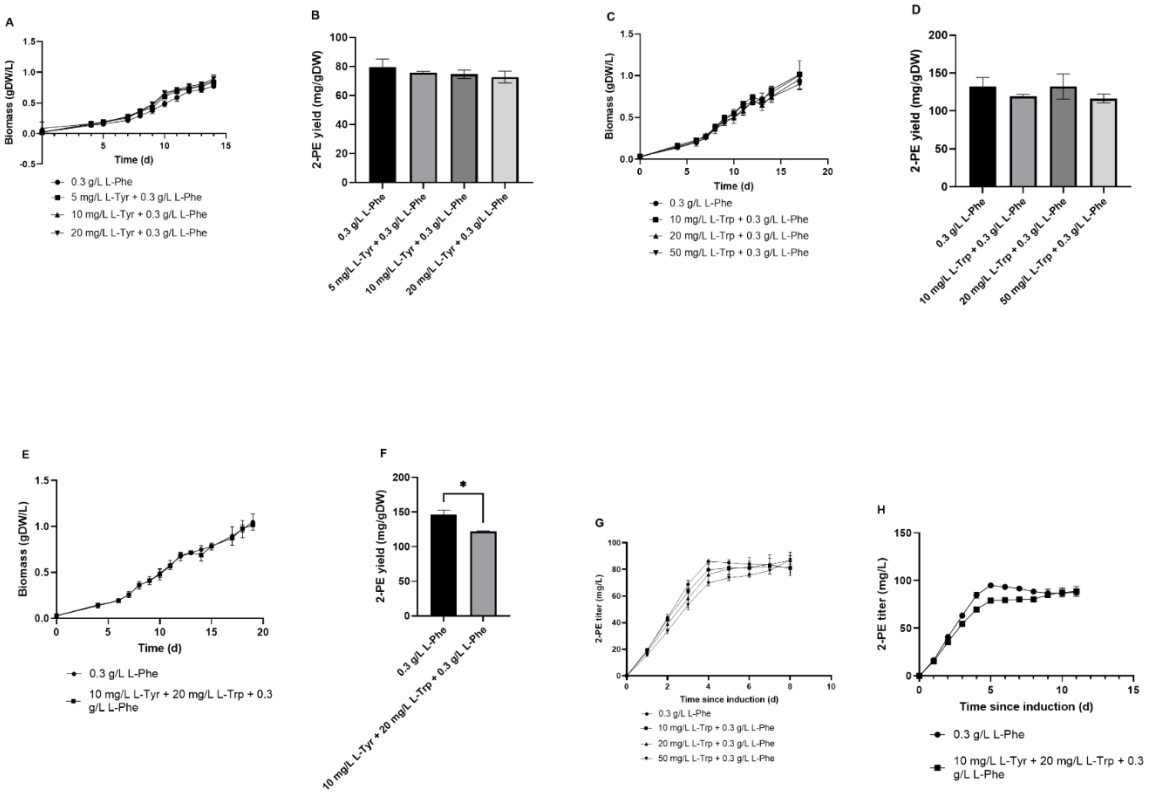
Supplementary Figure 3.1. Effect of IPTG addition for gene expression induction. *The growth kinetics, expressed as g of dry cell weight per liter, of both wild-type S. elongatus and the recombinant p120 strain subjected or not to IPTG. All tests were conducted by means of three biological replicates.*



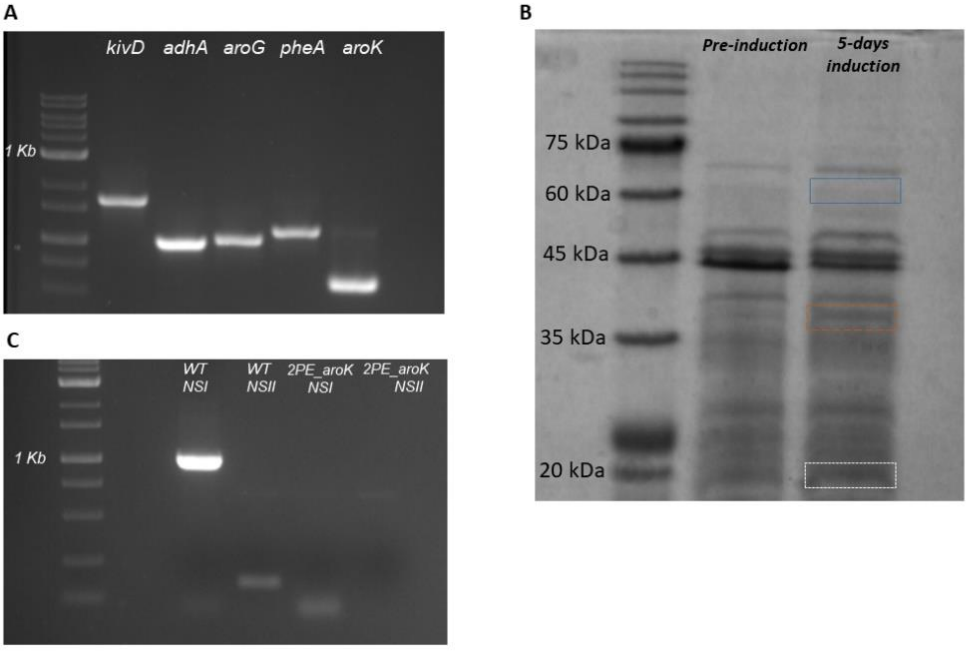
Supplementary Figure 3.2. Response of S. elongatus p120 strain growth and 2-PE production to the supplementation in BG11 medium of two aromatic vitamins. *All the results are means of three biological replicates and are relative of a reference condition (Control or 0.3 g L^{-1} L-Phe).* ***A***, ***C*** *and* ***B***, ***D*** *represent the p120 growth curve (gDW L^{-1}) and 2-PE yield (mg/gDW), respectively, at three different concentrations of folic acid or cyanocobalamin.* ***E***, ***G*** *and* ***F***, ***H*** *represent the p120 growth curve and 2-PE yield, respectively, when folic acid and cyanocobalamin were supplemented in combination with 0.3 g L^{-1} L-Phe. Statistical analyses were conducted as one-way ANOVA or unpaired two-tailed t-test (p-value < 0.05). For high resolution version see 10.3389/fbioe.2022.1005960.*



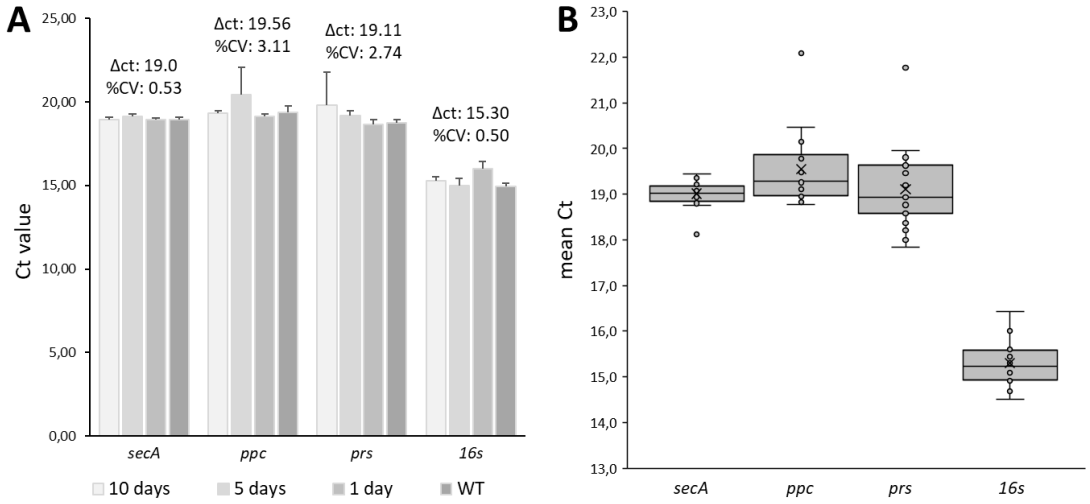
Supplementary Figure 3.3. Response of S. elongatus p120 strain growth and 2-PE production to the supplementation in BG11 medium of aromatic amino acids. *All the results are means of three biological replicates and are relative of a reference condition (0.3 g L^{-1} L-Phe).* ***A***, ***C*** *and* ***B***, ***D*** *represent the p120 growth curve (gDW L^{-1}) and 2-PE yield (mg gDW^{-1}), respectively, at three different concentrations of L-Tyr or L-Trp, when supplemented together with 0.3 g L^{-1} L-Phe.* ***E***, ***F*** *represent the p120 growth curve and 2-PE yield, respectively, in a combination of the three aromatic amino acids condition.* ***G***, ***H*** *show the 2-PE production kinetics in the presence of L-Phe and L-Trp or all the three aromatic amino acids. Statistical analyses were conducted as one-way ANOVA or Unpaired Two-tailed t-test (p-value < 0.05). Asterisk shows a statistical significance. For high resolution version see 10.3389/fbioe.2022.1005960.*



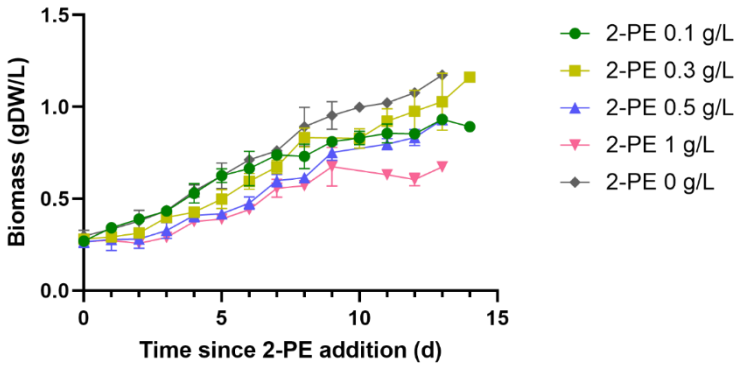
Supplementary Figure 3.4. Genetic and Protein profile of 2PE_aroK mutant. ***A)*** *Gene profile of 2PE_aroK mutant. kivD, 1647 bp; adhA, 1011 bp; aroG^{fbr}, 1065 bp; pheA^{fbr}, 1161 bp; aroK, 573 bp.* ***B)*** *Whole-cell protein profile of 2PE_aroK strain. 30 µg of proteins were loaded for both pre-induction and 5 days after induction samples. Phenylpyruvate decarboxylase, ≈ 61 kDa, blue box; 3-deoxy-D-arabino-heptulosonate 7-phosphate (DAHP) synthase, 38.5 kDa, and alcohol dehydrogenase A, ≈ 36 kDa, could be both part of the dashed box. Shikimate kinase, ≈ 21 kDa, white dotted box. The bifunctional chorismate mutase/prephenate dehydrogenase is ≈ 43 kDa could be included into the most intense band zone, due to endogenous proteins, which make it difficult to be distinguished. All five genes are under the control of IPTG-inducible promoter, which suffers from leaky expression, so it is possible to have a slight expression of the target proteins even before the actual gene expression induction. C) Segregation evaluation. The wild type NSI (1005 bp) and NSII (168 bp) were amplified in PCR. In 2PE_aroK strain the same sites were not amplified, because occupied by p120 insert and the aroK gene, respectively, indicating a complete segregation of the inserts in each S. elongatus chromosome.*



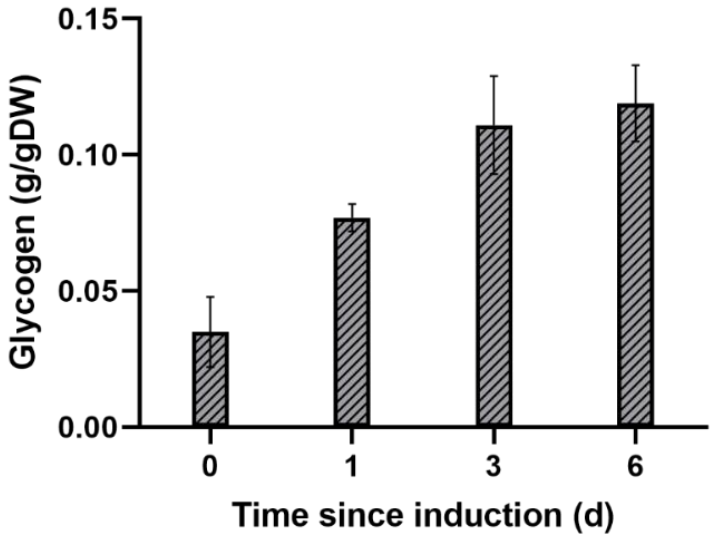
Supplementary Figure 3.5. qRT-PCR analysis of reference genes of S. elongatus PCC 7942. *A) range of cycle threshold (Ct) values of the four reference genes used in the present work (secA, ppc, prs, and 16s) across wild-type and 2PE_aroK engineered strain after one, five and ten days since gene expression induction, and the relative wild-type strain of S. elongatus PCC 7942. B) range of cycle threshold (Ct) values of the four candidate reference genes across all samples of S. elongatus PCC 7942. The box indicates the Ct value within the 25th and 75th percentiles. Whiskers include the Ct values in the 10th and 90th percentiles. The line across the box represents the median.*



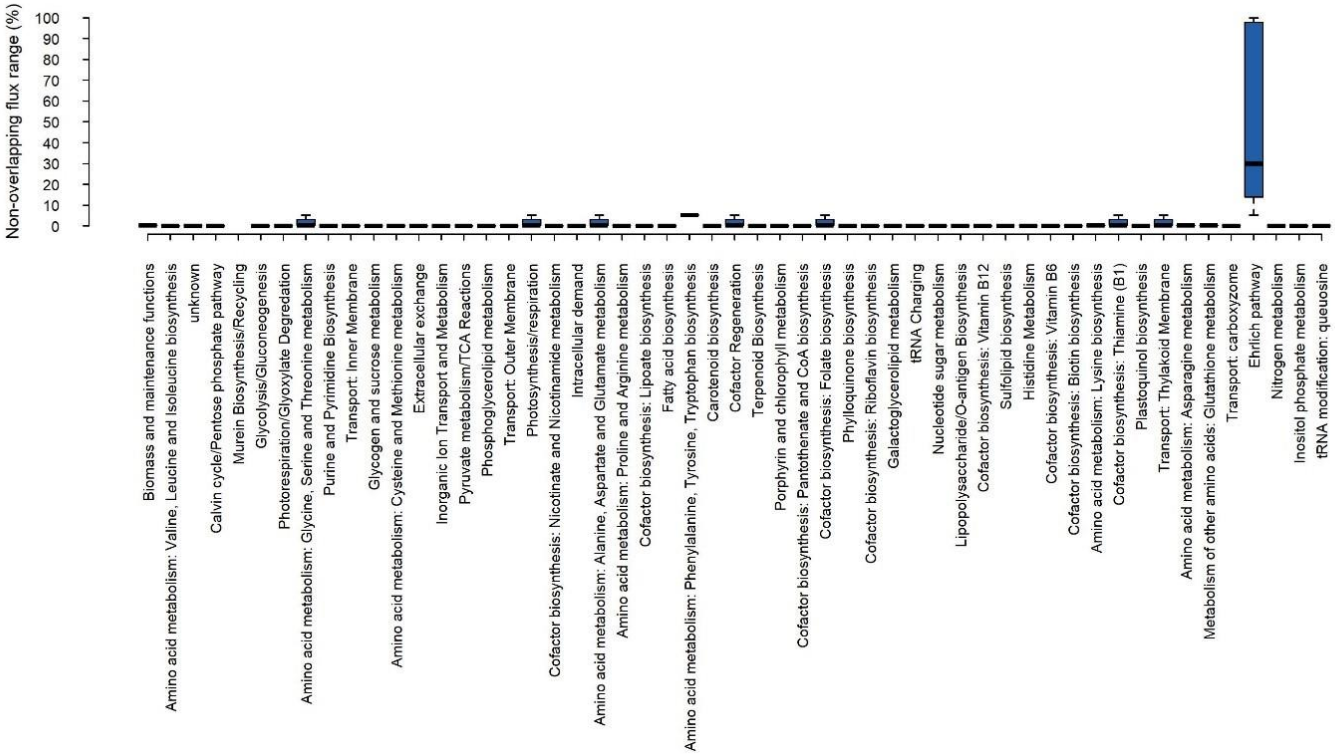
Supplementary Figure 3.6. Evaluation of toxicic effect of 2-phenylethanol on S. elongatus PCC 7942. *Four increasing 2-PE concentration were tested, from 0.1 to 1 g L^{-1}. 2-phenylethanol was added to the medium at around OD_{730} = 1 (0.26 gDW L^{-1}). Bars represent standard deviation. All tests were carried out in biological triplicate.*



Supplementary Figure 3.7. Glycogen content in 2PE_aroK mutant before and after the gene expression induction. *The glycogen content is reported as g of glycogen per g of cell dry weight (g gDW^{-1}). Bars represent standard deviation. All tests were carried on in biological triplicate.*



***Supplementary Figure 3.8*. Reactions of the metabolic reconstruction of the 2-PE-producing strain affected by medium supplementation with phenylalanine**. *L-phenylalanine supplementation affects mainly the fluxes through the reactions of the Ehrlich pathway. Shown is the simulated effect of phenylalanine addition to the medium on different functional categories. Flux variability analysis (FVA) was carried out in the absence/presence of Phe in the medium. Each reaction is assigned a range of allowed fluxes in the two conditions. For each reaction, the fraction (in percentage value) of allowed fluxes, which do not overlap between the two conditions, is computed. Shown is the distribution of the non-overlapping flux ranges of the reactions catalyzed by the enzymes belonging to different functional categories. For high resolution version see 10.3389/fbioe.2022.1005960.*



Due to the size and shape of the '**Supplementary Table 3.1, 3.2 and 3.3**', they have been collected in the attached file of thesis.

Supplementary Table 3.1. Alignment-based analysis of the S. elongatus PCC 7942 genome for genes encoding phenylalanine transaminases*. Alignment hits with statistical significance (E-value < 0.001) resulting from the alignment of known aromatic amino acid transaminases against the amino acid sequences of Synechococcus elongatus PCC 7942. For each retained hit, the table displays the scoring details corresponding to its top-scoring alignment. The table provides functional annotations retrieved from the UniProtKB database, both for the query and the hit proteins.*

Supplementary Table 3.3. Effects of medium supplementation with phenylalanine on the metabolic reactions of the S. elongatus PCC 7942 mutant producing 2-phenylethanol*. Flux variability analysis (FVA) was carried out in the absence/presence of phenylalanine in the medium. Each reaction is assigned a range of allowed fluxes in the two conditions. For each reaction, the fraction (in percentage value) of allowed fluxes, which do not overlap between the two conditions, is computed. Shown are the individual reactions whose flux ranges in the presence/absence of phenylalanine differ by at least 5%.*

Supplementary Table 3.2. Alignment-based analysis of the S. elongatus PCC 7942 genome for genes encoding L-amino acid deaminases, L-amino acid dehydrogenases and L-amino acid oxidases*. Alignment hits with statistical significance (E-value < 0.001) resulting from the alignment of known L-amino acid deaminases, dehydrogenases and oxidases against the amino acid sequences of S. elongatus PCC 7942. For each retained hit, the table displays the scoring details corresponding to its top-scoring alignment. The table provides functional annotations retrieved from the UniProtKB database, both for the query and the hit proteins. (*) The query gene is a known L-amino acid dehydrogenase in Synechocystics (Schriek et al., 2009). (**) Two genes known as L-amino acid oxidase in Synechococcus elongatus (Gau et al., 2007).*

Chapter 4

4. Metabolic Connection Between Photosynthesis And 2-PE Production In PBR: To What Extent Does Light Intensity Affect The 2-PE Synthesis?

4.0. Abstract

The development of a circular and bio-based economy is one of the striking challenges of this century. In this panorama, photosynthesis-based biomanufacturing fits in as attractive avenue for sustainable biochemicals production and simultaneous CO_2 recycling, which should contribute to address the carbon neutrality by 2050. However, several challenges need to be faced in developing such bio-based productions. One of the most impacting parameters is the light, which strongly affects the growth and productivity of photosynthetic microorganisms. While microalgae and cyanobacteria are being extensively explored for industrial applications, attention needs to be given to systematic investigations into the metabolic interplay between light and the synthesis of the desired product to optimize resource utilization efficiency.

Here, we focused on the heterologous production of 2-phenylethanol (2-PE) by an engineered strain of the model cyanobacterium *Synechococcus elongatus* PCC 7942, i.e. 2PE_*aroK*, under phenylalanine metabolite doping while exposed to several light conditions. 2-PE is a high-value aromatic compound, widely employed as fragrance in the food and cosmetics industry. The investigation was conducted in liquid batch mode in a flat panel photobioreactor under 0, 100, 150, 300 and 500 µmol photons m^{-2} s^{-1}. Biomass and 2-PE productivities, as well as carbon consumption were evaluated. Notably, in the darkness neither biomass nor 2-PE production were detected, stressing the light as main driving force of the bioprocess. Our data highlighted 150 µmol photons m^{-2} s^{-1} as the optimal setting, resulting in 282 mg L^{-1} 2-PE and an impressive productivity of 28.7 mg L^{-1} d^{-1}, representing one of the most significant goals of this study. Conversely, the highest light provoked a 30% decrease in 2-PE production. Additionally, carbon balance analysis showed that at lowest light intensities, 45-50% of carbon atoms partitioned into 2-PE, while at higher light it dropped to 28%. To better understand the impact of the photosynthetic rate on 2-PE production, the best performing light condition was further tested in turbidostat mode, where the 2-PE production was negatively affected by 42% compared to batch mode. Therefore, boosting the carbon flow through the photosynthesis did not inevitably enhance the target production, while the excess of carbon and energy is preferentially channeled into biomass formation. Interestingly, the carbon consumption analysis revealed that although 2-PE was quantified lower under the highest photon fluxes, a larger proportion could be synthesized using carbon atoms coming from CO_2 instead of phenylalanine. Finally, we explored how to potentially valorize the spent cyanobacterial biomass residual after 2-PE production. Thus, we quantified the content

in both photosynthetic pigments, known to be valuable and marketable compounds, and total carbohydrates, resulting in a potential substrate or additive for other fermentation bioprocess.

In conclusion, in this study we investigated the metabolic connection photosynthesis, carbon consumption and target product synthesis in the developed microbial factory, prospectively enabling a fine-tuned bioprocess for photosynthesis-based biomanufacturing.

4.1. Introduction

As a consequence of the worsening global climate change, accomplishing net zero carbon is the most pressing task on the Earth. This performance to date should be the result of reforming current global industrial settings to minimize greenhouse gas emissions, develop CO_2 capture technologies and promote natural carbon sinks (Wang *et al.*, 2021). Natural sinks, such as soil, forest and oceans, are capable to remove alone 9.5 - 11 gigatonne of CO_2 per year (General, 2020). Among them, photosynthetic organisms play a pivotal role; they are able to use CO_2 as sole carbon source, when light and water are both available and, thus, thrive into the environment. Both macroscopic or microscopic photosynthetic organisms are widely spread from marine or fresh waters to rocks and soil (Blankenship, 2010). Cyanobacteria constitute the largest community of photosynthetic prokaryotes (Demoulin *et al.*, 2019), characterized by the most efficient oxygenic photosynthesis (Janssen *et al.*, 2003; Schuurmans *et al.*, 2015). Due to their evolution in fluctuating environments, cyanobacteria possess a flexible metabolism and they are able to produce from CO_2 a plethora of valuable compounds for applications in food, pharmaceutical, and cosmetic industries, as well as for biofuels synthesis (Maltsev *et al.*, 2017; Barkia, Saari and Manning, 2019; Levasseur, Perré and Pozzobon, 2020; Hamouda and El-Naggar, 2021). Cyanobacteria have been extensively explored for industrial applications (Amadu, deGraft-Johnson and Ameka, 2021; Hamouda and El-Naggar, 2021). Indeed, cyanobacteria can tolerate water supplies that unsuit for agriculture, and they do not need arable land and freshwater (Catone *et al.*, 2021). Importantly, cyanobacteria are easy to manipulate genetically and engineering cyanobacteria for development of efficient strains allows to obtain higher production of a range of valuable compounds (Behler *et al.*, 2018; Santos-Merino, Singh and Ducat, 2019, 2021). However, several challenges need to be overcome when projecting a photosynthesis-based bioprocesses, and many steps are needed, from strain selection and optimization of the cultivation conditions, till the scale-up in PBR prior to the release of the target product into the market (Kamravamanesh, Lackner and Herwig, 2018). Generally, among all the factors that primarily affect cyanobacterial productivity, light is a key factor since it provides all the energy required for cell metabolism. Indeed, the influence of the light on photosynthesis has been extensively explored (Muhetaer *et al.*, 2020; Kwan *et al.*, 2021; Lisondro *et al.*, 2022; Rahman *et al.*, 2023). In both prokaryotic and eukaryotic microalgae cultivations, natural or artificial lighting can be adopted. Usually, natural light is exploited for growing microalgae in open systems. On the other hand, in closed

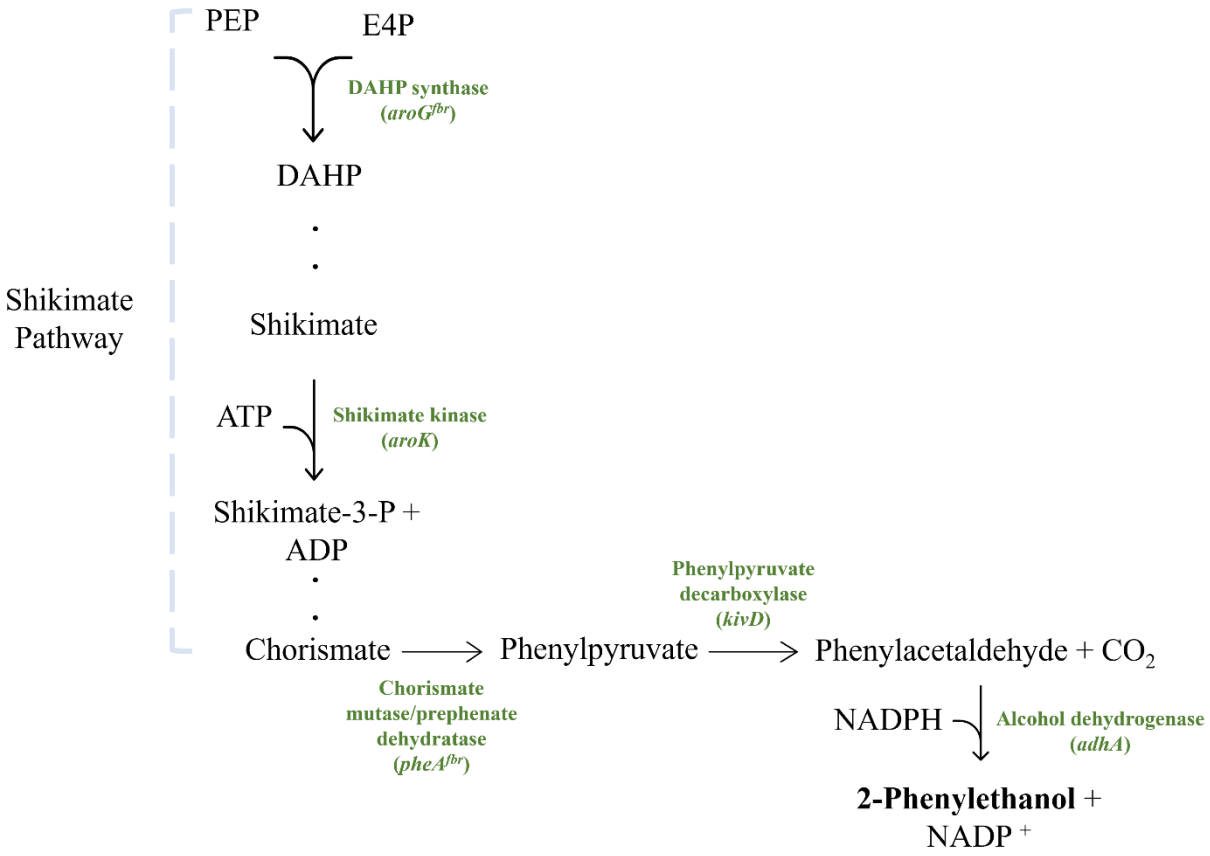
photobioreactors, artificial lighting is applicable and can be purposefully modulated to increase the productivity of microalgae biomass and the accumulation of valuable compounds. Usually, when designing photosynthesis-based bioprocess, the main light-related parameters to be considered are the photons flux, duration of lighting, and the use different spectral composition. These parameters can be tuned individually and in combination to address specific tasks. Furthermore, the energy cost for providing lighting should be evaluated, since largely influences the price of compounds produced by microalgae (Maltsev *et al.*, 2021). It has been estimated that up to 15.19 US$ kg DW^{-1} can be spent for light-emitting diodes (LED) illumination system (Blanken *et al.*, 2013; Singh and Mishra, 2023), which should be reduce by adopting alternative solutions, such as photovoltaic energy support (Sforza, Barbera and Bertucco, 2015) and Arduino microcontrollers (Alarde *et al.*, 2022; Tham *et al.*, 2022). Therefore, in order to better align with the physiological requests of the microalgae for optimal biomanufacturing, systematic studies are needed to find the best light conditions to apply to bioprocesses for achieving resource utilization efficiency. The second issue to be solved concerns understanding how the light and resulting photosynthetic rate affect the productivity of target compounds. This can be achieved by monitoring and unveiling the kinetic features of the bioprocess under development. The competition between biomass and target product formation for metabolic precursors is a common problem to deal with in bioprocess design. Coupling cellular fitness and compounds production is a phenomenon widely observed in nature for homo-fermenting microorganisms or accomplished under proper conditions (von Kamp and Klamt, 2017; Sharma *et al.*, 2020). In heterotrophic microorganisms under aerobic conditions, the growth-coupled overproduction is always associated with catabolic metabolism, in which the excess of the NADH is solved by respiration and much more ATP becomes available (von Kamp and Klamt, 2017). On the other hand, for anaerobes and photoautotrophs, the regeneration of the redox potential is regulated by excreting fermentation products (e.g. ethanol) and via the Calvin-Benson-Bassham cycle (Lassen *et al.*, 2014), respectively. The latter produces glyceraldehyde-3-phosphate, which goes into gluconeogenesis and lower glycolysis, thereby connecting to the central carbon metabolism and producing precursors for biomass synthesis. Additionally, examples of growth-coupled heterologous bioproduction are uncommon and more difficult to be studied. When a carbon sink is imposed in a wild-type or engineered autotroph, a likely imbalance of the redox potential can occur (Branco Dos Santos, Du and Hellingwerf, 2014; Du, Jongbloets, *et al.*, 2018), thus, the cells push side pathways to

stoichiometrically compensate the metabolic demand (Nogales *et al.*, 2012). One strategy to face this imbalance regards the deletion of those enzymes/pathways that interfere with the target production, but often compromise the fitness, resulting in a weaker organism (Nogales *et al.*, 2012), especially if designated for industrial application. Erdrich *et al*., (Erdrich *et al.*, 2014) proposed an *in silico* modelling study on *Synechocystis*, where they calculated that it would be feasible to reach a growth-coupled production when the target product is utilized by the cell as reduction equivalents sink. Moreover, their computational analysis suggested that a moderately increase of ATP turnover or energy dissipation is a promising approach to correct the stoichiometry necessary to balance biomass and target product synthesis.

Here, the heterologous production of 2-phenylethanol (2-PE) by the engineered strain of *S. elongatus* PCC 7942, i.e. 2PE_*aroK* (Usai *et al.*, 2022), involved five proteins, as reported in **Table 4.1,** and largely described in *Chapter 3* and Usai *et al.*, (Usai *et al.*, 2022). 2-PE is rose-scented aromatic alcohol with pleasant, which finds applications in the food, fragrance, and flavour industries, but still employable as antifungal or fuel additive (Etschmann *et al.*, 2002; Nielson, Machas and Mckenna, 2018; Fang and Sung, 2021). More in details, the protein product of *aroK* gene is the shikimate kinase, which is fifth protein of the shikimate pathway and catalyses the phosphorylation of the shikimate in shikimate-3-phosphate, by using ATP as co-substrate. The last step is mediated by the alcohol dehydrogenase A (*adhA* gene) from *Synechocystis* PCC 6803 (Vidal *et al.*, 2009), where the phenylacetaldehyde is reduced to 2-phenylethanol, by using NADPH as electron donor (**Figure 4.1**). Therefore, this investigation intends to find the interplay between the metabolic rate through photosynthesis and 2-PE production. The thorough analysis about the carbon consumption and carbon partitioning into the main two products (i.e. biomass and 2-PE), allowed to study the kinetics affecting the mutant while subjected to five light conditions (0-500 µmol photons m^{-2} s^{-1}) in a two-stage batch cultivation. Furthermore, the best light condition among those studied, was compared to turbidostatic growth mode. Thus, this study was thought to answer to the question: to what extent are photosynthesis and 2-PE production metabolically connected?

Additionally, the biomass composition was examined by the means of the photosynthetic pigments and glycogen content, either as physiological parameters and, since these are also valuable products with a variety of potential applications, as opportunity to further valorize the spent biomass, which, otherwise, would be wasted.

Figure 4.1. Scheme of the pathway for 2-PE biosynthesis in 2PE_aroK mutant strain. *All the overexpressed proteins are labelled in green.*



4.2. Materials and Methods

4.2.1. Cyanobacteria inoculum preparation for PBR

The whole set of experiments was conducted using the recombinant strain of *Synechococcus elongatus* PCC 7942, called 2PE_*aroK*, previously developed by our laboratory (Usai *et al.*, 2022). **Table 4.1** reports the gene and protein features that the mutant strain carries out. The mutant cyanobacteria inoculum to seed the PBR were grown in Erlenmeyer flasks, at 30°C, 130 rpm and constant illumination of 30 µmol photons m^{-2} s^{-1} (New Brunswick™ Innova® 44 Shaker). The culture were grown in BG11 medium, following the recipe as described: 1.5 g L^{-1} $NaNO_3$, 0.075 g L^{-1} $MgSO_4 \cdot 7H_2O$, 0.004 g L^{-1} $FeCl_3 \cdot 6H_2O$, 0.04 g L^{-1} K_2HPO_4, 0.036 g L^{-1} $CaCl_2$, 0.024 g L^{-1} $Na_2EDTA \cdot 2H_2O$, 2.86 g L^{-1} H_3BO_3, 1.81 mg L^{-1} $MnCl_2 \cdot 4H_2O$, 0.39 mg L^{-1} $Na_2MoO_4 \cdot 2H_2O$, 0.22 mg L^{-1} $ZnSO_4 \cdot 7H_2O$, mg L^{-1} $CuSO_4 \cdot 5H_2O$, mg L^{-1} $Co(NO_3)_2 \cdot 6H_2O$. The BG11 medium was buffered with 6.05 g L^{-1} TES (2-([Tris(hydroxymethyl)methyl]amino)ethane-1-sulfonic acid sodium salt) to pH = 8. The BG11 medium was supplemented with 20 µg mL^{-1} spectinomycin and 10 µg mL^{-1} kanamycin.

4.2.2. PBR general experimental conditions

2PE_*aroK* recombinant strain was studied in PBR. In details, the flat panel PBR adopted was the FMT150.2/400 (Photon Systems Instruments, Drasov, Czech Republic) (Nedbal *et al.*, 2008), equipped with a customized vessel of 450 mL of working volume. All the geometrical parameters were thoroughly described in (Vasile *et al.*, 2021). Cyanobacteria were grown in the BG11 medium as described above but supplemented with 10 mM of NaCHO3 as buffering system. The optical density (OD) was constantly measured by an integrated densitometer at 720 and 680 nm. The PBR is equipped with a probe for temperature and pH. The temperature was settled at 30 ± 1°C and pH = 8. A constant supply of CO_2 was provided by sparging the medium with 1% CO_2 (v/v) in N_2. A gas mixer (GMS150 micro, Photon Systems Instruments, Drásov, Czech Republic) coupled to a mass flow controller (EL-FLOW prestige FG-201CV, Bronkhorst High-Tech BV, AK Ruurlo, Netherland) to supply 150 mL min^{-1} of gas mixture to the PBR. The cyanobacteria cultures were illuminated with white light from one side of the PBR by emitting diodes (LEDs). PBR liquid batch experimental conditions

All tests were conducted following two stages: i) growth phase, the cells were gradually acclimated to the increasing light up to the chosen one, until the culture reached OD_{730} = 1; ii) production phase, triggered by adding to the mutant culture (OD_{730}=1) 1 mM IPTG and 0.3 g L^{-1} L-Phe, as gene expression inducer and metabolite doper, respectively. During the second stage, characterized by the induction of 2-PE synthesis pathway, the light was kept constant at 0, 100, 150, 300 or 500 µmol photons m^{-2} s^{-1} and this phase was preceded by an acclimation of 24-48 h at the target light. The OD was daily monitored at 730 nm and converted in biomass as g of dry cell weight per L of culture (gDW L^{-1}), by using the conversion factor of 0.26 previously determined in our laboratory.

4.2.2.1. ***PBR turbidostat experimental conditions***

The PBR was run in turbidostat (semicontinuous) mode by a controlled dilution of the growing cell population. Dilution was based on the changes at OD_{720}, measured by the integrated densitometer and calibrated to the benchtop spectrometer at OD_{730} to maintain the OD_{730} approximately at 1 ± 3%, keeping the culture in exponential phase. The turbidostat mode followed the same experimental set up described above. Firstly, the biomass was accumulated in batch mode until the cyanobacteria culture reached OD_{730}=1, then the turbidostat mode was activated. The cell culture was subjected to 24-48 h of turbidostat at 150 µmol photons m^{-2} s^{-1}, in order to acclimate the cells to both light and cultivation mode. To lunch the production phase 1 mM IPTG and 0.3 g L^{-1} L-Phe was directly supplemented into the vessel as well as into the BG11 medium for the controlled dilution, to avoid the washout of the gene expression inducer and the metabolite doper. Dilution was performed by a peristaltic pump automatically controlled by the software of the photobioreactor, accordingly to the selected OD_{720} range.

4.2.3. ***qRT-PCR analysis***

qRT-PCR analysis was performed as described in (Usai *et al.*, 2022). All the primers used are reported in **Supplementary Table 4.1**. The expression levels of the target genes (*kivD, adhA, aroG^{fbr}, pheA^{fbr}, aroK*) were relatively quantified against the reference *prs* gene (Luo *et al.*, 2019; Usai *et al.*, 2022) by the Pfaffl method (Mannino *et al.*, 2021), using the gene expression level at the lowest light intensity as control

condition. The analysis was conducted from the biomass harvested five days since the gene expression induction.

4.2.4. CO_2 consumption measurement

To measure the dissolved CO_2 (dC) into the cultural medium, the PBR was equipped with the CO_2 sensor InPro 5000/12/120 (Mettler Toledo, Columbus, Ohio, United States), based on the Severinghaus principle (SEVERINGHAUS and BRADLEY, 1958). Briefly, the electrode contains sodium bicarbonate, which reacts with the CO_2. The reaction changes the pH in the electrode, which corresponds to a change in potential difference, and this is measured. Therefore, the CO_2 is then inferred by changes in pH every minute. Furthermore, the dissolved CO_2 values were used to experimentally calculate the kLa, the volumetric mass transfer coefficient, under abiotic PBR condition. The CO_2 liquid transfer is represented by an exponential curve until a plateau, which represent the saturation limit (dC_{sat}) under the settled PBR condition. Thus, the CO_2 transfer rate (CTR) was determined from the measured dissolved CO_2 values (dC_n), as follows (**a**):

$$CTR = \Delta dC/\Delta t = \ln\left(\frac{dC_{sat}-dC_n}{dC_{sat}-dC_{n+1}}\right) \quad \textbf{(a)}$$

Being aware of the CTR every minute, the kLa values were calculated within the exponential phase of the dissolution curve and the resulting value was the average of those calculated (**b**):

$$kLa = CTR/dC_n \quad \textbf{(b)}$$

The resulting kLa was then used for calculating the CO_2 uptake by bacteria. First the theoretical dissolved CO_2 value (dCc) was calculated as follows (**c**):

$$dC_c = dC_{sat} - \left(\frac{dC_{sat}-dC_n}{\exp(kLa*\Delta t)}\right) \quad \textbf{(c)}$$

Finally, the CO_2 uptake was calculated every minute as (**d**):

$$C\,uptake = dC_c - dC_n \quad \textbf{(d)}$$

4.2.5. 2-PE and L-Phe HPLC quantification

2-PE and L-Phe were quantified as reported in (Usai *et al.*, 2022). Briefly, 2-PE production was assessed by UHPLC (UltiMate 3000, Thermo Fisher, Waltham, Massachusetts, United States) equipped with a Hypersil GOLD™ C18 reversed phase column (250 × 4.6 mm, 5 µm; Thermo Fisher Scientific). Acetonitrile and H_2O (50:50) was used with 1 mL/min flow rate, 40°C and UV-detection at 205 nm. L-phenylalanine was quantified through the Hypersil GOLD™ Amino column (120 × 4.6 mm, 5 µm; Thermo Fisher Scientific) at 210 nm and 9 mM sulfuric acid was pumped at 0.8 mL/min, column oven was heated at 50°C. For sample preparation, 1 ml of bacterial culture was collected and centrifuged at 12,000 g for 10 min, and 20 µL of the supernatant was injected for HPLC analysis.

4.2.6. Carbon balance

To determine the carbon distribution, the carbon balance was calculated considering together the two carbon sources, i.e. CO_2 and L-Phe, used to produce biomass and 2-PE. Each C source consumed and product synthesized was converted to the corresponding moles of carbon atoms. In the case of biomass, the carbon content of *S. elongatus* PCC 7942 biomass corresponds to approximately 46-48% of its dry weight (Mahlmann, Jahnke and Loosen, 2008). Thus, the carbon balance was calculated for both the biomass (**e**) and 2-PE (**f**):

$$C_{biomass} = \frac{Cmol\ biomass}{(Cmol\ CO_2 + Cmol\ L{-}Phe)} * 100 \qquad \textbf{(e)}$$

$$C_{2\text{-}PE} = \frac{Cmol\ 2{-}PE}{(Cmol\ CO_2 + Cmol\ L{-}Phe)} * 100 \qquad \textbf{(f)}$$

4.2.7. Glycogen content quantification

One mL of cell culture was collected before and after the induction of gene expression. The cell cultures were *centrifuged* at 12,000 *g* for 10 min and processed as previously

reported in (Usai *et al.*, 2022). Briefly, the cell pellet was lysed in 100 µL of 3.5% sulfuric acid and boiled for 40 min. Then, a centrifugation of 12,000 *g* for 2 min was followed by addition of 350 µL of 10% (w/v) trichloroacetic acid and incubated for 10 min at room temperature. The quantification was conducted from 150 µL of supernatant, by adding 750 µL of 6% (v/v) 2-aminotoluene (diluted in glacial acetic acid) and boiled again for 10 min. The absorbance was measured at 635 nm. The standard curve was performed with D-glucose (0-3 mg mL^{-1}).

4.2.8. ***Photosynthetic pigments quantification***

Phycocyanin (phy) Chlorophyll a (chla) and total carotenoids (car) were quantified in each sample. 1 mg of dried biomass was weighted and resuspended in 1 mL of PBS solution and kept on ice. The suspension was added to a tube containing 500 mg of glass beads (0.25-0.5 mm). The lysis was performed twice in a tissue lyser (Retsch MM 400, Haan, Germany), at 15 s^{-1} for 5 minutes. The lysate was then incubated on ice for 1 h and then centrifuged at +4° C, 15.000 g for 10 min. The supernatant was opportunely diluted and used for spectrophotometric measurements (PerkinElmer Lambda 650 UV/Vis). The absorbance was collected in the range from 800 nm to 500 nm. The phycocyanin concentration was measured through the following equation (Zavřel *et al.*, 2018):

$$\text{Phycocyanin [mg mL}^{-1}\text{]} = ((A615 - A720) - 0.474 \times (A652 - A720)) / 5.34$$

The remaining cell pellet was resuspended in 1 mL of cold methanol (≥ 99.9%) and incubated at 4°C in the darkness for 20 min. The cells debris were centrifuged (12,000 g, 10 min, 4°C) to recover the supernatant, which was properly diluted in methanol and then subjected to spectrophotometer in the range of 800 nm to 400 nm. To calculate the photosynthetic pigments concentration, the following equations were used (Wellburn, 1994):

$$\text{Chlorophyll a [µg mL}^{-1}\text{]} = 12.9447(A_{665} - A_{720})$$

$$\text{Total carotenoids [µg mL}^{-1}\text{]} = [1000(A_{470} - A_{720}) - 2.86(\text{Chla[µg mL}^{-1}\text{])}]/221$$

The relative pigments concentrations were normalised on the basis of the biomass used for the pigments extraction and the final results were expressed as mg of pigment per gDW (mg gDW^{-1}).

Gene	*HR Site*	*Protein*	*EC number*	*Reaction*	*Organism*	*Ref.*
aroG^{fbr}	NSI	feedback-inhibition resistant DAHP synthase	EC 2.5.1.54	PEP + E4P +H_2O ⇌ DAHP + Pi	*Escherichia coli*	(Ni *et al.*, 2018; Usai *et al.*, 2022)
pheA^{fbr}	NSI	feedback-inhibitionresistant chorismate mutase/prephenate dehydratase	EC 5.4.99.5/ EC 4.2.1.51	Chorismate ⇌ Prephenate ⇌ Phenylpyruvate + H_2O + CO_2	*Escherichia coli*	(Ni *et al.*, 2018; Usai *et al.*, 2022)
kivD	NSI	Phenylpyruvate decarboxylase	EC 4.1.1.43	Phenylpyruvate ⇌ phenylacetaldehyde + CO2	*Lactococcus lactis*	(Ni *et al.*, 2018; Usai *et al.*, 2022)
adhA	NSI	Alcohol dehydrogenase A	EC 1.1.1.1	Phenylacetaldehyde + NAD(P)H ⇌ 2-Phenylethanol + $NAD(P)^+$	*Synechocystis PCC 6803*	(Ni *et al.*, 2018; Usai *et al.*, 2022)
aroK	NSII	Shikimate kinase	EC 2.7.1.71	Shikimate + ATP ⇌ Shikimate-3-P + ADP	*S. elongatus PCC 7942*	(Usai *et al.*, 2022)

Table 4.1. Genetic features of 2PE_aroK recombinant strain of S. elongatus PCC 7942. *HR, homologous recombination; NS, neutral site; DAHP, 3-deoxy-7-phosphoheptulonate; PEP, phosphoenolpyruvate; E4P, erythrose-4-phosphate*

4.3. ***Results***

4.3.1. ***Growth of 2PE_aroK mutant strain under four photons fluxes in liquid batch mode***

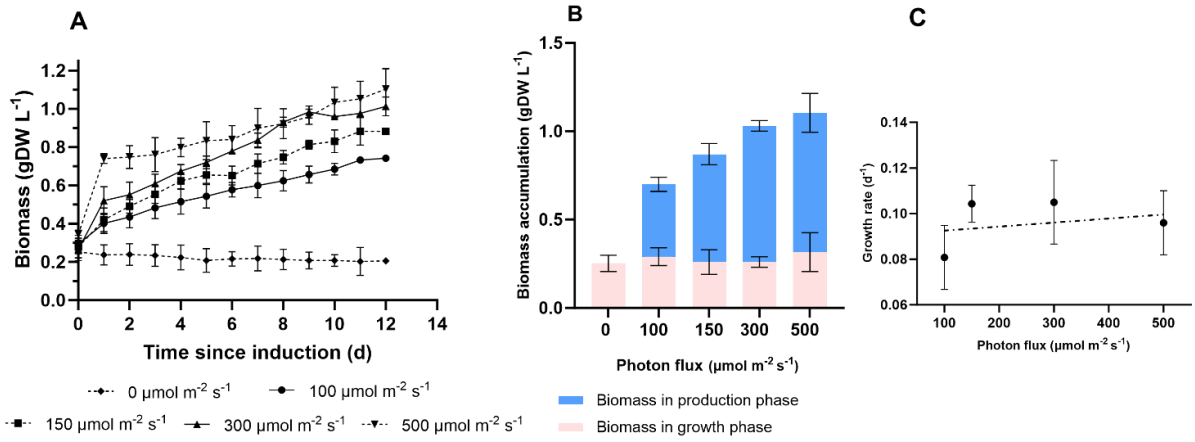
To expand knowledge about the metabolic relationship between the light, which acts directly on the photosynthesis, and the non-native pathway for 2-PE production in the 2PE_*aroK* mutant strain, five different light conditions (dark, 100, 150, 300 or 500 µmol photons m^{-2} s^{-1}) were assessed and compared. Data about cell growth, fitness, carbon consumption and 2-PE production were collected in each condition. Most of the data are related to the production phase (10-12 days), triggered by adding IPTG and L-Phe, which start the gene expression induction and the metabolite doping, respectively. The production phase started when the bacterial culture reached OD_{730} = 1, corresponding to 0.26 gDW L^{-1}, exposed to the relative photon flux for at least 24 h. **Table 4.2** reports a summary of the main data obtain in this study. Unsurprisingly, both

the highest biomass production (**Figure 4.2A, B**) and specific growth rate (**Figure 4.2C**; μ, d^{-1}) were obtained at the most intense light condition, following, however, a non-linear trend among the tested light conditions (R^2=0.034). Actually, the growth rate at the highest photon flux improved only by 19% compared to that at 100 μmol photons m^{-2} s^{-1}. Likely, this phenomenon was caused by a self-shading effect (Agustí, 1991; Ogbonna, Yada and Tanaka, 1995) usually occurring in batch culture, where the density of the culture plays a dominant role, and the mixing can no longer compensate the cell dispersion. Thereby, the culture is not able to receive the exact photons amount as the culture grew. During the production phase (2nd stage of the bioprocess), in almost all light conditions tested the biomass accumulated by 70-75% of the total biomass production, exception for the lowest light condition, where the biomass accumulated by 58% (**Figure 4.2B,** blue bars). Furthermore, in the dark condition no bacterial growth was detected, but the bacterial optical density slightly decreased day by day (**Figure 4.2A**). Additionally, a qRT-PCR analysis was performed to understand whether the light intensities or the environmental conditions could affect the gene expression level. The analysis has been conducted using the lowest light intensity as calibrator (and *prs* gene as reference gene as previously described (Luo *et al.*, 2019; Usai *et al.*, 2022) as one of the most stably expressed gene in cyanobacteria), but no worthy-of-mention results emerged in every light exposure (**Supplementary Figure 4.1**). Overall, all the genes were expressed in every light exposure condition, with no statistical significance among them (**Supplementary Figure 4.1**). Hence, the results obtained in the present investigation should be ascribed to physical-to-biological factors.

Photon flux	**μ (d^{-1})**		**Final Biomass (gDW L^{-1})**		**Max 2-PE titer (mg L^{-1})**		**Max 2-PE yield (mg gDW^{-1})**		**Average 2-PE productivity (mg L^{-1} d^{-1})**		**% L-Phe consumed**	
(μmol photons m^{-2} s^{-1})	**Average**	**SD**	**Average**	**SD**	**Average**	**SD**	**Average**	**SD**	**Average**	**SD**	**Average**	**SD**
100	0.081	0.014	0.70	0.049	259.4	27.4	349.3	27.5	24.1	2.1	79.3	5.8
150	0.104	0.008	0.87	0.068	282.0	21.1	329.0	7.3	28.7	3.4	77.3	4.3
300	0.105	0.018	1.03	0.029	268.5	31.6	299.9	9.1	26.5	3.6	52.5	10.3
500	0.096	0.014	1.10	0.107	197.7	24.6	182.3	36.2	19.2	2.1	33.0	4.5

Table 4.2. Summary of the main results obtained from the liquid batch cultures exposed to four different light conditions.

***Figure 4.2. 2PE_aroK growth data in batch cultures at four different light intensities and dark condition**. **A)** Growth curves; **B)** Biomass accumulation during the growth phase (pink bars) and production phase (blue bars); **C)** Growth rates. Four biological replicates were carried out. Error bars represent standard deviation.*



4.3.2. 2-PE production and L-Phe uptake by 2PE_aroK mutant strain under four photons fluxes in liquid batch mode

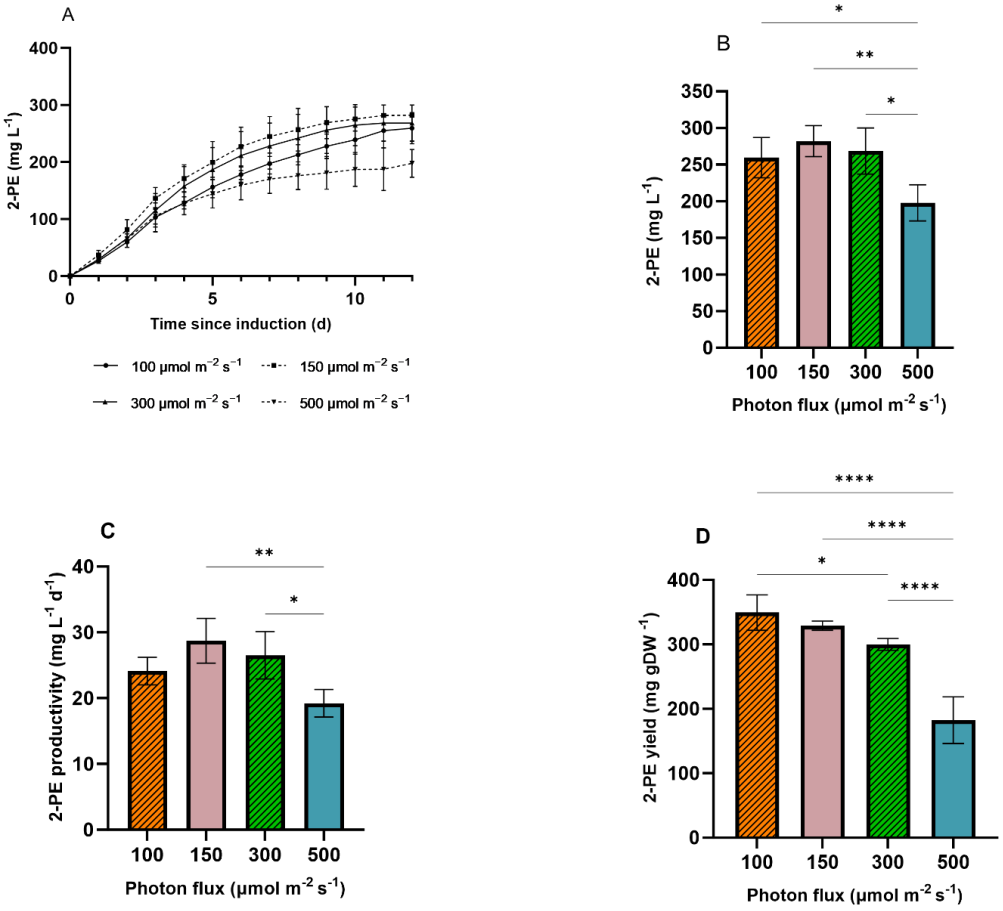
The ability to produce 2-PE resulted to be strongly affected by the light intensity. **Figure 4.3A** shows the 2-PE production kinetics under four light intensities. As expected, in dark condition, 2-PE was not produced at all, thereby, all the data about the dark condition were eliminated from any representation hereinafter.

The highest and lowest 2-PE concentration was reached at 150 and 500 µmol photons m^{-2} s^{-1}, respectively (**Figure 4.3A, B**). Particularly, at 150 µmol photons m^{-2} s^{-1} we achieved a 2-PE titer of 282 ± 21.1 mg L^{-1}. This result is not the highest production for the same mutant strain recorded in the literature, where it has previously reported 285 mg L^{-1} 2-PE in shaking flasks (Usai *et al.*, 2022). However, here we obtained 282 mg L^{-1} in ten days since the gene expression induction, truly increasing the volumetric productivity of the present bioprocess, accounting for 28.7 ± 3.4 mg L^{-1} d^{-1} under 150 µmol photons m^{-2} s^{-1} (**Figure 4.3C**). In addition, the 2-PE volumetric productivity recorded in this investigation is the highest reported in photoautotrophic condition compared to the literature, resulting in one of the most important achievements.

Furthermore, at the highest photon flux, i.e. 500 µmol photons m^{-2} s^{-1}, the 2-PE production was calculated as 198 ± 24.6 mg L^{-1}, resulting in a 30% decrease if compared to the highest 2-PE accumulation (**Figure 4.3B**).

In order to project a large-volume scale up, we found that while the higher light intensities push the biomass accumulation, the 2-PE yield resulted to be lower if compared to the lowest photon fluxes, where the yield ranged 339-349 mg of 2-PE per gram of dry cell biomass (mg gDW^{-1}, **Figure 4.3D**). These data suggest that we needed to accumulate a lower amount of cell biomass to reach the same amount of 2-PE, when the culture was exposed to the low light intensities among those tested. Overall, the most intense light condition (500 µmol photons m^{-2} s^{-1}) seems not to guarantee the best results in terms of target compound yield. Indeed, the photosynthesis and 2-PE production pathways likely uncoupled beyond 300 µmol photons m^{-2} s^{-1}, where increasing the photosynthesis-related carbon flux has no effect on the target compound synthesis profile, but even worsen the bioprocess. Thereby, here boosting the photosynthesis by rising the light intensity led to increase the biomass accumulation competing with the 2-PE production (**Figure 4.3B, D**).

Figure 4.3. 2-PE-related data of the 2PE_aroK mutant strain exposed to four light conditions in batch mode. *A) 2-PE kinetics production;* ***B****) 2-PE final concentration;* ***C****) 2-PE volumetric productivity;* ***D****) 2-PE production normalised by the biomass necessary for producing 2-PE, expressed as mg of 2-PE per gDW. All the tests were carried out as four biological replicates. Error bars represent standard deviation. The statistics was performed as one-way ANOVA (α ≤ 0.05). Asterisks refer statistical significance. *, p-value ≤ 0.05; **, p-value ≤ 0.002; ***, p-value ≤ 0.0002; ****, p-value ≤ 0.0001.*

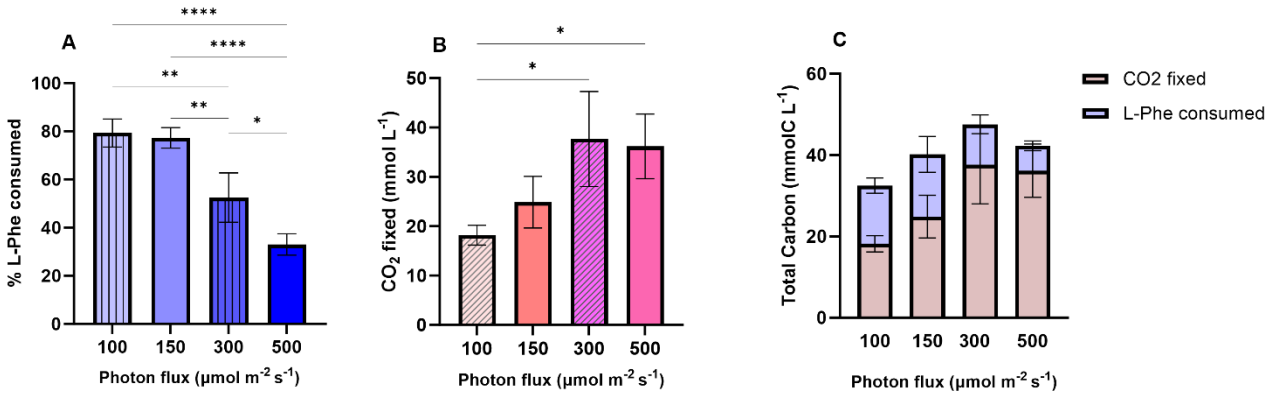


4.3.3. CO_2 and L-Phe uptake, and glycogen accumulation by 2PE_aroK mutant strain under four photons fluxes in liquid batch mode

1% CO_2 was supplied in a mixture with N_2 with a gas flow rate of 150 mL min^{-1}. To start the 2-PE production phase we added 1mM IPTG and 0.3 g L^{-1} L-Phe into the PBR, when the bacterial reached OD_{730} = 1 and the data collection stopped when the 2-PE productivity became negligible (about 10-12 days). Therefore, the present bioprocess was fed with both CO_2 and L-Phe, and their uptake appeared to be strongly influenced by the photon flux. In the dark production condition neither CO_2 nor L-Phe resulted to be consumed (data not shown), indicating that the light still remains the main driving force of the present biomanufacturing process. Furthermore, the L-Phe consumption was found to be altered, indeed, the highest the light intensity the lower the L-Phe uptake (**Figure 4.4A).** At the highest light intensities, i.e. 300 and 500 µmol photons m^{-2} s^{-1}, cyanobacteria consumed only the 33% and 46% of the available L-Phe, respectively. Conversely, almost all the L-Phe available was uptaken at 150 (78%) and 100 (79%) µmol photons m^{-2} s^{-1}, which approximately doubled if compared to the highest photon fluxes related data. The CO_2 consumption was also affected and, unsurprisingly, the highest amount was recorded at the most intense light conditions (**Figure 4.4B**). **Figure 4.4C** reports the sum of the carbon atoms consumed from both CO_2 and L-Phe and it is expressed as mmolC L^{-1}. To what extent CO_2 and L-Phe were exploited into the present bioprocess will be discussed in the following section.

Glycogen serves as the primary storage compound for CO_2 fixed through photosynthesis in cyanobacteria (De Porcellinis, Frigaard and Sakuragi, 2017; Shinde *et al.*, 2020), functioning as a crucial natural carbon sink. Our observations reveal that under low light conditions, glycogen accumulated steadily over time, constituting approximately 10% of the dry biomass (**Supplementary Figure 4.2**). Conversely, in conditions of higher light intensity, where photosynthetic activity is more stimulated, glycogen content is higher and exhibits periodic fluctuations (**Supplementary Figure 4.2**), reaching at the best up to 15% of the biomass.

Figure 4.4. Carbon consumption results of the 2PE_aroK mutant strain exposed to four light conditions in batch mode. ***A)*** *Percentage of L-Phe consumed of the available one;* ***B)*** *Carbon fixed through photosynthesis, expressed as mmol of carbon atoms consumed from the supplied CO2;* ***C)*** *Total amount of carbon consumed from CO2 (pink bars) and L-Phe (violet bars). All the tests were carried out as four biological replicates. Error bars represent standard deviation. The statistics was performed as one-way ANOVA (α ≤ 0.05). Asterisks express statistical significance. *, p-value ≤ 0.05; **, p-value ≤ 0.002; ***, p-value ≤ 0.0002; ****, p-value ≤ 0.0001.*

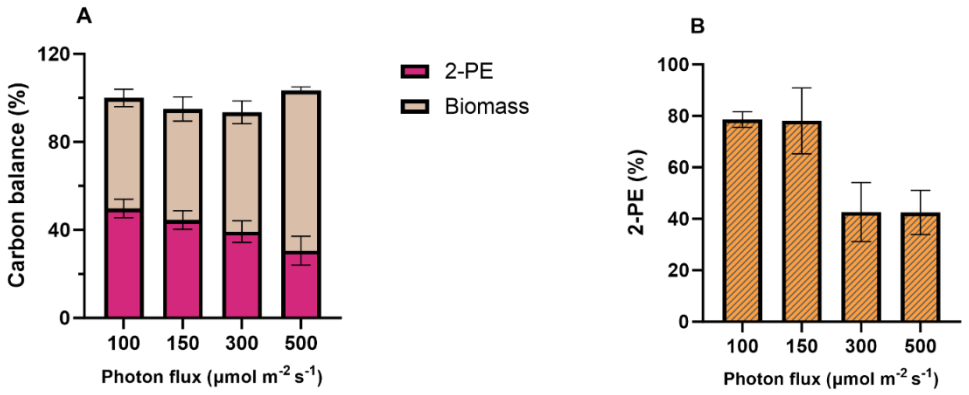


4.3.4. ***Carbon Balance between biomass and 2-PE***

All the carbon atoms coming from both the uptaken CO_2 and L-Phe were considered together in order to better understand how carbon atoms were differently distributed between biomass and 2-PE (**Figure 4.5A**), i.e. the two main products of this biomanufacturing process. No other by-product was considered for the present carbon analysis. The cyanobacterial photoautotrophic metabolism releases relatively few metabolic intermediates into the extracellular space (Pérez *et al.*, 2019). Thereby, the carbon balance offered here should be rather precise. **Table 4.3** shows the detailed data regarding the carbon analysis. At the highest light intensity (500 µmol photons m^{-2} s^{-1}), a larger percentage of carbon atoms (ca. 72 ± 1.58 %) went to biomass. On the other hand, at the other three light conditions the percentage of biomass obtained from the total carbons consumed was quantified in a range of 50-54% (**Figure 4.5A,** pink bars). Consequently, the percentage of carbon atoms as part of 2-PE ranged from 30 to 50% (**Figure 4.5A,** magenta bars). Apart from the predictable relationship observed between the CO_2 uptake and high light condition, the most interesting results were about the L-Phe utilization. The fate of the L-Phe inside the cell of 2PE_*aroK*

recombinant strain has been previously speculated (Usai *et al.*, 2022) and briefly discussed later on in this chapter. As already mentioned, the L-Phe uptake lowered as the photon fluxes increased (**Figure 4.4A**). Therefore, by assuming that the consumed L-Phe was fully employed to produce 2-PE, we calculated how the L-Phe can actually contribute to 2-PE synthesis. Theoretically, the yield between 2-PE (C8) and L-Phe (C9) is 0.89 molC molC^{-1}, thus, a dramatic difference between low and high light intensities emerged (**Figure 4.5B**): under the two low light conditions, the consumed L-Phe might generate up to 78% of the synthetized 2-PE; under the highest photon fluxes only the 43% of 2-PE could be produced from L-Phe, and the residual 2-PE should has been synthesized from CO_2. This truly interesting finding suggests that, even if increasing the light intensity leads to a lower amount of 2-PE, a larger fraction of the target compound is produced by the photosynthetic carbons coming as CO_2. Therefore, summing up all the results 150 and 300 µmol photons m^{-2} s^{-1} seemed to be the most successful production conditions. Importantly, this kind of remarks should be thoroughly faced while a specific bioprocess must be designed, and carbon sources must be chosen. Finally, to better understand the nature of this bioprocess and its biocatalyst (2PE_*aroK* mutant) we chose a light condition among the best ones and assayed the production of the 2-PE in turbidostat cultivation mode, as discussed later on in this chapter.

Figure 4.5. Carbon distribution analysis of the 2PE_aroK mutant strain exposed to four light conditions in batch mode. ***A)*** *Carbon balance indicates the percentage of the total consumed carbon atoms partitioning between 2-PE (magenta bars) and biomass (pink bars);* ***B)*** *Percentage of 2-PE producible from the L-Phe effectively consumed in every light conditions. The experiments were conducted by the means of four biological replicates. Error bars refer to standard deviation.*



Photon flux	CO_2 fixed (mmolC L^{-1})		L-Phe consumed (mmolC L^{-1})		C balance (%)				% 2-PE/L-Phe	
(µmol photons m^{-2} s^{-1})	Average	SD	Average	SD	Biomass		2-PE		Average	SD
					Average	SD	Average	SD		
100	18.2	2	14.3	1.9	50.3	3.9	49.7	4.2	78.6	3.1
150	24.88	5.2	15.3	4.4	50.5	5.6	44.5	4.2	78.1	12.8
300	37.68	9.6	9.9	2.3	54.2	5.2	39.3	4.9	42.6	11.5
500	36.18	6.5	6.1	1.2	72.9	1.6	30.6	6.5	42.5	8.6

Table 4.3. Summary of the carbon-related data obtained from the liquid batch cultures exposed to four different light conditions.

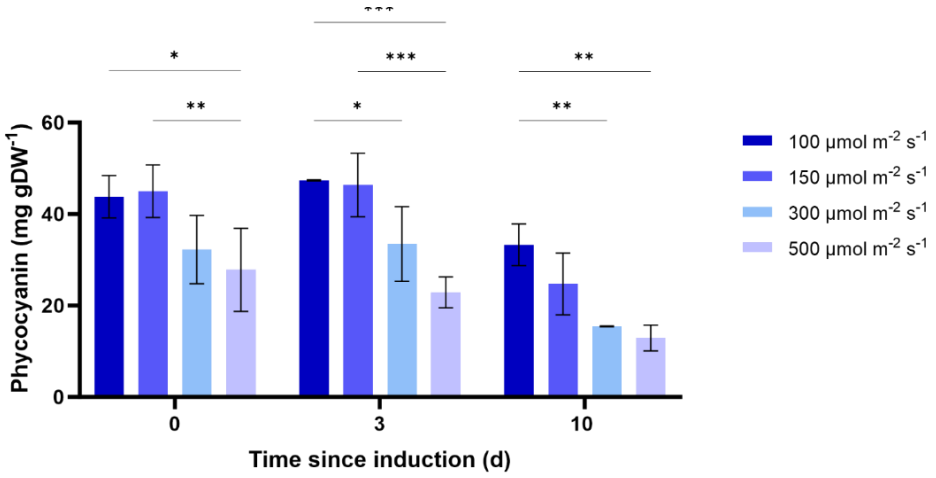
4.3.5. Photosynthetic pigments in 2PE-*aroK* mutant biomass under four photons fluxes in liquid batch mode

Phycocyanin (phy), chlorophyll a (chla) and total carotenoids (car) were quantified**.** Chla is the main pigment involved in photosynthesis, particularly in light harvesting as well as in converting energy of absorbed photons to chemical energy. Chla is universally distributed in all the oxygenic photosynthetic organisms and in small amount in green sulfur bacteria and anaerobic phototrophs. Other chlorophylls (e.g. b, c, d, f) are diffused differently among cyanobacteria, microalgae, macroalgae and higher plants (Björn *et al.*, 2009). Here, the chla content results constant over the time and among the light intensities (**Supplementary Figure 4.3A**), with some slight differences but not statistically significant. Indeed, the chla content in cyanobacteria tends to be constant unless the microorganisms are subjected to very stressful conditions (e.g. light, temperature, nitrogen and phosphorous depletion (da Silva Ferreira and Sant'Anna, 2016; Rahman *et al.*, 2023)). It does not seem the case of our investigation. Similarly, the content in carotenoids appeared to be higher accordingly with the highest light intensity exposure (**Supplementary Figure 4.3B**). Indeed, carotenoids are notoriously associated to stress condition, especially light related (Steiger, Schäfer and Sandmann, 1999; Masojídek, Torzillo and Koblížek, 2013; Lopes, Clarinha and Vasconcelos, 2020). In our investigation, the largest carotenoids content was recorded for the highest light intensity at the moment of the gene

expression induction. This data could be due to the 24 hours exposure to 500 µmol photons m^{-2} s^{-1} before the gene expression induction. However, even if the light was gradually increased during the 1st stage of this bioprocess (i.e. cellular growth), probably this exposure could cause that carotenoids rise, which relaxed in the following days.

Currently, phycocyanin is one of the most explored natural pigments. It is water-soluble and blue-colored, and contributes significantly to the natural shade of cyanobacteria, also known as blue-green algae. Here, we quantified phy in our mutant strain of *S. elongatus* PCC 7942, 2PE_*aroK*, in non-targeted condition for pigments production and extraction. Thus, we detected the highest amount at the lowest light intensities (**Figure 4.6**). Over the time, the amount of phy evolved, especially at both the highest light intensities, where the phy content decreased from 3 to 1.3% of the biomass at the end of the experiment. Also, at the lowest photon fluxes the quantified phy from the biomass decreased within ten days by 24 and 45% of the initial amount at 100 and 150 µmol photons m^{-2} s^{-1}, respectively (**Figure 4.6**). This phenomenon could be due to the stationary phase which characterized all the culture in this investigation between the 10th and 12th days (**Figure 4.2A**).

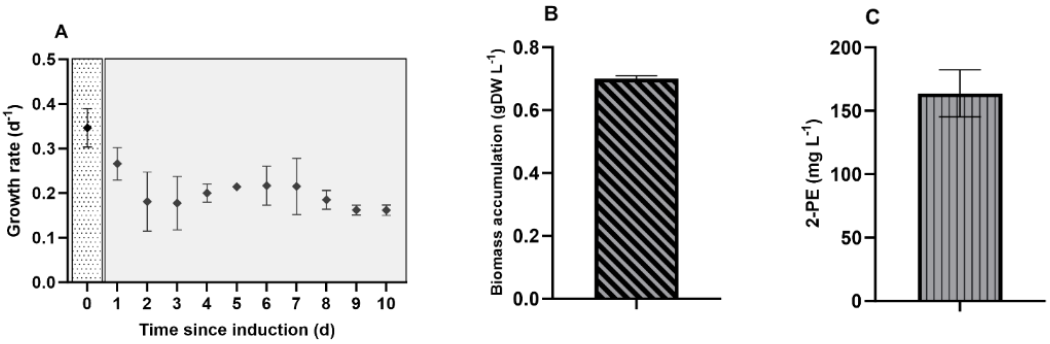
Figure 4.6. Phycocyanin profile over the time of the 2PE_aroK mutant strain exposed to four light conditions in batch mode. *All the tests were carried out as four biological replicates. Error bars represent standard deviation. The statistics was performed as two-way ANOVA (α ≤ 0.05). Asterisks express statistical significance. *, p-value ≤ 0.05; **, p-value ≤ 0.002; ***, p-value ≤ 0.0002; ****, p-value ≤ 0.0001.*



4.3.5. 2PE_aroK mutant characterization in turbidostat mode

One of the most promising light conditions tested in batch mode was selected for further analysis in turbidostat cultivation mode. The recombinant strain was subjected to semicontinuous cultivation as follow: 1% CO_2 (150 mL min^{-1} in N_2), 30°C and the periodical dilution was performed to keep the OD_{730} constant to 1 (± 3%), by adding fresh medium supplemented with 1 mM IPTG and 0.3 g L^{-1} L-Phe. The light condition was set at 150 µmol photons m^{-2} s^{-1}. This cultivation mode allowed to get knowledge about the combinatorial effect of light exposure and gene expression induction. **Figure 4.7A** reports the growth rate over the time before and after the gene expression induction within ten days of the production phase at 150 µmol photons m^{-2} s^{-1}. Noteworthy, the growth rate stabilized after two days since the gene expression induction, and on average it halved with respect of the growth rate before (**Figure 4.7A**, dotted box) the induction of the genes transcription, involved in 2-PE synthesis. This finding suggests that the induction of gene expression actually might provoke a slowdown of the cell fitness after the gene expression induction (**Supplementary Figure 4.4**). The final biomass production in this cultivation condition were found to be 0.7 gDW L^{-1} (**Figure 4.7B**), which resulted to be slightly improved if compared to the biomass accumulation in batch mode at the same light condition, i.e. 150 µmol photons m^{-2} s^{-1}. On the other hand, the 2-PE synthesis was severely reduced to 164 mg L^{-1} at the end of the test (**Figure 4.7C**), decreasing by 42% in 2-PE production abilities of the recombinant strain. The present operative modes comparison suggested that the batch cultivation outdid the turbidostat one taking into account both the growth and 2-PE biomanufacturing.

Figure 4.7. 2PE_aroK mutant strain under turbidostat cultivation mode at 150 µmol photons m^{-2} s^{-1}. *A) Growth rates calculated over the time before (dotted box) and after the gene expression induction and metabolite doping (grey box).* ***B****) Biomass accumulation as the sum of the biomass calculated from each turbidostat cycle.* ***C****) 2-PE production in turbidostat mode. All the experiments were performed by the means of biological triplicates. Error bars represent standard deviation.*



4.4. ***Discussion***

Although many cyanobacteria strains, both recombinant and wild-type, can be exploited for high-value compounds biomanufacturing, massive technical and scientific efforts have to be spent to develop an effective and sustainable bioprocess. Notoriously, the physiology of cyanobacteria and eukaryotic microalgae strongly changes when grown in photobioreactors if compared to the standard and comfortable laboratory equipment, e.g. Erlenmeyer flasks. Indeed, we can better control and tune many parameters in a photobioreactor, such as light exposure, light diffusion, CO_2 mixing, temperature and pH. Consequently, several biological factors (growth rate, target compound productivity, carbon uptake, etc.) could evolve differently during a scale-up process. Thus, a systematic analysis becomes obligatory to find the engineering rules suitable for a specific cyanobacteria-based bioproduction. Accordingly, often the light resulted to be the limiting factor mainly impacting on photoautotrophy-oriented bioprocesses. Here, we studied the production ability of a metabolically engineered strain of *Synechococcus elongatus* PCC 7942 to heterologously produce 2-PE in FMT150 photobioreactor (PBR), when subjected to different light intensities. The FMT150 PBR (Nedbal *et al.*, 2008) is a flat panel reactor system, in which the surface area per culture volume is maximized, so, it is the best

tool to study the effect of light irradiance to the cell physiology. The abovementioned mutant strain, already published, is capable of synthesizing 2-PE by overexpressing five genes (Usai *et al.*, 2022). **Table 4.1** reports the genetic features of this recombinant strain, also known as 2PE_*aroK*, and the relative protein products involved in this heterologous 2-PE bioproduction (**Figure 4.1**). The 2PE_*aroK* has been previously reported in *Chapter 3* to produce up to 285 mg L^{-1} 2-PE in three weeks when doped with 0.3 g L^{-1} L-Phe in laboratory scale (Usai *et al.*, 2022). Here, the 2PE_*aroK* mutant strain was subjected to four light intensities (100, 150, 300 and 500 µmol photons m^{-2} s^{-1}) and dark condition in a batch operational mode, constituted of two separate stages: i) growth and light acclimation stage (until culture reaches OD_{730} = 1); ii) 2-PE production stage (triggered by the addition of 1 mM IPTG and 0.3 g L^{-1} L-Phe as gene expression inducer and metabolite doper, respectively). As expected, the biomass accumulation increased as light intensity intensified (**Figure 4.2A, B**), but non-linearly (**Figure 4.2C**). Indeed, the growth rate at the highest photon flux grew only by 19% if compared to that at the lowest light condition. These data suggest a possible self-shading effect, where the high cell density (reaching around 1 gDW L^{-1}) reduces the light penetration into the vessel by negatively affecting further biomass production. Otherwise, no extra clues suggested any possible light stress event in each light exposure test, such as stress-related carotenoids, which were not statistically significant (**Supplementary Figure 4.3B**). However, a lowered biomass production did not correspond to a diminished 2-PE production and productivity (**Figure 4.3B, C**). Indeed, at the lowest two light conditions and at 300 µmol photons m^{-2} s^{-1} the 2-PE concentrations were the highest, ranging 260-282 mg L^{-1} (**Figure 4.3B**). Importantly, in the same conditions we reached the highest 2-PE productivity obtained so far via photoautotrophy (**Figure 4.3C**). Such an improvement in 2-PE productivity of 28.7 ± 3.4 mg L^{-1} d^{-1} at the best condition assessed represents one of the key achievements in our investigation, where the production time was dramatically reduced. On the other hand, at the highest light condition of 500 µmol photons m^{-2} s^{-1}, the 2-PE concentration resulted to be severely compromised by 30% of the highest 2-PE titer. This result is even more clear if considering the 2-PE yield normalized per g of dry biomass (**Figure 4.3D**). Thus, at the lowest light intensities less biomass is needed to obtain the highest 2-PE production. At 100 and 150 µmol photons m^{-2} s^{-1}, we achieved yields of 350 and 329 mg gDW^{-1} were, respectively, which are so far the highest 2-PE yield reported in photoautotrophic conditions (see **Table 4.2** for more details). Therefore, this study suggests how increasing the carbon flow through the photosynthesis does not lead

inevitably to the best performances, if considering the targeted production of a specific compound, while the excess of carbon and energy is preferentially regulated via biomass accumulation. This finding is consistent with some investigation previously reported in the literature concerning the competition between biomass and target product formation for metabolic precursors, showing that they could be mutually exclusive (Andreas, Michal and J., 2012; Du *et al.*, 2017; Du, Burbano, *et al.*, 2018; Pérez *et al.*, 2019). More in details, ATP and NADPH are produced during the photosynthesis in a ratio of 1.28 (Alric, Lavergne and Rappaport, 2010; Kugler and Stensjö, 2023), which is not enough to feed the Calvin–Benson cycle for carbon fixation (ATP/NADPH = 1.5) (Allen, 2003; Kugler and Stensjö, 2023), so, just at the beginning of the carbon metabolism an imbalance appears. Fortunately, the photoautotrophs evolved several alternative electron flow pathways, which is flexibly modulated on the basis of the metabolic demand (Nogales *et al.*, 2012). Obviously, other central routes generate ATP and reducing power (mainly as NADH), such as glycolysis and the TCA cycle. Here, theoretically, we exploited a feasible carbon sink for photoautotrophic production regime. Indeed, the 2PE_*aroK* mutant strain produces 2-PE by the alcohol dehydrogenase A using NADPH, as final step of the heterologous pathway (**Figure 4.1**). This strategy has been proposed as useful in easing the stoichiometric imbalance that could affect organisms while photosynthesizing under heterologous production systems (Erdrich *et al.*, 2014; Pérez *et al.*, 2019). An alternative strategy proposes the insertion of ATP-consuming steps (Erdrich *et al.*, 2014; Noguchi *et al.*, 2016). In the present study, the *aroK* gene overexpression by the 2PE_*aroK* mutant strain, led to overproduce the shikimate kinase, a protein involved in the shikimate pathway and consuming ATP as co-substrate. The effectiveness of the shikimate kinase overexpression was already reported as essential to really improve 2-PE production in 2PE_*aroK* mutant (*Chapter 3* (Usai *et al.*, 2022)), especially when compared to the previously described cyanobacterial mutants for 2-PE biomanufacturing (Ni *et al.*, 2018).

Additionally, we considered that the carbohydrate synthesis pathway is the most competitive, because cyanobacteria store glycogen as main transient energy reserve. Accordingly, we recorded an increased glycogen accumulation into the mutant biomass exposed to the highest photon fluxes (**Supplementary Figure 4.2**). As reported in the literature, many studies tried to impaired or disturbed the glycogen metabolism that often led, unfortunately, to severely weaken cellular fitness or cause overflow of intermediate metabolites (Eiji *et al.*, 2010; Gründel *et al.*, 2012; Cano *et al.*, 2018; Luan

et al., 2019). However, due to the high content in carbohydrates, as glycogen or starch (in eukaryotic microalgae), and proteins, the exhausted cyanobacterial/microalgal biomass might be interestingly utilized for further valorization as feedstock or additive for yeasts or bacterial fermentations (Aikawa *et al.*, 2014; Möllers *et al.*, 2014; Hays and Ducat, 2018; Comer *et al.*, 2020). In this regard, studying thoroughly the delicate relationship between the main carbon input, i.e. photosynthesis, and a target pathway becomes even more important, in order to balance all the resources in a photosynthetic microbial factory. Furthermore, our analysis about the carbon fate into the cell can help to add further insights into this topic (**Figure 4.4, 4.5, Table 4.3**). In fact, the carbon atoms becoming part of the 2-PE or biomass, could come from both CO_2 and L-Phe (supplemented as metabolite doper). As expected, at the highest light intensities assessed (i.e. 300 and 500 µmol photons m^{-2} s^{-1}) the amount of fixed carbon atoms was higher (**Figure 4.4B**). However, we noticed that the higher the light intensity the lower the L-Phe uptake (**Figure 4.4A**). A L-Phe uptake in wild-type *S. elongatus* PCC 7942 and other cyanobacteria strains has been previously reported (PING and MCAULEY, 1990; Usai *et al.*, 2022; Kukil *et al.*, 2023). The L-Phe uptake is energy-demand and mediated by an ABC-transport system (Labarre, Thuriaux and Chauvat, 1987; Quintero *et al.*, 2001). But to date, to the best of our knowledge, there are no further indications about the L-Phe employment once inside the cells. Thus, this topic is worth of additional investigations to be actually applied in aromatics bioproduction. On the other hand, we already speculated (Usai *et al.*, 2022) that the combination of some of the overexpressed proteins in 2PE_*aroK* mutant (*kivD* and *adhA* protein products) might reproduce a sort of Ehrlich pathway, usually exploited in yeast for the production of 2-PE starting from L-Phe (H. Liu *et al.*, 2019; Gu *et al.*, 2020; Dai *et al.*, 2021) (see *Chapter 3* for in-depth discussion). Nevertheless, this speculation provides no extra explanation about the massive effect of shikimate kinase (*aroK*) overexpression (located upstream to this putative Ehrlich pathway) on the 2-PE production. Moreover, the carbon balance analysis conducted in this study highlighted how the carbon atoms partition differently between the biomass and the target product (i.e. 2-PE) when the microbial cells were exposed to different light intensities. Firstly, the carbon atoms from CO_2 contributed mostly to this bioprocess in all the light conditions tested (**Figure 4.4C**), particularly, by 56% and 86% of the total carbon atoms used at the lowest and highest light intensities, respectively. In particular, at the highest light intensity up to 72% of carbon atoms were employed to build biomass instead of 2-PE (**Figure 4.5A**). Significantly, at the two lowest photon fluxes 50% and 45% of carbons were directed

to synthesize 2-PE (**Figure 4.5A**). Increasing the carbon partitioning towards the target compound so that it is ≥ 50% is one of the main target in creating a biomanufacturing process, necessary for qualifying such a strain as a microbial cell factory (C. *et al.*, 2012; Gao *et al.*, 2012; Savakis, Angermayr and Hellingwerf, 2013; Pérez *et al.*, 2019). In order to better understand to what extent the consumed L-Phe contributes to 2-PE production, we relied on the theoretical yield of 2-PE (C8) production from L-Phe (C9), i.e. 0.89 molC molC^{-1}. Significantly, at the highest light intensities of 300 and 500 µmol photons m^{-2} s^{-1} only 40% of the 2-PE could be synthesized from the consumed L-Phe in those conditions. Under the lowest photon fluxes the amount rose to 78% (**Figure 4.5B**). Such an evaluation can be considered only by assuming that the total amount of the consumed L-Phe was used to solely produce 2-PE, with no competition with biomass synthesis. However, these very interesting findings point out that even if the final 2-PE titer was lower at the highest light intensity, a larger proportion (at least the 60%) should be produced from CO_2 instead of L-Phe. This phenomenon inspires different observations and could be dissected from two different point of views. Traditionally, bioprocess engineering approaches are target compound-oriented, so, all the process stages are designed to maximize the productivity, by adopting ideal conditions, and synthetic media that provide excess of nutrients. On the other hand, the opportunity to exploit flue gas streams, at high CO_2 concentration (3-85% vol.) (Zieliński *et al.*, 2023), makes the CO_2 fixation abilities of cyanobacteria and microalgae even more attractive (Stewart and Hessami, 2005; Li *et al.*, 2011; Yen *et al.*, 2015). So, the design of ad hoc bioprocesses for flue gas recovery for stimulated CO_2 capture would be both economically and environmentally beneficial, even if, as in our case, the target molecule productivity would be partially reduced.

While the aim of this work was the characterization of the 2PE_*aroK* recombinant strain exposed to different light conditions, it is still important to stress the opportunities of an exhausted biomass coming from a photosynthesis-based bioprocess, where the target compound is not biomass-related but extruded into the culture broth. Indeed, cyanobacterial biomass is rich in photosynthetic pigments, and among them, phycocyanin (phy) is one of the most studied and it has a huge global market size, which will reach $6.3 billion by 2028 (Fernandes *et al.*, 2023). Over the year, the phycocyanin has been studied for anti-oxidation effect, anti-cancer and anti-inflammatory activity, photo-induced cytotoxicity and stimulating the immune system (Li *et al.*, 2010; Wang *et al.*, 2012; Pleonsil, Soogarun and Suwanwong, 2013; Zhu *et al.*, 2016). Besides the clinical potential applications, phycocyanin is largely required

for food and beverages, nutraceutics and cosmetics (Fernandes *et al.*, 2023). Biologically, phycocyanin is a pigment-protein complex and a major component of cyanobacterial light-harvesting antenna, which optimizes light energy gathering, where the chlorophyll cannot absorb. Accordingly, the quality and intensity of the light significantly influence the light-harvesting system of cyanobacteria, affecting mostly the accumulation of the photosynthetic pigments (Szwarc and Zieliński, 2018; Hsieh-Lo *et al.*, 2019). Therefore, when the light is low enough the production of phy is intensified to catch as much light as possible. Accordingly, we quantified a higher amount of phycocyanin in the biomass grown at the lowest light intensities (**Figure 4.6**). At the moment of the gene expression induction, the phy amount counted for 44 and 45 mg gDW^{-1} at 100 and 150 µmol photons m^{-2} s^{-1}, respectively. Afterwards, the phy amount decreased by 24% and 45% at the end of the experiment (**Figure 4.6**, 10^{th} day), probably indicating the beginning of the stationary phase, as shown for the growth kinetics in **Figure 4.2A**. At the highest light conditions, phy was lowered and at the end of the tests the amount was reduced over by 50% (**Figure 4.6**). About the chlorophyll a (chla) and carotenoids (car) no particular trends were detected, and the results were shown in **Supplementary Figure 4.3A, B**. The evolution over the time of the cellular composition about the photosynthetic pigments can be adopted as a physiological parameter to detect potential stress conditions, such as light excess or nutrient depletion, affecting the culture fitness. The present study has been conducted in excess of nutrients and CO_2, in standard synthetic medium, in order to focus on the light effect. Indeed. As mentioned earlier, the pigments composition did not indicate any light stress of the mutant biomass.

Subsequently to the batch tests, the best light condition (150 µmol photons m^{-2} s^{-1}) was compared to turbidostatic growth mode, to furtherly elucidate the relationship between the carbon metabolic rate influenced by photosynthesis and 2-PE synthesis, as interdependency in this bioprocess. Since the culture density inside the PBR is kept constant (± 3%) in turbidostat, the effect of the light intensity on the cyanobacteria physiology can be better studied over the time, avoiding the self-shading effect. In this study the turbidostat mode started ca. 24-48 h before the gene expression induction and metabolite doping (**Supplementary Figure 4.4**), in order to acclimate the culture to both the light and the cultivation mode. As in the batch mode, the gene expression and metabolite doping were activated by adding 1 mM IPTG and 0.3 g L^{-1} L-Phe, respectively. The periodical dilutions to maintain the cellular density constant were performed with standard medium supplemented with 1 mM IPTG and 0.3 g L^{-1} L-Phe,

not to washout the two molecules during this semicontinuous mode. The effect of the gene expression of the 2-PE heterologous pathway easily conveyed as a decrease in the growth rate of the mutant culture (**Figure 4.7A**). The growth rate stabilized from the 2nd day at an average value of 0.17 ± 0.02 d^{-1} (**Figure 4.7A**, grey box), which is almost half of one measured before inducing gene expression (**Figure 4.7A**, dotted box). While the biomass production was only slightly improved (**Figure 4.7B**) compared to the batch cultivation at the same light intensity (**Figure 4.2B**, **Table 4.2**), the 2-PE production was significantly affected with a reduction of more than 40% compared to the 2-PE titer obtained in batch mode (**Figure 4.7C**). Consequently, the volumetric productivities were also disturbed, counting for 16.4 mg L^{-1} d^{-1}, 1.75-fold lower than that recorded in the batch study. Thus, as already postulated for the high light conditions, increasing the metabolic rate at the photosynthesis level furtherly uncoupled the carbon flux into the heterologous 2-PE biosynthetic pathway, dramatically affecting the final 2-PE production. For all these reasons, no extra higher light intensities have been considered, while the main goal to be achieved was to find the optimal as well as the most advantageous and least energy-consuming process conditions to produce 2-PE.

Overall, our work is consistent with similar studies reported in the literature (Andreas, Michal and J., 2012; Du *et al.*, 2017; Du, Burbano, *et al.*, 2018; Pérez *et al.*, 2019) and provides useful information on design strategies for bioprocess based on engineering photosynthetic microorganisms, which heterologously produce a target product partially uncoupled from biomass production.

Finally, the data and information collected here could be used for building *in silico* models both metabolic and chemical-physical, to predict the behavior of this biocatalyst when subjected to different process conditions, including cultivation or nutritional modes or geometrically different PBRs.

4.5. Conclusions

Although the bioprocess engineering requires several challenging steps and appears occasionally frustrating, the intricate interaction of biological and chemical-physical systems can result in a charming phenomenon. On the whole, these scientific and engineering efforts make it possible to rationalize the resources dedicated to the implementation of an efficient microbial platform. Here, those efforts and implications related to the bioproduction of 2-PE (2-phenylethanol), utilizing a metabolically

engineered strain of *Synechococcus elongatus* PCC 7942, were technically discussed. The investigation spotlighted the non-obvious relationship between photosynthesis, biomass formation and heterologous production of a target compound, under varying the light intensity. Therefore, we experimentally demonstrated that the highest light intensity did not result in the highest 2-PE production. Only the biomass accumulation improved, as expected. Furthermore, the carbon consumption analysis pointed out at an intricate carbon partitioning. The highest amount of carbon atoms allocated to 2-PE were measured under the lowest light intensities. Intriguingly, under the highest light conditions the supplied CO_2 contributed more than phenylalanine to the 2-PE production, even if the total 2-PE production was reduced (by 30%). Overall, the study showed that if fine-tuned a bioprocess can effectively acts as microbial factory, whose carbon balance counted for 45-50% in 2-PE under the most performing conditions. Importantly, the darkness production tests confirmed that the light still remains the driving force behind the whole biomanufacturing process. In addition, since the target product here is secreted in the cultural medium, a huge amount of spent cell biomass can be further valorized. Indeed, cyanobacteria biomass possesses several valuable compounds, such as photosynthetic pigments. Thereby, we also suggested how to exploit those biomasses starting from pigments extraction up to the utilization as substrate or additive for other fermentation cultivations. Overall, these findings highlight the potential of a more finely tuned bioprocesses with the purpose to harnessing the effectiveness of photosynthetic microorganisms in biomanufacturing processes.

List of abbreviations:

2-PE: 2-phenylethanol

SKP: shikimate pathway

Phe: phenylalanine

***aroK*:** gene encoding for Shikimate Kinase

IPTG: Isopropyl β-D-1-thiogalactopyranoside

PBR: photobioreactor

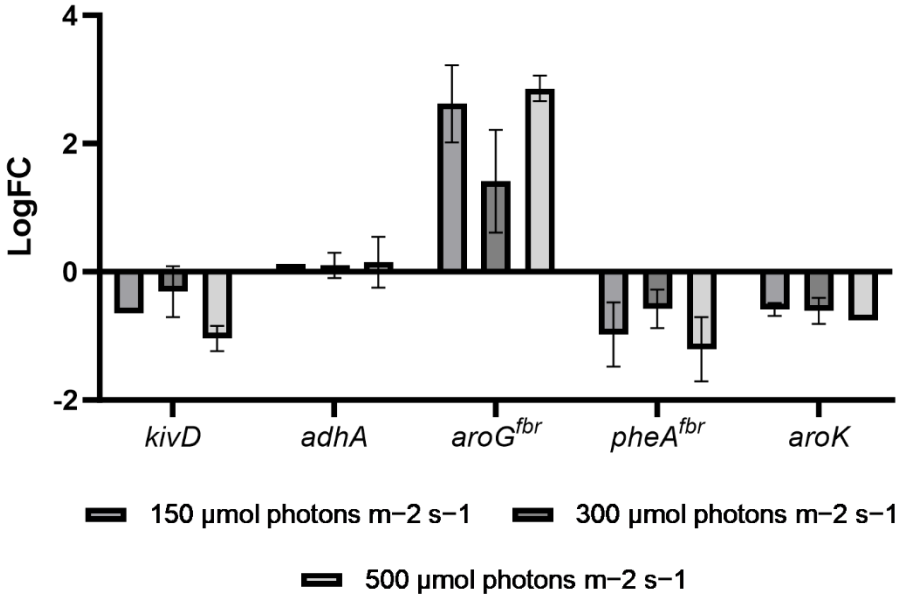
Chla: chlorophyll a

Car: carotenoids

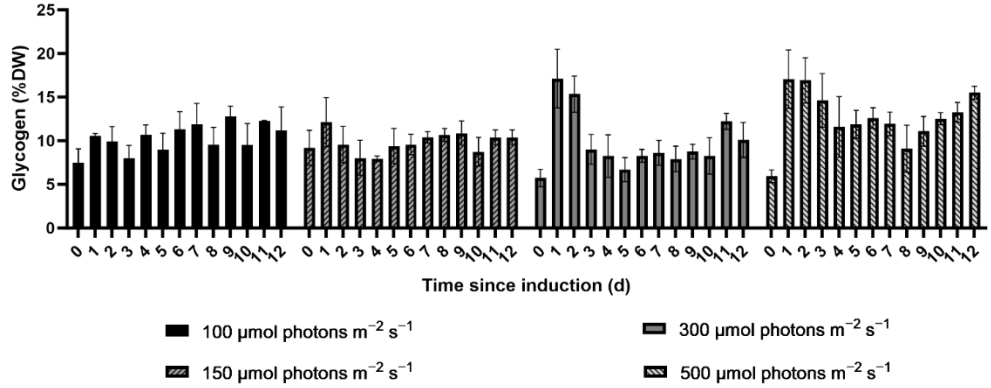
Phy: phycocyanin

*4.6. **Supplementary Materials***

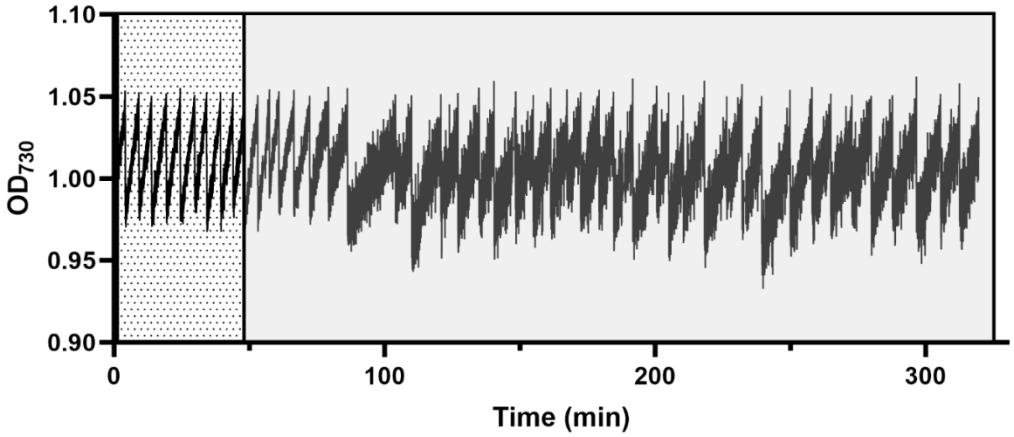
***Supplementary Figure 4.1. Gene expression analysis by qRT-PCR**. prs gene was used as reference gene and the lowest light condition was adopted as control condition. The analysis was conducted from the biomass harvested five days since the gene expression induction. Data are expressed as log(2^−ΔΔCt) ± standard deviation of the four biological replicates.*



***Supplementary Figure 4.2. Glycogen content in the biomass of 2PE_aroK mutant strain exposed to four light conditions**. The results are reported as glycogen percentage of the dry biomass over the time since the gene expression induction. The analysis was conducted on four biological replicates and the error bars indicate standard deviation.*



Supplementary Figure 4.3. Turbidostat pattern of the cellular density (expressed as OD_{730}), before (dotted box) and after (grey box) the gene expression induction.



Gene	Definition	Gene Type	Primer Sequence (5'-3')		Size
			Forward	Reverse	
prs	ribose-phosphate pyrophosphokinase	Reference	TCTTGCCCTACTACGGTTACGC	TCGCTCCAGCCTGAGTGATTAG	247
kivD	phenylpyruvate decarboxylase	Target	TCATCATCAACAACGACGGC	GCTGGCTAAAGAAGACGCTC	240
adhA	alcohol dehydrogenase A	Target	ACTTTGTTGGGGTGGTGTTG	ACTATGGCTGAGCACTACCC	239
aroG^{fbr}	DAHP synthase, feedback-inhibition-resistant	Target	CTGACGTTTGCCAGCAGATT	GCATTCGCCAGTTGACGTAA	184
pheA^{fbr}	chorismate mutase/prephenate dehydratase, feedback-inhibition-resistant	Target	GCGACAAAACTTCACCCGAT	CCAGACGGGGCATAATCAGA	167
aroK	shikimate kinase	Target	GCAAATCGAAACGCAGGTCT	CCGGAGCCTCAGTTTGTAGA	203

Supplementary Table 4.1. Genes employed for qRT-PCR analysis*. For each gene, the name, acronym, and nucleotide sequences for both Forward (F) and Reverse (R) primers are reported in the table.*

Chapter 5

5. Scale Up Of Photosynthetic 2-Phenylethanol Bioproduction In Photobioreactor: Opportunities And Challenges

Part of the research activity described in this chapter has been conducted at the Centre Algatech (Institute of Microbiology, Třebon, Czech Republic), under the kind supervision of Pavel Hrouzek (Ph.D), in the group of algal biotechnology.

5.0. Abstract

Microalgae are microorganisms that converts sunlight and carbon dioxide into oxygen and biomass that serves as food, feed and fuels. Microalgae and cyanobacteria mass cultivations are emerging as a worldwide industry but still face bottlenecks in contributing to the global economy. One of the most challenging limitations is the translation of the microscopic world of microalgae and the scale-up to a million times higher. The study focused on scaling up the production of 2-Phenylethanol (2-PE) by a recombinant strain of *Synechococcus elongatus* PCC 7942 (2PE_*aroK*) in different PBR configurations, including stirrer tanks, airlift flat panels, aquarium flat panels, and annular columns. 2-PE is a high-value aromatic compound, characterized by a rose scent and, so, widely employed as fragrance in the food and cosmetics industry. The study revealed that closed systems exhibit higher biomass productivity and growth rates, emphasizing the importance of PBR design in optimizing light distribution and minimizing energy consumption. Particularly the airlift flat panel showed the best performances as biomass productivity 0.226 gDW L^{-1} d^{-1}, while the 2-PE production resulted possible only in the stirrer tank, counting for 119 mg L^{-1} in four days. Unfortunately, biological contamination issues were faced in higher-scale PBRs, particularly the impact on 2-PE synthesis and strategies for prevention. The study also delved into the challenges of sterilization procedures and the potential of environmental stressors, such as high pH and high salinity, in controlling contaminations. Overall, the research suggests that a combination of diverse strategies, tailored to the specific physiology of the biocatalyst and contaminants, is essential for the successful implementation of photosynthesis-based bioprocesses in large-scale cultivation systems.

5.1. Introduction

Eukaryotic microalgae and cyanobacteria have emerged as promising alternatives for sustainable renewable production system, which need no arable lands for cultivation and can thrive on industrial wastewaters and flue gases. Currently, the microalgae market is dominated by the production of carotenoid pigments (e.g. β-carotene and astaxanthin), omega-3 fatty acids, and proteins. Despite being a relatively small industry globally, the interest and number of biotechnology companies in this field are steadily increasing (Araújo *et al.*, 2021). The European Algae Biomass Association (EABA) estimates the economic value of the microalgae field to be around € 850 million per year (*Blue bioeconomy – towards a strong and sustainable EU algae sector*, 2023).

Three primary methods of large-scale cultivation of microalgae and cyanobacteria are exploited now. Historically, phototrophic cultivation mainly focused on microalgal cultures in open ponds. While they are easy to build and relatively inexpensive, open ponds suffer from high contamination risks, require large land area and strictly depend on seasonality and weather conditions. On the other hand, the closed systems, usually known as photobioreactors (PBRs), offer several advantages (Pham *et al.*, 2017), despite they are more costly. More in details, PBRs are built with a high ratio of surface area to volume, in order to maximize the light exposure of microalgal culture. Often, PBRs are thought to be modulable, aim at increasing the culture volume and reduce the land area occupied by the PBRs, especially when artificially illuminated. Additionally, several parameters, such as light, CO_2, pH and temperature, can be finely tuned (Singh and Sharma, 2012), and the contaminations are minimized (Y. Wang *et al.*, 2016), although still possible. The last adopted method for microalgae cultivation regards biofilms (Bozan, Schmid and Bühler, 2022). They are inexpensive, require very little or no dewatering, and suitable for co-culture and complex consortia, including bacteria (Roostaei *et al.*, 2018).

The challenges associated with the scale-up of microalgae cultures have already been extensively discussed by various authors (da Silva and Reis, 2015; Borowitzka and Vonshak, 2017; Kamravamanesh *et al.*, 2019; Novoveská *et al.*, 2023). Particularly, biological contaminants are significantly impactful in mass microalgae cultivation (Zhu, Jiang and Fa, 2020), mainly in open ponds, but even the cultivation in enclosed PBR systems can be inflicted by this plague. Several mitigation and control approaches have been investigated and proposed as possible solutions, e.g. filtration, chemical treatment with pesticides or other additives, and changing environmental parameters

(Wang *et al.*, 2013; Krug *et al.*, 2019). Therefore, long-term production can be sustained under extreme conditions, such as high salinity, high or low pH, etc. (Parmar *et al.*, 2011; Deore, Beardall and Noronha, 2020; Di Caprio, 2020), depending on the specific requirements of both target and contaminant strains. Consequently, cleaning and sterilization procedures occupy a prominent role to prevent biological pollutants. Autoclaving and filtration of the growth media are feasible for working volume ≤ 20 L (Arndt and Sommer, 2014), while for higher volume UV radiation and ozonation are usually applied (Summerfelt, 2003). The PBRs, typically, are washed with chemicals, such as hypochlorite, for disinfection. However, the excessive applications of synthetic chemicals could potentially become hazard to the global environment and human health. Furthermore, based on the material and shape, the PBRs can have different blind angles, such as the gas injector, the pipe connections and the sampling systems, compromising the cleaning process. Those spots represent, therefore, the very source of contaminations, where biofilm accumulates, and spores and eggs deposit. For all these reasons, many studies have been focusing on the development of practical methods to improve *in situ* cleaning/sterilization of PBRs, here some interesting reports (Nawar *et al.*, 2017; Morselli, N.; Altunoz, M.; Puglia, M.; Arru, L.; Tartarini, 2019; Keyvan Hosseini *et al.*, 2023).

In the present Chapter, four geometrically different PBR systems, from laboratory to pilot scale, have been assessed to implement a photosynthetic microbial cell factory, based on a metabolically engineered strain of *Synechococcus elongatus* PCC 7942, i.e. 2PE_*aroK*. The 2PE_*aroK* strain has been published in Usai *et al.*, 2022 (Usai *et al.*, 2022) and extensively described in *Chapters 3* and *4*. The gene and protein features of the recombinant strain are reported in **Table 5.1**. The strain shows enhanced ability to heterologously synthesize 2-Phenylethanol (2-PE), an aromatic molecule characterized by a powerful smell of rose and, so, mainly employed as fragrance (Gosset, 2009; Nielson, Machas and Mckenna, 2018). The PBRs configurations investigated in the present study were: i) 4-L stirrer tank; ii) 6-L airlift flat panel; iii) 20-L conventional flat panel (aquarium); iv) 30-L annular column (internal illumination). The scale up tests were conducted by evaluating both the cyanobacterial growth kinetics and 2-PE production ability.

5.2. Materials and Methods

5.2.5. Cyanobacteria recombinant strain for 2-PE production in large scale

The recombinant strain of *S. elongatus* PCC 7942, called 2PE_*aroK*, previously developed by us (Usai *et al.*, 2022) was used for the scale up experiments. **Table 5.1** described the gene and protein features that the mutant strain carries out. The 2-PE synthesis was started by adding to the mutant culture, when optical density equal to 1, 1 mM IPTG and 0.3 g L-1 L-Phe, as gene expression inducer and metabolite doper, respectively.

5.2.6. Inoculum preparation for PBRs

All the PBRs were seeded with ca. 10% of the total working volume of the PBRs. The inoculi were grown on BG11: 1.5 g L^{-1} $NaNO_3$, 0.075 g L^{-1} $MgSO_4 \cdot 7H2O$, 0.004 g L^{-1} $FeCl_3 \cdot 6H2O$, 0.04 g L^{-1} K_2HPO_4, 0.036 g L^{-1} $CaCl_2$, 0.024 g L^{-1} $Na_2EDTA \cdot 2H_2O$, 2.86 mg L^{-1} H_3BO_3, 1.81 mg L^{-1}, $MnCl_2 \cdot 4H_2O$, 0.39 mg L^{-1} $Na_2MoO_4 \cdot 2H_2O$, 0.22 mg L^{-1} $ZnSO_4 \cdot 7H2O$, 0.05 mg L^{-1} $CuSO_4 \cdot 5H_2O$, 0.03 mg L^{-1} $Co(NO_3)_2 \cdot 6H_2O$. Finally, the growth medium was supplemented with 10 mM sodium bicarbonate as buffering system with 20 µg mL^{-1} spectinomycin and 10 µg mL^{-1} kanamycin. Starting from 50 mL Erlenmeyer flasks, the seed cultures were grown in increasing volume up to 1 L Erlenmeyer flasks at 30 °C 130 rpm and constant illumination of 30 µmol photons m^{-2} s^{-1}. For the largest PBRs, the flask cultures were also cultivated in 400 mL cylinders in a glass vessel with a water bath at 30°C and each cylinder was constantly bubbled with 1% CO_2 enriched air and irradiated at 100 µmol photons m^{-2} s^{-1} as light intensity. The PBRs described and used in the present chapter are: i) stirrer tank; ii) airlift flat panel; iii) conventional flat panel, here called 'Aquarium'; iv) annular column. The main features as well as the advantages and disadvantages of each PBR are reported in **Table 5.2**.

5.2.7. Scale Up tests for cultivating 2PE_aroK mutant strain in pilot scale

5.2.7.1. Stirrer Tank

The adopted stirrer tank is a Solaris Jupiter 4.0 (https://www.solarisbiotech.com/en/). It consists of a 4L jacketed borosilicate glass vessel, equipable with temperature, dO2, pH and cell density sensors (**Figure 5.1**). The thermoregulation is performed with heating blanket and cooling finger. The working volume is 3 L and the height to

diameter ratio is 3:1. The stirring was performed with a brushless motor. It was sterilized by autoclaving (121°C, 40 min). All the tests were conducted in batch mode, at 33°C, 150 ml min^{-1} 1% CO_2 in N_2. The stirring was assessed from 30 to 100 rpm. The light was provided by an external home-made LEDs panel, equipped with both warm and cold white light, and was studied between 40-250 µmol photons m^{-2} s^{-1}. The regime operation was conducted with photon flux at 250 µmol photons m^{-2} s^{-1} and 30 rpm. The cellular population was daily monitored by recording the OD at 730 nm and converted in biomass as g of dry cell weight per L of culture (gDW L^{-1}), by using the conversion factor of 0.26 previously determined in our laboratory. The culture was daily checked at the optical microscope in order to assess contaminations.

5.2.7.2. Airlift Flat Panel

The Airlift Flat Panel (**Figure 5.4, 5.5**) was provided by Subitec GmbH (Köngen, Germany, https://subitec.com/en/home/). The working volume is 6 L and it is made of plastic transparent material and has 0.6 m^2 of surface exposed to the light. The air is injected through a microsparger at the bottom of the panel. The air generates a flow to the top and thanks to the downcomer compartment, the liquid comes back to the bottom (**Figure 5.4B**). The geometrical configuration (**Figure 5.4A**) assures simultaneously a horizontal and vertical mixing and results to be a homogeneous as well as gentle mixing for the cell culture. Additionally, this gas supply set up increases the CO_2 mass transfer trough the injection of microbubbles, increasing the residence time. The present test was conducted in batch mode with a constant gas supply (1% CO_2 in air) and illuminated by one side (150 µmol photons m^{-2} s^{-1}), at 30°C. The cellular population was daily monitored as described above. The optical microscope was used to check for contaminations. The panel was sterilized with 70% ethanol over-night, bubbled by air, then was twice washed with sterile water.

5.2.7.3. Aquarium Flat Panel

The Aquarium flat panel is a conventional flat panel (https://www.alga.cz/en/a-106-centre-algatech.html). It consists of a glass vessel able to hold 20 L as working volume and a light path of 15 cm (**Figure 5.7**). The vessel is fully equipped with sensors for pH, OD, O_2 and temperature. The gas was injected through a tube without a sparger, and the mixing relies on the gas supply itself. The CO_2 injection is pH-dependent; thus, the CO_2 is supplied only when the pH runs over a settled threshold. The temperature is controlled by heat exchange coils. The pool of tests ran in Aquarium was conducted in

batch mode with a constant air bubbling at 30°C. The light panel was initially set at 150 µmol photons m^{-2} s^{-1} at the moment of the inoculum and then daily increased as the biomass grew. The cellular density was daily monitored as described above. The optical microscope was used to check for contaminations one or twice per day. The vessel was sterilized with bleach over-night, bubbled by air, then was twice washed with sterile water just before the test.

5.2.7.4. Annular column

The Annular column PBR was designed and developed in the Centre Algatech (Třebon, Czech Republic; https://www.alga.cz/en/a-106-centre-algatech.html) and thoroughly described in (Ranglová *et al.*, 2022) (**Figure 5.9**). Briefly, it is made of transparent PLEXIGLAS XT: height 70 cm; outer diameter 40 cm; an inner diameter 30 cm. The cultivation layer is thick 4.5 cm, and because of the short light path it can be considered a different configuration of a flat panel (Ranglová *et al.*, 2022; Štěrbová *et al.*, 2023). The light source is internal and the light intensity that could be achieved is 1600 µmol photons m^{-2} s^{-1}. The tests were performed in batch mode with 1% CO_2-enriched air constantly bubbled, which also represented the mixing force. The working volume was 30 L and the working temperature was 30 °C. The column was sterilized with bleach over-night, bubbled by air, then was twice washed with sterile water just before the test.

5.2.8. 2-PE and L-Phe HPLC analysis

2-PE and L-Phe were quantified as described in both the previous *Chapters* (Usai *et al.*, 2022).

Gene	*HR Site*	*Protein*	*EC number*	*Reaction*	*Organism*	*Ref.*
aroG^{fbr}	NSI	feedback-inhibition resistant DAHP synthase	EC 2.5.1.54	PEP + E4P + H_2O ⇌ DAHP + Pi	*Escherichia coli*	(Ni *et al.*, 2018; Usai *et al.*, 2022)
pheA^{fbr}	NSI	feedback-inhibitionresistant chorismate mutase/prephenate dehydratase	EC 5.4.99.5/ EC 4.2.1.51	Chorismate ⇌ Prephenate ⇌ Phenylpyruvate + H_2O + CO_2	*Escherichia coli*	(Ni *et al.*, 2018; Usai *et al.*, 2022)
kivD	NSI	Phenylpyruvate decarboxylase	EC 4.1.1.43	Phenylpyruvate ⇌ phenylacetaldehyde + CO2	*Lactococcus lactis*	(Ni *et al.*, 2018; Usai *et al.*, 2022)
adhA	NSI	Alcohol dehydrogenase A	EC 1.1.1.1	Phenylacetaldehyde + NAD(P)H ⇌ 2-Phenylethanol + $NAD(P)^+$	*Synechocystis PCC 6803*	(Ni *et al.*, 2018; Usai *et al.*, 2022)
aroK	NSII	Shikimate kinase	EC 2.7.1.71	Shikimate + ATP ⇌ Shikimate-3-P + ADP	*S. elongatus PCC 7942*	(Usai *et al.*, 2022)

Table 5.1. Genetic features of 2PE_aroK recombinant strain of S. elongatus PCC 7942. *HR, homologous recombination; NS, neutral site; DAHP, 3-deoxy-7-phosphoheptulonate; PEP, phosphoenolpyruvate; E4P, erythrose-4-phosphate.*

Type	*Temperature Control*	*Mixing*	*Gas exchange*	*Features*
Stirrer Tank	Heat exchanger/ reactor jacket	Stirrer/impeller	Gas injected through sparger (N_2 + 1% CO_2)	Low surface/volume ratio, low light penetration and low productivity. Easy to manage; axenic controllability; low cleaning cost; high energy consumption.
Airlift Flat panel	Thermostatic room	Airlift/bubbles	Gas injected through microsparger (Air + 1% CO_2)	Large surface/volume ratio; high biomass productivity; Potential hydrodynamic stress; modulable; photoinhibition; high cleaning cost; low energy consumption.
Flat panel 'Aquarium'	Heat exchange coils	Bubbles	Gas injected through sparger (Air + 1% CO_2)	Large surface/volume ratio; high biomass productivity; modulable; Potential hydrodynamic stress; photoinhibition; low energy consumption.

Annular column	Heat exchange coils	Bubbles	Gas injection (Air + 1% CO_2)	Large surface/volume ratio; high biomass productivity; Potential hydrodynamic stress; photoinhibition; high cleaning cost; low energy consumption.

Table 5.2. Main features of the photobioreactors used in this investigation.

5.3. Results

5.3.5. Setting parameters in stirrer tank PBR with external light source

Figure 5.1 shows the 2PE_*aroK* mutant culture in a 4L stirrer tank at low (**A**) and high (**B**) cellular density. A first round of experiments was devoted to set all the parameters involved in cultivation, mainly light exposure and mixing. The light was provided as external light source equipped with both warm-white and cold-white LEDs. The mixing was allowed as mechanical stirrer with a Rushton turbine impeller. 1% CO_2 in N_2 was constantly bubbled through a sparger located at the bottom of the vessel. To avoid a high shearing effect, the agitation, expressed as rotation per minute (rpm), was gradually rose as the cyanobacterial culture grew (**Figure 5.2A**), starting with 30 rpm up to a maximum of 100 rpm. The stirring value over 100 rpm completely destroyed the cyanobacterial culture (data not shown). **Figure 5.2B** reports the results of this study by comparing the growth with the light exposure. The presence of a diauxic growth curve is evident, in which light supply (**Figure 5.2B**) appeared to have an impact on the growth more than the mixing (**Figure 5.2A**). Thereby, these two separate stages were detected with different growth factors. During the first part of the setting experiments (pink box) the bacteria have a growth rate of 0.35 ± 0.001 d^{-1} corresponding to 2.2 d of doubling time (Dt) and a biomass productivity of 0.061 ± 0.0004 gDW $L^{-1}d^{-1}$ (**Figure 5.2C**). The second phase (blue box) was characterized by a growth rate of 0.087 ± 0.025 d^{-1}, ca. 4-fold decrease even if the light was 40% higher than that in the previous days of cultivation. At the end of the experiment the biomass accumulation counted for 0.68 ± 0.002 gDW L^{-1}. For photosynthesis-based bioprocess the low surface-to-volume ratio, unfortunately, strictly affect the entire process, due to the limited exposure of the cyanobacterial cells to the light source, especially when the cellular density is high, causing the self-shading effect (Agustí, 1991).

Figure 5.1. Solaris Jupiter Stirrer Tank PBR used in this study. *The illustration shows the PBR at the moment of the inoculum (**A**) and at the end of the test (**B**).* https://www.solarisbiotech.com/en/.

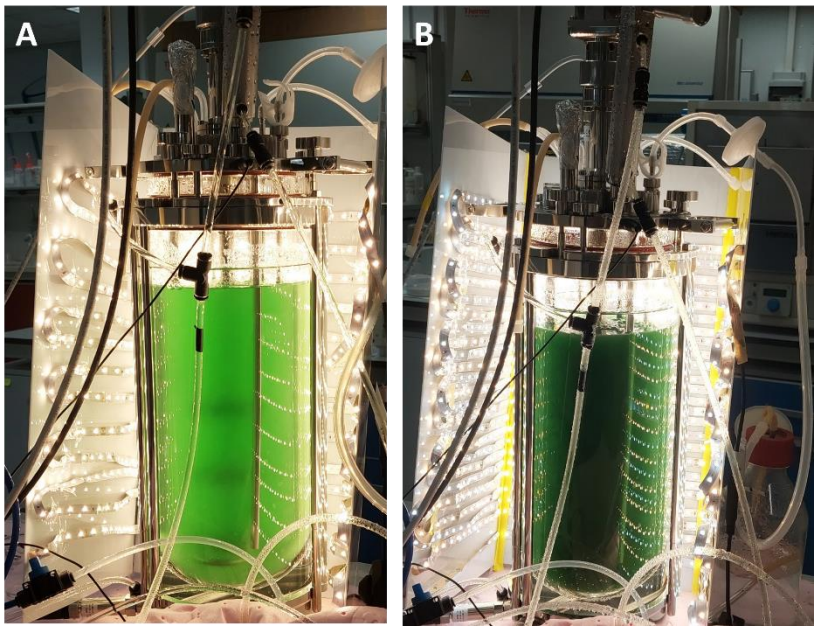
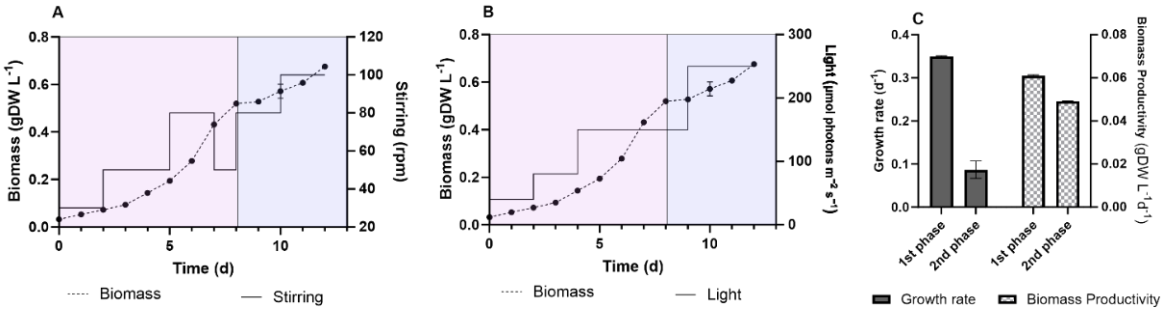


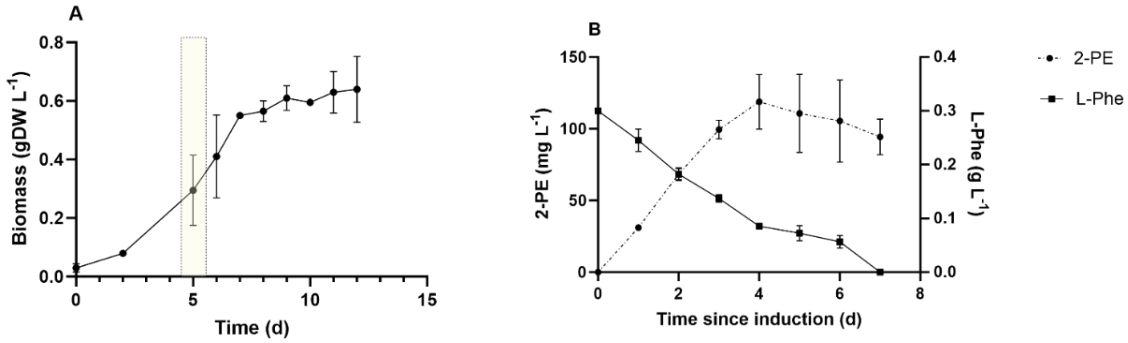
Figure 5.2. Set up of the main parameters related to their effect on the biomass production*. **A**) relationship between stirring force and biomass; **B**) relationship between light intensity and biomass. **C**) growth rate (grey bar) and biomass productivity (dotted bar) in the 1st and 2nd phases of the test.*



5.3.5.1.2-PE production by 2PE_aroK recombinant strain in 4-L stirrer tank

Once the parameters were settled, we conducted the 2-PE production as follow. To avoid any possibility of shear stress, we decided to set the stirring constant at 50 rpm. Due to the low light capture capacity of the stirrer tank, we chose to set the light as high as possible (250 µmol photons m^{-2} s^{-1}) with respect of the LEDs panel ability. The 2-PE production was started by adding into the tank 1 mM IPTG and 0.3 g L^{-1} L-Phe, as gene expression inducer and metabolite doper, respectively, as already described in *Chapter 3* and in (Usai *et al.*, 2022). The biomass accumulation profile confirmed the same trend as reported in the previous section, with an average biomass concentration of 0.64 ± 0.11 gDW L^{-1} (**Figure 5.3A**). At the highest production point (four days since the gene expression induction) the 2-PE concentration was 119 mg L^{-1} and all the available L-Phe was consumed (**Figure 5.3B**). This data resulted to be 2.4-fold lower than previously reported in the *Chapter 3* and *4,* but, curiously, the 2-PE volumetric productivity remained high 29.75 mg L^{-1} d^{-1} , resulting in a drastic reduction in production time.

Figure 5.3. 2-PE production of the 2PE_aroK mutant strain in stirrer tank. ***A)*** *biomass accumulation during the gene expression induction and metabolite doping, the box highlights the day of induction;* ***B)*** *2-PE production (●) and L-Phe consumption (■) profiles. Error bars represent standard deviation. The test was carried out by the means of three biological replicates.*



5.3.6. 2PE_aroK recombinant strain in pilot scale PBRs

5.3.6.1.Airlift Flat Panel – preliminary test

For this study an air lift flat panel was adopted (https://www.subitec.com/en/) (Bergmann *et al.*, 2013). The geometry of this device allows to maximize surface/volume ratio, increasing the light exposure and efficiently mixes the culture. The 1% CO_2 in air was provided by a microsparger, optimizing the contact surface of the gas bubbles. Moreover, the Airlift technology leads a special geometry that efficiently homogenizes the culture inside the PBR as shown in **Figure 5.4**. The light source was set by one side of the PBR at 150 µmol photons m^{-2} s^{-1} and kept it constant. **Figure 5.5** shows the cyanobacterial culture into the PBR at the moment of the inoculum (**A**) and at the end of the experiment (**B**). In this experiment we measured a growth rate of 0.62 d^{-1} (Dt = 1.11 d; **Figure 5.6B**), which allowed to reach 0.64 gDW L^{-1} in just two days (**Figure 5.6A**) and a biomass productivity of 0.226 gDW $L^{-1}d^{-1}$ (**Figure 5.6B**). Unfortunately, biological contaminations, which completely crashed the culture, emerged at the moment of the gene expression induction and metabolite doping. For this reason, no extra replicate was performed in this PBR, and the related data should be intended as preliminary. Nevertheless, it greatly showed its potentialities in photosynthesis-based bioproduction, especially for biomass accumulation.

***Figure 5.4. Airlift Flat Panel configuration**. **A**) illustration of the patented technology. **B**) Example of how the geometrical configuration allows the efficient mixing that characterizes this PBR. https://subitec.com/en/home/.*

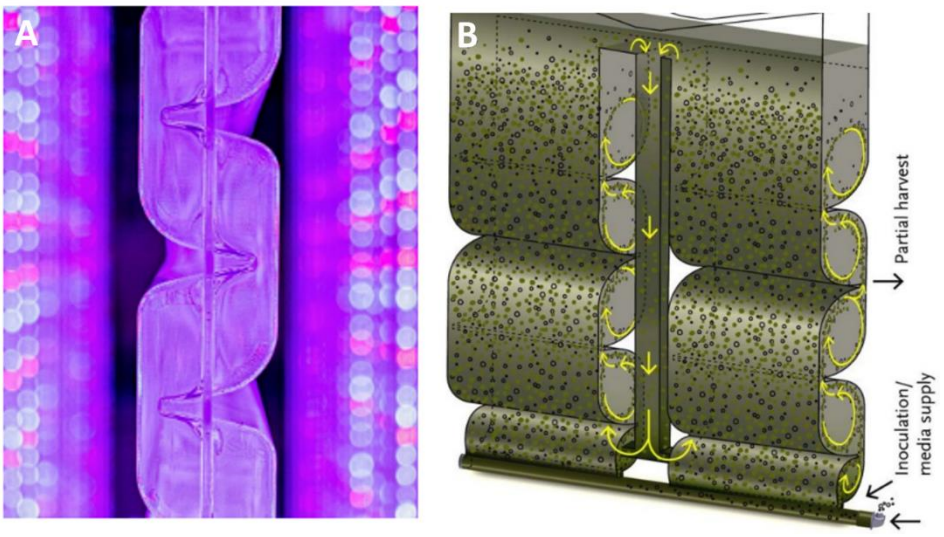


Figure 5.5. Realistic picture of the Airlift flat panel used in this study. *The picture illustrates the panel at the moment of the inoculum (**A**) and at the end of the study (**B**).*

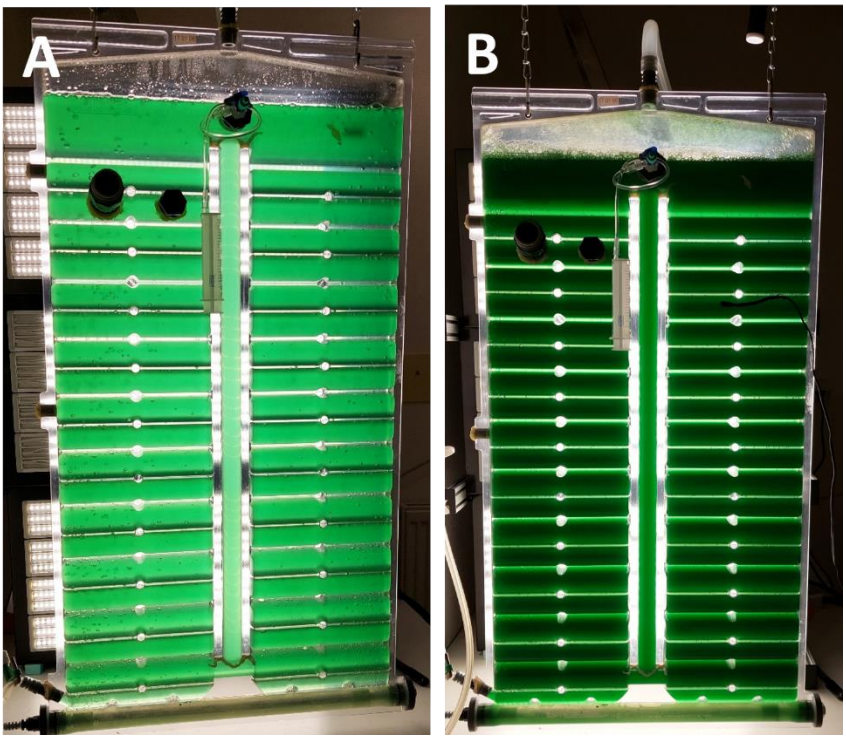
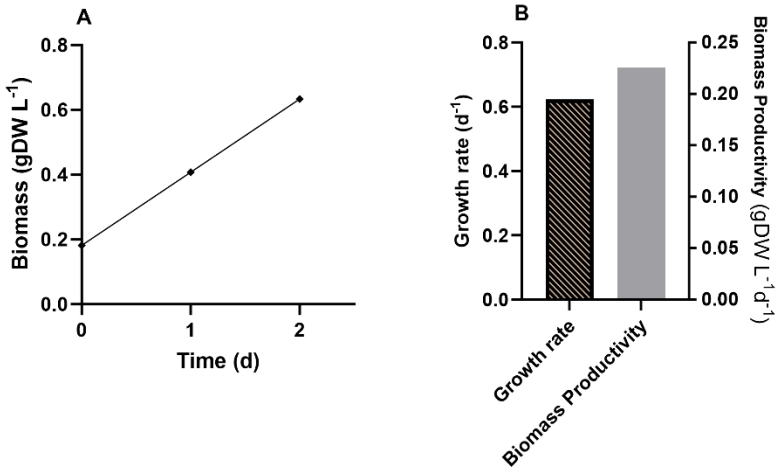


Figure 5.6. Data from the Airlift Flat Panel cultivation. ***A)*** *Growth curve, expressed as biomass produced (g dry weight per liter);* ***B)*** *Growth rate and biomass productivity, expressed as g of dry cell weight per liter per day.*



5.3.3.2. 'Aquarium', flat panel PBR

In this test, a flat-panel PBR was assessed, with standardized configuration. **Figure 5.7** shows the Aquarium with 20 L as working volume and light path of 15 cm, at the moment of the inoculum (**A**) and at the end of the test (**B**). The mixing was guaranteed by bubbling enriched air, with a strict pH control that release 1% CO_2 only when the pH rises over a settled threshold. Thus, the CO_2 is simultaneously used as carbon source and as pH buffering system. To date, this strategy to supply CO_2 is considered the most sustainable, fully avoiding gas wasting. The light panel was set at 150 µmol photons m^{-2} s^{-1} at the moment of the inoculum and then increased as the biomass grew. The growth lasted for five days (**Figure 5.8A**) and the average growth rate (**Figure 5.8B**) during the exponential phase counted for 0.42 ± 0.07 d^{-1} (Dt = 1.62 d), with a biomass productivity of 0.065 gDW L^{-1} d^{-1} (**Figure 5.8B**). The maximum biomass accumulation reached 0.41 gDW L^{-1} (**Figure 5.8A**) before the gene expression induction, which was followed, as described for the previous PBR, by a strong contamination leading the culture to be completely compromised.

Figure 5.7. Aquarium Flat panel. *It represents a conventional and standard flat panel. The picture shows the vessel at the moment of the cyanobacterial inoculum (**A**) and at the end of the test (**B**).* https://www.alga.cz/en/a-106-centre-algatech.html.

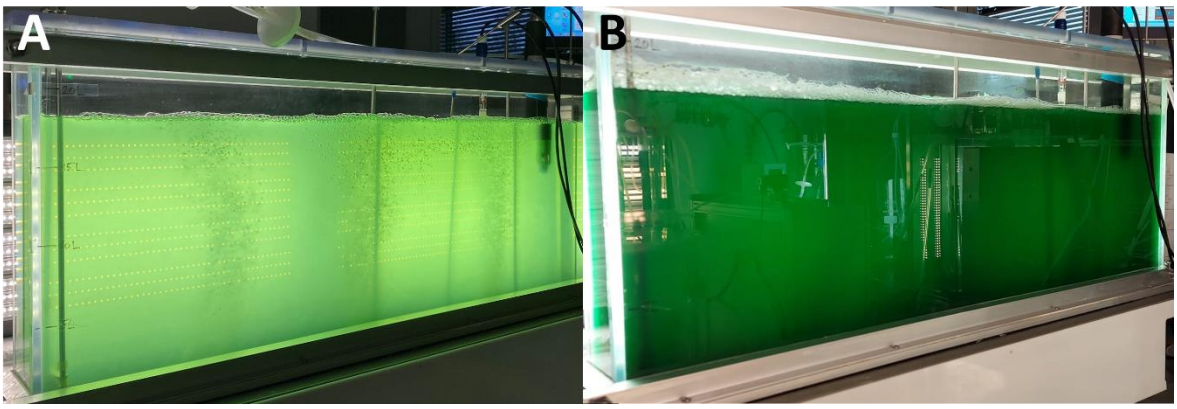
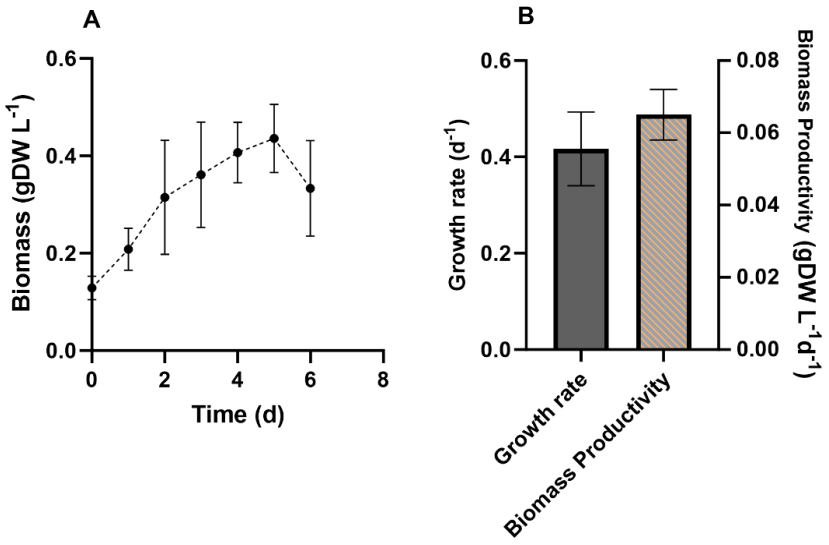


***Figure 5.8. Data from the Aquarium Flat Panel cultivation**. A) Growth curve, expressed as biomass produced (g dry weight per liter); **B**) Growth rate and biomass productivity, expressed as g of dry cell weight per liter per day. Three biological replicates were carried out. The error bars represent standard deviation.*



5.3.3.3. Annular-column PBR

The annular PBR used here was equipped with an internal illumination. **Figure 5.9** illustrates the PBR at the moment of the inoculum (**A**) and at the end of the test (**B**). The growth curve is reported in **Figure 5.10A**. The cyanobacterial culture showed a specific growth rate of 1.22 ± 0.004 d^{-1} (Dt = 0.57 d; **Figure 5.10B,** blue bar) during the first day of cultivation (light blue box), which corresponds to a volumetric biomass productivity of 0.131 gDW L^{-1} d^{-1} (**Figure 5.10C**). Unfortunately, as already mentioned, the gene expression induction coupled with the metabolite doping was always succeeded by a contamination, which will be discussed in the following section.

Figure 5.9. Annular column PBR. *The picture shows the vessel at the moment of the cyanobacterial inoculum (**A**) and at the end of the test (**B**).* https://www.alga.cz/en/a-106-centre-algatech.html.

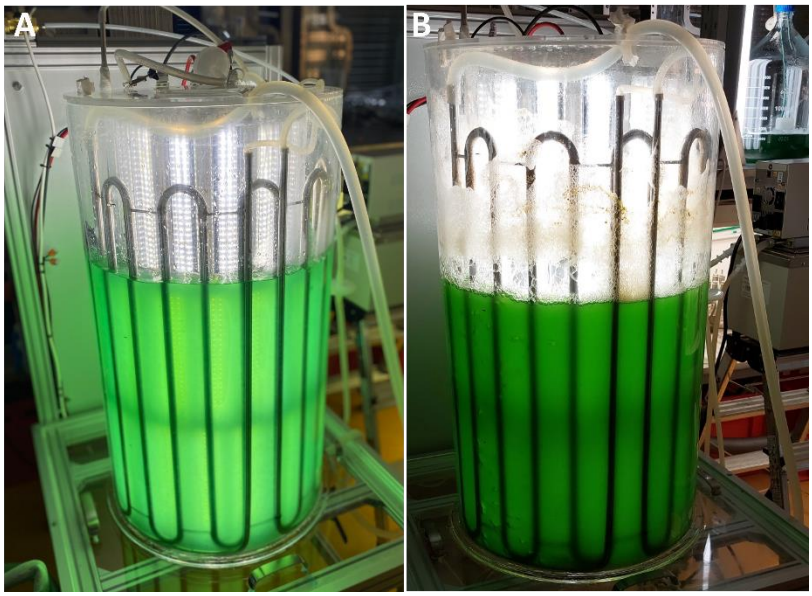
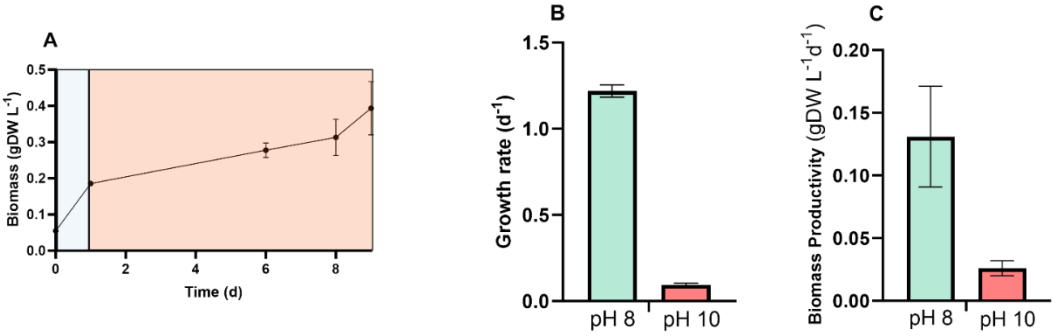


Figure 5.10. Data from the Annular column cultivation*. **A**) Growth curve, expressed as biomass produced (g dry weight per liter) at pH 8 (blue box) and pH 10 (red box); **B**) Growth rate at pH 8 (blue bar) and pH 10 (red bar); **C**) Biomass productivity, expressed as g of dry cell weight per liter per day, at pH 8. Two biological replicates were carried out. The error bars represent standard deviation.*

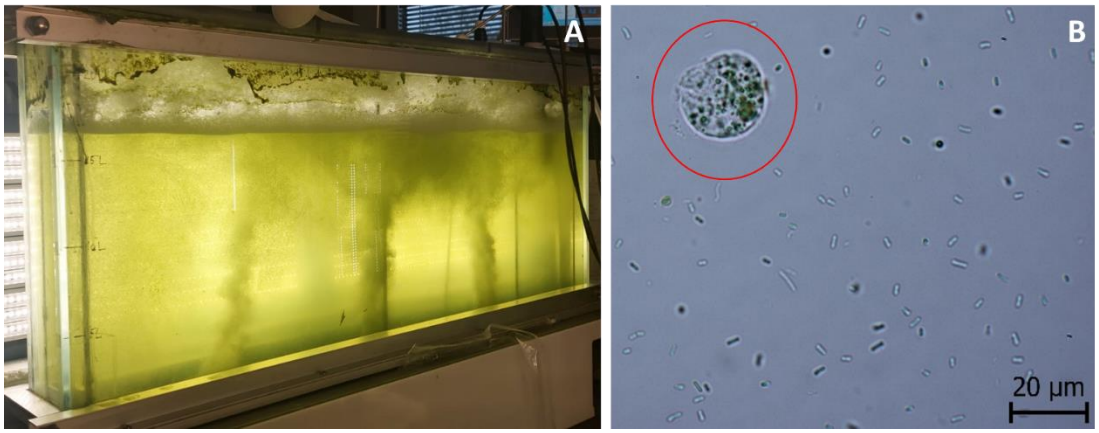


5.3.4. ***Biological contaminations affect PBR cultivations***

Besides the stirrer tank, it was never possible to evaluate the 2-PE production by the mutant strain 2PE_*aroK* in this bunch of scale-up tests, due to severe contaminations that completely destroyed the cyanobacterial culture, as shown in **Figure 5.11A**. The biological contaminant is illustrated in **Figure 5.11B** (red-circled), and it is a protozoan predator of cyanobacteria, which crashes the whole culture in a few days (Montemezzani *et al.*, 2015). The exact strain was not characterized, but morphologically resulted to be similar to a vast class of microzooplankton, such as amoeba, flagellates and ciliates (Day, Gong and Hu, 2017). They possess digestive vacuoles, which make them efficient phagotrophs, showing high growth rates, and have been identified as contaminants in microalgae and cyanobacteria mass cultures several years ago, especially for outdoor cultivations (Holen and Boraas, 1995; Leeper and Porter, 1995; Moreno-Garrido and Cañavate, 2001; Deruyck *et al.*, 2019). The most common strategy adopted to contrast this type of contaminant is represented by cultivation at high pH (≥ 10) (Touloupakis *et al.*, 2016; Haines *et al.*, 2022). Here, particularly during the annular column PBR cultivation, we tried to follow this common practice, but although we kept the mutant culture alive for some days, we never detected 2-PE produced in the supernant. Specifically, **Figure 5.10A** shows the growth curve at pH 10-11 (red box), where the growth kinetics was evidently affected, resulting in a reduced growth rate and biomass production (**Figure 5.10B, C**), a 13-fold decrease compared to the growth at neutral pH. Indeed, we noticed that after eight days of high pH exposure the culture went through photosynthetic pigments bleaching and gradually died. This contamination control method has been developed on *Synechocystis* as model cyanobacteria, which probably tolerates alkaline pH better than *Synechococcus*. Curiously, we noticed a reiterated event, thereby the contaminations appeared always the day after the gene expression induction and metabolite doping. Together, these data suggest that as long as the culture has a growth rate high enough to compete against the grazers, the cyanobacteria successfully reproduced themselves accumulating biomass. Indeed, at the optical microscope when the cyanobacteria culture was active and healthy the contaminants was not even detectable. Thus, the overexpression of the 2-PE synthesis pathway resulted to be a strong metabolic burden that affect the growth rate (as extensively described in the *Chapter 4*), which, consequently, compromised the natural fitness of *Synechococcus*. Additionally, both the cleaning and sterilization procedures of the PBRs adopted here were not evidently

strong enough, and, unsurprisingly, *in situ* cleaning/sterilization methods development are currently emerging as self-standing topic in microalgal research (Doud *et al.*, 2014; Zakova *et al.*, 2019; Fuchs *et al.*, 2021; Idris *et al.*, 2022).

***Figure 5.11. Picture about the biological contamination occurred during the scale up experiment**. **A)** Realistic picture of the cyanobacterial culture during a protozoan predator contamination. **B)** Microscopic picture of the protozoan contaminant (red circled) and the bacilli represent the target cyanobacterial culture.*



PBR	*µ (d^{-1})*	*Dt (d)*	*Biomass productivity ($gDW\ L^{-1}\ d^{-1}$)*
Stirrer tank	0.35	2.2	0.061
Airlift flat panel	0.62	1.11	0.226
Aquarium	0.42	1.62	0.065
Annular column	1.22	0.57	0.131

***Table 5.3. Biomass-related results obtained from each PBR.** µ, growth rate; Dt, doubling time (d, ln(2)/ µ); Biomass productivity, expressed as g of dry cell weight per liter per day.*

5.4. Discussion

Microalgae and cyanobacteria are cultivated in open ponds or closed PBR, which are selected based on performance, process control, strain, target product and total costs (Gao, Kong and Vigil, 2018). Generally, the performances of PBR depend on four factors: i) CO_2 mass transfer; ii) growth medium; iii) biocatalyst (photosynthetic microorganisms); iv) light, often the main limiting factor in photosynthesis-based bioprocess. Overall, closed systems have several advantages, e.g. contamination prevention, low water evaporation, enhancement of biomass productivity and ease of operation, so they are usually preferred for large scale cultivation of both microalgae and cyanobacteria in photoautotrophy cultivation mode (Chanquia, Vernet and Kara, 2022; Sirohi *et al.*, 2022). To make bioprocesses as efficient as possible, it is essential to characterize the photoautotrophic growth and product synthesis kinetics of cyanobacteria. It is common practice to use lab-scale photobioreactors to identify the optimal values of significant process variables. Thus, we started our scale up based on the production of the high value compound 2-PE by the recombinant strain of *S. elongatus* PCC 7942 (2PE_*aroK*) in stirrer tank (**Figure 5.1**) to set the operative parameters (**Figure 5.2**). The stirrer tank is the most employed bioreactor in several industries because improves mixing efficiency by agitating the culture with different types of impellers. However, the low surface to volume ratio severely affects the light distribution and penetration into the tank, and, consequently, the photosynthetic activity. Therefore, at the best condition, we reached a growth rate of 0.35 d^{-1}. Over that reached cell density the effect of low light penetration photo-limited the bacterial growth (**Figure 5.2B**). For a better light distribution flat panel PBRs have been developed with several configurations, to address photoautotrophy for CO_2 capture and simultaneous targeted production (Krujatz *et al.*, 2016; Fuchs *et al.*, 2021; Carone *et al.*, 2022; Gabrielyan *et al.*, 2022). The airlift flat panel (**Figure 5.4, 5.5**), the aquarium flat panel (**Figure 5.7**) and the annular column (**Figure 5.9**) are all photobioreactors featured of high surface-to-volume ratio with short light path, efficiently promoting photosynthesis. As far as concern the cyanobacterial biomass production, all these PBRs led to the highest growth rates obtained in this study. **Table 5.3** summarizes the maximum growth rates reached for each PBR configuration. The highest one was achieved in the annular column PBR, but, unfortunately, this data was related only to the first day of cultivation (**Figure 5.10**). However, this growth rate value is near to some growth rates reported in literature for wild type *S. elongatus* PCC 7942 (Mori,

Binder and Johnson, 1996; Kuan *et al.*, 2015). Obviously, the growth rate strongly depends on physical conditions, e.g. light exposure and PBR geometry, so, to determine reference values still remains a difficult task to accomplish. Indeed, even the light management during a PBR cultivation can significantly change depending on PBR design. The objective to be pursued when designing a bioprocess based on photosynthesis is the minimization of energy demands, first and foremost the demand for light. Thus, the amount of light should be the minimum necessary to guarantee the maximum photosynthesis efficiency, simultaneously limiting the mutual shading effect affecting the cells. Taking into account, there is a typical demand for nonstop or 8,000 working hours per year for industrial biorefineries using PBRs as an economic parameter (Kratky, Jirout and Belohlav, 2023). In this panorama, the airlift flat panel (**Figure 5.5**) adopted here shows higher potentialities (**Figure 5.6**), since moderated light intensity is needed to reach high cellular density. Herein, both the thickness and the geometrical design (**Figure 5.4**) enhance simultaneously light penetration and perfect homogeneous mixing. By provoking turbulence either the CO_2 mass transfer and cellular surface exposure are optimized (Bergmann *et al.*, 2013). So, overall, this device reduces energy consumption necessary for cyanobacteria cultivations. The Aquarium, i.e. a more standard flat panel, allowed to have 20L cultivation and, even if the mixing is not as good as the airlift system, the growth rate registered was 0.42 d^{-1}, which is 1.5-fold lower than that in the airlift and 1.2-fold higher than that in the stirrer tank (**Table 5.3**). From a more pragmatic point of view, the volumetric biomass productivity (**Table 5.3**), expressed as gDW L^{-1} d^{-1}, resulted to be really affected by the different PBR configurations assessed. For the purpose, only data from the best conditions, outside the contamination events, were considered. Thus, the airlift PBR ultimately emerged as the best option. Unfortunately, due to the contaminations no more replicates were assessed for this outstanding PBR, which showed great potential for photosynthesis-based bioprocesses.

Concerning the production of 2-PE, because of the contaminations occurred, in large volume PBRs the 2-PE synthesis was not detected. In the stirrer tank the 2-PE was detected 2.4-fold lower (**Figure 5.3B**) with respect of the best results previously obtained with the same mutant strain (see *Chapter 3* and *4*). The maximum 2-PE titer was 119 mg L^{-1}, with a volumetric productivity of 29.75 mg L^{-1} d^{-1}, which is coherent with the previous productivities reported so far, but the production time resulted to be drastically reduced (four days). Moreover, the L-Phe provided was fully consumed (**Figure 5.3B**), coherently with a low metabolic rate affecting the recombinant strain in

the stirrer tank, where the light absorption by the mutant resulted inevitably compromised.

The contaminations of cyanobacterial-based bioprocess is a commonly diffused plague (Touloupakis *et al.*, 2016; Zhu, Jiang and Fa, 2020; Toda *et al.*, 2021; Haines *et al.*, 2022; Nguyen *et al.*, 2022) and contributed mostly to the valorization of close PBRs (Borowitzka, 1999; Wang, Lan and Horsman, 2012), where the control on sterility and relative contaminations is theoretically higher than in open ponds. Additionally, the higher the PBR scale the more difficult the sterilization procedures, which supposed to strongly prevent contaminations. Here, as in many other mass cultivations, the killer was a predator (**Figure 5.11B**) of cyanobacteria, also known as 'grazers', which are part of the microzooplanktonic communities (Pierce and Turner, 1992; Day, Gong and Hu, 2017). Thus, over the years, many efforts have been spent to develop monitoring methods (Deore, Beardall and Noronha, 2020; Di Caprio, 2020) and to contrast these contaminations. One of the most exploited method is the cultivation of cyanobacteria at high pH (≥10) (Touloupakis *et al.*, 2016; Haines *et al.*, 2022). Therefore, in the efforts to scale up the photosynthetic 2-PE production by 2PE_*aroK* mutant strain, we performed a high pH (10-11) cultivation in the annular column PBR. As a result, even though the cyanobacterial culture was kept alive (**Figure 5.10A**), the growth rate resulted to be severely affected as well as the biomass accumulation (**Figure 5.10B, C**). Consequently, this strategy of controlling contamination for *S. elongatus* PCC 7942 did not seem to be proper. However, during the scale up tests for 2-PE production a very interesting result emerged. Indeed, we noticed that only after the induction of gene expression and metabolite doping the contamination appeared. Likely, the overexpression of the heterologous pathway for 2-PE synthesis is a metabolic burden too strong to be bearded, with a consequent reduction in the growth rate, as extensively discussed in *Chapter 4*. Thus, the contaminations, which may be latent into the PBRs, dominated the cultivation, leading to complete loss of the cyanobacteria culture in a few hours. Actually, the selection of fast growing species has been already used as strategy to keep grazer population in control (Lam *et al.*, 2018), allowing the cyanobacteria or microalgae to compete in open ponds.

Cleaning and sterilization phases are critical for PBRs to prevent contamination. Hypochlorite or bleach are widely used to disinfect the PBR before or even during the cultivation as microdosing. For example, (Park *et al.*, 2016) reported that sodium hypochlorite ranged from 0.45 to 0.6 mg Cl L^{-1} enabled for inhibiting the grazing activity of rotifers while maintaining the growth of *Chlorella kessleri*. Indeed, rotifers

or ciliates can be effectively killed by organophosphorus or organonitrogen insecticides, so, many different chemical strategies have been reported for several microalgae species (Benderliev, Pouneva and Ivanova, 1993; Sarma, Nandini and Flores, 2001; Marcial and Hagiwara, 2007; Molina *et al.*, 2019), as long as they have no toxic effect on the microalgae and cyanobacterial target cultures (Chen and Jiang, 2011). In addition, physical filtration, ultraviolet sterilization and ultrasound treatment have been considered as effective methods for *in situ* removal of biological contaminants, however, with insignificant effect on protozoans eggs and spores (Holm *et al.*, 2008; Nawar *et al.*, 2017; Zhu, Jiang and Fa, 2020). In this pessimistic panorama, along with the best options for cleaning/sterilization, the deep characterization of the photosynthetic biocatalyst would allow to find out an environmental stress range to apply to the cultivation in order to prevent and control biological contaminations, by reproducing non ideal conditions for the contaminants. As already described in the present investigation, the high pH could lead to control contaminant spread in some alkaline-tolerant strain (Touloupakis *et al.*, 2016), not the case for *S. elongatus* PCC 7942. In addition, the high salinity represents another successful strategy adopted for cyanobacterial and microalgal cultures (Vonshak *et al.*, 1983; Borowitzka and Borowitzka, 1990). Also, as reported in literature, light (Bader, Tsuchiya and Fredrickson, 1976) as well as temperature shock (Pleissner, Lindner and Ambati, 2020) could provide a helpful tool against biological predators. Thus, the construction of a preventing and control system of any cultivation should be the combination of different strategies and based on the specific physiology of both the biocatalyst and contaminants.

5.5. Conclusions

Cultivating photosynthetic microalgae and cyanobacteria is gaining globally interest. They find applications in food, feed, pharmaceutical, and cosmetic industries, as well as in the wastewater treatment. For fulfilling all these expectations, microalgae cultivation on a large scale is necessary. The scale-up process is often expensive and frequently carries high risks.

The scale-up of microalgae and cyanobacteria cultivation for the production of high-value compounds, such as 2-PE, involves careful consideration of various factors, including the choice of cultivation system, operational parameters, and strategies to mitigate contamination. The study presented here evaluated four different PBR

configurations, ranging from stirrer tanks to flat panels and an annular column, for cultivating the recombinant strain of *Synechococcus elongatus* PCC 7942 (2PE_*aroK*). The data demonstrated that enclosed PBR systems, particularly the airlift flat panel, exhibited superior performance in terms of biomass productivity and growth rates. Additionally, PBRs with very short light path enhance surface-to-volume ratio, improving light distribution, which is a crucial factor affecting the photosynthetic efficiency, and confirming their potential for large-scale photoautotrophic cultivation. Despite the promising outcomes as biomass formation, the challenge of biological contaminations remains a significant concern. The study encountered contamination issues, probably exacerbated by the metabolic burden imposed by the heterologous pathway overexpression for 2-PE synthesis. Strategies such as high pH cultivation, already positively proven on other cyanobacteria species, did not prove effective in controlling contaminations for *S. elongatus* PCC 7942, emphasizing the need for a tailored approach based on the specific features of the microorganism and contaminants together. Finally, the study highlighted how critical are both cleaning and sterilization among all the PBR operational procedures and the importance of selecting appropriate methods that do not compromise the target culture.

Thus, a successful scale-up of photosynthetic bioprocesses for microalgae and cyanobacteria cultivation should be the result of the combination of optimized PBR design, efficient light management, and robust contamination control strategies. Further research should focus on refining these strategies and exploring novel approaches to ensure the success of large-scale applications in the flourish field of microalgae and cyanobacteria biotechnology.

List of abbreviations:

2-PE: 2-phenylethanol

SKP: shikimate pathway

Phe: phenylalanine

***aroK*:** gene encoding for Shikimate Kinase

IPTG: Isopropyl β-D-1-thiogalactopyranoside

PBR: photobioreactor

Chapter 6

6. Coupling Dairy Wastewaters For Nutritional Balancing And Water Recycling: A Sustainable Heterologous 2-Phenyletanol Production By Engineered Cyanobacteria

This chapter was published as:

Usai G, Cordara A, Mazzocchi E, Re A, Fino D, Pirri CF and Menin B (March, 2024) ***Coupling dairy wastewaters for nutritional balancing and water recycling: sustainable heterologous 2-phenylethanol production by engineered cyanobacteria.*** Front. Bioeng. Biotechnol. 12:1359032. doi: 10.3389/fbioe.2024.1359032

6.0. Abstract

Microalgae biotechnology is hampered by the high production costs and the massive usage of water during large-volume cultivations. These drawbacks can be softened by the production of high-value compounds and adopting metabolic engineering strategies to improve their performances and productivity. Today, the most sustainable approach is the exploitation of industrial wastewaters for microalgae cultivations, which couples valuable biomass production with water resource recovery.

Among the food processing sectors, the dairy industry generates the largest volume of wastewaters through the manufacturing process. These effluents are typically rich in dissolved organic matter and nutrients, which make it a challenging and expensive waste stream for companies to manage. Nevertheless, these rich wastewaters represent an appealing resource for microalgal biotechnology.

In this study, we propose a sustainable approach for high-value compound production on dairy wastewaters through cyanobacteria. This strategy is based on a metabolically engineered strain of the model cyanobacterium *Synechococcus elongatus* PCC 7942 (already published elsewhere) for 2-phenylethanol (2-PE). 2-PE is a high-value aromatic compound, employed as a fragrance in the food and cosmetics industry, thanks to its pleasant floral scent.

Firstly, we assessed qualitatively the impact of four dairy effluents on cyanobacterial growth to identify the most promising substrates. Both tank washing waters and the liquid effluent of exhausted sludge resulted as suitable nutrient sources. Thus, we created an ideal buffer system by combining the two wastewaters, while simultaneously providing balanced nutrition and completely avoiding the need for fresh water. The combination of 75% liquid effluent of exhausted sludge and 25% tank washing waters, with a fine-tuning ammonium supplementation, yielded 180 mg L^{-1} of 2-PE and a biomass concentration of 0.6 gDW L^{-1} within ten days. While the mixture of 90% exhausted sludge and 10% washing waters allowed to the highest 2-PE (205 mg L^{-1}) and biomass accumulation (0.7 gDW L^{-1}), although in sixteen days. Through these treatments, the phosphates were completely consumed, and nitrogen was removed in a range of 74-77%.

Overall, our approach significantly valorized the water recycling and the exploitation of valuable wastewaters to circularly produce marketable compounds via microalgae biotechnology, laying promising groundwork for subsequent implementation and scale-up.

6.1. Introduction

Mass microalgae cultivation requires colossal volumes of water. For instance, microalgae have the largest water footprint among biofuel feedstocks (Zhang, Xie and Huang, 2014). As a possible strategy, reusing the cultural medium for microalgae production strongly reduces freshwater demand and nutrient usage, limiting the concerns on these cultivations (Yang *et al.*, 2011). However, reused water may lead to accumulated cell exudates, salts, bacteria, viruses, cell debris, which can potentially inhibit microalgae (Farooq *et al.*, 2015). Noteworthy, water is also an essential resource in almost all industrial sectors, including pharmaceutics, electronics, food and beverage, textile, petrochemicals, agrochemicals, oil and gas, and domestic purposes (Wollmann *et al.*, 2019; Abdelfattah *et al.*, 2023). The resulting effluents contain different contaminants, such as organic carbon (Venkata Mohan, Lalit Babu and Sarma, 2008), nitrogen (Carrera *et al.*, 2003), phosphorous (Bunce *et al.*, 2018), salts (Zhao *et al.*, 2020) heavy metals (Barakat, 2011), and solid organic matter, and must be treated prior to disposal. Therefore, new technologies aimed at removing pollutants and valorizing wastewaters are needed. For instance, the dairy industry utilizes large water volumes for its activities (e.g. cleaning equipment, milk processes, pasteurization and sterilization) and it has been estimated that from 1 to 10 m^3 of water per m^3 of processed milk are employed in this sector (Boguniewicz-Zablocka, Klosok-Bazan and Naddeo, 2019). In 2019, Europe has been the second largest producer of milk with 167.4 million tons (FAO, 2019) (UN-Food & Agriculture Organization (FAO), 2020). The production of wastewater calculated for liquid milk, cheeses, butterfat and fermented milk products (83% of dairy products) was 192.5 x 10^6 m^3 per year (Stasinakis, Charalambous and Vyrides, 2022). Particularly, Italy is the third European country, counting 18.9 x 10^6 m^3 of dairy effluents in 2019 (Stasinakis, Charalambous and Vyrides, 2022). The most abundant components are fats, organic compounds, proteins and minerals, with chemical oxygen demand (COD) ranging from 80 to 95 g L^{-1} and biochemical oxygen demand (BOD) of 40-48 g L^{-1} (Qasim and Mane, 2013). Additionally, dairy wastewaters contain large amounts of total nitrogen and total phosphorus (14–830 mg L^{-1} and 9–280 mg L^{-1}, respectively), while the pH ranges from very acidic to alkaline (Chokshi *et al.*, 2016). Thus, different kinds of liquid wastes are produced. The most biologically investigated for its recovery and valorization is the cheese whey (CW) (Atra *et al.*, 2005; Zandona, Blažić and Režek Jambrak, 2021; Sar *et al.*, 2022). CW is a nutrient-rich by-product and is derived from the milk coagulation

and the subsequent separation of the curd, it is estimated that about 8-9 kg of CW are produced every 1-2 kg of cheese product (Baldasso, Barros and Tessaro, 2011). Moreover, due to the content of phosphorus (0.124 - 0.54 kg m^{-3}) and nitrogen (0.2 - 1.76 kg m^{-3}) (Prazeres, Carvalho and Rivas, 2012), CW has a high eutrophication risk for the receiving environments (Carvalho, Prazeres and Rivas, 2013), but even biotechnologically exploitable (Carvalho, Prazeres and Rivas, 2013). However in Italy, CW itself represents a resource for the cheese industry, since it is employed to produce 'Ricotta' cheese, whose relative waste is called 'Scotta' (Maragkoudakis *et al.*, 2016). Scotta is characterized by high COD and BOD (Sansonetti *et al.*, 2009; Bergamaschi *et al.*, 2016; Monti *et al.*, 2018), and, so, environmentally dangerous if not properly processed (Ribeiro *et al.*, 2017). In addition, the large volume of effluents generated during the various production steps, related to cleaning of tanks and pipelines should be considered. Indeed, the washing procedures account for 75% of the total water used by the dairy industry (Buabeng-Baidoo *et al.*, 2017). These washing waters (WW) retain significant quantities of dissolved nutrients, proteins, fats and lactose (Brião *et al.*, 2019). Finally, the secondary wastewaters of the dairy industry derive from biological treatments of raw or primary dairy effluents, e.g. activated sludge treatment. Currently, it is applied as the main strategy for the removal of organic compounds and nitrogen from the dairy effluents (Lateef, Chaudhry and Ilyas, 2013). The resulting exhausted sludge still contains contaminants, mainly nitrogen and phosphorus as well as metals (Kaur, 2021) and so worthy of further processing, as tertiary treatments (Zagklis and Bampos, 2022). In this scenario, microalgae and cyanobacteria bioremediation, also known as phycoremediation, suits perfectly. Phycoremediation is a consolidated approach that not only exploits challenging wastewaters but also benefits bioeconomy by providing value-added products, i.e. pigments, lipids, carbohydrates, proteins and bioactive pharmaceutical metabolites (Kalra, Gaur and Goel, 2021; Uma *et al.*, 2023). The advantage of choosing microalgae or cyanobacteria for this purpose lies on their capability of growing on a variety of industrial effluents. In fact, these microorganisms photosynthesize by absorbing CO_2 from the atmosphere and use some of the pollutants found in wastewaters as nutrients (Ansari *et al.*, 2017). Particularly, a plethora of microalgal species, such as *Chlorella pyrenoidosa*, *Anabaena ambigua*, *Scenedesmus abundans*, *Chlorella vulgaris*, *Chlorella sorokininana, Chlamydomonas polypyrenoideum* and *Acutodesmus dimorphus* have been successfully cultivated in wastewaters from dairy industry (Kothari *et al.*, 2013; Qin *et al.*, 2014; Choi, 2016; Chokshi *et al.*, 2016; Brar, Kumar and Pareek, 2019;

Kusmayadi *et al.*, 2022). In all these studies, they reduced COD and BOD up to 90%, and nitrogen and phosphates by 70-90 and 80-100%, respectively. Eukaryotic microalgae biomass coming from these treatments is usually exploited as feedstock for biofuels production, since the biomass can contain up to 40-70% lipids (Kothari *et al.*, 2013; Chokshi *et al.*, 2016; Khalaji *et al.*, 2023; Paulenco *et al.*, 2023). On the other hand, cyanobacteria, which constitute a group of ancient ubiquitous phototrophic bacteria (Abed, Dobretsov and Sudesh, 2009; Garcia-Pichel, 2009), are resistant to extreme conditions of temperature, pH, heavy metals and high salinity, and, thus, suitable for bioremediation (Gaurav *et al.*, 2018; Ahmad, 2022b; Lakmali, Athukorala and Jayasundera, 2022). Although cyanobacteria conserve the ability to successfully remove nitrogen and phosphate from wastewaters (Lincoln, Wilkie and French, 1996; Dubey *et al.*, 2011; El-Sheekh, El-Otify and Saber, 2011; G and G, 2016; Of and Microbiology, 2016; Álvarez *et al.*, 2020; Ouhsassi *et al.*, 2020; Ahmad, 2022a), they have been mainly investigated for the production of high-value compounds, both naturally produced and using metabolically engineered thanks to their ease of genetic manipulation. These compounds can be extruded or derivatives of the biomass, such as pigments (H. Kabariya and M. Ramani, 2018; Menin *et al.*, 2019; Arashiro *et al.*, 2020; Thevarajah *et al.*, 2023). Alternatively, cyanobacteria have been exploited as disinfection treatment of waste effluents (Samiotis, Ziagova and Amanatidou, 2023) and their biomass has been used as substrate for fermentation processes (Möllers *et al.*, 2014; Álvarez *et al.*, 2020; Comer *et al.*, 2020; De Oliveira, Bassin and Cammarota, 2022). Thus, exploiting nutrient-rich wastewaters as growth substrate not only facilitates the cultivation of microalgae and cyanobacteria but also serves the dual purpose of contaminant removal and reduction in freshwater usage. Consequently, this approach plays a pivotal role in cost-cutting within the realm of microalgae and cyanobacteria biotechnology.

Here, we aimed at developing a sustainable heterologous production of the high-value compound 2-phenylethanol (2-PE) by a metabolically engineered strain of *Synechococcus elongatus* PCC 7942, known as 2PE_*aroK* (Usai *et al.*, 2022). 2-PE is an aromatic alcohol with pleasant rose-like scent, which finds application mostly in the food, fragrance, and flavor industries (Etschmann *et al.*, 2002; Nielson, Machas and Mckenna, 2018; Fang and Sung, 2021). The 2PE_*aroK* recombinant strain is able to overexpress five genes. *aroG*^{fbr} *and pheA*^{fbr} (from *E. coli*), *aroK* (native), related to the shikimate pathway, the metabolic route for aromatics production (Gosset, 2009); *kivD* (*L. lactis*) and *adhA* (*Synechocystis* PCC 6803), responsible for the final synthesis steps

(**Supplementary Table 6.1**). The 2PE_*aroK* has been extensively described in (Usai *et al.*, 2022). The herein proposed sustainable 2-PE bioproduction has been tailor-made by coupling wastewaters from a dairy industry, which allowed to balance pH and nutritional contributions, avoiding the use of freshwater and resulting in successful production of 2-PE.

6.2. Materials and Methods

6.2.1. Pre-treatment of dairy wastewaters

All the dairy waste streams were firstly subjected to natural sedimentation (overnight at 4°C), in order to eliminate the solid particulate. The liquid effluent of exhausted sludge was filtered with polyethersulfone filtration systems (pore size 0.22 µm). The effluents were stored at 4°C until use. Cheese whey, scotta and the tank washing waters were deproteinized (105°C, 5 min) and the protein aggregates were left to sediment and stored at 4°C. To prevent biological contamination, almost all the preparative steps were conducted at 4°C, rigorously avoiding frequent thermal changes of the effluents.

6.2.2. Hydrochemical analysis of dairy wastewaters

The pre-treated dairy effluents were analyzed by E.L.A. s.r.l. (Asti, Italy) for hydrochemical characterization. The following parameters were determined: pH and conductivity, chemical oxygen demand (COD), biochemical oxygen demand (BOD), total nitrogen, total phosphorous. Additionally, NH_4^+, NO_3^-, PO_4^{3-}, SO_4^{2-} and dissolved metal ions (Ca, Na, Cl, K, Fe, Al, As, Ba, Hg, Se, Mn, Ni, Cr, Cd, Cu). The methods utilized are reported in **Table 6.1**.

6.2.3. Cyanobacterial strain and culture maintenance

All the tests reported in the present investigation have been conducted by using a metabolically engineered strain of *S. elongatus* PCC 7942, known as 2PE_*aroK* and already developed by our laboratory (Usai *et al.*, 2022). This strain is able to heterologously produce 2-PE and the **Supplementary Table 6.1** reports all the genes and relative proteins involved in this pathway, while they were thoroughly described in (Usai *et al.*, 2022). The mutant strain was grown in BG11 (Cordara *et al.*, 2018; Vasile *et al.*, 2021) as a standard medium to define the control condition of the qualitative screening. Briefly, the present BG11 medium is composed as follow: 1.5 g

L^{-1} $NaNO_3$, 0.075 g L^{-1} $MgSO_4 \cdot 7H_2O$, 0.004 g L^{-1} $FeCl_3 \cdot 6H_2O$, 0.04 g L^{-1} K_2HPO_4, 0.036 g L^{-1} $CaCl_2$, 0.024g L-1 $Na_2EDTA \cdot 2H_2O$, 2.86 mg L^{-1} H_3BO_3, 1.81 mg L^{-1} $MnCl_2 \cdot 4H_2O$, 0.39 mg L^{-1} $Na_2MoO_4 \cdot 2H_2O$, 0.22mg L^{-1} $ZnSO_4 \cdot 7H_2O$, 0.05 mg L^{-1} $CuSO_4 \cdot 5H_2O$, 0.03 mg L^{-1} $Co(NO_3)_2 \cdot 6H_2O$. The BG11 medium was buffered with 6.05 g L^{-1} TES (2-([Tris(hydroxymethyl)methyl]amino)ethane-1-sulfonic acid sodium salt) to pH = 8. The BG11 medium was supplemented with 20 µg mL^{-1} spectinomycin and 10 µg mL^{-1} kanamycin. All the cyanobacteria cultures were grown at 30°C, 130 rpm and continuous illumination of 30 µmol photons m^{-2} s^{-1}.

6.2.4. Cyanobacteria growth conditions on dairy wastewaters

All the experiments were performed at the same environmental parameters: 30°C, 130 rpm, continuous light intensity of 30 µmol photons m^{-2} s^{-1}, with 20 µg mL^{-1} spectinomycin and 10 µg mL^{-1} kanamycin.

To evaluate the qualitative effect of the dairy wastewaters on the mutant strain of cyanobacteria, the bacterial growth was evaluated on 100, 75, 50% of singular wastewater using 6-well plates. Moreover, different supplementations were assessed in order to better understand the limiting nutritional factor associated with each waste and highlight the most potential growth conditions on dairy waste waters (**Figure 6.1**). For this purpose, trace element solution, nitrate or phosphates were supplemented singularly or in combination, at the same concentration reported for BG11 medium. Then, the combination between exhausted sludge (ES) and washing water (WW) was studied at different ratios: 90:10, 75:25 and 60:40. The pH tolerance of 2PE_*aroK* mutant strain on the previously selected conditions was evaluated. To assess the pH buffering system in ES and WW, the MOPS (4-(3-sulfonatopropyl)morpholin-4-ium) buffer was adopted (25, 50 and 75 mM), using TES as control buffer (**Supplementary Table 6.2**). The final physiological characterization of the mutant strain on 90:10 and 75:25 mixtures between ES and WW was performed in 250-mL Erlenmeyer flasks in the abovementioned parameters. All the experiments were conducted using a starting inoculum equivalent to OD_{730} = 0.2. The growth of the 2PE_*aroK* mutant strains of *S. elongatus* PCC 7942 was monitored by measuring optical density at 730 nm (OD_{730}) and then converted into biomass as gram of dry cell weight per liter (gDW L^{-1}), by using a conversion factor of 0.26 (previously developed in our laboratory, (Usai *et al.*, 2022)). Specific growth rate (µ, d^{-1}) was obtained from the slope of the logarithmic plot of OD_{730} versus time, for the growth curve points belonging to the exponential phase (**Table 6.2**). The gene expression was induced by adding 1mM IPTG (Isopropyl

β-d-1-thiogalactopyranoside) into the proper growth condition and the metabolite doping was launched with 0.3 g L^{-1} L-Phenylalanine (L-Phe).

6.2.5. ***Photosynthetic pigments quantification***

Chlorophyll α (chlα) and total carotenoids (car) were quantified. 1 mL of cyanobacterial culture was harvested at the end of each test about 75:25 and 90:10 ratios. The culture was pelleted 12,000 g for 10 min and the supernatant was discharged. The cell pellet was resuspended in 1 mL of cold methanol (≥ 99.9%) and incubated at 4°C in the darkness for 20 min. The lysed cells were centrifuged again (12,000 g, 10 min, 4°C) to recover the supernatant, which was properly diluted in methanol.
The spectrophotometric analyses were carried on a PerkinElmer Lambda 650 UV/Vis spectrophotometer using quartz cuvettes. The instrument was calibrated using methanol as blank. Each run was performed from 800 nm to 400 nm with slit width 1 nm.
To calculate the photosynthetic pigments concentration, the following equations were used (Wellburn, 1994):

$$\text{Chlorophyll } \alpha\ [\mu g\ mL^{-1}] = 12.9447(A_{665} - A_{720})$$

$$\text{Total carotenoids } [\mu g\ mL^{-1}] = [1000(A_{470} - A_{720}) - 2.86(\text{Chla}[\mu g\ mL^{-1}])]/221$$

6.2.6. ***2-PE and L-Phe HPLC analysis***

2-PE and L-Phe were quantified as described in previous the previous chapters.

6.3. Results

6.3.1. *Selection of proper dairy wastewaters for* S. elongatus *growth*

Here, the metabolically engineered strain of *S. elongatus* PCC 7942 2PE_*aroK* (**Supplementary Table 6.1**), has been adopted to design a sustainable heterologous 2-phenylethanol production based on the exploitation of dairy wastewaters.
In this investigation, a chemical analysis and a screening of the dairy effluents provided by a local Italian cheese factory have been conducted to firstly evaluate the possibility of specifically cultivating the 2-PE producing mutant strain. Detailed description will be provided in the following sections.

6.3.1.1. *Chemical characterization of dairy wastewaters*

Four dairy wastewaters coming from the cheese production plant were analyzed: i) cheese whey (from cheese production, CW); ii) scotta (from ricotta cheese production, Sc); iii) the washing water of pipelines and tanks (WW); iv) the liquid effluent of the exhausted sludge (ES; coming from the biological treatment of the previous effluents). **Table 6.1** shows the chemical characterization of the dairy streams. In the literature, for dairy effluents the ratio of the key macroelements is reported to be C/N/P ≈ 200/3.5/1, which is generally considered nitrogen deficient to drive any biological processes (Prazeres, Carvalho and Rivas, 2012)

6.3.1.2.*Nitrogen and Phosphates*

Nitrate (NO_3^-) and free ammonium (NH_4^+) are preferentially assimilated as nitrogen source in almost all microorganisms (J. Wang *et al.*, 2016), since nitrogen is an essential macronutrient needed for the biosynthesis of amino acids, proteins and nucleic acids. NO_3^- concentration into the present wastewaters was < 1.5mg L^{-1} in all the waste streams and the highest ammonium concentrations were 83 and 103 mg L^{-1} for ES and CW, respectively.
Here, the phosphates concentration as well as the total phosphorous (TP) resulted to be high in all the wastewaters if compared with the standard medium for cyanobacteria (which contains approx. 20 mg L^{-1} PO_4^{3-}) and, surely, higher than that should be in marine and fresh- water bodies for identifying them high quality and non-polluted. For these latest reasons, the present dairy wastewaters are great candidates for cyanobacteria treatments prior to disposal into the environment.

Description	Cheese whey	Scotta	Washing waters	Exhausted sludge	Analytical method
COD	48600	53800	5308	22	ISO 15705:2002
BOD	20100	22300	2200	< 10	M.I. 21 Rev. 0:2013
Total Nitrogen	475	466	166.8	5.91	
Ammonical Nitrogen	103	3.9	< 0.05	83	UNI 11669:2017
Nitric Nitrogen	< 1.5	< 1.5	< 1.5	< 1.5	APAT CNR IRSA 4020 Man 29 2003
Phosphates	649	1090	69.5	100	
Sulfates	113	117	6.69	< 5	
Chloride	7090	9610	54.4	287	
Total Phosphorous	249	382	27.8	33.4	UNI EN ISO 15587-1:2002 (Annex A) + UNI EN ISO 11885:2009
Na	3000	4470	29.8	414	
Ca	161.048	418.47	44.311	48.727	
K	1120	1220	44.2	61	
Al	0.047	0.062	0.03	0.021	
As	0.03	0.029	< 0.01	< 0.01	
Fe	0.059	0.077	0.042	0.06	
Mn	< 0.01	< 0.01	< 0.01	0.02	
Cu	0.011	0.018	0.015	< 0.01	
Se	0.016	0.029	0.012	< 0.01	
Ba	0.011	< 0.01	< 0.01	< 0.01	
Cd	< 0.01	< 0.01	< 0.01	< 0.01	
Cr	< 0.01	< 0.01	< 0.01	< 0.01	
Hg	< 0.01	< 0.01	< 0.01	< 0.01	
Ni	< 0.01	< 0.01	< 0.01	< 0.01	
Pb	< 0.01	< 0.01	< 0.01	< 0.01	
pH	5.78	3.84	4.57	8.43	APAT CNR IRSA 2060 Man 29 2003
Conductivity (mS/cm)	18.83	25.87	0.53	3.02	UNI EN 27888:1995

Table 6.1. Chemical analysis of four dairy wastewaters*: cheese whey, scotta, washing waters, liquid effluent of exhausted sludge. The data are expressed as mg* L^{-1}*. The analytical methods used for their quantification is reported in the last column.*

6.3.1.3. ***Sodium, chloride and calcium***

Often, some cheese producers add NaCl or $CaCl_2$ for specific cheese preparations (Guinee, 2004). Hence, high salinity is a peculiarity of the dairy streams, especially in the primary wastes. Here, CW and Sc had the highest salinity among the dairy streams (**Table 6.1**, conductivity 18.83 and 25.87 mS cm^{-1}, respectively).

6.3.1.4. ***Metals***

In prokaryotic and eukaryotic microalgae, Copper (Cu) covers a pivotal role for either photosynthesis or respiratory electron transport (López-Maury, Giner-Lamia and Florencio, 2012). In the dairy wastewaters (**Table 6.1**), the Cu content appears stable in a range 11-18 µg L^{-1}, which is near to the content in BG11 medium. Exception for ES, where the Cu was not even detected. Furthermore, iron (Fe) is fundamental for photosynthetic microorganisms, since it is a cofactor for all three photosynthetic electron transfer chain complexes (Shcolnick and Keren, 2006). Even in this case, Fe concentration in all the streams ranged of 42-77 µg L^{-1}, which is lower than that in standard BG11 medium.

6.3.1.5. ***pH, COD and BOD***

The range of pH associated to dairy wastewaters is wide. Here, the lowest pH was recorded for Sc (pH = 3.84) and the highest one was for ES (pH = 8.43). Generally, the optimum pH for cyanobacteria is 8, but it should never be as low as 7. Consequently, what concerns the pH values, WW, CW and Sc were not putative suitable for cyanobacteria cultivations. Additionally, the high COD (chemical Oxygen demand) and BOD (Biochemical Oxygen demand) represent a huge challenge to the applicability of non-diluted CW and Sc, caused by the rich content in organic carbon compounds. Indeed, for high-COD wastes a preliminary anaerobic digestion or activated sludge treatment (as in this specific case for secondary treatment) is usually adopted prior to any other downstream application or disposal (Kusmayadi *et al.*, 2022).

6.3.2. ***Qualitative screening of dairy wastewaters for cyanobacterial growth***

The screening took place in 6-well plates as described in materials and methods section. To evaluate qualitatively the impact of wastewaters for the *S. elongatus* PCC 7942 mutant strain (2PE_*aroK*) a reference condition has been adopted, i.e. the bacteria

grown on BG11 standard medium. Thus, the growth on dairy effluents was assessed as ratio against the control condition growth, represented by the heatmap in **Figure 6.1**, where the orange color represents no growth (equal to Ø) and dark green indicates a growth as the control condition (equal to 1). Furthermore, the percentage indicates the wastewater amount diluted with water (v/v). Thereby, to identify the limiting factor of each wastewater, we added singularly or in combination nitrogen (1.5 g L^{-1} $NaNO_3$), phosphates (0.04 g L^{-1} K_2HPO_4) or trace metals sources at the same concentration as specified for the BG11 medium. Additionally, to assess the effect of nitrogen, phosphates and trace metals some negative controls have been designed: i) BG11 with no N and P; ii) 75% diluted BG11; iii) 50% diluted BG11. As theoretically inferred by the chemical nature of CW and Sc, discussed earlier, those wastewaters resulted to be detrimental for the cyanobacteria and actually they did not support the growth even when 50%-diluted (data not shown). As depicted in **Figure 6.1**, the most promising conditions tested were 50-75% WW and 75% ES. Additionally, for ES the most limiting nutrient seemed to be the nitrogen, but supplementing phosphates in combination further improved the cyanobacterial growth. In WW the deficiency in both metals and nitrogen had the most pronounced effect. To clarify, more diluted conditions have been excluded, in order to avoid the use of further freshwater and to better align with the concept of wastewaters recycling. In fact, the aim of this study was to assess the viability of cultivating our metabolically engineered strain for a sustainable production of 2-PE on wastewaters. Due to the relevance of the nitrogen, we found here, we checked for the minimum ammonium concentration that would have guaranteed in ES a bacterial growth as in the control condition (BG11). We found 0.15 g L^{-1} NH_4^+ **(Figure 6.2)** as the best condition among those studied (0.03-0.15 g L^{-1} NH_4^+) for biomass accumulation. Subsequently, to maximize the utilization of wastewaters by the mutant strain, we combined ES and WW in various ratios, carefully considering their chemical features, and conducted a comprehensive examination of pH balance in the following section.

Additionally, as the complexity of a growth medium increases as the interaction among all the chemical parts could influence the exploitation by the bacteria. This is the case of wastewaters to be taken into account.

***Figure 6.1. Dairy wastewaters qualitative screening**. The screening has been conducted as biological triplicates for each tested condition against a control one (BG11). The study has considered the effect on the growth of the 2PE_aroK S. elongatus PCC 7942 mutant strain, ranging from no growth (red) to a growth equal to the control condition (dark green). The percentages indicate the ratio of each waste used in the single experiment.*

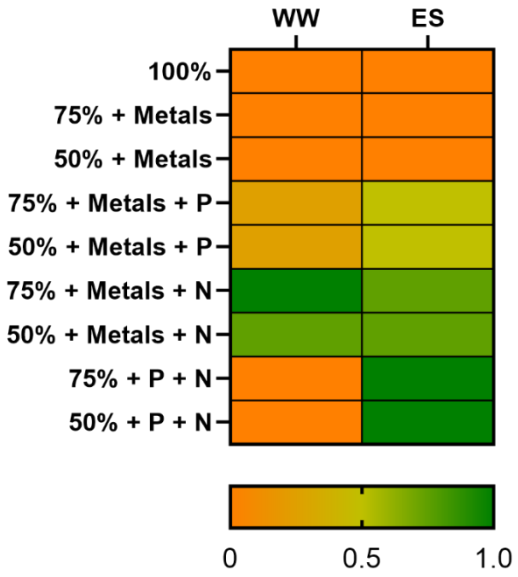
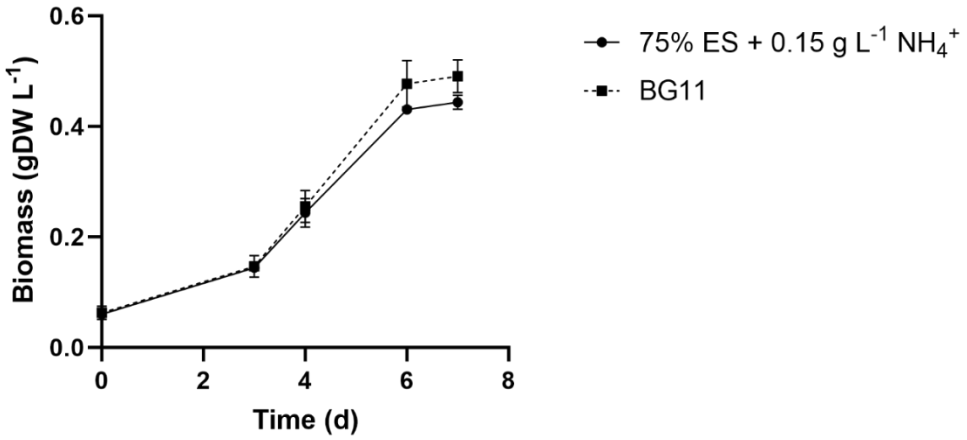


***Figure 6.2. Growth rate of 2PE_**arok* ***mutant on 75% exhausted sludge waste supplemented with 0.15 g L^{-1} NH_4^+**, which was found to be the minimum ammonium concentration able to lead a growth similar to the control condition (BG11). All tests were carried out in triplicate. Error bars represent standard deviation.*

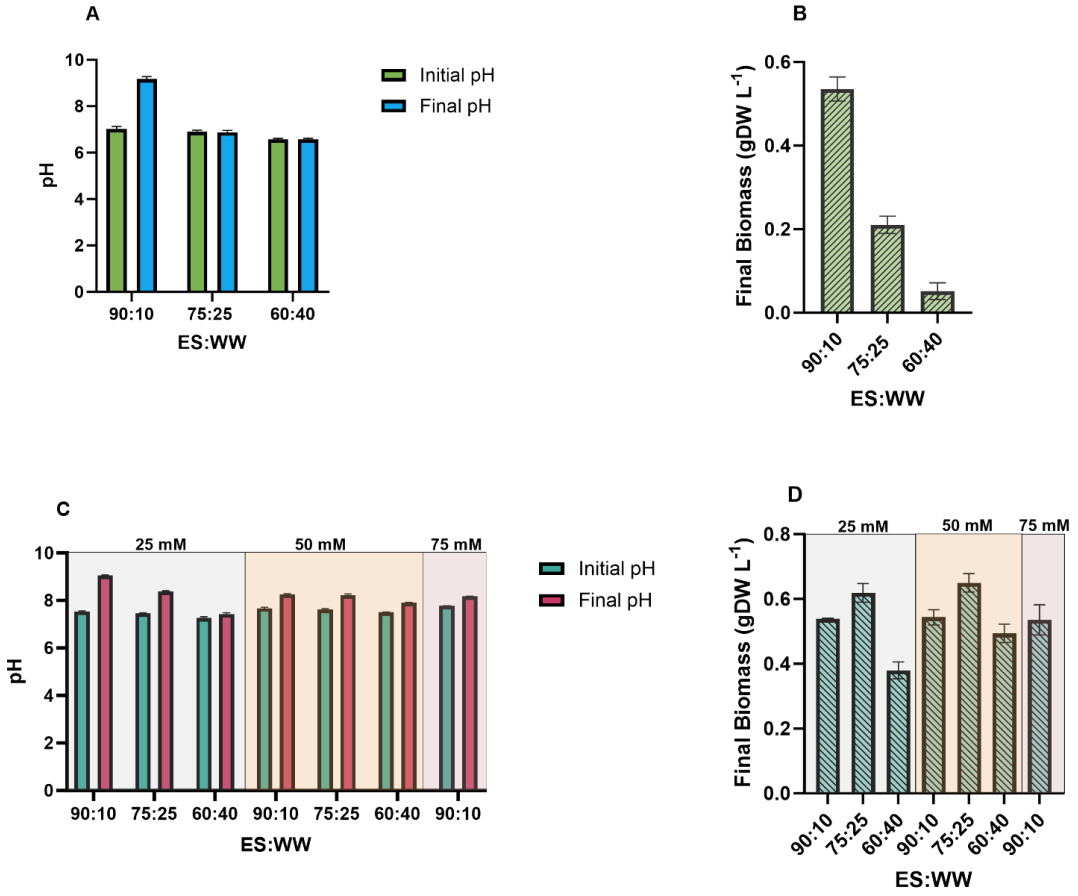


6.3.3. Coupling dairy wastewaters for nutritional balancing and water recycling

6.3.3.1. pH tolerance and pH control effect on the 2PE_aroK recombinant strain

S. elongatus PCC 7942 shows optimum growth at pH values ranging from 7.0 to 9.0 (Billini, Stamatakis and Sophianopoulou, 2008). In the effort to simultaneously balance the pH (at ca. 7.5) and the relative nutritional contribution, we mixed ES and WW in different ratio and 0.15 g L^{-1} NH_4^+ was supplemented in this pool of experiments. The data related to the pH screening are summarized in the **Supplementary Table 6.2**. **Figure 6.3** shows the outcomes of the wastewaters mixing without pH control. The best result was reached at 90 ES : 10 WW, where the initial pH was 7.5, coherently with the optimum for *S. elongatus*. Unfortunately, while the bacteria grew the pH increased rapidly to a final value of 9.2, which likely inhibited the growth. Conversely, because of the low pH, the mutant strain was not able to grow at 60:40 ratio (**Figure 6.3B**). To better understand the impact of pH on these cultivations, we selected a molecule capable of buffering at the desired pH, i.e. MOPS (range 6.5-7.9). Also, we evaluated the use of our reference buffer, present in our BG11 medium recipe, i.e. TES. However, we found out that TES supplementation led to the formation of particulate and, even if the cyanobacteria could grow (**Supplementary Table 6.2**), we decided not to further investigate this option. The MOPS buffer was tested at three different concentrations: 25, 50 and 75 mM (**Figure 6.3C, D**). Notably, 25 mM MOPS was able to keep the pH stable almost in all the mixtures tested and only 90:10 condition required to be buffered at the highest MOPS concentration of 75 mM, with no improvement for cyanobacterial growth (**Figure 6.3D**). Both 25- and 50 mM MOPS concentrations efficiently buffered the mixtures between ES and WW, but no quantitative effect on the bacterial growth was recorded and for this reason only 25 mM MOPS was selected for further investigations. Regarding the ratio between ES:WW, the 60:40 ratio proved unsuitable for this specific application. On the other hand, 75:25 and 90:10 emerged as the most promising ones and worthy for a deeper study, discussed in the following section.

***Figure 6.3. Study of the effect of no pH control and MOPS pH control on the growth performance of the 2PE_aroK mutant strain**, on different ratios between ES and WW: i) 90:10; ii) 75:25; iii) 60:40. All tests were carried out in triplicate. Error bars represent standard deviation.*



6.3.4. *Characterization of 2PE_aroK mutant in two mixtures of ES and WW*

6.3.4.1. *Growth of 2PE_aroK mutant strain in wastewaters*

Although the mixtures designed here contain a small amount of L-Phe (approximately 70 and 25 mg L^{-1} were quantified in the ratios 75:25 and 90:10, respectively), it was not sufficient to support 2-PE production. Indeed, in (Usai *et al.*, 2022) and *Chapter 3* the effect of the metabolite doping provided as L-Phe supplementation has been extensively described as necessary for improving 2-PE production by the mutant strain.

Thereby, extra L-Phe (0.3 g L^{-1}) was added to the wastewaters at the beginning of the test or at the moment of the gene expression induction (triggered by 1 mM IPTG at 6th day). Four different conditions were thought for both 75:25 and 90:10. All the conditions contain 25 mM MOPS as pH buffering system, in order to exclude the pH as object of this investigation.

i. **Control**: the 2PE_*aroK* mutant strain grown with no extra supplementations on ES:WW.
ii. **Condition I**: 0.3 g L^{-1} L-Phe was supplemented at 6-day growth.
iii. **Condition II**: 0.15 g L^{-1} NH_4^+ and 0.3 g L^{-1} L-Phe were supplemented at 6-day growth.
iv. **Condition III**: 0.15 g L^{-1} NH_4^+ + 0.3 g L^{-1} L-Phe (Nitrogen and L-Phe were added as part of the medium, at the beginning of the test).

Figures 6.4 and 6.**5** depict the results relatively to 75:25 and 90:10 ratio, respectively, regarding the bacterial growth and 2-PE production. The data were collected until the 2-PE synthesis was detected, resulting in a production time of 10 days for 75:25 and 16 days for 90:10 after the induction of the gene expression. All the main findings are summed up in **Table 6.2**, where the results of the statistical analysis are reported and performed as multiple t-test (unpaired, $\alpha \leq 0.05$) versus the control condition. Almost all the results were statistically significant against the control condition (with only some exceptions for the pigment quantification). Significantly, in 75:25 the specific growth rate (μ, d^{-1}) for all the supplemented conditions and control averaged 2-fold higher than those detected in 90:10 (**Table 6.2**). Unsurprisingly, the nitrogen supplementation positively affected the biomass formation in both the ratios (**Figure 6.4A**, **6.5A**; conditions II and III), leading to a biomass accumulation of averaged 0.6 and 0.7 gDW L^{-1} in 75:25 and 90:10, respectively. On the other hand, the L-Phe addition at the beginning of the test (**Figure 6.4A**, **6.5A**; condition III) seemed not to improve the mutant growth.

***Figure 6.4. Comparison between 2PE_aroK grown on three different conditions on 75 ES : 25 WW**. **A)** Growth curves, expressed as biomass (gDW L^{-1}). **B)** 2-PE prodution kinetics obtained in sixteen days (mg L^{-1}). **C)** 2-PE yield, expressed as mg 2-PE normalized by the biomass produced. **D)** 2-PE daily productivity (mg L^{-1} d^{-1}). All tests were carried out in biological triplicate. Error bars represent standard deviation. The statistical tests were performed as unpaired t-test ($\alpha \leq 0.05$) versus the control condition. *, p-value ≤ 0.05; **, p-value ≤ 0.002; ***, p-value ≤ 0.0002; ****, p-value ≤ 0.0001.*

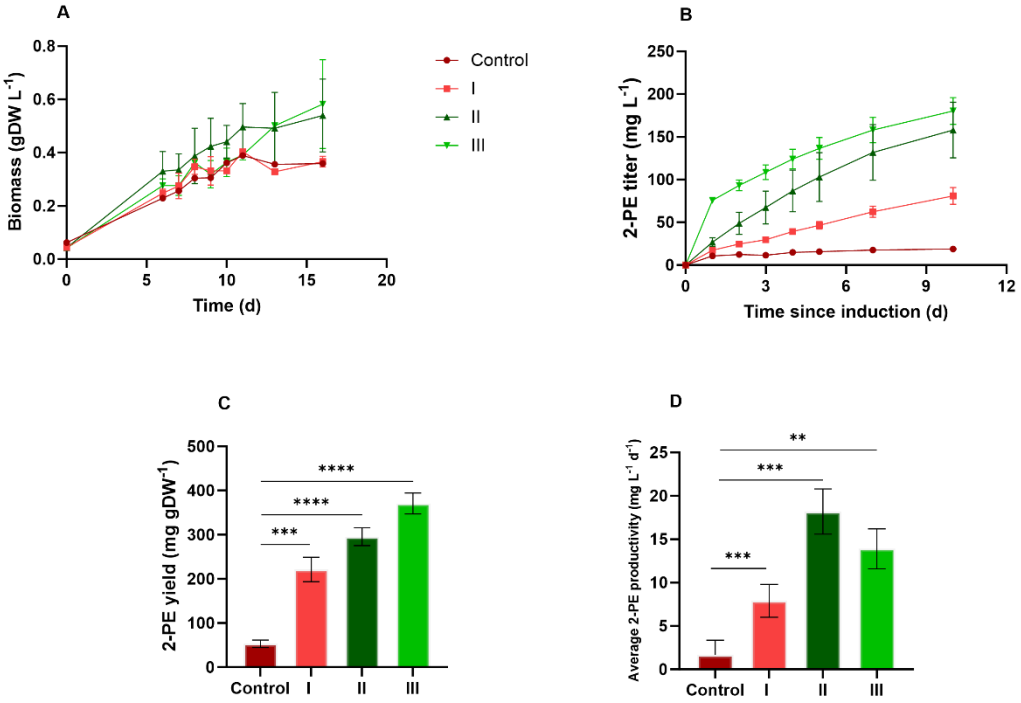
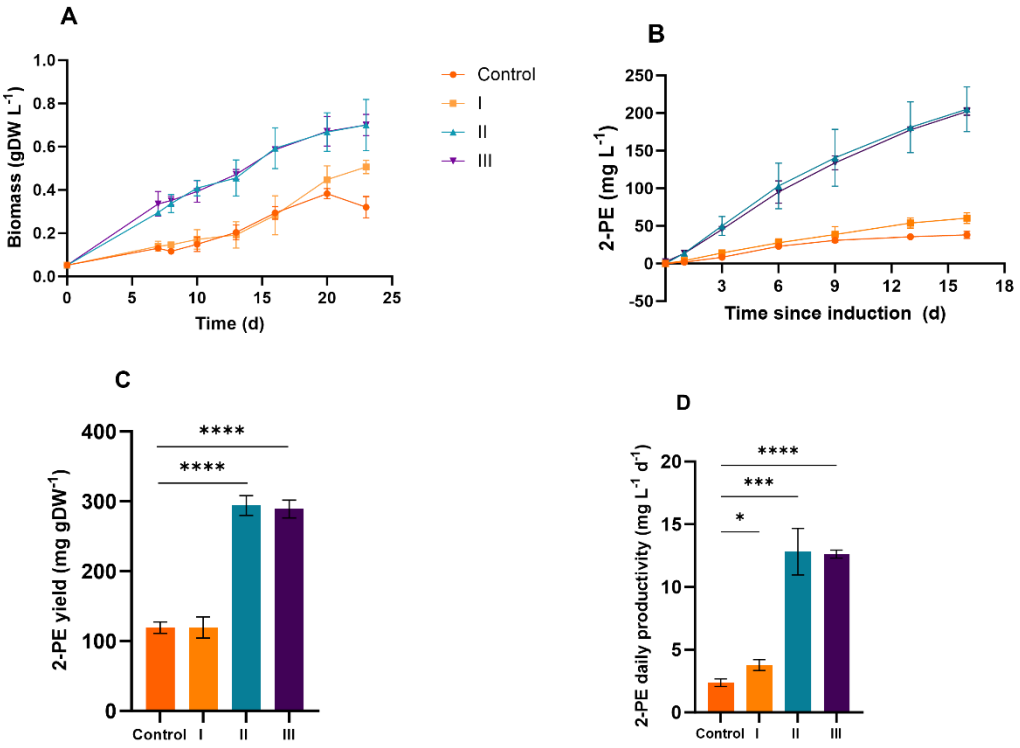


***Figure 6.5. Comparison between 2PE_aroK grown on three different conditions on 90 ES : 10 WW**. **A)** Growth curves, expressed as biomass (gDW/L). **B)** 2-PE prodution kinetics obtained in sixteen days (mg/L). **C)** 2-PE yield, expressed as mg 2-PE normalized by the biomass produced. **D)** 2-PE daily productivity (mg/L per day). All tests were carried out in biological triplicate. Error bars represent standard deviation. The statistical tests were performed as unpaired t-test ($\alpha \leq 0.05$) versus the control condition. *, p-value ≤ 0.05; **, p-value ≤ 0.002; ***, p-value ≤ 0.0002; ****, p-value ≤ 0.0001.*



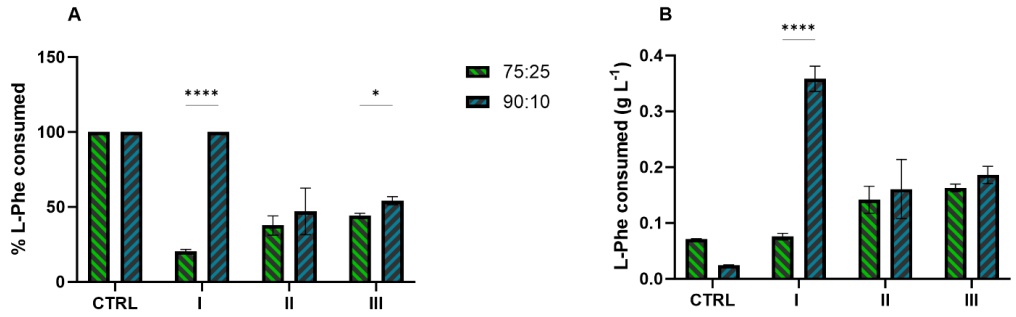
6.3.4.2. ***2-PE production and L-Phe consumption in wastewaters***

The 2-PE production ability of the mutant strain in wastewaters resulted to be improved if compared to the control conditions (no extra supplementations on ES:WW), yielding to 19 and 38 mg L^{-1}, at 75:25 and 90:10 respectively (**Figure 6.4B, 6.5B**). However, at both the ratios the highest titers were obtained in conditions II and III, accounting for 180 and 205 mg L^{-1} for 75:25 and 90:10, respectively. In both 90:10 and 75:25, conditions II and III were not statistically comparable, so, the addition of L-Phe at the

beginning of the experiment or later on did not improve the bioprocess. On the other hand, the volumetric productivity significantly changed between the two mixtures. Indeed, a productivity of 12.82 mg L^{-1} d^{-1} was detected in 90:10 (**Figure 6.5D**) against 18.03 mg L^{-1} d^{-1}, in 75:25 (**Figure 6.4D).** This means that the production time in 90:10 mixture necessary to reach the highest 2-PE concentration is longer (16 days) than in 75:25 (10 days).

Concerning the metabolite doping, the L-Phe consumption profiled differently between 75:25 and 90:10 (**Figure 6.6A, B**). In both the ratios, in conditions II and III, where the L-Phe was supplemented at 6th day or at the beginning of growth, respectively, a range of 34-54% (**Figure 6.6A**) of the available L-Phe (0.3 g L^{-1} supplemented in addition to the amount already inside) was consumed. Conversely, in condition I (i.e. L-Phe supplementation at 6th day, with no extra N) of 90:10 mixture, the L-Phe was uptaken by 100% (**Figure 6.6A**), with no effect on both bacterial growth and 2-PE production (**Figure 6.5A, B**). Additionally, the control conditions for both ratios consumed all the available L-Phe (**Figure 6.6B**).

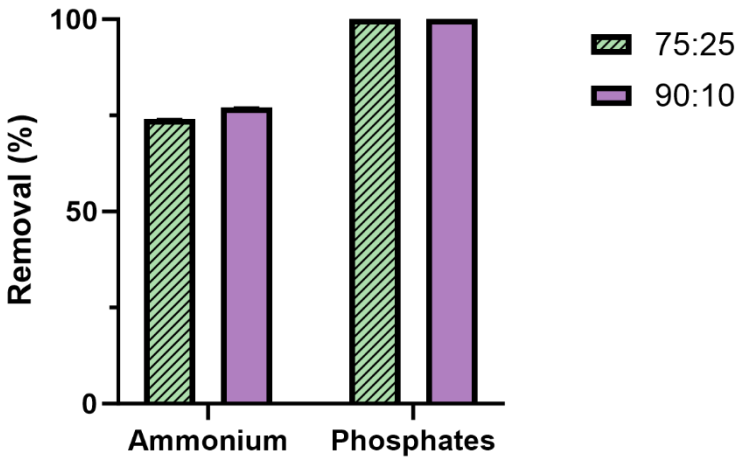
Figure 6.6. L-Phe consumption by 2PE_aroK mutant strain grown on 75:25 and 90:10 ratios between ES and WW. ***A****) percentage of L-Phe consumed over the L-Phe available.* ***B****) total amount of L-Phe consumed (g L^{-1}) in all the conditions tested and control of the two wastewaters mixtures. All tests were carried out in biological triplicate. Error bars represent standard deviation. Asterisks refer to statistical significance (unpaired t-test, $\alpha \leq 0.05$).*



6.3.4.3. Nutrients removal from wastewaters

A chemical analysis of the effluent following microbial treatment (**Figure 6.7A, B**) was conducted under the two best conditions for bacterial growth and 2-PE production (i.e. ammonium and L-Phe supplementation). N consumption counted for 74 and 77% in 75:25 and 90:10 conditions, respectively. In both the mixtures, P was completely removed (100%).

Figure 6.7. Percentage of N and P removal from the mixture 75 ES : 25 WW (patterned) and 90 ES : 10 WW (violet). *The quantification was carried out in biological triplicate. The error bars represent the standard deviation.*

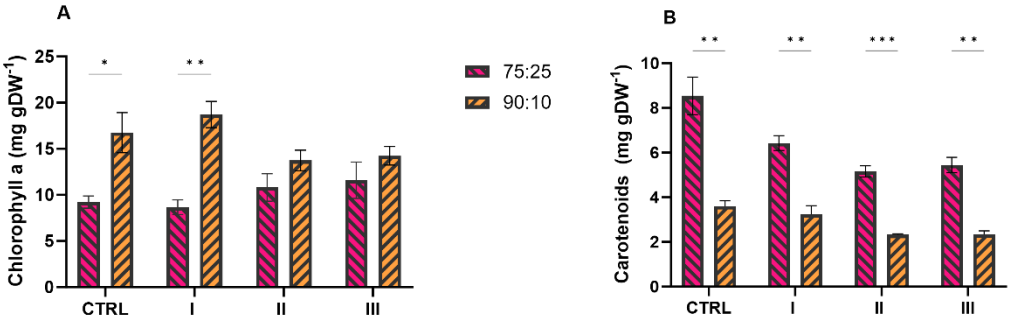


6.3.4.4. Photosynthetic pigments accumulation by 2PE_aroK mutant strain in wastewaters

The main photosynthetic pigments, i.e. chlorophyll a (chla) and carotenoids (car), were investigated because they can be used as physiological parameters to assess the quality of the cyanobacterial culture. **Figure 6.8** shows the pigments profile, expressed as mg of pigment per g of dry biomass (mg gDW^{-1}), in both 75:25 and 90:10 ratios (see the **Table 6.2** for more details). The chla content, measured at the end of the cultivation, was comparable in both 75:25 and 90:10 mixtures (**Figure 6.8A**) in conditions II and III, resulting in a range of 11-14 mg gDW^{-1}. Within the two ratios, the main difference in chlorophyll content was detected for control and condition I of 90:10, where the chla content was almost doubled with respect to 75:25, reaching almost 20 mg gDW^{-1} (**Figure 6.8A**). Otherwise, the content of carotenoids was found to be higher in all the

conditions exposed to 75:25 instead of 90:10 (**Figure 6.8B**). The control condition in 75:25 showed the highest carotenoids quantification, with 8.5 mg gDW^{-1}.

Figure 6.8. Photosynthetic pigments profile of 2PE_arok mutant strain growth on 75:25 and 90:10 mixtures between ES and WW *in three conditions and a control. All tests were carried out in biological triplicate. Error bars represent standard deviation. Asterisks refer to statistical significance (unpaired t-test, $\alpha \leq 0.05$).*



6.4. ***Discussion***

The reuse of wastewaters as nutritional sources for cultivating microorganisms and producing chemicals promotes the concept of a circular economy and ultimately enhances the economic and ecological sustainability of the whole biotechnology. Firstly, to design the sustainable bioprocess, the selection of the proper wastewater for specific microorganisms, or *vice versa*, is the preliminary step as well as the very challenging task to accomplish. To optimize resource allocation and minimize inefficiencies, it is mandatory to consider the physiological requirements and the final purpose of the relative bioprocess. In this instance, the mutant strain of *S. elongatus* PCC 7942, named 2PE_*aroK*, has been used to evaluate a sustainable 2-PE bioproduction design on dairy wastewaters. The 2PE_*aroK* mutant strain overexpresses five genes and their rules are summarized in **Supplementary Table 6.1**. As already reported (Usai *et al.*, 2022), the 2PE_*aroK* mutant strain needs L-phenylalanine (L-Phe) as metabolite doping to enhance the 2-PE production.

S. elongatus is an obligate photoautotroph and the uptake of organic carbon has been obtained solely by genetic engineering (McEwen *et al.*, 2013; Sarnaik, Pandit and Lali, 2017; Sarnaik *et al.*, 2018). However, its excellent ability to rapidly absorb nutrients, such as P and N, simple nutritional requirements and metabolic plasticity, make it a promising biofactory for producing high-value compounds coupled with the treatment of nutrient-rich effluents. The dairy sector generates different types of effluent, appealing for biotechnological applications due to the high content of dissolved organic matter and nutrients, such as nitrogen, phosphates, fats, salts, proteins, free amino acids, metals, minerals, and their inherent composition, including the relative pH, varies based on the unique production line and specific plant cleaning procedures (Sarkar *et al.*, 2006; Vourch *et al.*, 2008; Carvalho, Prazeres and Rivas, 2013; Licata *et al.*, 2021). Importantly, the need of substantial volume of freshwater represents a challenge of the milk and cheese industries, resulting in generation of a considerable excess of wastewater. It has been estimated that the amount of wastewater is one to three times higher than the volume of processed milk (Usmani *et al.*, 2022), and solely in Italy the effluent volume has been evaluated as 18.9×10^6 m^3 per year (Stasinakis, Charalambous and Vyrides, 2022). Consequently, recovering as much water as possible from the dairy streams should be a main practice towards the water quality and resource management in biotechnology. Indeed, different kinds of liquid wastes are produced by dairy industries as primary wastes like cheese whey (CW), scotta (Sc),

pipelines and tank washing waters (WW) or secondary as exhausted sludge (ES). Early in this study, all the dairy waste streams have been considered for this biotechnological application, and, at the same time, discussed for their employability in microalgae/cyanobacteria-based applications, highlighting potentialities and challenges. Firstly, they were chemically characterized, and the analysis is reported in **Table 6.1**. In the literature, for dairy effluents the ratio of the key macroelements is reported to be C/N/P ≈ 200/3.5/1, which is generally considered nitrogen deficient to drive any biological processes (Prazeres, Carvalho and Rivas, 2012; Lu *et al.*, 2016). Concerning the nitrogen source, the most used in synthetic cultural media is nitrate (NO_3^-). Even if the nitrate uptake is ATP demanding, nitrate is harmless at high concentration (Flores and Herrero, 1994) and so commonly preferred as nitrogen supply for microbial cultivations. However, in dairy effluents the most diffused nitrogen form is ammonium (NH_4^+), as in several wastewaters (Li *et al.*, 2017). Fortunately, both cyanobacteria and eukaryotic microalgae are able to assimilate also free ammonium as nitrogen source, but often in wastewaters the concentration is too high to be tolerated by these microbes. As reported, ammonium would inhibit the photosynthesis of some cyanobacteria species even at ca. 30 mg L^{-1} NH_4^+ (Belkin and Boussiba, 1991; Dai *et al.*, 2008). Indeed, sometimes strong dilution (Park and Craggs, 2011; Xia and Murphy, 2016) or nitrification (Sekine *et al.*, 2020; Casagli *et al.*, 2021; Das, Kundu and Adhikari (Nee Pramanik), 2022; H. Liu *et al.*, 2022) of ammonium-rich wastewaters are crucial prior to feed photosynthetic microorganisms. Nevertheless, here, we quantified a putative deficiency in ready-to-use nitrogen sources, such as NO_3^- and NH_4^+. The nitrate ion in the present wastewaters was under the detection limit (< 1.5 mg L^{-1} NO_3^-). To be precise, the nitrate ion concentration in BG11 medium is 1.09 g L^{-1}. On the other hand, phosphates resulted to be sufficient for supporting cyanobacteria growth, even at the lowest concentrations measured (**Table 6.1**). High phosphate loads definitely promote the cyanobacterial biomass accumulation (Burberg, Petzoldt and von Elert, 2020), as indicated in the context of eutrophication. Actually, this phenomenon is often attributed to the high content of phosphates in cleaning agents and fertilizers and even the influence of climate change can promote phosphates accumulation in water bodies (Forber *et al.*, 2018; Wilson *et al.*, 2019). Additionally, aquatic habitats are characterized by temporally fluctuations in phosphate availability, so, to cope with this, cyanobacteria evolved several smart strategies to thrive even at low phosphate concentration (Riegman *et al.*, 2000; Adams *et al.*, 2008; Van Mooy *et al.*, 2009).

Often, the salinity is the main issue affecting the employability of dairy wastes in non-halotolerant microalgae and cyanobacteria bioprocess, sometimes requiring strong dilutions. On the other hand, the osmotic stress caused by high salts concentration is used as strategy to boost the high-value carotenoids synthesis in several microalgae, e.g. *Dunaliella salina* and *Haematococcus pluvialis* (Sedjati *et al.*, 2019; Li *et al.*, 2022). Nevertheless, the salinity seems not to be a problem for *S. elongatus* PCC 7942, which has been reported to have a high salinity tolerance up to 0.4 M (23 g L^{-1}) (Dong *et al.*, 2023), quite high value for a freshwater microorganism.

Microalgae and cyanobacteria are proficient to reduce heavy metals content into wastewaters, e.g. Chromium, Copper, Lead, Arsenic, Mercury, Nickel and Cadmium by bioaccumulation and biosorption (Chakravorty *et al.*, 2023). Instead, many heavy metals, such as Zinc, Iron, Cobalt, Manganese are crucial for microalgae/cyanobacteria metabolism (Balzano *et al.*, 2020). In fact, metal homeostasis is especially important in cyanobacteria, because the photosynthetic machinery imposes high demand for metals, acting as cofactors of several proteins (Huertas *et al.*, 2014). Even at higher concentrations of some heavy metals, microalgae show elevated biomass, thereby proving to be a suitable candidate for bioremediation (Upadhyay *et al.*, 2016). Here, Cu and Fe were discussed, because of their rule either in photosynthesis or respiratory electron chains (Shcolnick and Keren, 2006; López-Maury, Giner-Lamia and Florencio, 2012). Only Cu in ES resulted to be under the detection limit (**Table 6.1**), while in the other wastewaters the concentration of both metals could hypothetically sustain cyanobacteria as well as microalgae cultivation. Worthy of mention, pH and COD can strongly influence this type of cultivations (Giraldez-Ruiz *et al.*, 1997). In fact, cyanobacteria show growth at pH values ranging from 7.5 to 11, and they are practically absent in habitats with pH < 5 (Brock, 1973). Moreover, the pH also strongly affects the CO_2 concentrating mechanism (CCM) (Mangan *et al.*, 2016). Otherwise, some eukaryotic microalgae have been successfully cultivated in very acidic wastewaters (Abinandan, Venkateswarlu and Megharaj, 2021; Yu *et al.*, 2022). Given the importance of pH, a detailed investigation of pH effect on our strain has been accomplished and will be discussed later on. Following the chemical characterization of the dairy wastewaters, those were qualitatively screened for cyanobacterial growth. This test was conducted on 2PE_*aroK* mutant strain, being our chassis for addressing this bioprocess aimed at producing biologically 2-PE. As expected, the qualitative screening highlighted that both CW and Sc were unsuitable for cyanobacteria, even when diluted by 50% (data not shown). Conversely, ES and WW showed that they can

support cyanobacteria, if opportunely treated and supplemented (**Figure 6.1**). The nitrogen source was found to be the main limitation factor in both ES and WW. For this reason, we searched for the minimum ammonium concentration allowing cyanobacteria to grow in 75% ES similarly to the standard medium. We found 0.15 g L^{-1} as the best condition (**Figure 6.2**). This is not the first example where nitrogen supplementation was necessary for microalgae applications, especially for secondary wastewater treatments (Huang *et al.*, 2017; Rodrigues-Sousa *et al.*, 2021), such as ES. Additionally, the so-called Redfield ratio (N:P = 16:1) assumes that the balancing between nitrogen and phosphates in the medium really affects marine photosynthetic microorganisms growth (Redfield, 1934). However, for freshwater microalgae, the Redfield ratio seems to be an exception and the N:P molar ratios can range between 8:1 and 45:1 with a species specific preferences (Hecky, Campbell and Hendzel, 1993). Here, using ES as reference we had N:P ca. 4, which is definitely too low to sustain cyanobacteria. By supplementing extra nitrogen as ammonium, we reached the ratio of 12.26, while in BG11 N/P molar ratio is approx. 76. Curiously, as reported in (Choi and Lee, 2015), the biomass production highly depends on the N/P ratio, and they noticed that increasing ratio up to 10 proportionally promotes the biomass accumulation and then decreases to a constant value, even furtherly rising the ratio. So, theoretically, considering the intrinsic stoichiometry of specific microalgae, the wastewater bioremediation approach could be tailor-made and, thus, optimized to address specific sustainability goals.

To simultaneously balance the pH (ca. 7.5) and the nutritional contribution, as discussed earlier, we mixed ES and WW in different ratio, supplemented with 0.15 g L^{-1} NH_4^+. We assessed also the evolution of pH level during the cyanobacterial growth with no pH control system (**Figure 6.3A**). The best condition found was 90:10, where highest biomass production was allowed (**Figure 6.3B**), but the pH rose rapidly from 7.02 to 9.2, probably preventing further cell accumulation. Thus, to better understand how the pH was impacting the cyanobacterial growth, we used a buffering system, i.e. MOPS (6.5-7.9). Three different concentrations were tested on the three mixtures between ES and WW, but the lowest one (i.e. 25 mM MOPS) resulted to be suitable for our purposes, while higher concentrations improved the pH control but did not affect the biomass production (**Figure 6.3C, D**). Additionally, we noticed that controlling the pH level improved the biomass formation, mainly at 75:25 (**Figure 6.3D**). Thereby, established the minimal requirements for the cyanobacteria growth, a deeper analysis concerning the target molecule (2-PE) production skills in wastewaters

has been conducted. Particularly, both 75:25 and 90:10 ratios were selected for the following tests, while 60:40, once again, resulted in failing cyanobacteria culture. Noteworthy, the implementation of buffers into wastewater treatment bioprocesses is not uncommon, especially when the wastewaters are mixed with standard cultural media, which usually contain buffer agents (Song *et al.*, 2020; Lee, Lee and Sim, 2023). Particularly, this is the case of studies at laboratory scale, where the pH control relies on manual addition of buffers or acid/bases. In photobioreactors manage the pH is a consolidated practice and nowadays on/off strategy is largely exploited. Thereby, the pH is constantly monitored and when the pH rises beyond a setpoint (depending on the microorganisms or to avoid ammonia volatilization) the injection of CO_2 is activated and so the pH will be lowered.

Next, four different conditions were designed for both 75:25 and 90:10. All the cultivation conditions contain 25mM MOPS as pH buffering system and they were differentiated by the supplementation of ammonium and/or L-Phe. Actually, in the control condition (no nitrogen or L-Phe supplementation) both the growth and the 2-PE synthesis resulted to be drastically reduced. At 75:25 ratio, the bacterial growth resulted to be affected mostly by the nitrogen addition (**Figure 6.4A**, conditions II and III), while the L-Phe addition at the beginning of the test (**Figure 6.4A**, condition III) seemed not to improve the growth. The same trend was detected in the 90:10 ratio for both growth (**Figure 6.5A**) and 2-PE production (**Figure 6.5B**) kinetics. However, the specific growth rate (μ, d^{-1}) was 2-fold higher in 75:25 than in 90:10 in all the conditions and control (**Table 6.2**), although the final biomass accumulation was higher (0.7 gDW L^{-1}) than that at 75:25 (0.6 gDW L^{-1}).

The 2-PE synthesis was directly improved by the supplementation of L-Phe (either at 6^{th} day of cultivation or at the beginning of the test) and indirectly due to the addition of extra nitrogen, which increased the biomass accumulation (condition II and III). Comparing to the control, in both the wastewater mixtures, the 2-PE production was enhanced 5-fold and 9-fold in 90:10 and 75:25, respectively. While the highest final 2-PE titer was reached in 90:10 ratio (205 mg L^{-1} in condition II, **Figure 6.5B**), the daily productivity lowered (12.8 mg L^{-1} d^{-1}, **Figure 6.5D**), which is a 30% decrement of the highest one in 75:25 ratio (18.03 mg L^{-1} d^{-1}, **Figure 6.4D**). Therefore, the production kinetics in 90:10 mixture necessary to reach the highest 2-PE concentration was longer (16 days) than in 75:25 (10 days), where 180 mg L^{-1} were achieved. Overall, the 2-PE production on wastewaters recorded here resulted lowered by 37% (in 75:25) and 28%

(in 90:10) in comparison with the highest 2-PE titer reported in literature for the same mutant strain, but under ideal and synthetic laboratory conditions (Usai *et al.*, 2022).
While the mutant strain was subjected to the metabolite doping, carried out by adding L-Phe, the metabolite doper resulted to be differentially consumed in the tested conditions (**Figure 6.6A, B**). In both the ratios when the L-Phe was supplemented at 6^{th} day (condition II) or at the beginning of growth (condition III), the consumption was ranging from 34% to 54% (**Figure 6.6A**) of the available L-Phe. Interestingly, those test conditions in both the ratios led to the highest 2-PE production of 180 and 205 mg L^{-1} for 75:25 and 90:10, respectively. Indeed, considering the theoretical carbon yield between 2-PE (C8) and L-Phe (C9) of 0.89 molC $molC^{-1}$, the actual amount of L-Phe consumed (**Figure 6.6B**) on average (between condition II and III) of 7.28 molC L^{-1} and 9.51 molC L^{-1} (75:25 and 90:10, respectively) may contribute to 59% and 64% of the 2-PE produced in the two mixtures. These findings support the hypothesis (Usai *et al.*, 2022) that L-Phe would not be completely used by the mutant for 2-PE synthesis. Probably, the amino acid partially helps the 2PE_*aroK* strain to overcome some metabolic constraints, whose affect this mutant when overexpressing the 2-PE heterologous pathway. Curiously, when L-Phe was supplemented at 6^{th} day in 90:10 mixture (condition I), the uptake accounted for 100%, i.e. 0.347 g L^{-1} (**Figure 6.6A**), an outlier of this investigation, however, this massive L-Phe uptake had no effect on both growth and 2-PE production (**Figure 6.5A, B**). Analysis of the removal of the main macronutrients, i.e. N and P, confirmed the strong capability of cyanobacteria to phycoremediate wastewaters (**Figure 6.7**). Indeed, the 100% of the available phosphates was consumed and ammonium resulted in a reduction by 74 and 77% in the 75:25 and 90:10 mixtures, respectively. The present results are perfectly consistent with previous studies, conducted in both prokaryotic and eukaryotic microalgae (Kothari *et al.*, 2013; Qin *et al.*, 2014; Choi, 2016; Chokshi *et al.*, 2016; Brar, Kumar and Pareek, 2019; Kusmayadi *et al.*, 2022; Praveen *et al.*, 2023).
Interestingly, we have observed that the photosynthetic pigments production exhibited distinct profiles within the different mixture conditions. (**Figure 6.8; Table 6.2**). Indeed, the assessment of photosynthetic pigments is a common physiological parameter to evaluate the quality of cyanobacteria/microalgae cultures. The chla content, measured at the end of the cultivation, was comparable in both 75:25 and 90:10 mixtures (**Figure 6.8A**), while the amount of carotenoids profiled differently between the two wastewater ratios (**Figure 6.8B**). Within the two ratios, the main difference in chlorophyll content was found in control e condition I, while in 90:10 the chla content

was almost doubled with respect to 75:25 (**Figure 6.8A**). On the other hand, the carotenoids content resulted to be strongly increased in all the conditions tested for 75:25 ratio (**Figure 6.8B**) if compared with 90:10 (p-values ≤ 0.002). It is important to stress that all the tested conditions here were subjected to the same environmental parameters (light intensity, temperature, shaking), thereby, only the medium composition was the study object. Indeed, excluding the light as stressing factor affecting the chla content in both the wastewater mixtures, the limiting factor should be searched elsewhere. As reported in the literature, under iron deficiency the amount of chlorophyll decreases and carotenoids increases (Ivanov *et al.*, 2007; Jia *et al.*, 2021). Accordingly, from the chemical analysis reported in **Table 6.1**, the iron content in the effluents (42-60 μg L^{-1}) was approximately 17-fold lower than that in the standard BG11 medium. This hypothesis could explain the different carotenoids amount between the two ratios, but, still, could not provide any clue about the higher content in the control of 75:25 (**Figure 6.8B**). The control condition, actually, may suffer from the strongest stress conditions, where no N or L-Phe supplementation was supplied. Here, several combined stressors could have affected the control growth and pigments accumulations. Indeed, even if carotenoids are mainly involved in light-induced stress, they have been found related also with any type of stress generating reactive oxygen species (ROSs) (Masojídek, Torzillo and Koblížek, 2013). Consequently, it is possible that in 75:25 mixture, where the WW proportion is higher than in 90:10, the oxidative effect was more severe due to the higher COD/BOD (**Table 6.1**) and, thus, resulting in higher accumulation of carotenoids. Furthermore, this putative oxidative effect in 75:25 ratio seemed not to have effect on the growth and 2-PE synthesis, that, instead, resulted to be improved than those at 90:10 (**Table 6.2**). Moreover, the supplementation of N and/or L-Phe appeared to be relieving for this putative oxidative condition. Indeed, in condition II and III the carotenoids content was lower than control (**Figure 6.8B**) in both 75:25 and 90:10 ratios. Being a wastewater treatment based on photosynthesis, these pigment content related consideration can help define optimal conditions under which the microorganisms should operate.

However, in scaling up a process, several issues have to be faced. Indeed, nutrient-rich effluents are difficult to fully sterilize, and suffer from frequent biological contaminations. Nevertheless, some smart strategies have been proposed to allow microalgae and cyanobacteria to compete to contaminants, in wastewater treatment as well as in massive volume cultivations. Mainly, for instance, the recreation of the optimal environment for the target strain, such as stoichiometrically balancing the

C/N/P accordingly with the microalgal biomass (Chang *et al.*, 2023), or cultivating at high value of pH (Touloupakis *et al.*, 2016; Haines *et al.*, 2022) or salinity (Vonshak *et al.*, 1983; Borowitzka and Borowitzka, 1990). Thus, accordingly with the physiological needs and the chemical features of wastewaters could be possible to design a process where the target cultures can thrive. In addition, to reduce biological contaminations for large-volume microalgae cultivation, physical filtration, ultraviolet sterilization and ultrasound treatment have been considered as effective methods for in situ removal of biological pollutants with insignificant effect on protozoans eggs and spores (Holm *et al.*, 2008; Nawar *et al.*, 2017; Zhu, Jiang and Fa, 2020).

Significantly, cultivating engineered cyanobacteria strains in wastewater for sophisticated production is not so common, while wild-type strains are preferred, such as *Spirulina* (Lim *et al.*, 2021; Zapata *et al.*, 2021). Furthermore, traditionally, antibiotics are commonly used as selection markers for recombinant strains and adopted for strain maintenance, as in our case. This is considered as inconvenient for environment-oriented biotechnological approaches, especially in wastewaters treatment. Indeed, researchers are focused on the development of alternative selection markers to avoid antibiotics utilization. For instance, nutritional markers involve mutations into essential metabolic pathways, rendering cells dependent on specific nutrients for growth (Dormatey *et al.*, 2021). Additionally, auxotrophic markers are similar to the previous ones, so, the mutant cells can then be selected by their inability to grow in the absence of required nutrients (Ulfstedt *et al.*, 2017). As the optimal choice, marker-free recombinant strains represent the avant-garde, allowing to the most environmentally suitable solution (Rajveer Singh *et al.*, 2022).

Overall, only a few reports, nowadays, have been published for chemicals production that involve engineered cyanobacteria on wastewater (Hollinshead *et al.*, 2014; Cao *et al.*, 2019). Thus, this investigation proposes a case of study as tertiary treatments via engineered cyanobacteria for sustainable added-value compounds bioproduction, worthy of further development for larger volume applications.

6.5. Conclusions

Nowadays, the (almost) unique controversy related to microalgae biotechnology regards the costs of their mass cultivation and the huge volume of water needed. To cut these concerns, many strategies have been proposed among growth medium recycling

and the exploitation of wastewaters, which need to be properly treated prior to disposal. As a natural consequence, the utilization of wastewaters in bioprocessing has vast potential for environmental and economic sustainability, aligning with the principles of circular economy, in which resources are recycled and waste minimized.

Here, we propose a sustainable approach to produce 2-phenylethanol using a metabolically engineered cyanobacteria (2PE_*aroK*), by combining dairy wastewaters to harmonize microbial physiology with the peculiar composition of these effluents. In this study, the resource optimization for both specific microbial cultivations and sustainability targets is spotlighted. Indeed, while eukaryotic microalgae support better COD-high dairy wastewater treatments oriented to biomass-related products (e.g. lipids, proteins), cyanobacteria can promote more sophisticated biomanufacturing for high-value compounds even in not-so-rich wastewaters, keeping high growth rates via photoautotrophy. Consequently, freshwater conservation is directly supported, merging the future targets of water management and water quality enhancement. Dairy wastewaters, known for their rich organic carbon content, minerals, nitrogen, and phosphates, are generally considered suitable for microbial cultivation. However, the specific composition of these wastewaters, including pH and nutrient ratios, varied depending on the dairy production process and cleaning procedure. Therefore, to efficiently valorize such wastewaters for bioprocessing requires careful consideration of their chemistry. Thereby, we collected some clues aimed at building a tailor-made process to really improved the bioprocess *in-toto*. Consequently, customizing the bioprocess to match the specific composition of different wastewater streams with the biological needs of the microbial chassis, we obtained an effective production of 2-PE on wastewaters, counting for 180 and 205 mg L^{-1} as the best conditions. Thus, these findings ultimately offer a promising case of study for future research and the practical application of sustainable industrial practices, thereby fostering a greener and more responsible approach to photosynthetic biotechnology and bioprocessing.

List of abbreviations

CW: cheese whey

Sc: scotta

WW: washing water

ES: exhausted sludge

2-PE: 2-phenylethanol

***aroK*:** gene encoding for shikimate kinase

Phe: phenylalanine

COD: chemical oxygen demand

BOD: biochemical oxygen demand

Chla: chlorophyll a

		μ (d^{-1})			Max 2-PE titer (mg L^{-1})			Max 2-PE yield (mg gDW^{-1})			Average 2-PE productivity (mg L^{-1} d^{-1})			Chl α (mg gDW^{-1})			Car (mg gDW^{-1})		
Ratio ES:WW	**Condition**	**Average**	**SD**	**p-value**	**Average**	**SD**	**p-value**	**Average**	**SD**	**p-value**	**Average**	**SD**	**p-value**	**Average**	**SD**	**p-value**	**Average**	**SD**	**p-value**
75 : 25	***CTRL***	0.168	0.003		18.9	0.4		53.30	8.32		1.89	0.04		9.35	0.89		8.54	0.84	
	I	0.199	0.002	***	81.0	9.8	***	221.22	27.73	***	8.10	0.98	***	8.67	0.79	ns	6.42	0.33	*
	II	0.223	0.015	**	158.1	32.5	**	295.41	20.28	****	15.81	3.25	**	10.81	1.49	ns	5.16	0.25	*
	III	0.207	0.006	***	180.3	15.6	****	370.53	23.75	****	18.03	1.56	****	11.59	1.96	ns	5.45	0.34	*
90 : 10	***CTRL***	0.085	0.003		38.12	4.80		119.37	8.27		2.38	0.30		16.75	2.18		3.60	0.25	
	I	0.103	0.006	**	60.39	7.04	*	119.59	14.93	ns	3.77	0.44	*	18.70	1.43	ns	3.24	0.38	ns
	II	0.106	0.005	**	205.10	29.73	**	294.00	14.22	***	12.82	1.86	**	13.74	1.11	ns	2.32	0.04	**
	III	0.119	0.002	***	202.01	5.19	****	289.08	12.78	***	12.63	0.32	****	14.24	1.01	ns	2.34	0.16	**

Table 6.2. Sum up of the main results of the present investigation about the growth of 2PE_aroK mutant strain in 75:25 and 90:10 ratios of ES and WW. *SD, standard deviation. The statistical tests were performed as unpaired t-test (α ≤ 0.05) versus the control condition. *, p-value ≤ 0.05; **, p-value ≤ 0.002; ***, p-value ≤ 0.0002; ****, p-value ≤ 0.0001. Chl α, chlorophyll α. Car, carotenoids.*

6.6. *Supplementary Materials*

Gene	*HR Site*	*Protein*	*EC number*	*Reaction*	*Organism*	*Ref.*
aroG^{fbr}	NSI	feedback-inhibition resistant DAHP synthase	EC 2.5.1.54	PEP + E4P +H_2O ⇌ DAHP + Pi	*Escherichia coli*	(Ni *et al.*, 2018; Usai *et al.*, 2022)
pheA^{fbr}	NSI	feedback-inhibitionresistant chorismate mutase/prephenate dehydratase	EC 5.4.99.5/ EC 4.2.1.51	Chorismate ⇌ Prephenate ⇌ Phenylpyruvate + H_2O + CO_2	*Escherichia coli*	(Ni *et al.*, 2018; Usai *et al.*, 2022)
kivD	NSI	Phenylpyruvate decarboxylase	EC 4.1.1.43	Phenylpyruvate ⇌ phenylacet aldehyde + CO2	*Lactococcus lactis*	(Ni *et al.*, 2018; Usai *et al.*, 2022)
adhA	NSI	Alcohol dehydrogenase A	EC 1.1.1.1	Phenylacetaldehyde + NAD(P)H ⇌ 2-Phenylethanol + $NAD(P)^+$	*Synechocystis PCC 6803*	(Ni *et al.*, 2018; Usai *et al.*, 2022)
aroK	NSII	Shikimate kinase	EC 2.7.1.71	Shikimate + ATP ⇌ Shikimate-3-P + ADP	*S. elongatus PCC 7942*	(Usai *et al.*, 2022)

Supplementary Table 6.1. Genetic features of 2PE_aroK recombinant strain of S. elongatus PCC 7942*. HR, homologous recombination; DAHP, 3-deoxy-7-phosphoheptulonate; PEP, phosphoenolpyruvate; E4P, erythrose-4-phosphate.*

Buffer	Molarity	ES:WW	Initial pH	Final pH		Final OD_{730}	
		Ratio		Average	SD	Average	SD
No Buffer	/	90:10	7.02	9.17	0.11	0.536	0.029
	/	75:25	6.9	6.88	0.07	0.210	0.021
	/	60:40	6.57	6.57	0.05	0.052	0.020
TES	**30 mM**	90:10	7.69	8.8	0.03	0.595	0.029
	30 mM	75:25	7.56	8.6	0	0.616	0.065
	30 mM	60:40	7.41	7.96	0.03	0.510	0.026
MOPS	**25 mM**	90:10	7.53	9.05	0.03	0.538	0.003
	25 mM	75:25	7.45	8.38	0.03	0.619	0.029
	25 mM	60:40	7.26	7.43	0.05	0.379	0.026
	50 mM	90:10	7.67	8.25	0.04	0.543	0.023
	50 mM	75:25	7.61	8.23	0.04	0.650	0.028
	50 mM	60:40	7.5	7.91	0.01	0.494	0.028
	75 mM	90:10	7.77	8.17	0.01	0.536	0.047

Supplementary Table 6.2. Detailed results of the pH control system screening in ES:WW mixtures. SD, standard deviation. *All tests were carried out in biological triplicate. Error bars represent standard deviation.*

Chapter 7

7. Conclusions and Outlook

In this comprehensive study, a recombinant photosynthetic cell factory was successfully enhanced for 2-phenylethanol (2-PE) production, i.e. an aromatic, rosy-scented high-value compound, employed in cosmetics, and food and beverage industries. The combination of several disciplines from molecular biology, synthetic biology, microbiology, bioinformatics to engineering, bioprocess development and environmental sciences allowed to reach a wider picture about what biotechnology truly means.

Here, the attention is paid to process-to-industry biotechnology in the effort to propose a photosynthesis-based biomanufacturing for high-value compound production. That was realized by coupling metabolic engineering, through the overexpression of five proteins involved in 2-PE production, and process engineering, by setting all the parameters and conditions for improving 2-PE production process *in toto*.

Firstly, the cyanobacteria recombinant strain, called 2PE_*aroK*, was created and characterized (***Chapter 3***), achieving a 2.4-fold increase in 2-PE production compared to the previous report. Interestingly, the overexpression of the native shikimate kinase addressed a bottleneck in cyanobacterial metabolism, suggesting its potential as a target for various aromatics and derived compound production strategies. A follow-up in laboratory scale photobioreactor revealed the non-obvious relationship between photosynthesis, biomass formation, and heterologous production of 2-PE, under varying light intensity (***Chapter 4***). Contrary to expectations, the highest light intensity, among those assessed, did not result in the highest 2-PE production, while the bacterial growth and 2-PE synthesis resulted uncoupled. Carbon consumption analysis elucidated the intricate carbon distribution, with the highest carbon allocation to 2-PE observed under the lowest light intensities, with the carbon balance accounting for 45-50%.

The study extended to the scale-up of photosynthetic microbial factory for 2-PE production, evaluating different photobioreactor configurations (***Chapter 5***). Enclosed

PBR systems, particularly the airlift flat panel, exhibited superior performance in terms of biomass productivity and growth rates, while acknowledging the challenge of biological contaminations. The importance of tailored contamination control strategies and efficient cleaning and sterilization methods for PBR operational procedures emerged in the present thesis, as obligatory task for improving the sustainability of microalgal biotechnology.

Finally, addressing concerns about the environmental and economic sustainability of microalgae cultivation, the study proposed a sustainable approach to produce 2-PE using this metabolically engineered cyanobacteria and dairy wastewaters (***Chapter 6***). The combination of two dairy wastewaters was presented as a potential solution aligning with the principles of circular economy, highlighting the need for careful consideration of effluent chemistry to tailor the bioprocess effectively on the microbial factory. Thus, under tailored conditions 2-PE was successfully synthesized on dairy effluents. The results offered a promising case for future research and practical application of sustainable industrial practices in photosynthetic biotechnology and bioprocessing.

Additionally, the secretion of the target product into the cultural medium allows for the valorization of a significant amount of spent cell biomass. Cyanobacteria biomass, rich in valuable compounds such as photosynthetic pigments, can be exploited further. Indeed, in the thesis it is possible to find suggested strategies to valorize pigments and utilize carbohydrates from biomass as a substrate or additive for other fermentation cultivations.

Overall, all together these findings underline the potential of finely tuned bioprocesses to harness the effectiveness of photosynthetic microorganisms in biomanufacturing processes, displaying the multifaceted aspects of optimizing microbial platforms for efficient production.

Further research will refine these strategies and explore novel approaches for large-scale and practical applications in the evolving field of microalgae and cyanobacteria biotechnology, with a focus on sustainability, scalability, and interdisciplinary collaboration.

References

2-Phenylethanol Market - By Product (Synthetic, Natural), By Application (Cosmetics & Personal Care, Laundry & Home Care, Food & Beverages, Pharmaceuticals) & Forecast, 2022-2028 (2022). Available at: https://www.gminsights.com/industry-analysis/2-phenylethanol-market.

Abdelfattah, A. *et al.* (2023) 'Microalgae-based wastewater treatment: Mechanisms, challenges, recent advances, and future prospects', *Environmental Science and Ecotechnology*, 13, p. 100205. doi: https://doi.org/10.1016/j.ese.2022.100205.

Abed, R. M. M., Dobretsov, S. and Sudesh, K. (2009) 'Applications of cyanobacteria in biotechnology', *Journal of Applied Microbiology*, 106(1), pp. 1–12. doi: 10.1111/j.1365-2672.2008.03918.x.

Abinandan, S., Venkateswarlu, K. and Megharaj, M. (2021) 'Phenotypic changes in microalgae at acidic pH mediate their tolerance to higher concentrations of transition metals', *Current Research in Microbial Sciences*, 2, p. 100081. doi: https://doi.org/10.1016/j.crmicr.2021.100081.

Acién Fernández, F. G. *et al.* (2001) 'Airlift-driven external-loop tubular photobioreactors for outdoor production of microalgae: assessment of design and performance', *Chemical Engineering Science*, 56(8), pp. 2721–2732. doi: https://doi.org/10.1016/S0009-2509(00)00521-2.

Adame-Soto, P. J. *et al.* (2019) 'Potential production of 2-phenylethanol and 2-phenylethylacetate by non-Saccharomyces yeasts from Agave durangensis', *Annals of Microbiology*, 69(9), pp. 989–1000. doi: 10.1007/s13213-019-01489-0.

Adams, M. M. *et al.* (2008) 'Phosphorus Deprivation Responses and Phosphonate Utilization in a Thermophilic *Synechococcus* sp. from Microbial Mats', *Journal of Bacteriology*, 190(24), pp. 8171–8184. doi: 10.1128/jb.01011-08.

Adams, T. B. *et al.* (2005) 'The FEMA GRAS assessment of phenethyl alcohol, aldehyde, acid, and related acetals and esters used as flavor ingredients', *Food and Chemical Toxicology*, 43(8), pp. 1179–1206. doi: https://doi.org/10.1016/j.fct.2004.11.013.

Agustí, S. (1991) 'Light environment within dense algal populations: cell size influences on self-shading', *Journal of Plankton Research*, 13(4), pp. 863–871. doi: 10.1093/plankt/13.4.863.

Ahmad, A. and Ashraf, S. S. (2023) 'Sustainable food and feed sources from microalgae: Food security and the circular bioeconomy', *Algal Research*, 74, p. 103185. doi: https://doi.org/10.1016/j.algal.2023.103185.

Ahmad, I. Z. (2022a) 'The usage of Cyanobacteria in wastewater treatment: prospects and limitations', *Letters in Applied Microbiology*, 75(4), pp. 718–730. doi: 10.1111/lam.13587.

Ahmad, I. Z. (2022b) 'The usage of Cyanobacteria in wastewater treatment: prospects and limitations', *Letters in Applied Microbiology*, 75(4), pp. 718–730. doi: 10.1111/lam.13587.

Ahmadi, M. K. *et al.* (2016) 'E. coli metabolic engineering for gram scale production of a plant-based anti-inflammatory agent', *Metabolic Engineering*, 38, pp. 382–388. doi: https://doi.org/10.1016/j.ymben.2016.10.001.

Ahn, J. *et al.* (2011) 'NADPH-dependent pgi-gene knockout Escherichia coli metabolism producing shikimate on different carbon sources', *FEMS Microbiology Letters*, 324(1), pp. 10–16. doi: 10.1111/j.1574-6968.2011.02378.x.

Aikawa, S. *et al.* (2014) 'Glycogen production for biofuels by the euryhaline cyanobacteria Synechococcus sp. strain PCC 7002 from an oceanic environment', *Biotechnology for Biofuels*, 7(1), p. 88. doi: 10.1186/1754-6834-7-88.

Al-Jabri, H. *et al.* (2021) 'Treatment of Wastewaters by Microalgae and the Potential Applications of the Produced Biomass—A Review', *Water*. doi: 10.3390/w13010027.

Al-Tohamy, R. *et al.* (2022) 'A critical review on the treatment of dye-containing wastewater: Ecotoxicological and health concerns of textile dyes and possible remediation approaches for environmental safety', *Ecotoxicology and Environmental Safety*, 231, p. 113160. doi: https://doi.org/10.1016/j.ecoenv.2021.113160.

Alarde, H. P. S. *et al.* (2022) 'Development of an Arduino-based photobioreactor to investigate algae growth rate and CO_2 removal efficiency', *IAES International Journal of Robotics and Automation (IJRA)*, 11(2), p. 141. doi: 10.11591/ijra.v11i2.pp141-160.

Allen, J. F. (2003) 'Cyclic, pseudocyclic and noncyclic photophosphorylation: new links in the chain', *Trends in Plant Science*, 8(1), pp. 15–19. doi: https://doi.org/10.1016/S1360-1385(02)00006-7.

Alric, J., Lavergne, J. and Rappaport, F. (2010) 'Redox and ATP control of photosynthetic cyclic electron flow in Chlamydomonas reinhardtii (I) aerobic conditions', *Biochimica et Biophysica Acta (BBA) - Bioenergetics*, 1797(1), pp. 44–51. doi: https://doi.org/10.1016/j.bbabio.2009.07.009.

Álvarez, X. *et al.* (2020) 'Cyanobacterial Biomass Produced in the Wastewater of the Dairy Industry and Its Evaluation in Anaerobic Co-Digestion with Cattle Manure for Enhanced Methane Production', *Processes*. doi: 10.3390/pr8101290.

Amadu, A. A., deGraft-Johnson, K. A. A. and Ameka, G. K. (2021) 'Industrial Applications of Cyanobacteria', in Hozzein, W. N. (ed.). Rijeka: IntechOpen, p. Ch. 2. doi: 10.5772/intechopen.98859.

America, N. and Europe, W. (2020) 'What is the demand for coffee on the European market ? Contents of this page 1 . What makes Europe an interesting market for coffee ?', c(November).

Andreas, A. S., Michal, P. and J., H. K. (2012) 'Engineering a Cyanobacterial Cell Factory for Production of Lactic Acid', *Applied and Environmental Microbiology*, 78(19), pp. 7098–7106. doi: 10.1128/AEM.01587-12.

Andreotti, G. *et al.* (1994) 'Characterization of aromatic aminotransferases from the hyperthermophilic archaeon Thermococcus litoralis.', *European journal of biochemistry*, 220(2), pp. 543–549. doi: 10.1111/j.1432-1033.1994.tb18654.x.

Anfelt, J. *et al.* (2015) 'Genetic and nutrient modulation of acetyl-CoA levels in Synechocystis for n-butanol production', *Microbial Cell Factories*, 14(1), p. 167. doi: 10.1186/s12934-015-0355-9.

Ansari, F. A. *et al.* (2017) 'Microalgal cultivation using aquaculture wastewater: Integrated biomass generation and nutrient remediation', *Algal Research*, 21, pp. 169–177. doi: https://doi.org/10.1016/j.algal.2016.11.015.

Arad, S. and Cohen, E. (1991) 'Outdoor Cultivation of Microalgae in a Closed System for the Production of Valuable Biochemicals', *Biotechnology: Bridging Research and Applications*, pp. 301–316. doi: 10.1007/978-94-011-3456-9_20.

Arashiro, L. T. *et al.* (2020) 'Natural Pigments and Biogas Recovery from

Microalgae Grown in Wastewater', *ACS Sustainable Chemistry and Engineering*, 8(29), pp. 10691–10701. doi: 10.1021/acssuschemeng.0c01106.

Araújo, R. *et al.* (2021) 'Current Status of the Algae Production Industry in Europe: An Emerging Sector of the Blue Bioeconomy', *Frontiers in Marine Science*, 7. doi: 10.3389/fmars.2020.626389.

Arndt, C. and Sommer, U. (2014) 'Effect of algal species and concentration on development and fatty acid composition of two harpacticoid copepods, Tisbe sp. and Tachidius discipes, and a discussion about their suitability for marine fish larvae', *Aquaculture Nutrition*, 20(1), pp. 44–59. doi: https://doi.org/10.1111/anu.12051.

de Assis, L. R. *et al.* (2019) 'Evaluation of the performance of different materials to support the attached growth of algal biomass', *Algal Research*, 39, p. 101440. doi: https://doi.org/10.1016/j.algal.2019.101440.

Atra, R. *et al.* (2005) 'Investigation of ultra- and nanofiltration for utilization of whey protein and lactose', *Journal of Food Engineering*, 67(3), pp. 325–332. doi: https://doi.org/10.1016/j.jfoodeng.2004.04.035.

Averesch, N. J. H. and Krömer, J. O. (2018) 'Metabolic Engineering of the Shikimate Pathway for Production of Aromatics and Derived Compounds—Present and Future Strain Construction Strategies', *Frontiers in Bioengineering and Biotechnology*, 6. doi: 10.3389/fbioe.2018.00032.

Al Azad, S. *et al.* (2017) 'Assessment of Nutrients in Seaweed Tank from Land Based Integrated Multitrophic Aquaculture Module', *Journal of Geoscience and Environment Protection*, 05(08), pp. 137–147. doi: 10.4236/gep.2017.58012.

Babaoğlu Aydaş, S., Ozturk, S. and Aslım, B. (2013) 'Phenylalanine ammonia lyase (PAL) enzyme activity and antioxidant properties of some cyanobacteria isolates.', *Food chemistry*, 136(1), pp. 164–169. doi: 10.1016/j.foodchem.2012.07.119.

Babel, W. (2009) 'The Auxiliary Substrate Concept: From simple considerations to heuristically valuable knowledge', *Engineering in Life Sciences*, 9(4), pp. 285–290. doi: 10.1002/elsc.200900027.

Bader, F. G., Tsuchiya, H. M. and Fredrickson, A. G. (1976) 'Grazing of ciliates on blue–green algae: Effects of light shock on the grazing relation and on the algal population', *Biotechnology and Bioengineering*, 18(3), pp. 333–348. doi: https://doi.org/10.1002/bit.260180305.

Báez-Viveros, J. L. *et al.* (2004) 'Metabolic engineering and protein directed evolution increase the yield of L-phenylalanine synthesized from glucose in Escherichia coli.', *Biotechnology and bioengineering*, 87(4), pp. 516–524. doi: 10.1002/bit.20159.

Bahadur, A., Zubair, M. and Khan, M. B. (2013) 'Design, construction and evaluation of solarized airlift tubular photobioreactor', *Journal of Physics: Conference Series*, 439(1). doi: 10.1088/1742-6596/439/1/012036.

Baldasso, C., Barros, T. C. and Tessaro, I. C. (2011) 'Concentration and purification of whey proteins by ultrafiltration', *Desalination*, 278(1), pp. 381–386. doi: https://doi.org/10.1016/j.desal.2011.05.055.

Balzano, S. *et al.* (2020) 'Microalgal Metallothioneins and Phytochelatins and Their Potential Use in Bioremediation', *Frontiers in Microbiology*, 11(April), pp. 1–16. doi: 10.3389/fmicb.2020.00517.

Bar-Even, A., Noor, E. and Milo, R. (2012) 'A survey of carbon fixation pathways through a quantitative lens', *Journal of Experimental Botany*, 63(6), pp. 2325–2342. doi: 10.1093/jxb/err417.

Barakat, M. A. (2011) 'New trends in removing heavy metals from industrial wastewater', *Arabian Journal of Chemistry*, 4(4), pp. 361–377. doi: https://doi.org/10.1016/j.arabjc.2010.07.019.

Barbosa, M. J. *et al.* (2023) 'Hypes, hopes, and the way forward for microalgal biotechnology', *Trends in Biotechnology*, 41(3), pp. 452–471. doi: 10.1016/j.tibtech.2022.12.017.

Barkia, I., Saari, N. and Manning, S. R. (2019) 'Microalgae for High-Value Products Towards Human Health and Nutrition.', *Marine drugs*, 17(5). doi: 10.3390/md17050304.

Behler, J. *et al.* (2018) 'CRISPR-Based Technologies for Metabolic Engineering in Cyanobacteria', *Trends in Biotechnology*, 36(10), pp. 996–1010. doi: https://doi.org/10.1016/j.tibtech.2018.05.011.

Belkin, S. and Boussiba, S. (1991) 'Resistance of Spirulina platensis to Ammonia at High pH Values', *Plant and Cell Physiology*, 32(7), pp. 953–958. doi: 10.1093/oxfordjournals.pcp.a078182.

Benderliev, K. M., Pouneva, I. D. and Ivanova, N. I. (1993) 'Fungicide effect of

Triton-N on Phlyctidium', *Biotechnology Techniques*, 7(5), pp. 335–338. doi: 10.1007/BF00152537.

Bergamaschi, M. *et al.* (2016) 'Cheesemaking in highland pastures: Milk technological properties, cream, cheese and ricotta yields, milk nutrients recovery, and products composition', *Journal of Dairy Science*, 99(12), pp. 9631–9646. doi: https://doi.org/10.3168/jds.2016-11199.

Bergmann, P. *et al.* (2013) 'Disposable flat panel airlift photobioreactors', *Chemie-Ingenieur-Technik*, 85(1–2), pp. 202–205. doi: 10.1002/cite.201200132.

Berla, B. M. *et al.* (2013) 'Synthetic biology of cyanobacteria: unique challenges and opportunities', *Frontiers in microbiology*, 4, p. 246. doi: 10.3389/fmicb.2013.00246.

Billini, M., Stamatakis, K. and Sophianopoulou, V. (2008) 'Two members of a network of putative Na+/H+ antiporters are involved in salt and pH tolerance of the freshwater cyanobacterium Synechococcus elongatus.', *Journal of bacteriology*, 190(19), pp. 6318–6329. doi: 10.1128/JB.00696-08.

Bishé, B., Taton, A. and Golden, J. W. (2019) 'Modification of RSF1010-Based Broad-Host-Range Plasmids for Improved Conjugation and Cyanobacterial Bioprospecting.', *iScience*, 20, pp. 216–228. doi: 10.1016/j.isci.2019.09.002.

Björn, L. O. *et al.* (2009) 'A viewpoint: Why chlorophyll a?', *Photosynthesis Research*, 99(2), pp. 85–98. doi: 10.1007/s11120-008-9395-x.

Blanken, W. *et al.* (2013) 'Cultivation of microalgae on artificial light comes at a cost', *Algal Research*, 2(4), pp. 333–340. doi: https://doi.org/10.1016/j.algal.2013.09.004.

Blankenship, R. E. (2010) 'Early evolution of photosynthesis.', *Plant physiology*, 154(2), pp. 434–438. doi: 10.1104/pp.110.161687.

Blue bioeconomy – towards a strong and sustainable EU algae sector (2023). Available at: https://ec.europa.eu/info/law/better-regulation/have-your-say/initiatives/12780-Blue-bioeconomy-towards-a-strong-and-sustainable-EU-algae-sector_en.

BOBBY MAGILL & CLIMATE CENTRAL (2016) *Sewage Plants Overlooked Source of CO2*. Available at: https://www.scientificamerican.com/article/sewage-plants-overlooked-source-of-co2/.

Boguniewicz-Zablocka, J., Klosok-Bazan, I. and Naddeo, V. (2019) 'Water quality and resource management in the dairy industry', *Environmental Science and Pollution Research*, 26(2), pp. 1208–1216. doi: 10.1007/s11356-017-0608-8.

Bongaerts, J. *et al.* (2001) 'Metabolic engineering for microbial production of aromatic amino acids and derived compounds.', *Metabolic engineering*, 3(4), pp. 289–300. doi: 10.1006/mben.2001.0196.

Borowitzka, L. and Borowitzka, M. (1990) 'Commercial Production of β-Carotene by Dunaliella Salina in Open Ponds', *Bulletin of Marine Science*, 47, pp. 244–252.

Borowitzka, M. A. (1999) 'Commercial production of microalgae: ponds, tanks, and fermenters', in Osinga, R. et al. (eds) *Marine Bioprocess Engineering*. Elsevier, pp. 313–321. doi: https://doi.org/10.1016/S0079-6352(99)80123-4.

Borowitzka, M. A. and Vonshak, A. (2017) 'Scaling up microalgal cultures to commercial scale', *European Journal of Phycology*, 52(4), pp. 407–418. doi: 10.1080/09670262.2017.1365177.

Bozan, M., Schmid, A. and Bühler, K. (2022) 'Evaluation of self-sustaining cyanobacterial biofilms for technical applications.', *Biofilm*, 4, p. 100073. doi: 10.1016/j.bioflm.2022.100073.

Braga, A. and Faria, N. (2020) 'Bioprocess Optimization for the Production of Aromatic Compounds With Metabolically Engineered Hosts: Recent Developments and Future Challenges', *Frontiers in Bioengineering and Biotechnology*, 8(February). doi: 10.3389/fbioe.2020.00096.

Braga, A. and Faria, N. (2022) 'Biotechnological production of specialty aromatic and aromatic-derivative compounds', *World journal of microbiology & biotechnology*. CEB-Centre of Biological Engineering, Universidade do Minho, Campus de Gualtar, 4710-057, Braga, Portugal. abraga@deb.uminho.pt., p. 80. doi: 10.1007/s11274-022-03263-y.

Branco Dos Santos, F., Du, W. and Hellingwerf, K. J. (2014) 'Synechocystis: Not Just a Plug-Bug for CO2, but a Green E. coli.', *Frontiers in bioengineering and biotechnology*, 2, p. 36. doi: 10.3389/fbioe.2014.00036.

Brar, A., Kumar, M. and Pareek, N. (2019) 'Comparative appraisal of biomass production, remediation, and bioenergy generation potential of microalgae in dairy wastewater', *Frontiers in Microbiology*, 10(MAR), pp. 1–12. doi: 10.3389/fmicb.2019.00678.

Brey, L. F. *et al.* (2020) 'Metabolic engineering of Synechocystis sp. PCC 6803 for the production of aromatic amino acids and derived phenylpropanoids', *Metabolic Engineering*, 57, pp. 129–139. doi: https://doi.org/10.1016/j.ymben.2019.11.002.

Brião, V. B. *et al.* (2019) 'Water recovery from dairy rinse water by reverse osmosis: Giving value to water and milk solids', *Resources, Conservation and Recycling*, 140, pp. 313–323. doi: https://doi.org/10.1016/j.resconrec.2018.10.007.

Brock, T. D. (1973) 'Lower pH limit for the existence of blue-green algae: evolutionary and ecological implications.', *Science (New York, N.Y.)*, 179(4072), pp. 480–483. doi: 10.1126/science.179.4072.480.

Broddrick, J. T. *et al.* (2016) 'Unique attributes of cyanobacterial metabolism revealed by improved genome-scale metabolic modeling and essential gene analysis', *Proceedings of the National Academy of Sciences of the United States of America*, 113(51), pp. E8344–E8353. doi: 10.1073/pnas.1613446113.

Broddrick, J. T. *et al.* (2019) 'Predicting the metabolic capabilities of Synechococcus elongatus PCC 7942 adapted to different light regimes', *Metabolic Engineering*, 52, pp. 42–56. doi: 10.1016/j.ymben.2018.11.001.

Buabeng-Baidoo, E. *et al.* (2017) 'Study of water reuse opportunities in a large-scale milk processing plant through process integration', *Chemical Engineering Research and Design*, 121, pp. 81–91. doi: https://doi.org/10.1016/j.cherd.2017.02.031.

Bui, M. *et al.* (2018) 'Carbon capture and storage (CCS): the way forward', *Energy & Environmental Science*, 11(5), pp. 1062–1176. doi: 10.1039/C7EE02342A.

Bunce, J. T. *et al.* (2018) 'A Review of Phosphorus Removal Technologies and Their Applicability to Small-Scale Domestic Wastewater Treatment Systems', *Frontiers in Environmental Science*, 6. doi: 10.3389/fenvs.2018.00008.

Burak, H., Dunbar, A. and Gilmour, D. J. (2019) 'Enhancement of Dunaliella salina growth by using wavelength shifting dyes', *Journal of Applied Phycology*, 31(5), pp. 2791–2796. doi: 10.1007/s10811-019-01819-4.

Burberg, C., Petzoldt, T. and von Elert, E. (2020) 'Phosphate Limitation Increases Content of Protease Inhibitors in the Cyanobacterium Microcystis aeruginosa', *Toxins*. doi: 10.3390/toxins12010033.

C., D. D. *et al.* (2012) 'Rerouting Carbon Flux To Enhance Photosynthetic

Productivity', *Applied and Environmental Microbiology*, 78(8), pp. 2660–2668. doi: 10.1128/AEM.07901-11.

Campobenedetto, C. *et al.* (2020) 'Transcriptome Analyses and Antioxidant Activity Profiling Reveal the Role of a Lignin-Derived Biostimulant Seed Treatment in Enhancing Heat Stress Tolerance in Soybean', *Plants*, 9(10). doi: 10.3390/plants9101308.

Cano, M. *et al.* (2018) 'Glycogen Synthesis and Metabolite Overflow Contribute to Energy Balancing in Cyanobacteria', *Cell Reports*, 23(3), pp. 667–672. doi: 10.1016/j.celrep.2018.03.083.

Cao, T. P. *et al.* (2016) 'Development of the feedback resistant pheA FBR from E. coli and studies on its biochemical characteristics', in.

Cao, Y. *et al.* (2019) 'Engineered cyanobacteria as a potential organic degrader for wastewater treatment', *Proceedings, Annual Conference - Canadian Society for Civil Engineering*, 2019-June(Ccm), pp. 1–9.

Di Caprio, F. (2020) 'Methods to quantify biological contaminants in microalgae cultures', *Algal Research*, 49, p. 101943. doi: https://doi.org/10.1016/j.algal.2020.101943.

Carbon Capture (2023). Available at: https://www.c2es.org/content/carbon-capture/.

Cardona, T., Shao, S. and Nixon, P. J. (2018) 'Enhancing photosynthesis in plants: the light reactions.', *Essays in biochemistry*, 62(1), pp. 85–94. doi: 10.1042/EBC20170015.

Cardoso, L. G. *et al.* (2021) 'Spirulina sp. as a Bioremediation Agent for Aquaculture Wastewater: Production of High Added Value Compounds and Estimation of Theoretical Biodiesel', *BioEnergy Research*, 14(1), pp. 254–264. doi: 10.1007/s12155-020-10153-4.

Carone, M. *et al.* (2022) 'Design and characterization of a new pressurized flat panel photobioreactor for microalgae cultivation and CO2 bio-fixation', *Chemosphere*, 307, p. 135755. doi: https://doi.org/10.1016/j.chemosphere.2022.135755.

Carrera, J. *et al.* (2003) 'Biological nitrogen removal of high-strength ammonium industrial wastewater with two-sludge system', *Water Research*, 37(17), pp. 4211–4221. doi: https://doi.org/10.1016/S0043-1354(03)00338-5.

Carvalho, F., Prazeres, A. R. and Rivas, J. (2013) 'Cheese whey wastewater: Characterization and treatment', *Science of The Total Environment*, 445–446, pp. 385–396. doi: https://doi.org/10.1016/j.scitotenv.2012.12.038.

Casagli, F. *et al.* (2021) 'Balancing Microalgae and Nitrifiers for Wastewater Treatment: Can Inorganic Carbon Limitation Cause an Environmental Threat?', *Environmental Science & Technology*, 55(6), pp. 3940–3955. doi: 10.1021/acs.est.0c05264.

Catone, C. M. *et al.* (2021) 'Bio-products from algae-based biorefinery on wastewater: A review', *Journal of Environmental Management*, 293, p. 112792. doi: https://doi.org/10.1016/j.jenvman.2021.112792.

Cazzaniga, S. *et al.* (2014) 'Domestication of the green alga Chlorella sorokiniana: reduction of antenna size improves light-use efficiency in a photobioreactor', *Biotechnology for Biofuels*, 7(1), p. 157. doi: 10.1186/s13068-014-0157-z.

Chakravorty, M. *et al.* (2023) 'Heavy metal tolerance in microalgae: Detoxification mechanisms and applications', *Aquatic Toxicology*, 260, p. 106555. doi: https://doi.org/10.1016/j.aquatox.2023.106555.

Chang, S. *et al.* (2021) 'Improved Bio-Synthesis of 2,5-bis(hydroxymethyl)furan by Burkholderia contaminans NJPI-15 With Co-substrate', *Frontiers in Chemistry*, 9. doi: 10.3389/fchem.2021.635191.

Chang, Y. L. *et al.* (2023) 'Microalgae-bacteria consortia for the treatment of raw dairy manure wastewater using a novel two-stage process: Process optimization and bacterial community analysis', *Chemical Engineering Journal*, 473(August). doi: 10.1016/j.cej.2023.145388.

Chanquia, S. N., Vernet, G. and Kara, S. (2022) 'Photobioreactors for cultivation and synthesis: Specifications, challenges, and perspectives', *Engineering in Life Sciences*, 22(12), pp. 712–724. doi: https://doi.org/10.1002/elsc.202100070.

Chaumont, D. (1993) 'Biotechnology of algal biomass production: a review of systems for outdoor mass culture', *Journal of Applied Phycology*, 5(6), pp. 593–604. doi: 10.1007/BF02184638.

Chávez-Béjar, M. I. *et al.* (2012) 'Biotechnological production of l-tyrosine and derived compounds', *Process Biochemistry*, 47(7), pp. 1017–1026. doi: https://doi.org/10.1016/j.procbio.2012.04.005.

Chen, G.-Q. (2012) 'New challenges and opportunities for industrial biotechnology.', *Microbial cell factories*. England, p. 111. doi: 10.1186/1475-2859-11-111.

Chen, G.-Q. and Patel, M. K. (2012) 'Plastics Derived from Biological Sources: Present and Future: A Technical and Environmental Review', *Chemical Reviews*, 112(4), pp. 2082–2099. doi: 10.1021/cr200162d.

Chen, H. and Jiang, J.-G. (2011) 'Toxic effects of chemical pesticides (trichlorfon and dimehypo) on Dunaliella salina.', *Chemosphere*, 84(5), pp. 664–670. doi: 10.1016/j.chemosphere.2011.03.032.

Chen, H. and Wang, Q. (2022) 'Microalgae-Based Green Bio-Manufacturing—How Far From Us', *Frontiers in Microbiology*, 13(February), pp. 1–5. doi: 10.3389/fmicb.2022.832097.

Chen, J. *et al.* (2022) 'Recent Progress on Systems and Synthetic Biology of Diatoms for Improving Algal Productivity', *Frontiers in Bioengineering and Biotechnology*, 10(May), pp. 1–15. doi: 10.3389/fbioe.2022.908804.

Chen, K. *et al.* (2012) 'Deletion of the aroK gene is essential for high shikimic acid accumulation through the shikimate pathway in E. coli.', *Bioresource technology*, 119, pp. 141–147. doi: 10.1016/j.biortech.2012.05.100.

Chen, X. *et al.* (2017) 'Regulation of general amino acid permeases Gap1p, GATA transcription factors Gln3p and Gat1p on 2-phenylethanol biosynthesis via Ehrlich pathway.', *Journal of biotechnology*, 242, pp. 83–91. doi: 10.1016/j.jbiotec.2016.11.028.

Chisti, Y. (2008) 'Biodiesel from microalgae beats bioethanol', *Trends in Biotechnology*, 26(3), pp. 126–131. doi: https://doi.org/10.1016/j.tibtech.2007.12.002.

Cho, C. *et al.* (2019) 'Multi-bandgap Solar Energy Conversion via Combination of Microalgal Photosynthesis and Spectrally Selective Photovoltaic Cell', *Scientific Reports*, 9(1), p. 18999. doi: 10.1038/s41598-019-55358-6.

Cho, J. S. *et al.* (2022) 'Designing Microbial Cell Factories for the Production of Chemicals', *JACS Au*, 2(8), pp. 1781–1799. doi: 10.1021/jacsau.2c00344.

Choi, H.-J. (2016) 'Dairy wastewater treatment using microalgae for potential biodiesel application', *Environmental Engineering Research*, 21(4), pp. 393–400. doi: 10.4491/eer.2015.151.

Choi, H. J. and Lee, S. M. (2015) 'Effect of the N/P ratio on biomass productivity and nutrient removal from municipal wastewater', *Bioprocess and Biosystems Engineering*, 38(4), pp. 761–766. doi: 10.1007/s00449-014-1317-z.

Choi, Y.-N. and Park, J. M. (2016) 'Enhancing biomass and ethanol production by increasing NADPH production in Synechocystis sp. PCC 6803.', *Bioresource technology*, 213, pp. 54–57. doi: 10.1016/j.biortech.2016.02.056.

Chokshi, K. *et al.* (2016) 'Microalgal biomass generation by phycoremediation of dairy industry wastewater: An integrated approach towards sustainable biofuel production', *Bioresource Technology*, 221, pp. 455–460. doi: https://doi.org/10.1016/j.biortech.2016.09.070.

Chreptowicz, K. *et al.* (2018) 'Screening of yeasts for the production of 2-phenylethanol (rose aroma) in organic waste-based media.', *Letters in applied microbiology*, 66(2), pp. 153–160. doi: 10.1111/lam.12835.

Comer, A. D. *et al.* (2020) 'Enhancing Photosynthetic Production of Glycogen-Rich Biomass for Use as a Fermentation Feedstock', *Frontiers in Energy Research*, 8. doi: 10.3389/fenrg.2020.00093.

Cordara, A. *et al.* (2018) 'Analysis of the light intensity dependence of the growth of Synechocystis and of the light distribution in a photobioreactor energized by 635 nm light', *PeerJ*. Edited by E. Eroglu, 6, p. e5256. doi: 10.7717/peerj.5256.

Corre, J. *et al.* (1990) 'Antibacterial activity of phenethyl alcohol and resulting membrane alterations', *Research in Microbiology*, 141(4), pp. 483–497. doi: https://doi.org/10.1016/0923-2508(90)90074-Z.

Costa, J. A. V. and de Morais, M. G. (2013) *An Open Pond System for Microalgal Cultivation*, *Biofuels from Algae*. Elsevier B.V. doi: 10.1016/B978-0-444-59558-4.00001-2.

Craggs, R. J., Lundquist, T. J. and Benemann, J. R. (2013) 'Wastewater Treatment and Algal Biofuel Production BT - Algae for Biofuels and Energy', in Borowitzka, M. A. and Moheimani, N. R. (eds). Dordrecht: Springer Netherlands, pp. 153–163. doi: 10.1007/978-94-007-5479-9_9.

Crofcheck, C. *et al.* (2013) 'Influence of flue gas components on the growth rate of chlorella vulgaris and scenedesmus acutus', *Transactions of the ASABE*, 56(6), pp. 1421–1429. doi: 10.13031/trans.56.10094.

Dai, G. *et al.* (2008) 'Differential sensitivity of five cyanobacterial strains to ammonium toxicity and its inhibitory mechanism on the photosynthesis of rice-field cyanobacterium Ge–Xian–Mi (Nostoc)', *Aquatic Toxicology*, 89(2), pp. 113–121. doi: https://doi.org/10.1016/j.aquatox.2008.06.007.

Dai, J. *et al.* (2021) 'Sensing, Uptake and Catabolism of L-Phenylalanine During 2-Phenylethanol Biosynthesis via the Ehrlich Pathway in Saccharomyces cerevisiae', *Frontiers in microbiology*, 12, p. 601963. doi: 10.3389/fmicb.2021.601963.

Dall'Osto, L. *et al.* (2019) 'Combined resistance to oxidative stress and reduced antenna size enhance light-to-biomass conversion efficiency in Chlorella vulgaris cultures', *Biotechnology for Biofuels*, 12(1), p. 221. doi: 10.1186/s13068-019-1566-9.

Daneshvar, E. *et al.* (2019) 'Sequential cultivation of microalgae in raw and recycled dairy wastewater: Microalgal growth, wastewater treatment and biochemical composition', *Bioresource Technology*, 273, pp. 556–564. doi: https://doi.org/10.1016/j.biortech.2018.11.059.

Daneshvar, E. *et al.* (2022) 'Biologically-mediated carbon capture and utilization by microalgae towards sustainable CO2 biofixation and biomass valorization – A review', *Chemical Engineering Journal*, 427, p. 130884. doi: https://doi.org/10.1016/j.cej.2021.130884.

Darmawi, J. *et al.* (2012) 'Modular Engineering of l-Tyrosine Production in Escherichia coli ', *Applied and Environmental Microbiology*, 78(1), pp. 89–98. doi: 10.1128/AEM.06017-11.

Das, A., Kundu, P. and Adhikari (Nee Pramanik), S. (2022) 'Two stage treatability and biokinetic study of dairy wastewater using bacterial consortium and microalgae', *Biocatalysis and Agricultural Biotechnology*, 43, p. 102387. doi: https://doi.org/10.1016/j.bcab.2022.102387.

Das, P. and Karar Paul, K. (2022) 'Present scenario of dairy wastewater treatment: A state of art review', *Research Square*, pp. 1–22. Available at: https://doi.org/10.21203/rs.3.rs-1774888/v1.

Daverey, A. *et al.* (2019) 'Recent advances in energy efficient biological treatment of municipal wastewater', *Bioresource Technology Reports*, 7, p. 100252. doi: https://doi.org/10.1016/j.biteb.2019.100252.

Day, J. G., Gong, Y. and Hu, Q. (2017) 'Microzooplanktonic grazers – A potentially devastating threat to the commercial success of microalgal mass culture',

Algal Research, 27, pp. 356–365. doi: https://doi.org/10.1016/j.algal.2017.08.024.

Dayana Priyadharshini, S. *et al.* (2021) 'Phycoremediation of wastewater for pollutant removal: A green approach to environmental protection and long-term remediation', *Environmental Pollution*, 290, p. 117989. doi: https://doi.org/10.1016/j.envpol.2021.117989.

Delbeke, J. *et al.* (2019) 'The paris agreement', *Towards a Climate-Neutral Europe: Curbing the Trend*, pp. 24–45. doi: 10.4324/9789276082569-2.

Demoulin, C. F. *et al.* (2019) 'Cyanobacteria evolution: Insight from the fossil record', *Free Radical Biology and Medicine*, 140, pp. 206–223. doi: https://doi.org/10.1016/j.freeradbiomed.2019.05.007.

Deore, P., Beardall, J. and Noronha, S. (2020) 'A perspective on the current status of approaches for early detection of microalgal grazing', *Journal of Applied Phycology*, 32(6), pp. 3723–3733. doi: 10.1007/s10811-020-02241-x.

Deprá, M. C. *et al.* (2019) 'A new hybrid photobioreactor design for microalgae culture', *Chemical Engineering Research and Design*, 144, pp. 1–10. doi: https://doi.org/10.1016/j.cherd.2019.01.023.

Deruyck, B. *et al.* (2019) 'Modeling the impact of rotifer contamination on microalgal production in open pond, photobioreactor and thin layer cultivation systems', *Algal Research*, 38(July 2018), p. 101398. doi: 10.1016/j.algal.2018.101398.

Deshpande, A., Vue, J. and Morgan, J. (2020) 'Combining Random Mutagenesis and Metabolic Engineering for Enhanced Tryptophan Production in Synechocystis sp. Strain PCC 6803', *Applied and environmental microbiology*, 86(9), pp. e02816-19. doi: 10.1128/AEM.02816-19.

Dhakal, D. *et al.* (2021) 'Heterologous production of cyanobacterial compounds', *Journal of Industrial Microbiology and Biotechnology*, 48(3–4), p. kuab003. doi: 10.1093/jimb/kuab003.

Díaz, J. P., Inostroza, C. and Acién Fernández, F. G. (2019) 'Fibonacci-type tubular photobioreactor for the production of microalgae', *Process Biochemistry*, 86(April), pp. 1–8. doi: 10.1016/j.procbio.2019.08.008.

Dickey, R. M., Forti, A. M. and Kunjapur, A. M. (2021) 'Advances in engineering microbial biosynthesis of aromatic compounds and related compounds', *Bioresources and Bioprocessing*, 8(1), p. 91. doi: 10.1186/s40643-021-00434-x.

Ding, Y. *et al.* (2020) 'Improving nutrient and organic matter removal by novel integration of a high-rate algal pond and submerged macrophyte pond', *Polish Journal of Environmental Studies*, 29(1), pp. 997–1001. doi: 10.15244/pjoes/99824.

Diotto, D. *et al.* (2022) 'Modeling Approach to Capture the Effect of High Frequency Flashing Light in Steady-State Microalgae Cultures', *Industrial & Engineering Chemistry Research*, 61(50), pp. 18258–18269. doi: 10.1021/acs.iecr.2c03258.

Dong, Z. *et al.* (2023) 'Improved salt tolerance of Synechococcus elongatus PCC 7942 by heterologous synthesis of compatible solute ectoine', *Frontiers in Microbiology*, 14. doi: 10.3389/fmicb.2023.1123081.

Dormatey, R. *et al.* (2021) 'ptxD/Phi as alternative selectable marker system for genetic transformation for bio-safety concerns: a review.', *PeerJ*, 9, p. e11809. doi: 10.7717/peerj.11809.

Doucha, J., Straka, F. and Lívanský, K. (2005) 'Utilization of flue gas for cultivation of microalgae Chlorella sp.) in an outdoor open thin-layer photobioreactor', *Journal of Applied Phycology*, 17(5), pp. 403–412. doi: 10.1007/s10811-005-8701-7.

Doud, D. F. R. *et al.* (2014) 'In Situ UV Disinfection of a Waveguide-Based Photobioreactor', *Environmental Science & Technology*, 48(19), pp. 11521–11526. doi: 10.1021/es502812k.

Du, J., Shao, Z. and Zhao, H. (2011) 'Engineering microbial factories for synthesis of value-added products.', *Journal of industrial microbiology & biotechnology*, 38(8), pp. 873–890. doi: 10.1007/s10295-011-0970-3.

Du, W. *et al.* (2017) 'Nonhierarchical Flux Regulation Exposes the Fitness Burden Associated with Lactate Production in Synechocystis sp. PCC6803', *ACS Synthetic Biology*, 6(3), pp. 395–401. doi: 10.1021/acssynbio.6b00235.

Du, W., Jongbloets, J. A., *et al.* (2018) 'Alignment of microbial fitness with engineered product formation: obligatory coupling between acetate production and photoautotrophic growth', *Biotechnology for Biofuels*, 11(1), p. 38. doi: 10.1186/s13068-018-1037-8.

Du, W., Burbano, P. C., *et al.* (2018) 'Challenges in the Application of Synthetic Biology Toward Synthesis of Commodity Products by Cyanobacteria via "Direct Conversion" BT - Synthetic Biology of Cyanobacteria', in Zhang, W. and Song, X. (eds). Singapore: Springer Singapore, pp. 3–26. doi: 10.1007/978-981-13-0854-3_1.

Dubey, S. K. *et al.* (2011) 'Potential use of cyanobacterial species in bioremediation of industrial effluents', *African Journal of Biotechnology*, 10(7), pp. 1125–1132. doi: 10.5897/AJB10.908.

Ducat, D. C., Way, J. C. and Silver, P. A. (2011) 'Engineering cyanobacteria to generate high-value products', *Trends in Biotechnology*, 29(2), pp. 95–103. doi: https://doi.org/10.1016/j.tibtech.2010.12.003.

EC (2019) 'The European Green Deal', *European Commission*, 53(9), p. 24. Available at: https://eur-lex.europa.eu/legal-content/EN/TXT/PDF/?uri=CELEX:52019DC0640&from=EN.

Eiji, S. *et al.* (2010) 'Carbohydrate Metabolism in Mutants of the Cyanobacterium Synechococcus elongatus PCC 7942 Defective in Glycogen Synthesis', *Applied and Environmental Microbiology*, 76(10), pp. 3153–3159. doi: 10.1128/AEM.00397-08.

Eilertsen, H. C. *et al.* (2022) 'Mass Cultivation of Microalgae: I. Experiences with Vertical Column Airlift Photobioreactors, Diatoms and CO2 Sequestration', *Applied Sciences*. doi: 10.3390/app12063082.

Eilertsen, H. C. *et al.* (2023) 'Mass Cultivation of Microalgae: II. A Large Species Pulsing Blue Light Concept', *BioTech*. doi: 10.3390/biotech12020040.

El-sheekh, M. *et al.* (2021) 'Green technology for bioremediation of the eutrophication phenomenon in aquatic ecosystems: a review', *African Journal of Aquatic Science*, 46, pp. 274–292. Available at: https://api.semanticscholar.org/CorpusID:233826505.

El-Sheekh, M. M., El-Otify, A. M. and Saber, H. (2011) 'Alterations in proteins and amino acids of the Nile cyanobacteria Pseudanabaena limnetica and Anabaena wisconsinense in response to industrial wastewater pollution', *Brazilian Archives of Biology and Technology*, 54(4), pp. 810–820. doi: 10.1590/s1516-89132011000400022.

Erdrich, P. *et al.* (2014) 'Cyanobacterial biofuels: new insights and strain design strategies revealed by computational modeling', *Microbial Cell Factories*, 13(1), p. 128. doi: 10.1186/s12934-014-0128-x.

Escobar, N. and Laibach, N. (2021) 'Sustainability check for bio-based technologies: A review of process-based and life cycle approaches', *Renewable and Sustainable Energy Reviews*, 135, p. 110213. doi: https://doi.org/10.1016/j.rser.2020.110213.

Escolà Oliva, G. *et al.* (2022) 'Dairy wastewater as growth substrate for biomass and biocompound production by Spirulina platensis', *Proceedings of the 16th International Conference on Environmental Science and Technology*, 16(September), pp. 1–2. doi: 10.30955/gnc2019.00222.

Espinosa, M. F. *et al.* (2021) 'Reduction and partitioning of viral and bacterial indicators in a UASB reactor followed by high rate algal ponds treating domestic sewage', *Science of The Total Environment*, 760, p. 144309. doi: https://doi.org/10.1016/j.scitotenv.2020.144309.

Etschmann, M. M. W. *et al.* (2002) 'Biotechnological production of 2-phenylethanol.', *Applied microbiology and biotechnology*, 59(1), pp. 1–8. doi: 10.1007/s00253-002-0992-x.

Fal, S., Smouni, A. and Arroussi, H. El (2023) 'Integrated microalgae-based biorefinery for wastewater treatment, industrial CO2 sequestration and microalgal biomass valorization: A circular bioeconomy approach', *Environmental Advances*, 12, p. 100365. doi: https://doi.org/10.1016/j.envadv.2023.100365.

Fang, R. and Sung, C. J. (2021) 'A rapid compression machine study of 2-phenylethanol autoignition at low-to-intermediate temperatures', *Energies*, 14(22). doi: 10.3390/en14227708.

Farooq, W. *et al.* (2015) 'Water use and its recycling in microalgae cultivation for biofuel application', *Bioresource Technology*, 184, pp. 73–81. doi: https://doi.org/10.1016/j.biortech.2014.10.140.

Fernandes, R. *et al.* (2023) 'Exploring the Benefits of Phycocyanin: From Spirulina Cultivation to Its Widespread Applications.', *Pharmaceuticals (Basel, Switzerland)*, 16(4). doi: 10.3390/ph16040592.

Fernández, I. *et al.* (2014) 'First Principles Model of a Tubular Photobioreactor for Microalgal Production', *Industrial & Engineering Chemistry Research*, 53(27), pp. 11121–11136. doi: 10.1021/ie501438r.

Flores, E. and Herrero, A. (1994) 'Assimilatory Nitrogen Metabolism and Its Regulation BT - The Molecular Biology of Cyanobacteria', in Bryant, D. A. (ed.). Dordrecht: Springer Netherlands, pp. 487–517. doi: 10.1007/978-94-011-0227-8_16.

Forber, K. J. *et al.* (2018) 'The Phosphorus Transfer Continuum: A Framework for Exploring Effects of Climate Change', *Agricultural & Environmental Letters*, 3(1), p. 180036. doi: https://doi.org/10.2134/ael2018.06.0036.

Franchino, M. *et al.* (2013) 'Growth of three microalgae strains and nutrient removal from an agro-zootechnical digestate', *Chemosphere*, 92(6), pp. 738–744. doi: https://doi.org/10.1016/j.chemosphere.2013.04.023.

Fraud, S. *et al.* (2003) 'Aromatic alcohols and their effect on Gram-negative bacteria, cocci and mycobacteria', *Journal of Antimicrobial Chemotherapy*, 51(6), pp. 1435–1436. doi: 10.1093/jac/dkg246.

Fu, W. *et al.* (2017) 'Intracellular spectral recompositioning of light enhances algal photosynthetic efficiency.', *Science advances*, 3(9), p. e1603096. doi: 10.1126/sciadv.1603096.

Fuchs, T. *et al.* (2021) 'A Newly Designed Automatically Controlled, Sterilizable Flat Panel Photobioreactor for Axenic Algae Culture', *Frontiers in Bioengineering and Biotechnology*, 9. doi: 10.3389/fbioe.2021.697354.

Fujiwara, R. *et al.* (2020) 'Metabolic engineering of Escherichia coli for shikimate pathway derivative production from glucose–xylose co-substrate', *Nature Communications*, 11(1), p. 279. doi: 10.1038/s41467-019-14024-1.

G, J. and G, M. (2016) 'Cultivation of Oscillatoria SP in Dairy Waste Water in Two Stage Photo Bioreactors for Biodiesel Production', *Civil Engineering and Urban Planning: An International Journal (CiVEJ)*, 3(2), pp. 87–96. doi: 10.5121/civej.2016.3207.

Gabrielyan, D. A. *et al.* (2022) 'Cultivation of Chlorella sorokiniana IPPAS C-1 in Flat-Panel Photobioreactors: From a Laboratory to a Pilot Scale', *Life*, 12(9). doi: 10.3390/life12091309.

Gao, X., Kong, B. and Vigil, R. D. (2018) 'Simulation of algal photobioreactors: recent developments and challenges.', *Biotechnology letters*, 40(9–10), pp. 1311–1327. doi: 10.1007/s10529-018-2595-3.

Gao, Z. *et al.* (2012) 'Photosynthetic production of ethanol from carbon dioxide in genetically engineered cyanobacteria', *Energy and Environmental Science*, 5(12), pp. 9857–9865. doi: 10.1039/c2ee22675h.

Garbowski, T. *et al.* (2020) 'The use of a natural substrate for immobilization of microalgae cultivated in wastewater', *Scientific Reports*, 10(1), p. 7915. doi: 10.1038/s41598-020-64656-3.

Garcia-Pichel, F. (2009) 'Cyanobacteria', in Schaechter, M. B. T.-E. of M. (Third

E. (ed.). Oxford: Academic Press, pp. 107–124. doi: https://doi.org/10.1016/B978-012373944-5.00250-9.

la Gatta, S. *et al.* (2019) 'A highly efficient heptamethine cyanine antenna for photosynthetic Reaction Center: From chemical design to ultrafast energy transfer investigation of the hybrid system.', *Biochimica et biophysica acta. Bioenergetics*, 1860(4), pp. 350–359. doi: 10.1016/j.bbabio.2019.01.009.

Gau, A. E. *et al.* (2007) 'L-amino acid oxidases with specificity for basic L-amino acids in cyanobacteria.', *Zeitschrift fur Naturforschung. C, Journal of biosciences*, 62(3–4), pp. 273–284. doi: 10.1515/znc-2007-3-419.

Gaurav, S. *et al.* (2018) 'Bioremediation of Cr(VI) Using Live Cyanobacteria: Experimentation and Kinetic Modeling', *Journal of Environmental Engineering*, 144(9), p. 4018089. doi: 10.1061/(ASCE)EE.1943-7870.0001425.

Gayathri, R. *et al.* (2021) 'A review on biological carbon sequestration: A sustainable solution for a cleaner air environment, less pollution and lower health risks', *Journal of King Saud University - Science*, 33(2), p. 101282. doi: https://doi.org/10.1016/j.jksus.2020.101282.

General, D. (2020) 'Achieved By 2050 ?', pp. 1–4.

Georgeson, L., Maslin, M. and Poessinouw, M. (2017) 'The global green economy: a review of concepts, definitions, measurement methodologies and their interactions', *Geo: Geography and Environment*, 4(1), p. e00036. doi: https://doi.org/10.1002/geo2.36.

Geremia, E. *et al.* (2021) 'A Review about Microalgae Wastewater Treatment for Bioremediation and Biomass Production—A New Challenge for Europe', *Environments*. doi: 10.3390/environments8120136.

Gifuni, I. *et al.* (2018) 'New ultra-flat photobioreactor for intensive microalgal production: The effect of light irradiance', *Algal Research*, 34, pp. 134–142. doi: https://doi.org/10.1016/j.algal.2018.07.014.

Giraldez-Ruiz, N. *et al.* (1997) 'The relationship between intracellular pH, growth characteristics and calcium in the cyanobacterium Anabaena sp. strain PCC7120 exposed to low pH', *New Phytologist*, 137(4), pp. 599–605. doi: 10.1046/j.1469-8137.1997.00864.x.

Goldfinger, V. *et al.* (2023) 'Metabolic engineering of the shikimate pathway in

Amycolatopsis strains for optimized glycopeptide antibiotic production.', *Metabolic engineering*, 78, pp. 84–92. doi: 10.1016/j.ymben.2023.05.005.

Gosset, G. (2009) 'Production of aromatic compounds in bacteria', *Current Opinion in Biotechnology*, 20(6), pp. 651–658. doi: https://doi.org/10.1016/j.copbio.2009.09.012.

Gottlieb, K., Albermann, C. and Sprenger, G. A. (2014) 'Improvement of L-phenylalanine production from glycerol by recombinant Escherichia coli strains: The role of extra copies of glpK, glpX, and tktA genes', *Microbial Cell Factories*, 13(1), p. 96. doi: 10.1186/s12934-014-0096-1.

Grace, J. (2013) 'Carbon Cycle', in Levin, S. A. B. T.-E. of B. (Second E. (ed.). Waltham: Academic Press, pp. 674–684. doi: https://doi.org/10.1016/B978-0-12-384719-5.00306-3.

Gramegna, G. *et al.* (2020) 'Exploring the potential of microalgae in the recycling of dairy wastes', *Bioresource Technology Reports*, 12, p. 100604. doi: https://doi.org/10.1016/j.biteb.2020.100604.

Grogan, D. W. (2012) 'Chapter 50 - Physiology of Prokaryotic Cells', in Sperelakis, N. B. T.-C. P. S. B. (Fourth E. (ed.). San Diego: Academic Press, pp. 891–906. doi: https://doi.org/10.1016/B978-0-12-387738-3.00050-0.

Gründel, M. *et al.* (2012) 'Impaired glycogen synthesis causes metabolic overflow reactions and affects stress responses in the cyanobacterium Synechocystis sp. PCC 6803', *Microbiology*, 158(12), pp. 3032–3043. doi: https://doi.org/10.1099/mic.0.062950-0.

Gu, P. *et al.* (2017) 'Novel technologies combined with traditional metabolic engineering strategies facilitate the construction of shikimate-producing Escherichia coli', *Microbial Cell Factories*, 16(1), p. 167. doi: 10.1186/s12934-017-0773-y.

Gu, Y. *et al.* (2020) 'Refactoring Ehrlich Pathway for High-Yield 2-Phenylethanol Production in Yarrowia lipolytica', *ACS Synthetic Biology*, 9(3), pp. 623–633. doi: 10.1021/acssynbio.9b00468.

Guardini, Z. *et al.* (2021) 'High Carotenoid Mutants of Chlorella vulgaris Show Enhanced Biomass Yield under High Irradiance', *Plants*. doi: 10.3390/plants10050911.

Guinee, T. P. (2004) 'Salting and the role of salt in cheese', *International Journal*

of Dairy Technology, 57(2–3), pp. 99–109. doi: https://doi.org/10.1111/j.1471-0307.2004.00145.x.

H. Kabariya, J. and M. Ramani, V. (2018) 'Dairy Wastewater Treatment by Cyanobacteria for Removal of Nutrients with Extraction of High Value Compounds from Biomass', *International Journal of Current Microbiology and Applied Sciences*, 7(04), pp. 1527–1538. doi: 10.20546/ijcmas.2018.704.172.

Hahn, M. W., Koll, U. and Schmidt, J. (2019) 'Isolation and Cultivation of Bacteria', *Advances in Environmental Microbiology*. Available at: https://api.semanticscholar.org/CorpusID:182520984.

Haines, M. *et al.* (2022) 'Pilot-scale outdoor trial of a cyanobacterial consortium at pH 11 in a photobioreactor at high latitude', *Bioresource Technology*, 354, p. 127173. doi: https://doi.org/10.1016/j.biortech.2022.127173.

Hall, G. C. and Jensen, R. A. (1980) 'Enzymological basis for growth inhibition by L-phenylalanine in the cyanobacterium Synechocystis sp. 29108.', *Journal of bacteriology*, 144(3), pp. 1034–1042. doi: 10.1128/jb.144.3.1034-1042.1980.

Hamouda, R. A. and El-Naggar, N. E.-A. (2021) 'Chapter 14 - Cyanobacteria-based microbial cell factories for production of industrial products', in Singh, V. B. T.-M. C. F. E. for P. of B. (ed.). Academic Press, pp. 277–302. doi: https://doi.org/10.1016/B978-0-12-821477-0.00007-6.

Han, F. *et al.* (2015) 'Optimization and lipid production enhancement of microalgae culture by efficiently changing the conditions along with the growth-state', *Energy Conversion and Management*, 90, pp. 315–322. doi: https://doi.org/10.1016/j.enconman.2014.11.032.

Handayani, T. *et al.* (2020) 'Utilization of Dairy Industry Wastewater for Nutrition of Microalgae Chlorella vulgaris', *Journal of Physics: Conference Series*, 1655(1). doi: 10.1088/1742-6596/1655/1/012123.

Hansen, E. H. *et al.* (2009) 'De novo biosynthesis of vanillin in fission yeast (Schizosaccharomyces pombe) and baker's yeast (Saccharomyces cerevisiae).', *Applied and environmental microbiology*, 75(9), pp. 2765–2774. doi: 10.1128/AEM.02681-08.

Hartline, C. J. *et al.* (2021) 'Dynamic control in metabolic engineering: Theories, tools, and applications', *Metabolic Engineering*, 63, pp. 126–140. doi: https://doi.org/10.1016/j.ymben.2020.08.015.

Hartmann, M. *et al.* (2003) 'Evolution of feedback-inhibited β/α barrel isoenzymes by gene duplication and a single mutation', *Proceedings of the National Academy of Sciences*, 100(3), pp. 862–867. doi: 10.1073/pnas.0337566100.

Hasunuma, T. *et al.* (2013) 'Dynamic metabolic profiling of cyanobacterial glycogen biosynthesis under conditions of nitrate depletion.', *Journal of experimental botany*, 64(10), pp. 2943–2954. doi: 10.1093/jxb/ert134.

Haveren, J. van, Scott, E. L. and Sanders, J. (2008) 'Bulk chemicals from biomass', *Biofuels, Bioproducts and Biorefining*, 2(1), pp. 41–57. doi: https://doi.org/10.1002/bbb.43.

Hays, S. G. and Ducat, D. C. (2015) 'Engineering cyanobacteria as photosynthetic feedstock factories', *Photosynthesis Research*, 123(3), pp. 285–295. doi: 10.1007/s11120-014-9980-0.

Hays, S. G. and Ducat, D. C. (2018) 'factories', 123(3), pp. 285–295. doi: 10.1007/s11120-014-9980-0.Engineering.

Hazelwood, L. A. *et al.* (2008) 'The Ehrlich pathway for fusel alcohol production: a century of research on Saccharomyces cerevisiae metabolism', *Applied and environmental microbiology*. 2008/02/15, 74(8), pp. 2259–2266. doi: 10.1128/AEM.02625-07.

He, L. *et al.* (2013) 'Optimize flue gas settings to promote microalgae growth in photobioreactors via computer simulations.', *Journal of visualized experiments : JoVE*, (80). doi: 10.3791/50718.

Hecky, R. E., Campbell, P. and Hendzel, L. L. (1993) 'The stoichiometry of carbon, nitrogen, and phosphorus in particulate matter of lakes and oceans', *Limnology and Oceanography*, 38(4), pp. 709–724. doi: https://doi.org/10.4319/lo.1993.38.4.0709.

Hedges, S. B. *et al.* (2001) 'A genomic timescale for the origin of eukaryotes.', *BMC evolutionary biology*, 1, p. 4. doi: 10.1186/1471-2148-1-4.

Herrmann, K. M. (1995) 'The shikimate pathway: Early steps in the biosynthesis of aromatic compounds', *Plant Cell*, 7(7), pp. 907–919. doi: 10.2307/3870046.

Hirokawa, Y., Suzuki, I. and Hanai, T. (2015) 'Optimization of isopropanol production by engineered cyanobacteria with a synthetic metabolic pathway', *Journal of Bioscience and Bioengineering*, 119(5), pp. 585–590. doi:

https://doi.org/10.1016/j.jbiosc.2014.10.005.

Holen, D. A. and Boraas, M. E. (1995) 'Mixotrophy in chrysophytes', *Chrysophyte algae: ecology, phylogeny and development*, 119.

Hollinshead, W. D. *et al.* (2014) 'Boosting d-lactate production in engineered cyanobacteria using sterilized anaerobic digestion effluents', *Bioresource Technology*, 169, pp. 462–467. doi: https://doi.org/10.1016/j.biortech.2014.07.003.

Holm, E. R. *et al.* (2008) 'Sonication of bacteria, phytoplankton and zooplankton: Application to treatment of ballast water', *Marine Pollution Bulletin*, 56(6), pp. 1201–1208. doi: https://doi.org/10.1016/j.marpolbul.2008.02.007.

Hong, J.-W. *et al.* (2019) 'Polyhydroxybutyrate production in halophilic marine bacteria Vibrio proteolyticus isolated from the Korean peninsula.', *Bioprocess and biosystems engineering*, 42(4), pp. 603–610. doi: 10.1007/s00449-018-02066-6.

Hsieh-Lo, M. *et al.* (2019) 'Phycocyanin and phycoerythrin: Strategies to improve production yield and chemical stability', *Algal Research*, 42, p. 101600. doi: https://doi.org/10.1016/j.algal.2019.101600.

Hu, C. *et al.* (2003) 'Mutation analysis of the feedback inhibition site of phenylalanine-sensitive 3-deoxy-D-arabino-heptulosonate 7-phosphate synthase of Escherichia coli', *Journal of Basic Microbiology*, 43(5), pp. 399–406. doi: https://doi.org/10.1002/jobm.200310244.

Hua, D. and Xu, P. (2011) 'Recent advances in biotechnological production of 2-phenylethanol.', *Biotechnology advances*, 29(6), pp. 654–660. doi: 10.1016/j.biotechadv.2011.05.001.

Hua, S.-S. *et al.* (2014) 'The major volatile compound 2-phenylethanol from the biocontrol yeast, Pichia anomala, inhibits growth and expression of aflatoxin biosynthetic genes of Aspergillus flavus', *Mycotoxin research*, 30. doi: 10.1007/s12550-014-0189-z.

Huang, C. *et al.* (2020) 'The quorum-sensing molecule 2-phenylethanol impaired conidial germination, hyphal membrane integrity and growth of Penicillium expansum and Penicillium nordicum.', *Journal of applied microbiology*, 129(2), pp. 278–286. doi: 10.1111/jam.14621.

Huang, J. *et al.* (2016) 'Development of a novel multi-column airlift photobioreactor with easy scalability by means of computational fluid dynamics

simulations and experiments', *Bioresource Technology*, 222, pp. 399–407. doi: https://doi.org/10.1016/j.biortech.2016.09.109.

Huang, Yong *et al.* (2017) 'Improving phosphorus removal efficiency and Chlorella vulgaris growth in high-phosphate MFC wastewater by frequent addition of small amounts of nitrate', *International Journal of Hydrogen Energy*, 42(45), pp. 27749–27758. doi: https://doi.org/10.1016/j.ijhydene.2017.05.069.

Huccetogullari, D., Luo, Z. W. and Lee, S. Y. (2019) 'Metabolic engineering of microorganisms for production of aromatic compounds', *Microbial Cell Factories*, 18(1), p. 41. doi: 10.1186/s12934-019-1090-4.

Huertas, M. J. *et al.* (2014) 'Metals in cyanobacteria: analysis of the copper, nickel, cobalt and arsenic homeostasis mechanisms.', *Life (Basel, Switzerland)*, 4(4), pp. 865–886. doi: 10.3390/life4040865.

Huo, S. *et al.* (2018) 'Biomass Accumulation of Chlorella Zofingiensis G1 Cultures Grown Outdoors in Photobioreactors', *Frontiers in Energy Research*, 6. doi: 10.3389/fenrg.2018.00049.

Huy, M. *et al.* (2018) 'Photoautotrophic cultivation of mixed microalgae consortia using various organic waste streams towards remediation and resource recovery', *Bioresource Technology*, 247, pp. 576–581. doi: https://doi.org/10.1016/j.biortech.2017.09.108.

Idris, N. *et al.* (2022) 'In-situ sterilization of microalgae photobioreactor via ozone-rich macrobubbles', *AIP Conference Proceedings*, 2454(1), p. 30026. doi: 10.1063/5.0078258.

International Energy Agency (2017) 'Energy Technology Perspectives 2017 - Tracking Clean Energy Progress', *Technology*, p. 112. Available at: http://www.iea.org/media/etp/Tracking_Clean_Energy_Progress.pdf.

International Energy Agency (IEA) (2022) 'Global CO2 emissions rebounded to their highest level in history in 2021', *Global Energy Review: CO2 Emissions in 2021*, pp. 1–3. Available at: https://www.iea.org/news/global-co2-emissions-rebounded-to-their-highest-level-in-history-in-2021.

Inventory of U.S. Greenhouse Gas Emissions and Sinks: 1990-2021 (2021). Available at: https://www.epa.gov/ghgemissions/inventory-us-greenhouse-gas-emissions-and-sinks.

Iraqui, I. *et al.* (1998) 'Characterisation of Saccharomyces cerevisiae ARO8 and ARO9 genes encoding aromatic aminotransferases I and II reveals a new aminotransferase subfamily', *Molecular and General Genetics MGG*, 257(2), pp. 238–248. doi: 10.1007/s004380050644.

Ivanov, A. G. *et al.* (2007) 'The induction of CP43′ by iron-stress in Synechococcus sp. PCC 7942 is associated with carotenoid accumulation and enhanced fatty acid unsaturation', *Biochimica et Biophysica Acta (BBA) - Bioenergetics*, 1767(6), pp. 807–813. doi: https://doi.org/10.1016/j.bbabio.2007.02.006.

Janssen, M. *et al.* (2003) 'Enclosed outdoor photobioreactors: light regime, photosynthetic efficiency, scale-up, and future prospects.', *Biotechnology and bioengineering*, 81(2), pp. 193–210. doi: 10.1002/bit.10468.

Jenkins, P. A. (1991) 'Mycobacteria in the environment', *Journal of Applied Bacteriology Symposium Supplement*, (20). doi: 10.1128/JCM.37.1.49-55.1999.

Jia, A. *et al.* (2021) 'Regulation and Functional Complexity of the Chlorophyll-Binding Protein IsiA.', *Frontiers in microbiology*, 12, p. 774107. doi: 10.3389/fmicb.2021.774107.

Jiang, M. and Zhang, H. (2016) 'Engineering the shikimate pathway for biosynthesis of molecules with pharmaceutical activities in E. coli', *Current Opinion in Biotechnology*, 42, pp. 1–6. doi: https://doi.org/10.1016/j.copbio.2016.01.016.

Jiang, P.-H. *et al.* (2000) 'Effect of F209S Mutation of Escherichia coli AroG on Resistance to Phenylalanine Feedback Inhibition.', *Sheng wu hua xue yu sheng wu wu li xue bao Acta biochimica et biophysica Sinica*, 32(5), pp. 441–444.

Jin, H. *et al.* (2021) 'Potential of Producing Flavonoids Using Cyanobacteria As a Sustainable Chassis', *Journal of Agricultural and Food Chemistry*, 69(42), pp. 12385–12401. doi: 10.1021/acs.jafc.1c04632.

Jones, E. R. *et al.* (2021) 'Country-level and gridded estimates of wastewater production, collection, treatment and reuse', *Earth System Science Data*, 13(2), pp. 237–254. doi: 10.5194/essd-13-237-2021.

Jossek, R., Bongaerts, J. and Sprenger, G. A. (2001) 'Characterization of a new feedback-resistant 3-deoxy-D-arabino-heptulosonate 7-phosphate synthase AroF of Escherichia coli.', *FEMS microbiology letters*, 202(1), pp. 145–148. doi: 10.1111/j.1574-6968.2001.tb10795.x.

Jung, K. A. *et al.* (2013) 'Potentials of macroalgae as feedstocks for biorefinery', *Bioresource Technology*, 135, pp. 182–190. doi: https://doi.org/10.1016/j.biortech.2012.10.025.

K.W. Thoning, A.M. Crotwell, and J. W. M. (2023) *Atmospheric Carbon Dioxide Dry Air Mole Fractions from continuous measurements at Mauna Loa, Hawaii, Barrow, Alaska, American Samoa and South Pole*. Boulder, Colorado, USA. doi: 10.15138/yaf1-bk21.

Kakade, A. *et al.* (2021) 'World eutrophic pollution of lake and river: Biotreatment potential and future perspectives', *Environmental Technology & Innovation*, 23, p. 101604. doi: https://doi.org/10.1016/j.eti.2021.101604.

Kallio, P. *et al.* (2021) 'Photoautotrophic production of renewable ethylene by engineered cyanobacteria: Steering the cell metabolism towards biotechnological use', *Physiologia Plantarum*, 173(2), pp. 579–590. doi: https://doi.org/10.1111/ppl.13430.

Kalra, R., Gaur, S. and Goel, M. (2021) 'Microalgae bioremediation: A perspective towards wastewater treatment along with industrial carotenoids production', *Journal of Water Process Engineering*, 40, p. 101794. doi: https://doi.org/10.1016/j.jwpe.2020.101794.

von Kamp, A. and Klamt, S. (2017) 'Growth-coupled overproduction is feasible for almost all metabolites in five major production organisms.', *Nature communications*, 8, p. 15956. doi: 10.1038/ncomms15956.

Kamravamanesh, D. *et al.* (2019) 'Scale-up challenges and requirement of technology-transfer for cyanobacterial poly (3-hydroxybutyrate) production in industrial scale', *International Journal of Biobased Plastics*, 1(1), pp. 60–71. doi: 10.1080/24759651.2019.1688604.

Kamravamanesh, D., Lackner, M. and Herwig, C. (2018) 'Bioprocess Engineering Aspects of Sustainable Polyhydroxyalkanoate Production in Cyanobacteria.', *Bioengineering (Basel, Switzerland)*, 5(4). doi: 10.3390/bioengineering5040111.

Kang, Z. *et al.* (2014) 'Metabolic engineering of Escherichia coli for production of 2-phenylethanol from renewable glucose.', *Applied biochemistry and biotechnology*, 172(4), pp. 2012–2021. doi: 10.1007/s12010-013-0659-3.

Kastberg, L. L. B. *et al.* (2022) 'Burden Imposed by Heterologous Protein Production in Two Major Industrial Yeast Cell Factories: Identifying Sources and Mitigation Strategies', *Frontiers in Fungal Biology*, 3. doi:

10.3389/ffunb.2022.827704.

Kätelhön, A. *et al.* (2019) 'Climate change mitigation potential of carbon capture and utilization in the chemical industry', *Proceedings of the National Academy of Sciences*, 116(23), pp. 11187–11194. doi: 10.1073/pnas.1821029116.

Kaur, N. (2021) 'Different treatment techniques of dairy wastewater', *Groundwater for Sustainable Development*, 14, p. 100640. doi: https://doi.org/10.1016/j.gsd.2021.100640.

Keasling, J. D. and Chou, H. (2008) 'Metabolic engineering delivers next-generation biofuels', *Nature Biotechnology*, 26(3), pp. 298–299. doi: 10.1038/nbt0308-298.

Keyvan Hosseini, M. *et al.* (2023) 'The comparison between two methods of membrane cleaning to control membrane fouling in a hybrid membrane photobioreactor (HMPBR).', *Preparative biochemistry & biotechnology*, 53(4), pp. 394–400. doi: 10.1080/10826068.2022.2095574.

Khalaji, M. *et al.* (2023) 'Treatment of dairy wastewater by microalgae Chlorella vulgaris for biofuels production', *Biomass Conversion and Biorefinery*, 13(4), pp. 3259–3265. doi: 10.1007/s13399-021-01287-2.

Khemka, A. and Saraf, M. (2017) 'Strategic enhancement of Desertifilum tharense MSAK01 on dairy wastewater: an integrated approach for remediation and biomass production', *Applied Water Science*, 7(6), pp. 2779–2785. doi: 10.1007/s13201-017-0525-5.

Kikuchi, Y., Tsujimoto, K. and Kurahashi, O. (1997) 'Mutational analysis of the feedback sites of phenylalanine-sensitive 3-deoxy-D-arabino-heptulosonate-7-phosphate synthase of Escherichia coli.', *Applied and environmental microbiology*, 63(2), pp. 761–762. doi: 10.1128/aem.63.2.761-762.1997.

Kim, B., Cho, B.-R. and Hahn, J.-S. (2014) 'Metabolic engineering of Saccharomyces cerevisiae for the production of 2-phenylethanol via Ehrlich pathway.', *Biotechnology and bioengineering*, 111(1), pp. 115–124. doi: 10.1002/bit.24993.

Kim, T.-Y., Lee, S.-W. and Oh, M.-K. (2014) 'Biosynthesis of 2-phenylethanol from glucose with genetically engineered Kluyveromyces marxianus.', *Enzyme and microbial technology*, 61–62, pp. 44–47. doi: 10.1016/j.enzmictec.2014.04.011.

King, Z. A. *et al.* (2016) 'BiGG Models: A platform for integrating, standardizing and sharing genome-scale models', *Nucleic Acids Research*, 44(D1), pp. D515–D522. doi: 10.1093/nar/gkv1049.

Kleinwächter, I. S. *et al.* (2021) 'The Bacteriostatic Activity of 2-Phenylethanol Derivatives Correlates with Membrane Binding Affinity.', *Membranes*, 11(4). doi: 10.3390/membranes11040254.

Koksharova, O. A. and Wolk, C. P. (2002) 'Genetic tools for cyanobacteria.', *Applied microbiology and biotechnology*, 58(2), pp. 123–137. doi: 10.1007/s00253-001-0864-9.

Koma, D. *et al.* (2020) 'Chromosome Engineering To Generate Plasmid-Free Phenylalanine- and Tyrosine-Overproducing Escherichia coli Strains That Can Be Applied in the Generation of Aromatic-Compound-Producing Bacteria.', *Applied and environmental microbiology*, 86(14). doi: 10.1128/AEM.00525-20.

Kondaveeti, S. *et al.* (2020) 'Advanced Routes of Biological and Bio-electrocatalytic Carbon Dioxide (CO2) Mitigation Toward Carbon Neutrality', *Frontiers in Energy Research*, 8. doi: 10.3389/fenrg.2020.00094.

Kong, S. *et al.* (2020) 'De novo biosynthesis of 2-phenylethanol in engineered Pichia pastoris', *Enzyme and Microbial Technology*, 133, p. 109459. doi: https://doi.org/10.1016/j.enzmictec.2019.109459.

Kopka, J. *et al.* (2017) 'Systems analysis of ethanol production in the genetically engineered cyanobacterium Synechococcus sp. PCC 7002', *Biotechnology for Biofuels*, 10(1), p. 56. doi: 10.1186/s13068-017-0741-0.

Kothari, R. *et al.* (2013) 'Production of biodiesel from microalgae Chlamydomonas polypyrenoideum grown on dairy industry wastewater', *Bioresource Technology*, 144, pp. 499–503. doi: https://doi.org/10.1016/j.biortech.2013.06.116.

Kratky, L., Jirout, T. and Belohlav, V. (2023) 'Economic feasibility study for artificial lighting of microalgal flat-panel photobioreactors', *International Journal of Environmental Science and Technology*. doi: 10.1007/s13762-023-04804-0.

Krauss, R. W. (1962) 'Mass Culture of Algae for Food and Other Organic Compounds', *American Journal of Botany*, 49(4), pp. 425–435. doi: 10.2307/2439085.

Krug, L. *et al.* (2019) 'A novel, nature-based alternative for photobioreactor decontaminations', *Scientific Reports*, 9(1), p. 2864. doi: 10.1038/s41598-019-39673-

6.

Krujatz, F. *et al.* (2016) 'MicrOLED-photobioreactor: Design and characterization of a milliliter-scale Flat-Panel-Airlift-photobioreactor with optical process monitoring', *Algal Research*, 18, pp. 225–234. doi: https://doi.org/10.1016/j.algal.2016.06.018.

Kuan, D. *et al.* (2015) 'Growth optimization of Synechococcus elongatus PCC7942 in lab flasks and a 2-D photobioreactor', *The Canadian Journal of Chemical Engineering*, 93(4), pp. 640–647. doi: https://doi.org/10.1002/cjce.22154.

Kugler, A. and Stensjö, K. (2023) 'Optimal energy and redox metabolism in the cyanobacterium Synechocystis sp. PCC 6803.', *NPJ systems biology and applications*, 9(1), p. 47. doi: 10.1038/s41540-023-00307-3.

Kukil, K. *et al.* (2023) 'Laboratory evolution of Synechocystis sp. PCC 6803 for phenylpropanoid production', *Metabolic Engineering*, 79, pp. 27–37. doi: https://doi.org/10.1016/j.ymben.2023.06.014.

Kulagina, N. *et al.* (2021) 'Peroxisomes: A New Hub for Metabolic Engineering in Yeast', *Frontiers in Bioengineering and Biotechnology*, 9. doi: 10.3389/fbioe.2021.659431.

Kumar, P. K. *et al.* (2018) 'Phycoremediation of sewage wastewater and industrial flue gases for biomass generation from microalgae', *South African Journal of Chemical Engineering*, 25, pp. 133–146. doi: https://doi.org/10.1016/j.sajce.2018.04.006.

Kusmayadi, A. *et al.* (2022) 'Integrating anaerobic digestion and microalgae cultivation for dairy wastewater treatment and potential biochemicals production from the harvested microalgal biomass', *Chemosphere*, 291, p. 133057. doi: https://doi.org/10.1016/j.chemosphere.2021.133057.

Kwan, P. P. *et al.* (2021) 'Influence of light on biomass and lipid production in microalgae cultivation', *Aquaculture Research*, 52(4), pp. 1337–1347. doi: https://doi.org/10.1111/are.15023.

Labarre, J., Thuriaux, P. and Chauvat, F. (1987) 'Genetic analysis of amino acid transport in the facultatively heterotrophic cyanobacterium Synechocystis sp. strain 6803.', *Journal of bacteriology*, 169(10), pp. 4668–4673. doi: 10.1128/jb.169.10.4668-4673.1987.

Lafarga, T. and Acién, G. (2022) 'Microalgae for the Food Industry: From Biomass

Production to the Development of Functional Foods.', *Foods (Basel, Switzerland)*. Switzerland. doi: 10.3390/foods11050765.

Lai, M. C. and Lan, E. I. (2015) 'Advances in Metabolic Engineering of Cyanobacteria for Photosynthetic Biochemical Production', *Metabolites* . doi: 10.3390/metabo5040636.

Lakmali, W. G. M., Athukorala, A. D. S. N. P. and Jayasundera, K. B. (2022) 'Investigation of Pb(II) bioremediation potential of algae and cyanobacteria strains isolated from polluted water', *Water Science and Engineering*, 15(3), pp. 237–246. doi: https://doi.org/10.1016/j.wse.2022.04.003.

Lam, T. P. *et al.* (2018) 'Strategies to control biological contaminants during microalgal cultivation in open ponds', *Bioresource Technology*, 252, pp. 180–187. doi: https://doi.org/10.1016/j.biortech.2017.12.088.

Lassen, L. M. *et al.* (2014) 'Redirecting photosynthetic electron flow into light-driven synthesis of alternative products including high-value bioactive natural compounds.', *ACS synthetic biology*, 3(1), pp. 1–12. doi: 10.1021/sb400136f.

Lateef, A., Chaudhry, M. N. and Ilyas, S. (2013) 'Biological treatment of dairy wastewater using activated sludge', *ScienceAsia*, 39(2), pp. 179–185. doi: 10.2306/scienceasia1513-1874.2013.39.179.

Lau, N.-S., Matsui, M. and Abdullah, A. A.-A. (2015) 'Cyanobacteria: Photoautotrophic Microbial Factories for the Sustainable Synthesis of Industrial Products', *BioMed Research International*. Edited by Z. K. Zhao, 2015, p. 754934. doi: 10.1155/2015/754934.

Lee, J.-H. and Wendisch, V. F. (2017) 'Biotechnological production of aromatic compounds of the extended shikimate pathway from renewable biomass.', *Journal of biotechnology*, 257, pp. 211–221. doi: 10.1016/j.jbiotec.2016.11.016.

Lee, J. W. *et al.* (2012) 'Systems metabolic engineering of microorganisms for natural and non-natural chemicals', *Nature Chemical Biology*, 8(6), pp. 536–546. doi: 10.1038/nchembio.970.

Lee, S. Y., Lee, J. S. and Sim, S. J. (2023) 'Enhancement of microalgal biomass productivity through mixotrophic culture process utilizing waste soy sauce and industrial flue gas', *Bioresource Technology*, 373, p. 128719. doi: https://doi.org/10.1016/j.biortech.2023.128719.

Lee, Y.-K. (2001) 'Microalgal mass culture systems and methods: Their limitation and potential', in *Journal of Applied Phycology*, pp. 307–315. doi: 10.1023/A:1017560006941.

Leeper, D. A. and Porter, K. G. (1995) 'Toxicity of the mixotrophic chrysophyte Poterioochromonas malhamensis to the cladoceran Daphnia ambigua', *Archiv für Hydrobiologie*, 134(2), pp. 207–222. doi: 10.1127/archiv-hydrobiol/134/1995/207.

Leone, G. *et al.* (2021) 'Incorporating a molecular antenna in diatom microalgae cells enhances photosynthesis', *Scientific Reports*, 11(1), p. 5209. doi: 10.1038/s41598-021-84690-z.

Levasseur, W., Perré, P. and Pozzobon, V. (2020) 'A review of high value-added molecules production by microalgae in light of the classification', *Biotechnology Advances*, 41, p. 107545. doi: https://doi.org/10.1016/j.biotechadv.2020.107545.

Li, B. *et al.* (2010) 'Apoptotic mechanism of MCF-7 breast cells in vivo and in vitro induced by photodynamic therapy with C-phycocyanin.', *Acta biochimica et biophysica Sinica*, 42(1), pp. 80–89. doi: 10.1093/abbs/gmp104.

Li, F.-F. *et al.* (2011) 'Microalgae Capture of CO2 from Actual Flue Gas Discharged from a Combustion Chamber', *Industrial & Engineering Chemistry Research*, 50(10), pp. 6496–6502. doi: 10.1021/ie200040q.

Li, L. *et al.* (2020) 'A comparative long-term operation using up-flow anaerobic sludge blanket (UASB) and anaerobic membrane bioreactor (AnMBR) for the upgrading of anaerobic treatment of N, N-dimethylformamide-containing wastewater', *Science of The Total Environment*, 699, p. 134370. doi: https://doi.org/10.1016/j.scitotenv.2019.134370.

Li, Q. *et al.* (2022) 'Sodium chloride stimulates the biomass and astaxanthin production by Haematococcus pluvialis via a two-stage cultivation strategy', *Bioresource Technology*, 344, p. 126214. doi: https://doi.org/10.1016/j.biortech.2021.126214.

Li, Y., Horsman, M., Wu, N., *et al.* (2008) 'Biofuels from Microalgae', *Biotechnology Progress*, 24(4), pp. 815–820. doi: https://doi.org/10.1021/bp070371k.

Li, Y., Horsman, M., Wang, B., *et al.* (2008) 'Effects of nitrogen sources on cell growth and lipid accumulation of green alga Neochloris oleoabundans.', *Applied microbiology and biotechnology*, 81(4), pp. 629–636. doi: 10.1007/s00253-008-1681-1.

Li, Y. *et al.* (2017) 'Fate of nitrogen in subsurface infiltration system for treating secondary effluent', *Water Science and Engineering*, 10(3), pp. 217–224. doi: https://doi.org/10.1016/j.wse.2017.10.002.

Li, Z. *et al.* (2020) 'Metabolic engineering of Escherichia coli for production of chemicals derived from the shikimate pathway', *Journal of Industrial Microbiology & Biotechnology*, 47(6), pp. 525–535. doi: 10.1007/s10295-020-02288-2.

Liao, H. F. *et al.* (2001) 'Serine 187 is a crucial residue for allosteric regulation of Corynebacterium glutamicum 3-deoxy-D-arabino-heptulosonate-7-phosphate synthase.', *FEMS microbiology letters*, 194(1), pp. 59–64. doi: 10.1111/j.1574-6968.2001.tb09446.x.

Licata, M. *et al.* (2021) 'Treatment of Combined Dairy and Domestic Wastewater with Constructed Wetland System in Sicily (Italy). Pollutant Removal Efficiency and Effect of Vegetation', *Water*. doi: 10.3390/w13081086.

'Light–Dependent Reactions of Photosynthesis' (2015) *The Plant Cell*, 27(11), p. tpc.115.tt1115. doi: 10.1105/tpc.115.tt1115.

Lim, H. R. *et al.* (2021) 'Perspective of Spirulina culture with wastewater into a sustainable circular bioeconomy', *Environmental Pollution*, 284, p. 117492. doi: https://doi.org/10.1016/j.envpol.2021.117492.

Lincoln, E. P., Wilkie, A. C. and French, B. T. (1996) 'Cyanobacterial process for renovating dairy wastewater', *Biomass and Bioenergy*, 10(1), pp. 63–68. doi: https://doi.org/10.1016/0961-9534(95)00055-0.

Lisondro, I. *et al.* (2022) 'Influence of irradiance on the growth and biochemical composition of Nitzschia aff. pellucida', *Journal of Applied Phycology*, 34(1), pp. 19–30. doi: 10.1007/s10811-021-02605-x.

Liu, C., Men, X., *et al.* (2018) 'A systematic optimization of styrene biosynthesis in Escherichia coli BL21(DE3)', *Biotechnology for Biofuels*, 11(1), p. 14. doi: 10.1186/s13068-018-1017-z.

Liu, C., Zhang, K., *et al.* (2018) 'Genome mining of 2-phenylethanol biosynthetic genes from Enterobacter sp. CGMCC 5087 and heterologous overproduction in Escherichia coli', *Biotechnology for Biofuels*, 11(1), p. 305. doi: 10.1186/s13068-018-1297-3.

Liu, H. *et al.* (2019) 'Engineering acetyl-CoA metabolic shortcut for eco-friendly

production of polyketides triacetic acid lactone in Yarrowia lipolytica.', *Metabolic engineering*, 56, pp. 60–68. doi: 10.1016/j.ymben.2019.08.017.

Liu, H. *et al.* (2022) 'Comparison of Swine Wastewater Treatment by Microalgae and Heterotrophic Nitrifiers: Focusing on Nitrogen Removal Mechanism Revealed by Microbiological Correlation Analysis', *Water, Air, & Soil Pollution*, 233(8), p. 294. doi: 10.1007/s11270-022-05783-7.

Liu, J., Jiang, J., Bai, Y., *et al.* (2018) 'Mimicking a New 2-Phenylethanol Production Pathway from Proteus mirabilis JN458 in Escherichia coli', *Journal of Agricultural and Food Chemistry*, 66(13), pp. 3498–3504. doi: 10.1021/acs.jafc.8b00627.

Liu, N., Santala, S. and Stephanopoulos, G. (2020) 'Mixed carbon substrates: a necessary nuisance or a missed opportunity?', *Current Opinion in Biotechnology*, 62, pp. 15–21. doi: https://doi.org/10.1016/j.copbio.2019.07.003.

Liu, Q. *et al.* (2019) 'Rewiring carbon metabolism in yeast for high level production of aromatic chemicals', *Nature Communications*, 10(1), p. 4976. doi: 10.1038/s41467-019-12961-5.

Liu, X. *et al.* (2022) 'Current advances in engineering cyanobacteria and their applications for photosynthetic butanol production', *Current Opinion in Biotechnology*, 73, pp. 143–150. doi: https://doi.org/10.1016/j.copbio.2021.07.014.

Liu, Y., Xu, Y., Ding, D., *et al.* (2018) 'Genetic engineering of Escherichia coli to improve L-phenylalanine production', *BMC Biotechnology*, 18(1), p. 5. doi: 10.1186/s12896-018-0418-1.

Löffelhardt, W. and Bohnert, H. J. (1994) 'Molecular Biology of Cyanelles BT - The Molecular Biology of Cyanobacteria', in Bryant, D. A. (ed.). Dordrecht: Springer Netherlands, pp. 65–89. doi: 10.1007/978-94-011-0227-8_4.

Lopes, G., Clarinha, D. and Vasconcelos, V. (2020) 'Carotenoids from Cyanobacteria: A Biotechnological Approach for the Topical Treatment of Psoriasis.', *Microorganisms*, 8(2). doi: 10.3390/microorganisms8020302.

López-Maury, L., Giner-Lamia, J. and Florencio, F. J. (2012) 'Redox control of copper homeostasis in cyanobacteria.', *Plant signaling & behavior*, 7(12), pp. 1712–1714. doi: 10.4161/psb.22323.

Lopez, F. B. and Barclay, G. F. (2017) *Plant Anatomy and Physiology*,

Pharmacognosy: Fundamentals, Applications and Strategy. Elsevier Inc. doi: 10.1016/B978-0-12-802104-0.00004-4.

Lu, J. *et al.* (2023) 'Natural product 2-Phenylethanol inhibits ATP synthesis of P. infestans by blocking the oxidative phosphorylation pathway to prevent potato late blight', *Postharvest Biology and Technology*, 199, p. 112310. doi: https://doi.org/10.1016/j.postharvbio.2023.112310.

Lu, Q. *et al.* (2016) 'Mitigating ammonia nitrogen deficiency in dairy wastewaters for algae cultivation', *Bioresource Technology*, 201, pp. 33–40. doi: 10.1016/j.biortech.2015.11.029.

Luan, G. *et al.* (2019) 'Progress and perspective on cyanobacterial glycogen metabolism engineering', *Biotechnology Advances*, 37(5), pp. 771–786. doi: https://doi.org/10.1016/j.biotechadv.2019.04.005.

Luo, X. *et al.* (2019) 'Stable Reference Gene Selection for RT-qPCR Analysis in *Synechococcus elongatus* PCC 7942 under Abiotic Stresses', *BioMed Research International*. Edited by M. El-Matbouli, 2019, p. 7630601. doi: 10.1155/2019/7630601.

Lütke-Eversloh, T. and Stephanopoulos, G. (2005) 'Feedback inhibition of chorismate mutase/prephenate dehydrogenase (TyrA) of Escherichia coli: generation and characterization of tyrosine-insensitive mutants.', *Applied and environmental microbiology*, 71(11), pp. 7224–7228. doi: 10.1128/AEM.71.11.7224-7228.2005.

Lütke-Eversloh, T. and Stephanopoulos, G. (2008) 'Combinatorial pathway analysis for improved L-tyrosine production in Escherichia coli: Identification of enzymatic bottlenecks by systematic gene overexpression', *Metabolic Engineering*, 10(2), pp. 69–77. doi: https://doi.org/10.1016/j.ymben.2007.12.001.

Luttik, M. A. H. *et al.* (2008) 'Alleviation of feedback inhibition in Saccharomyces cerevisiae aromatic amino acid biosynthesis: Quantification of metabolic impact', *Metabolic Engineering*, 10(3), pp. 141–153. doi: https://doi.org/10.1016/j.ymben.2008.02.002.

M. Ciani;G. Daly;R. De Philippis;A. Adessi (2023) 'Cyanobacteria for heavy metals removal: from pure metal solutions to electroplating industry wastewaters', in *6th IWA International Conference on eco-Technologies for Wastewater Treatment*. Available at: https://hdl.handle.net/2158/1328772.

Magalhães, I. B. *et al.* (2021) 'Technologies for improving microalgae biomass

production coupled to effluent treatment: A life cycle approach', *Algal Research*, 57, p. 102346. doi: https://doi.org/10.1016/j.algal.2021.102346.

Mahlmann, D. M., Jahnke, J. and Loosen, P. (2008) 'Rapid determination of the dry weight of single, living cyanobacterial cells using the Mach-Zehnder double-beam interference microscope', *European Journal of Phycology*, 43(4), pp. 355–364. doi: 10.1080/09670260802168625.

Majdabadi, N. *et al.* (2018) 'Effect of 2-Phenylethanol as Antifungal Agent and Common Antifungals (Amphotericin B, Fluconazole, and Itraconazole) on Candida Species Isolated from Chronic and Recurrent Cases of Candidal Vulvovaginitis.', *Assay and drug development technologies*, 16(3), pp. 141–149. doi: 10.1089/adt.2017.837.

Majhi, S. and Das, D. (2021) 'Chemical derivatization of natural products: Semisynthesis and pharmacological aspects- A decade update', *Tetrahedron*, 78, p. 131801. doi: https://doi.org/10.1016/j.tet.2020.131801.

Maltsev, Y. *et al.* (2017) 'Prospects of using algae in biofuel production', *Regulatory Mechanisms in Biosystems*, 8, pp. 455–460.

Maltsev, Y. *et al.* (2021) 'Influence of Light Conditions on Microalgae Growth and Content of Lipids, Carotenoids, and Fatty Acid Composition', *Biology*, 10(10). doi: 10.3390/biology10101060.

Mangan, N. M. *et al.* (2016) 'pH determines the energetic efficiency of the cyanobacterial CO2 concentrating mechanism', *Proceedings of the National Academy of Sciences*, 113(36), pp. E5354–E5362. doi: 10.1073/pnas.1525145113.

Mangi, K. H. *et al.* (2021) 'Passive thermal regulation approach for Algofilm © photobioreactor through phase change', *Chemical Engineering Research and Design*, 168, pp. 411–425. doi: https://doi.org/10.1016/j.cherd.2021.02.013.

Mannino, G. *et al.* (2021) 'Bioactive Triterpenes of Protium heptaphyllum Gum Resin Extract Display Cholesterol-Lowering Potential', *International Journal of Molecular Sciences*, 22(5). doi: 10.3390/ijms22052664.

Maragkoudakis, P. *et al.* (2016) 'Potential use of scotta, the by-product of the ricotta cheese manufacturing process, for the production of fermented drinks.', *The Journal of dairy research*, 83(1), pp. 104–108. doi: 10.1017/S002202991500059X.

Marcial, H. S. and Hagiwara, A. (2007) 'Effect of diazinon on life stages and

resting egg hatchability of rotifer Brachionus plicatilis', *Hydrobiologia*, 593(1), pp. 219–225. doi: 10.1007/s10750-007-9070-9.

Marella, T. K., Parine, N. R. and Tiwari, A. (2018) 'Potential of diatom consortium developed by nutrient enrichment for biodiesel production and simultaneous nutrient removal from waste water', *Saudi Journal of Biological Sciences*, 25(4), pp. 704–709. doi: https://doi.org/10.1016/j.sjbs.2017.05.011.

Martín-Girela, I., Curt, M. D. and Fernández, J. (2017) 'Flashing light effects on CO2 absorption by microalgae grown on a biofilm photobioreactor', *Algal Research*, 25, pp. 421–430. doi: https://doi.org/10.1016/j.algal.2017.06.008.

Martínez-Avila, O. *et al.* (2018) 'Bioprocesses for 2-phenylethanol and 2-phenylethyl acetate production: current state and perspectives', *Applied Microbiology and Biotechnology*, 102(23), pp. 9991–10004. doi: 10.1007/s00253-018-9384-8.

Masojídek, J. and Prášil, O. (2010) 'The development of microalgal biotechnology in the Czech Republic.', *Journal of industrial microbiology & biotechnology*, 37(12), pp. 1307–1317. doi: 10.1007/s10295-010-0802-x.

Masojídek, J. and Torzillo, G. (2014) 'Mass cultivation of freshwater microalgae'.

Masojídek, J., Torzillo, G. and Koblížek, M. (2013) 'Photosynthesis in Microalgae', in *Handbook of Microalgal Culture*, pp. 21–36. doi: https://doi.org/10.1002/9781118567166.ch2.

McEwen, J. T. *et al.* (2013) 'Engineering Synechococcus elongatus PCC 7942 for continuous growth under diurnal conditions.', *Applied and environmental microbiology*, 79(5), pp. 1668–1675. doi: 10.1128/AEM.03326-12.

Melis, A. (2009) 'Solar energy conversion efficiencies in photosynthesis: Minimizing the chlorophyll antennae to maximize efficiency', *Plant Science*, 177(4), pp. 272–280. doi: https://doi.org/10.1016/j.plantsci.2009.06.005.

Menin, B. *et al.* (2019) 'Non-endogenous ketocarotenoid accumulation in engineered Synechocystis sp. PCC 6803', *Physiologia Plantarum*, 166(1), pp. 403–412. doi: https://doi.org/10.1111/ppl.12900.

Meyer, M. T. *et al.* (2020) 'Assembly of the algal CO(2)-fixing organelle, the pyrenoid, is guided by a Rubisco-binding motif.', *Science advances*, 6(46). doi: 10.1126/sciadv.abd2408.

Milano, F. *et al.* (2012) 'Enhancing the Light Harvesting Capability of a Photosynthetic Reaction Center by a Tailored Molecular Fluorophore', *Angewandte Chemie International Edition*, 51(44), pp. 11019–11023. doi: https://doi.org/10.1002/anie.201203404.

Mir, R., Jallu, S. and Singh, T. P. (2015) 'The shikimate pathway: review of amino acid sequence, function and three-dimensional structures of the enzymes.', *Critical reviews in microbiology*, 41(2), pp. 172–189. doi: 10.3109/1040841X.2013.813901.

Mitri, S., Koubaa, M., Maroun, R. G., Rossignol, T., Nicaud, J.-M., *et al.* (2022) 'Bioproduction of 2-Phenylethanol through Yeast Fermentation on Synthetic Media and on Agro-Industrial Waste and By-Products: A Review.', *Foods (Basel, Switzerland)*, 11(1). doi: 10.3390/foods11010109.

Mitri, S., Koubaa, M., Maroun, R. G., Rossignol, T., Nicaud, J., *et al.* (2022) 'on Synthetic Media and on Agro-Industrial Waste and By-Products : A Review'.

Moffitt, M. C. *et al.* (2007) 'Discovery of two cyanobacterial phenylalanine ammonia lyases: kinetic and structural characterization.', *Biochemistry*, 46(4), pp. 1004–1012. doi: 10.1021/bi061774g.

Mohsenpour, S. F., Richards, B. and Willoughby, N. (2012) 'Spectral conversion of light for enhanced microalgae growth rates and photosynthetic pigment production', *Bioresource Technology*, 125, pp. 75–81. doi: https://doi.org/10.1016/j.biortech.2012.08.072.

Molina, D. *et al.* (2019) 'Biological contamination and its chemical control in microalgal mass cultures', *Applied Microbiology and Biotechnology*, 103(23), pp. 9345–9358. doi: 10.1007/s00253-019-10193-7.

Molitor, H. R. and Schnoor, J. L. (2020) 'Using Simulated Flue Gas to Rapidly Grow Nutritious Microalgae with Enhanced Settleability.', *ACS omega*, 5(42), pp. 27269–27277. doi: 10.1021/acsomega.0c03492.

Möllers, K. B. *et al.* (2014) 'Cyanobacterial biomass as carbohydrate and nutrient feedstock for bioethanol production by yeast fermentation', *Biotechnology for Biofuels*, 7(1), p. 64. doi: 10.1186/1754-6834-7-64.

Montemezzani, V. *et al.* (2015) 'A review of potential methods for zooplankton control in wastewater treatment High Rate Algal Ponds and algal production raceways', *Algal Research*, 11, pp. 211–226. doi: https://doi.org/10.1016/j.algal.2015.06.024.

Monti, L. *et al.* (2018) 'Application of membrane technologies to bovine Ricotta cheese exhausted whey (scotta)', *International Dairy Journal*, 85, pp. 121–128. doi: https://doi.org/10.1016/j.idairyj.2018.05.007.

de Mooij, T. *et al.* (2015) 'Antenna size reduction as a strategy to increase biomass productivity: a great potential not yet realized', *Journal of Applied Phycology*, 27(3), pp. 1063–1077. doi: 10.1007/s10811-014-0427-y.

Van Mooy, B. A. S. *et al.* (2009) 'Phytoplankton in the ocean use non-phosphorus lipids in response to phosphorus scarcity', *Nature*, 458(7234), pp. 69–72. doi: 10.1038/nature07659.

Morales, M., Hélias, A. and Bernard, O. (2019) 'Optimal integration of microalgae production with photovoltaic panels: environmental impacts and energy balance', *Biotechnology for Biofuels*, 12(1), p. 239. doi: 10.1186/s13068-019-1579-4.

Moreno-Garrido, I. and Cañavate, J. P. (2001) 'Assessing chemical compounds for controlling predator ciliates in outdoor mass cultures of the green algae Dunaliella salina', *Aquacultural Engineering*, 24(2), pp. 107–114. doi: https://doi.org/10.1016/S0144-8609(00)00067-4.

Moreno Osorio, J. H. *et al.* (2019) 'Start-up of a nutrient removal system using Scenedesmus vacuolatus and Chlorella vulgaris biofilms', *Bioresources and Bioprocessing*, 6(1), p. 27. doi: 10.1186/s40643-019-0259-3.

Mori, T., Binder, B. and Johnson, C. H. (1996) 'Circadian gating of cell division in cyanobacteria growing with average doubling times of less than 24 hours.', *Proceedings of the National Academy of Sciences of the United States of America*, 93(19), pp. 10183–10188. doi: 10.1073/pnas.93.19.10183.

Morselli, N.; Altunoz, M.; Puglia, M.; Arru, L.; Tartarini, P. (2019) 'Passive system for internal surface cleaning and homogenization in the air-lift vertical column photobioreactors', in *27th European Biomass Conference and Exhibition, EUBCE 2019*, pp. 268–275. doi: 10.5071/27thEUBCE2019-1DV.1.25.

Muharam, Y., Putri, A. D. and Hamzah, A. (2019) 'Phenomenological model for the prediction of the performance of a slurry bubble column reactor for green diesel production', *Journal of Physics: Conference Series*, 1349(1). doi: 10.1088/1742-6596/1349/1/012057.

Muhetaer, G. *et al.* (2020) 'Effects of Light Intensity and Exposure Period on the Growth and Stress Responses of Two Cyanobacteria Species: Pseudanabaena galeata

and Microcystis aeruginosa', *Water*, 12(2). doi: 10.3390/w12020407.

Myerson, A. L. (1954) *Algal culture: From laboratory to pilot plant*, *Journal of the Franklin Institute*. doi: 10.1016/0016-0032(54)90075-7.

Nagi, M. *et al.* (2020) 'Utilization of tannery wastewater for biofuel production: New insights on microalgae growth and biomass production', *Scientific Reports*, 10(1), p. 1530. doi: 10.1038/s41598-019-57120-4.

Nawar, A. *et al.* (2017) 'Physical abrasion method using submerged spike balls to remove algal biofilm from photobioreactors', *BMC Research Notes*, 10(1), p. 666. doi: 10.1186/s13104-017-2995-9.

Nayak, M., Karemore, A. and Sen, R. (2016) 'Sustainable valorization of flue gas CO2 and wastewater for the production of microalgal biomass as a biofuel feedstock in closed and open reactor systems', *RSC Advances*, 6(94), pp. 9111–91120. doi: 10.1039/c6ra17899e.

Ndayisenga, F. *et al.* (2021) 'Co-substrate facilitated charge transfer for bioelectricity evolution in a toxic blue-green alga-fed microbial fuel cell technology', *Clean Technologies and Environmental Policy*. doi: 10.1007/s10098-021-02173-1.

Nedbal, L. *et al.* (2008) 'A photobioreactor system for precision cultivation of photoautotrophic microorganisms and for high-content analysis of suspension dynamics.', *Biotechnology and bioengineering*, 100(5), pp. 902–910. doi: 10.1002/bit.21833.

Ng, I.-S. *et al.* (2017) 'Recent Developments on Genetic Engineering of Microalgae for Biofuels and Bio-Based Chemicals', *Biotechnology Journal*, 12(10), p. 1600644. doi: https://doi.org/10.1002/biot.201600644.

Nguyen, D. D. *et al.* (2022) 'Grazer-induced changes in molecular signatures of cyanobacteria', *Algal Research*, 61, p. 102575. doi: https://doi.org/10.1016/j.algal.2021.102575.

Ni, J. *et al.* (2018) 'Remodeling of the Photosynthetic Chain Promotes Direct CO2 Conversion into Valuable Aromatic Compounds', *Angewandte Chemie - International Edition*, 57(49), pp. 15990–15994. doi: 10.1002/anie.201808402.

Nielson, D., Machas, M. and Mckenna, R. (2018) 'Microbial production of 2-phenylethanol from renewable substrates', p. 5630.

Niu, H. *et al.* (2019) 'Metabolic engineering for improving L-tryptophan production in Escherichia coli.', *Journal of industrial microbiology & biotechnology*, 46(1), pp. 55–65. doi: 10.1007/s10295-018-2106-5.

Noda, S. and Kondo, A. (2017) 'Recent Advances in Microbial Production of Aromatic Chemicals and Derivatives.', *Trends in biotechnology*, 35(8), pp. 785–796. doi: 10.1016/j.tibtech.2017.05.006.

Nogales, J. *et al.* (2012) 'Detailing the optimality of photosynthesis in cyanobacteria through systems biology analysis', *Proceedings of the National Academy of Sciences*, 109(7), pp. 2678–2683. doi: 10.1073/pnas.1117907109.

Noguchi, S. *et al.* (2016) 'Quantitative target analysis and kinetic profiling of acyl-CoAs reveal the rate-limiting step in cyanobacterial 1-butanol production', *Metabolomics*, 12(2), p. 26. doi: 10.1007/s11306-015-0940-2.

Norsker, N.-H. *et al.* (2011) 'Microalgal production — A close look at the economics', *Biotechnology Advances*, 29(1), pp. 24–27. doi: https://doi.org/10.1016/j.biotechadv.2010.08.005.

Norsker, N. H. *et al.* (2019) 'Productivity of Nannochloropsis oceanica in an industrial closely spaced flat panel photobioreactor', *Algal Research*, 43, p. 101632. doi: https://doi.org/10.1016/j.algal.2019.101632.

Novoveská, L. *et al.* (2023) 'Overview and Challenges of Large-Scale Cultivation of Photosynthetic Microalgae and Cyanobacteria.', *Marine drugs*, 21(8). doi: 10.3390/md21080445.

Nowicka, B. and Kruk, J. (2016) 'Cyanobacteria use both p-hydroxybenozate and homogentisate as a precursor of plastoquinone head group', *Acta Physiologiae Plantarum*, 38(2), p. 49. doi: 10.1007/s11738-015-2043-0.

Nozzi, N. E. and Atsumi, S. (2015) 'Genome Engineering of the 2,3-Butanediol Biosynthetic Pathway for Tight Regulation in Cyanobacteria', *ACS Synthetic Biology*, 4(11), pp. 1197–1204. doi: 10.1021/acssynbio.5b00057.

Nozzi, N., Oliver, J. and Atsumi, S. (2013) 'Cyanobacteria as a Platform for Biofuel Production', *Frontiers in Bioengineering and Biotechnology*, 1. doi: 10.3389/fbioe.2013.00007.

Nshimiyimana, P., Liu, L. and Du, G. (2019) 'Engineering of L-amino acid deaminases for the production of α-keto acids from L-amino acids', *Bioengineered*,

10(1), pp. 43–51. doi: 10.1080/21655979.2019.1595990.

Nwoba, E. G. *et al.* (2019) 'Light management technologies for increasing algal photobioreactor efficiency', *Algal Research*, 39. doi: 10.1016/j.algal.2019.101433.

Nwoba, E. G. *et al.* (2020) 'Energy efficiency analysis of outdoor standalone photovoltaic-powered photobioreactors coproducing lipid-rich algal biomass and electricity', *Applied Energy*, 275, p. 115403. doi: 10.1016/j.apenergy.2020.115403.

Odunlami, O. A. *et al.* (2022) 'Advanced techniques for the capturing and separation of CO2 – A review', *Results in Engineering*, 15, p. 100512. doi: https://doi.org/10.1016/j.rineng.2022.100512.

Of, J. and Microbiology, P. (2016) 'Cyanobacterial Cultivation on Dairy Effluent for Removal of Nutrient and its Biomass Production for Biofuel', 8(January), pp. 4917–4925.

Ogawa, T. *et al.* (2015) 'Enhancement of photosynthetic capacity in Euglena gracilis by expression of cyanobacterial fructose-1,6-/sedoheptulose-1,7-bisphosphatase leads to increases in biomass and wax ester production', *Biotechnology for Biofuels*, 8(1), p. 80. doi: 10.1186/s13068-015-0264-5.

Ogbonna, J. C., Yada, H. and Tanaka, H. (1995) 'Kinetic study on light-limited batch cultivation of photosynthetic cells', *Journal of Fermentation and Bioengineering*, 80(3), pp. 259–264. doi: https://doi.org/10.1016/0922-338X(95)90826-L.

Olaizola, M. and Grewe, C. (2019) 'Commercial Microalgal Cultivation Systems BT - Grand Challenges in Algae Biotechnology', in Hallmann, A. and Rampelotto, P. H. (eds). Cham: Springer International Publishing, pp. 3–34. doi: 10.1007/978-3-030-25233-5_1.

De Oliveira, M. C., Bassin, I. D. and Cammarota, M. C. (2022) 'Microalgae and Cyanobacteria Biomass Pretreatment Methods: A Comparative Analysis of Chemical and Thermochemical Pretreatment Methods Aimed at Methane Production', *Fermentation*. doi: 10.3390/fermentation8100497.

Oliver, J. W. K. and Atsumi, S. (2015) 'A carbon sink pathway increases carbon productivity in cyanobacteria.', *Metabolic engineering*, 29, pp. 106–112. doi: 10.1016/j.ymben.2015.03.006.

Osanai, T. *et al.* (2011) 'Genetic engineering of group 2 sigma factor SigE widely

activates expressions of sugar catabolic genes in Synechocystis species PCC 6803.', *The Journal of biological chemistry*, 286(35), pp. 30962–30971. doi: 10.1074/jbc.M111.231183.

Ouhsassi, M. *et al.* (2020) 'Evaluation of self-purifying power of cyanobacteria Pseudanabaena galeata: case of dairy factory effluents', *Applied Water Science*, 10(7), p. 181. doi: 10.1007/s13201-020-01270-8.

P R., Y., Das, M. and Maiti, S. K. (2021) 'Recent progress and challenges in cyanobacterial autotrophic production of polyhydroxybutyrate (PHB), a bioplastic', *Journal of Environmental Chemical Engineering*, 9(4), p. 105379. doi: https://doi.org/10.1016/j.jece.2021.105379.

Palmer, C. M. (1969) 'A COMPOSITE RATING OF ALGAE TOLERATING ORGANIC POLLUTION2', *Journal of Phycology*, 5(1), pp. 78–82. doi: https://doi.org/10.1111/j.1529-8817.1969.tb02581.x.

Pan, M. *et al.* (2021) 'Mitigating antibiotic pollution using cyanobacteria: Removal efficiency, pathways and metabolism', *Water Research*, 190, p. 116735. doi: https://doi.org/10.1016/j.watres.2020.116735.

Papadopoulos, K. P. *et al.* (2020) 'Brewery wastewater treatment using cyanobacterial-bacterial settleable aggregates', *Algal Research*, 49, p. 101957. doi: https://doi.org/10.1016/j.algal.2020.101957.

Papazi, A. *et al.* (2012) 'High Yields of Hydrogen Production Induced by Meta-Substituted Dichlorophenols Biodegradation from the Green Alga Scenedesmus obliquus', *PLOS ONE*, 7(11), p. e49037. Available at: https://doi.org/10.1371/journal.pone.0049037.

Parichehreh, R. *et al.* (2019) 'Optimization of lipid production in Chlorella vulgaris for biodiesel production using flux balance analysis', *Biochemical Engineering Journal*, 141, pp. 131–145. doi: https://doi.org/10.1016/j.bej.2018.10.011.

Park, J. B. K. and Craggs, R. J. (2011) 'Algal production in wastewater treatment high rate algal ponds for potential biofuel use', *Water Science and Technology*, 63(10), pp. 2403–2410. doi: 10.2166/wst.2011.200.

Park, J. O. *et al.* (2019) 'Synergistic substrate cofeeding stimulates reductive metabolism', *Nature Metabolism*, 1(6), pp. 643–651. doi: 10.1038/s42255-019-0077-0.

Park, K.-H. and Lee, C.-G. (2000) 'Optimization of algal photobioreactors using flashing lights', *Biotechnology and Bioprocess Engineering*, 5(3), pp. 186–190. doi: 10.1007/BF02936592.

Park, S. *et al.* (2016) 'The Selective Use of Hypochlorite to Prevent Pond Crashes for Algae-Biofuel Production.', *Water environment research : a research publication of the Water Environment Federation*, 88(1), pp. 70–78. doi: 10.2175/106143015X14362865227670.

Park, S. *et al.* (2019) 'Microalgae Cultivation in Pilot Scale for Biomass Production Using Exhaust Gas from Thermal Power Plants', *Energies*. doi: 10.3390/en12183497.

Parmar, A. *et al.* (2011) 'Cyanobacteria and microalgae: A positive prospect for biofuels', *Bioresource Technology*, 102(22), pp. 10163–10172. doi: https://doi.org/10.1016/j.biortech.2011.08.030.

Paulenco, A. *et al.* (2023) 'Nannochloris sp. Microalgae Strain for Treatment of Dairy Wastewaters', *Microorganisms*. doi: 10.3390/microorganisms11061469.

Pereira, M. I. B. *et al.* (2019) 'Mixotrophic cultivation of Spirulina platensis in dairy wastewater: Effects on the production of biomass, biochemical composition and antioxidant capacity', *PLOS ONE*, 14(10), p. e0224294. Available at: https://doi.org/10.1371/journal.pone.0224294.

Pérez, A. A. *et al.* (2019) 'On the use of oxygenic photosynthesis for the sustainable production of commodity chemicals.', *Physiologia plantarum*, 166(1), pp. 413–427. doi: 10.1111/ppl.12946.

Pham, H.-M. *et al.* (2017) 'Development of an X-Shape airlift photobioreactor for increasing algal biomass and biodiesel production', *Bioresource Technology*, 239, pp. 211–218. doi: https://doi.org/10.1016/j.biortech.2017.05.030.

Pierce, R. W. and Turner, J. T. (1992) 'Ecology of Planktonic Ciliates in Marine Food Webs', *Reviews in Aquatic Sciences*, 6(January 1992), pp. 139–181.

PING, X. and MCAULEY, P. J. (1990) 'Uptake of amino acids by the cyanobacterium Anabaena ATCC 27893', *New Phytologist*, 115(4), pp. 581–585. doi: 10.1111/j.1469-8137.1990.tb00488.x.

Pittard, J. and Yang, J. (2008) 'Biosynthesis of the Aromatic Amino Acids.', *EcoSal Plus*, 3(1). doi: 10.1128/ecosalplus.3.6.1.8.

Pleissner, D., Lindner, A. V. and Ambati, R. R. (2020) 'Techniques to Control Microbial Contaminants in Nonsterile Microalgae Cultivation.', *Applied biochemistry and biotechnology*, 192(4), pp. 1376–1385. doi: 10.1007/s12010-020-03414-7.

Pleonsil, P., Soogarun, S. and Suwanwong, Y. (2013) 'Anti-oxidant activity of holo- and apo-c-phycocyanin and their protective effects on human erythrocytes.', *International journal of biological macromolecules*, 60, pp. 393–398. doi: 10.1016/j.ijbiomac.2013.06.016.

De Porcellinis, A., Frigaard, N.-U. and Sakuragi, Y. (2017) 'Determination of the Glycogen Content in Cyanobacteria', *Journal of visualized experiments : JoVE*, (125), p. 56068. doi: 10.3791/56068.

Praveen, K. *et al.* (2023) 'Harnessing Extremophilic Trait and Metabolic Flexibility of Microalgal Strains for the Treatment of Highly Alkaline Winery Wastewater', *ACS ES&T Engineering*. doi: 10.1021/acsestengg.3c00386.

Prazeres, A. R., Carvalho, F. and Rivas, J. (2012) 'Cheese whey management: A review', *Journal of Environmental Management*, 110, pp. 48–68. doi: 10.1016/j.jenvman.2012.05.018.

Prokop, A. *et al.* (1984) 'Spectral shifting by dyes to enhance algae growth', *Biotechnology and Bioengineering*, 26(11), pp. 1313–1322. doi: https://doi.org/10.1002/bit.260261108.

Pruvost, J. *et al.* (2017) 'Development of a thin-film solar photobioreactor with high biomass volumetric productivity (AlgoFilm©) based on process intensification principles', *Algal Research*, 21, pp. 120–137. doi: https://doi.org/10.1016/j.algal.2016.10.012.

Qasim, W. and Mane, A. V (2013) 'Characterization and treatment of selected food industrial effluents by coagulation and adsorption techniques', *Water Resources and Industry*, 4, pp. 1–12. doi: https://doi.org/10.1016/j.wri.2013.09.005.

Qian, X. *et al.* (2019) 'Current status and perspectives of 2-phenylethanol production through biological processes.', *Critical reviews in biotechnology*, 39(2), pp. 235–248. doi: 10.1080/07388551.2018.1530634.

Qin, L. *et al.* (2014) 'Cultivation of chlorella vulgaris in dairy wastewater pretreated by UV irradiation and sodium hypochlorite', *Applied Biochemistry and Biotechnology*, 172(2), pp. 1121–1130. doi: 10.1007/s12010-013-0576-5.

Qin, S. *et al.* (2023) 'Biotechnologies for bulk production of microalgal biomass: from mass cultivation to dried biomass acquisition', *Biotechnology for Biofuels and Bioproducts*, 16(1), pp. 1–25. doi: 10.1186/s13068-023-02382-4.

Le Quéré, C. *et al.* (2018) 'Global Carbon Budget 2018', *Earth System Science Data*, 10(4), pp. 2141–2194. doi: 10.5194/essd-10-2141-2018.

Quintero, M. J. *et al.* (2001) 'Identification of genes encoding amino acid permeases by inactivation of selected ORFs from the Synechocystis genomic sequence.', *Genome research*, 11(12), pp. 2034–2040. doi: 10.1101/gr.196301.

Rahman, M. *et al.* (2023) 'An Assessment of the Effects of Light Intensities and Temperature Changes on Cyanobacteria’s Oxidative Stress via the Use of Hydrogen Peroxide as an Indicator', *Water*, 15(13). doi: 10.3390/w15132429.

Rajabloo, T. *et al.* (2023) 'Carbon capture and utilization for industrial applications', *Energy Reports*, 9, pp. 111–116. doi: https://doi.org/10.1016/j.egyr.2022.12.009.

Ramanna, L., Rawat, I. and Bux, F. (2017) 'Light enhancement strategies improve microalgal biomass productivity', *Renewable and Sustainable Energy Reviews*, 80, pp. 765–773. doi: https://doi.org/10.1016/j.rser.2017.05.202.

Ranglová, K. *et al.* (2022) 'Efficient microalgae feed production for fish hatcheries using an annular column photobioreactor characterized by a short light path and central LED illumination', *Journal of Applied Phycology*, 34(1), pp. 31–41. doi: 10.1007/s10811-021-02647-1.

Redfield, A. C. (1934) *On the Proportions of Organic Derivatives in Sea Water and Their Relation to the Composition of Plankton*. University Press of Liverpool. Available at: https://books.google.it/books?id=szAezQEACAAJ.

Ribeiro, J. E. S. *et al.* (2017) 'Production of Chlorella protothecoides biomass, chlorophyll and carotenoids using the dairy industry by-product scotta as a substrate', *Biocatalysis and Agricultural Biotechnology*, 11, pp. 207–213. doi: https://doi.org/10.1016/j.bcab.2017.07.007.

Riegman, R. *et al.* (2000) 'Nutrient uptake and alkaline phosphatase (ec 3:1:3:1) activity of emiliania huxleyi (PRYMNESIOPHYCEAE) during growth under n and p limitation in continuous cultures', *Journal of Phycology*, 36(1), pp. 87–96. doi: https://doi.org/10.1046/j.1529-8817.2000.99023.x.

Rodrigues-Sousa, A. E. *et al.* (2021) 'Nitrogen supplementation for the production of Chlorella vulgaris biomass in secondary effluent from dairy industry', *Biochemical Engineering Journal*, 165, p. 107818. doi: https://doi.org/10.1016/j.bej.2020.107818.

Rodríguez-Romero, J. de J. *et al.* (2020) '2-Phenylethanol and 2-phenylethylacetate production by nonconventional yeasts using tequila vinasses as a substrate', *Biotechnology Reports*, 25, p. e00420. doi: https://doi.org/10.1016/j.btre.2020.e00420.

Rodriguez, A. *et al.* (2014) 'Engineering Escherichia coli to overproduce aromatic amino acids and derived compounds', *Microbial Cell Factories*, 13(1), p. 126. doi: 10.1186/s12934-014-0126-z.

Rodriguez, A. *et al.* (2015) 'Establishment of a yeast platform strain for production of p-coumaric acid through metabolic engineering of aromatic amino acid biosynthesis', *Metabolic Engineering*, 31, pp. 181–188. doi: https://doi.org/10.1016/j.ymben.2015.08.003.

Roell, G. W. *et al.* (2019) 'Engineering microbial consortia by division of labor', *Microbial Cell Factories*, 18(1), p. 35. doi: 10.1186/s12934-019-1083-3.

Romagnoli, G. *et al.* (2015) 'Deletion of the Saccharomyces cerevisiae ARO8 gene, encoding an aromatic amino acid transaminase, enhances phenylethanol production from glucose.', *Yeast (Chichester, England)*, 32(1), pp. 29–45. doi: 10.1002/yea.3015.

Romero-Villegas, G. I. *et al.* (2018) 'Utilization of centrate for the outdoor production of marine microalgae at pilot-scale in flat-panel photobioreactors', *Journal of Biotechnology*, 284, pp. 102–114. doi: https://doi.org/10.1016/j.jbiotec.2018.08.006.

Roostaei, J. *et al.* (2018) 'Mixotrophic Microalgae Biofilm: A Novel Algae Cultivation Strategy for Improved Productivity and Cost-efficiency of Biofuel Feedstock Production', *Scientific Reports*, 8(1), p. 12528. doi: 10.1038/s41598-018-31016-1.

Ruffing, A. M. (2014) 'Improved free fatty acid production in cyanobacteria with Synechococcus sp. PCC 7002 as host', *Frontiers in Bioengineering and Biotechnology*, 2(MAY), pp. 1–10. doi: 10.3389/fbioe.2014.00017.

S., D. P. and A.K., B. (2019) 'A comparative study on growth and degradation behavior of C. pyrenoidosa on synthetic phenol and phenolic wastewater of a coal gasification plant', *Journal of Environmental Chemical Engineering*, 7(3), p. 103079.

doi: https://doi.org/10.1016/j.jece.2019.103079.

Sabina Asanova (CARSA), Demetrius Klitou (CARSA), T. L. (CARSA) and (PwC), L. A. (CARSA); in cooperation with K. D. (2017) *Bio-based aromatics Report on promising KETs-based product nr . 2 KETs Observatory Phase II*.

SAKAI, M. *et al.* (2007) 'Production of 2-Phenylethanol in Roses as the Dominant Floral Scent Compound from l-Phenylalanine by Two Key Enzymes, a PLP-Dependent Decarboxylase and a Phenylacetaldehyde Reductase', *Bioscience, Biotechnology, and Biochemistry*, 71(10), pp. 2408–2419. doi: 10.1271/bbb.70090.

Samiotis, G., Ziagova, M. G. and Amanatidou, E. (2023) 'Wastewater substrate disinfection for cyanobacteria cultivation as tertiary treatment.', *Environmental science and pollution research international*, 30(4), pp. 8746–8758. doi: 10.1007/s11356-022-20369-w.

Sánchez-Baracaldo, P. and Cardona, T. (2020) 'On the origin of oxygenic photosynthesis and Cyanobacteria', *New Phytologist*, 225(4), pp. 1440–1446. doi: https://doi.org/10.1111/nph.16249.

Sánchez-Bayo, A. *et al.* (2020) 'Cultivation of Microalgae and Cyanobacteria: Effect of Operating Conditions on Growth and Biomass Composition', *Molecules (Basel, Switzerland)*, 25(12), p. 2834. doi: 10.3390/molecules25122834.

Sansonetti, S. *et al.* (2009) 'Bio-ethanol production by fermentation of ricotta cheese whey as an effective alternative non-vegetable source', *Biomass and Bioenergy*, 33(12), pp. 1687–1692. doi: https://doi.org/10.1016/j.biombioe.2009.09.002.

Santos-Merino, M., Singh, A. K. and Ducat, D. C. (2019) 'New Applications of Synthetic Biology Tools for Cyanobacterial Metabolic Engineering', *Frontiers in Bioengineering and Biotechnology*, 7. doi: 10.3389/fbioe.2019.00033.

Santos-Merino, M., Singh, A. K. and Ducat, D. C. (2021) 'Sink Engineering in Photosynthetic Microbes', in *Cyanobacteria Biotechnology*. John Wiley & Sons, Ltd, pp. 171–209. doi: https://doi.org/10.1002/9783527824908.ch6.

dos Santos, R. R. *et al.* (2016) 'Cultivation of Spirulina maxima in medium supplemented with sugarcane vinasse', *Bioresource Technology*, 204, pp. 38–48. doi: https://doi.org/10.1016/j.biortech.2015.12.077.

Sar, T. *et al.* (2022) 'Potential utilization of dairy industries by-products and wastes through microbial processes: A critical review', *Science of The Total Environment*,

810, p. 152253. doi: https://doi.org/10.1016/j.scitotenv.2021.152253.

Sarkar, B. *et al.* (2006) 'Wastewater treatment in dairy industries — possibility of reuse', *Desalination*, 195(1), pp. 141–152. doi: https://doi.org/10.1016/j.desal.2005.11.015.

Sarma, S. S., Nandini, S. and Flores, J. L. (2001) 'Effect of methyl parathion on the population growth of the rotifer Brachionus patulus (O. F. Müller) under different algal food (Chlorella vulgaris) densities.', *Ecotoxicology and environmental safety*, 48(2), pp. 190–195. doi: 10.1006/eesa.2000.2014.

Sarnaik, A. *et al.* (2018) 'Recombinant Synechococcus elongatus PCC 7942 for improved zeaxanthin production under natural light conditions', *Algal Research*, 36, pp. 139–151. doi: https://doi.org/10.1016/j.algal.2018.10.021.

Sarnaik, A., Pandit, R. and Lali, A. (2017) 'Growth engineering of Synechococcus elongatus PCC 7942 for mixotrophy under natural light conditions for improved feedstock production.', *Biotechnology progress*, 33(5), pp. 1182–1192. doi: 10.1002/btpr.2490.

Savakis, P. E., Angermayr, S. A. and Hellingwerf, K. J. (2013) 'Synthesis of 2,3-butanediol by Synechocystis sp. PCC6803 via heterologous expression of a catabolic pathway from lactic acid- and enterobacteria', *Metabolic Engineering*, 20, pp. 121–130. doi: https://doi.org/10.1016/j.ymben.2013.09.008.

Saygin, D. and Gielen, D. (2021) 'Zero-Emission Pathway for the Global Chemical and Petrochemical Sector', *Energies*. doi: 10.3390/en14133772.

Schmidt, O., Padel, S. and Levidow, L. (2012) 'The Bio-Economy Concept and Knowledge Base in a Public Goods and Farmer Perspective', *Bio-based and Applied Economics*, 1(1 SE-Reviews Articles), pp. 47–63. doi: 10.13128/BAE-10770.

Schriek, S. *et al.* (2009) 'Detection of an L-amino acid dehydrogenase activity in Synechocystis sp. PCC 6803', *Journal of Experimental Botany*, 60(3), pp. 1035–1046. doi: 10.1093/jxb/ern352.

Schuurmans, R. M. *et al.* (2015) 'Comparison of the Photosynthetic Yield of Cyanobacteria and Green Algae: Different Methods Give Different Answers', *PLOS ONE*, 10(9), p. e0139061. Available at: https://doi.org/10.1371/journal.pone.0139061.

Scognamiglio, J. *et al.* (2012) 'Fragrance material review on phenylethyl alcohol.', *Food and chemical toxicology : an international journal published for the British*

Industrial Biological Research Association, 50 Suppl 2, pp. S224-39. doi: 10.1016/j.fct.2011.10.028.

Sedjati, S. *et al.* (2019) 'Chlorophyll and Carotenoid Content of Dunaliella salina at Various Salinity Stress and Harvesting Time', *IOP Conference Series: Earth and Environmental Science*, 246(1), p. 12025. doi: 10.1088/1755-1315/246/1/012025.

Sekine, M. *et al.* (2020) 'Microalgae cultivation using undiluted anaerobic digestate by introducing aerobic nitrification–desulfurization treatment', *Water Science and Technology*, 82(6), pp. 1070–1080. doi: 10.2166/wst.2020.153.

Sengupta, A. *et al.* (2019) 'Fine-Tuning Native Promoters of Synechococcus elongatus PCC 7942 To Develop a Synthetic Toolbox for Heterologous Protein Expression', *ACS Synthetic Biology*, 8(5), pp. 1219–1223. doi: 10.1021/acssynbio.9b00066.

Seo, Y. H. *et al.* (2014) 'Enhancement of growth and lipid production from microalgae using fluorescent paint under the solar radiation', *Bioresource Technology*, 173, pp. 193–197. doi: https://doi.org/10.1016/j.biortech.2014.09.012.

SEVERINGHAUS, J. W. and BRADLEY, A. F. (1958) 'Electrodes for blood pO2 and pCO2 determination.', *Journal of applied physiology*, 13(3), pp. 515–520. doi: 10.1152/jappl.1958.13.3.515.

Sforza, E., Barbera, E. and Bertucco, A. (2015) 'Improving the photoconversion efficiency: An integrated photovoltaic-photobioreactor system for microalgal cultivation', *Algal Research*, 10, pp. 202–209. doi: https://doi.org/10.1016/j.algal.2015.05.005.

Shabana, E., Senousy, H. and Khourshid, E. (2019) 'Pharmaceutical wastewater treatment using free and immobilized Cyanobacteria', *Egyptian Journal of Phycology*, 20(1), pp. 123–154. doi: 10.21608/egyjs.2019.116025.

Shankar, V. S. B. *et al.* (2017) 'Antiknock quality and ignition kinetics of 2-phenylethanol, a novel lignocellulosic octane booster', *Proceedings of the Combustion Institute*, 36(3), pp. 3515–3522. doi: https://doi.org/10.1016/j.proci.2016.05.041.

Sharma, A. *et al.* (2020) 'Tailoring cellular metabolism in lactic acid bacteria through metabolic engineering', *Journal of Microbiological Methods*, 170, p. 105862. doi: https://doi.org/10.1016/j.mimet.2020.105862.

Sharwood, R. E. (2017) 'Engineering chloroplasts to improve Rubisco catalysis:

prospects for translating improvements into food and fiber crops', *New Phytologist*, 213(2), pp. 494–510. doi: https://doi.org/10.1111/nph.14351.

Shcolnick, S. and Keren, N. (2006) 'Metal Homeostasis in Cyanobacteria and Chloroplasts. Balancing Benefits and Risks to the Photosynthetic Apparatus', *Plant Physiology*, 141(3), pp. 805–810. doi: 10.1104/pp.106.079251.

Shen, L. and Yin, X. (2022) 'Solar spectral management for natural photosynthesis: from photonics designs to potential applications', *Nano Convergence*, 9(1), p. 36. doi: 10.1186/s40580-022-00327-5.

Shin, W.-S. *et al.* (2016) 'Truncated light-harvesting chlorophyll antenna size in Chlorella vulgaris improves biomass productivity', *Journal of Applied Phycology*, 28(6), pp. 3193–3202. doi: 10.1007/s10811-016-0874-8.

Shinde, S. *et al.* (2020) 'Glycogen Metabolism Supports Photosynthesis Start through the Oxidative Pentose Phosphate Pathway in Cyanobacteria.', *Plant physiology*, 182(1), pp. 507–517. doi: 10.1104/pp.19.01184.

Sierra, E. *et al.* (2008) 'Characterization of a flat plate photobioreactor for the production of microalgae', *Chemical Engineering Journal*, 138(1), pp. 136–147. doi: https://doi.org/10.1016/j.cej.2007.06.004.

da Silva Ferreira, V. and Sant'Anna, C. (2016) 'Impact of culture conditions on the chlorophyll content of microalgae for biotechnological applications', *World Journal of Microbiology and Biotechnology*, 33(1), p. 20. doi: 10.1007/s11274-016-2181-6.

da Silva, T. L. and Reis, A. (2015) 'Scale-up Problems for the Large Scale Production of Algae BT - Algal Biorefinery: An Integrated Approach', in Das, D. (ed.). Cham: Springer International Publishing, pp. 125–149. doi: 10.1007/978-3-319-22813-6_6.

Singh, Rajveer *et al.* (2022) 'A Prospective Review on Selectable Marker-Free Genome Engineered Rice: Past, Present and Future Scientific Realm', *Frontiers in Genetics*, 13(June), pp. 1–15. doi: 10.3389/fgene.2022.882836.

Singh, Ravikant *et al.* (2022) 'Enhanced Production of Plant Aromatic Compounds Through Metabolic Engineering BT - Metabolic Engineering in Plants', in Aftab, T. and Hakeem, K. R. (eds). Singapore: Springer Nature Singapore, pp. 209–237. doi: 10.1007/978-981-16-7262-0_9.

Singh, R. N. and Sharma, S. (2012) 'Development of suitable photobioreactor for

algae production – A review', *Renewable and Sustainable Energy Reviews*, 16(4), pp. 2347–2353. doi: https://doi.org/10.1016/j.rser.2012.01.026.

Singh, V. and Mishra, V. (2023) 'A review on the current application of light-emitting diodes for microalgae cultivation and its fiscal analysis', *Critical Reviews in Biotechnology*, 43(5), pp. 665–679. doi: 10.1080/07388551.2022.2057274.

Sirohi, R. *et al.* (2022) 'Design and applications of photobioreactors- a review', *Bioresource Technology*, 349, p. 126858. doi: https://doi.org/10.1016/j.biortech.2022.126858.

Slegers, P. M. *et al.* (2011) 'Design scenarios for flat panel photobioreactors', *Applied Energy*, 88(10), pp. 3342–3353. doi: https://doi.org/10.1016/j.apenergy.2010.12.037.

Song, C. *et al.* (2020) 'Microalgae carbon fixation integrated with organic matters recycling from soybean wastewater: Effect of pH on the performance of hybrid system', *Chemosphere*, 248, p. 126094. doi: https://doi.org/10.1016/j.chemosphere.2020.126094.

Spoalore, P. *et al.* (2006) 'Commercial application of microalgae', *J Biosci Bioeng*, 101, pp. 87–96.

Sriram, S., A., H. K. and Robert, T. F. (2019) 'Selection of Cyanobacterial (Synechococcus sp. Strain PCC 6301) RubisCO Variants with Improved Functional Properties That Confer Enhanced CO2-Dependent Growth of Rhodobacter capsulatus, a Photosynthetic Bacterium', *mBio*, 10(4), pp. 10.1128/mbio.01537-19. doi: 10.1128/mbio.01537-19.

Srisawat, P., Higuchi-Takeuchi, M. and Numata, K. (2022) 'Microbial autotrophic biorefineries: Perspectives for biopolymer production', *Polymer Journal*, 54(10), pp. 1139–1151. doi: 10.1038/s41428-022-00675-3.

STAL, L. J. (1995) 'Physiological ecology of cyanobacteria in microbial mats and other communities', *New Phytologist*, 131(1), pp. 1–32. doi: https://doi.org/10.1111/j.1469-8137.1995.tb03051.x.

Stal, L. J. and Moezelaar, R. (1997) 'Fermentation in cyanobacteria1Publication 2274 of the Centre of Estuarine and Coastal Ecology, Yerseke, The Netherlands.1', *FEMS Microbiology Reviews*, 21(2), pp. 179–211. doi: https://doi.org/10.1016/S0168-6445(97)00056-9.

Stanier, R. Y. *et al.* (1971) 'Purification and properties of unicellular blue-green algae (order Chroococcales)', *Bacteriological reviews*, 35(2), pp. 171–205. doi: 10.1128/br.35.2.171-205.1971.

Stasinakis, A. S., Charalambous, P. and Vyrides, I. (2022) 'Dairy wastewater management in EU: Produced amounts, existing legislation, applied treatment processes and future challenges', *Journal of Environmental Management*, 303, p. 114152. doi: https://doi.org/10.1016/j.jenvman.2021.114152.

Steiger, S., Schäfer, L. and Sandmann, G. (1999) 'High-light-dependent upregulation of carotenoids and their antioxidative properties in the cyanobacterium Synechocystis PCC 6803', *Journal of Photochemistry and Photobiology B: Biology*, 52(1), pp. 14–18. doi: https://doi.org/10.1016/S1011-1344(99)00094-9.

Štěrbová, K. *et al.* (2023) 'Microalgae as an aquaculture feed produced in a short light-path annular column photobioreactor', *Journal of Applied Phycology*, 35(2), pp. 603–611. doi: 10.1007/s10811-023-02928-x.

Stewart, C. and Hessami, M.-A. (2005) 'A study of methods of carbon dioxide capture and sequestration—the sustainability of a photosynthetic bioreactor approach', *Energy Conversion and Management*, 46(3), pp. 403–420. doi: https://doi.org/10.1016/j.enconman.2004.03.009.

Su, B. *et al.* (2020) 'Engineering a growth-phase-dependent biosynthetic pathway for carotenoid production in Saccharomyces cerevisiae', *Journal of Industrial Microbiology and Biotechnology*, 47(4–5), pp. 383–393. doi: 10.1007/s10295-020-02271-x.

Summerfelt, S. T. (2003) 'Ozonation and UV irradiation—an introduction and examples of current applications', *Aquacultural Engineering*, 28(1), pp. 21–36. doi: https://doi.org/10.1016/S0144-8609(02)00069-9.

Sutherland, D. L. *et al.* (2020) 'Improved microalgal productivity and nutrient removal through operating wastewater high rate algal ponds in series', *Algal Research*, 47, p. 101850. doi: https://doi.org/10.1016/j.algal.2020.101850.

Sveshnikova, A., MohammadiPeyhani, H. and Hatzimanikatis, V. (2022) 'Computational tools and resources for designing new pathways to small molecules', *Current Opinion in Biotechnology*, 76, p. 102722. doi: 10.1016/j.copbio.2022.102722.

Szwarc, D. and Zieliński, M. (2018) 'Effect of Lighting on the Intensification of Phycocyanin Production in a Culture of Arthrospira platensis', *Proceedings*. doi:

10.3390/proceedings2201305.

Takai A, Nishi R, Joe Y, I. H. (2009) '(12) Patent Application Publication (10) Pub. No.: US 2009/0104683 A1'.

Tamoi, M. *et al.* (2005) 'The Calvin cycle in cyanobacteria is regulated by CP12 via the NAD(H)/NADP(H) ratio under light/dark conditions', *The Plant Journal*, 42(4), pp. 504–513. doi: https://doi.org/10.1111/j.1365-313X.2005.02391.x.

Tan, J. Sen *et al.* (2020) 'A review on microalgae cultivation and harvesting, and their biomass extraction processing using ionic liquids.', *Bioengineered*, 11(1), pp. 116–129. doi: 10.1080/21655979.2020.1711626.

Tan, X. B. *et al.* (2018) 'Cultivation of microalgae for biodiesel production: A review on upstream and downstream processing', *Chinese Journal of Chemical Engineering*, 26(1), pp. 17–30. doi: https://doi.org/10.1016/j.cjche.2017.08.010.

Terezinha Schneider, A. *et al.* (2023) 'Chapter 5 - Microalgae as superfood', in Arunkumar, K. et al. (eds) *Developments in Applied Microbiology and Biotechnology*. Academic Press, pp. 93–102. doi: https://doi.org/10.1016/B978-0-443-18816-9.00023-X.

Terry, K. L. (1986) 'Photosynthesis in modulated light: Quantitative dependence of photosynthetic enhancement on flashing rate', *Biotechnology and Bioengineering*, 28(7), pp. 988–995. doi: https://doi.org/10.1002/bit.260280709.

Tham, P. E. *et al.* (2022) 'Sustainable smart photobioreactor for continuous cultivation of microalgae embedded with Internet of Things', *Bioresource Technology*, 346, p. 126558. doi: https://doi.org/10.1016/j.biortech.2021.126558.

Thevarajah, B. *et al.* (2023) 'Cyanobacterial pigment production in wastewaters treated for heavy metal removal: Current status and perspectives', *Journal of Environmental Chemical Engineering*, 11(1), p. 108999. doi: https://doi.org/10.1016/j.jece.2022.108999.

Ting, H. *et al.* (2017) 'Progress in microalgae cultivation photobioreactors and applications in wastewater treatment: A review', *International Journal of Agricultural and Biological Engineering*, 10(1), pp. 1–29. doi: 10.3965/j.ijabe.20171001.2705.

Toda, N. *et al.* (2021) 'Phosphite Reduces the Predation Impact of Poterioochromonasmalhamensis on Cyanobacterial Culture.', *Plants (Basel, Switzerland)*, 10(7). doi: 10.3390/plants10071361.

Torzillo, G. *et al.* (1993) 'A two-plane tubular photobioreactor for outdoor culture of Spirulina.', *Biotechnology and bioengineering*, 42(7), pp. 891–898. doi: 10.1002/bit.260420714.

Touloupakis, E. *et al.* (2016) 'Effect of high pH on growth of Synechocystis sp. PCC 6803 cultures and their contamination by golden algae (Poterioochromonas sp.)', *Applied Microbiology and Biotechnology*, 100(3), pp. 1333–1341. doi: 10.1007/s00253-015-7024-0.

Toyama, T. *et al.* (2018) 'Growth promotion of three microalgae, Chlamydomonas reinhardtii, Chlorella vulgaris and Euglena gracilis, by in situ indigenous bacteria in wastewater effluent', *Biotechnology for Biofuels*, 11(1), p. 176. doi: 10.1186/s13068-018-1174-0.

Tredici, M. R. *et al.* (2015) 'Energy balance of algal biomass production in a 1-ha "Green Wall Panel" plant: How to produce algal biomass in a closed reactor achieving a high Net Energy Ratio', *Applied Energy*, 154, pp. 1103–1111. doi: https://doi.org/10.1016/j.apenergy.2015.01.086.

Turnbull, J. and Morrison, J. F. (1990) 'Chorismate mutase-prephenate dehydrogenase from Escherichia coli. 2. Evidence for two different active sites.', *Biochemistry*, 29(44), pp. 10255–10261. doi: 10.1021/bi00496a015.

Tzin, V. and Galili, G. (2010) 'The Biosynthetic Pathways for Shikimate and Aromatic Amino Acids in Arabidopsis thaliana.', *The arabidopsis book*, 8, p. e0132. doi: 10.1199/tab.0132.

Ueno, H. *et al.* (2019) 'Anti-depressive-like effect of 2-phenylethanol inhalation in mice.', *Biomedicine & pharmacotherapy = Biomedecine & pharmacotherapie*, 111, pp. 1499–1506. doi: 10.1016/j.biopha.2018.10.073.

Ugwu, C. U., Aoyagi, H. and Uchiyama, H. (2008) 'Photobioreactors for mass cultivation of algae', *Bioresource Technology*, 99(10), pp. 4021–4028. doi: https://doi.org/10.1016/j.biortech.2007.01.046.

Ulfstedt, M. *et al.* (2017) 'Testing of Auxotrophic Selection Markers for Use in the Moss Physcomitrella Provides New Insights into the Mechanisms of Targeted Recombination', *Frontiers in Plant Science*, 8. doi: 10.3389/fpls.2017.01850.

Uma, V. S. *et al.* (2023) 'Valorisation of algal biomass to value-added metabolites: emerging trends and opportunities', *Phytochemistry Reviews*, 22(4), pp. 1015–1040. doi: 10.1007/s11101-022-09805-4.

Ummalyma, S. B. *et al.* (2023) 'Sustainable microalgal biomass production in food industry wastewater for low-cost biorefinery products: a review', *Phytochemistry Reviews*, 22(4), pp. 969–991. doi: 10.1007/s11101-022-09814-3.

UN-Food & Agriculture Organization (FAO) (2020) 'Dairy market review, March 2020', *Food and Agriculture Organization of the United Nations*, (March), pp. 1–15. Available at: http://www.fao.org/3/cb4230en/cb4230en.pdf.

Untergasser, A. *et al.* (2012) 'Primer3—new capabilities and interfaces', *Nucleic Acids Research*, 40(15), pp. e115–e115. doi: 10.1093/nar/gks596.

Upadhyay, A. K. *et al.* (2016) 'Augmentation of arsenic enhances lipid yield and defense responses in alga Nannochloropsis sp.', *Bioresource Technology*, 221, pp. 430–437. doi: https://doi.org/10.1016/j.biortech.2016.09.061.

Usai, G. *et al.* (2022) 'Combining metabolite doping and metabolic engineering to improve 2-phenylethanol production by engineered cyanobacteria', *Frontiers in Bioengineering and Biotechnology*, 10(September), pp. 1–18. doi: 10.3389/fbioe.2022.1005960.

Usmani, Z. *et al.* (2022) 'Valorization of dairy waste and by-products through microbial bioprocesses', *Bioresource Technology*, 346, p. 126444. doi: https://doi.org/10.1016/j.biortech.2021.126444.

Vasile, N. S. *et al.* (2021) 'Computational Analysis of Dynamic Light Exposure of Unicellular Algal Cells in a Flat-Panel Photobioreactor to Support Light-Induced CO2 Bioprocess Development', *Frontiers in Microbiology*, 12, p. 579. doi: 10.3389/fmicb.2021.639482.

Vasudevan, R. *et al.* (2019) 'CyanoGate: A Modular Cloning Suite for Engineering Cyanobacteria Based on the Plant MoClo Syntax.', *Plant physiology*, 180(1), pp. 39–55. doi: 10.1104/pp.18.01401.

Venkata Mohan, S., Lalit Babu, V. and Sarma, P. N. (2008) 'Effect of various pretreatment methods on anaerobic mixed microflora to enhance biohydrogen production utilizing dairy wastewater as substrate', *Bioresource Technology*, 99(1), pp. 59–67. doi: https://doi.org/10.1016/j.biortech.2006.12.004.

Vidal, R. *et al.* (2009) 'Characterization of an alcohol dehydrogenase from the Cyanobacterium Synechocystis sp. strain PCC 6803 that responds to environmental stress conditions via the Hik34-Rre1 two-component system.', *Journal of bacteriology*, 191(13), pp. 4383–4391. doi: 10.1128/JB.00183-09.

Vieira, J. G. *et al.* (2012) 'Uptake of phosphorus from dairy wastewater by heterotrophic cultures of cyanobacteria', *Desalination and Water Treatment*, 40(1–3), pp. 224–230. doi: 10.1080/19443994.2012.671249.

Vincent, S. *et al.* (2002) 'Probing the overlap of chorismate mutase and prephenate dehydrogenase sites in the escherichia coli T-protein: a dehydrogenase-selective inhibitor.', *Bioorganic & medicinal chemistry letters*, 12(6), pp. 929–931. doi: 10.1016/s0960-894x(02)00053-7.

Vonshak, A. *et al.* (1983) 'Production of Spirulina biomass: Maintenance of monoalgal culture outdoors', *Biotechnology and Bioengineering*, 25. Available at: https://api.semanticscholar.org/CorpusID:22459010.

Vourch, M. *et al.* (2008) 'Treatment of dairy industry wastewater by reverse osmosis for water reuse', *Desalination*, 219(1), pp. 190–202. doi: https://doi.org/10.1016/j.desal.2007.05.013.

Wang, B. and Dai, Z. (2023) 'Engineering Photosynthetic Microbial Consortia for Carbon-Negative Biosynthesis', *Angewandte Chemie International Edition*, 62(17), p. e202217961. doi: https://doi.org/10.1002/anie.202217961.

Wang, B., Lan, C. Q. and Horsman, M. (2012) 'Closed photobioreactors for production of microalgal biomasses', *Biotechnology Advances*, 30(4), pp. 904–912. doi: https://doi.org/10.1016/j.biotechadv.2012.01.019.

Wang, C. *et al.* (2012) 'Photosensitization of phycocyanin extracted from Microcystis in human hepatocellular carcinoma cells: Implication of mitochondria-dependent apoptosis', *Journal of Photochemistry and Photobiology B: Biology*, 117, pp. 70–79. doi: https://doi.org/10.1016/j.jphotobiol.2012.09.001.

Wang, F., Gao, Y. and Yang, G. (2020) 'Recent advances in synthetic biology of cyanobacteria for improved chemicals production', *Bioengineered*, 11(1), pp. 1208–1220. doi: 10.1080/21655979.2020.1837458.

Wang, Fang *et al.* (2021) 'Technologies and perspectives for achieving carbon neutrality', *The Innovation*, 2(4), p. 100180. doi: https://doi.org/10.1016/j.xinn.2021.100180.

Wang, H. *et al.* (2011) 'Synergistic inhibition effect of 2-phenylethanol and ethanol on bioproduction of natural 2-phenylethanol by Saccharomyces cerevisiae and process enhancement.', *Journal of bioscience and bioengineering*, 112(1), pp. 26–31. doi: 10.1016/j.jbiosc.2011.03.006.

Wang, H. *et al.* (2013) 'The contamination and control of biological pollutants in mass cultivation of microalgae', *Bioresource Technology*, 128, pp. 745–750. doi: https://doi.org/10.1016/j.biortech.2012.10.158.

Wang, J. *et al.* (2016) 'Deciphering the Principles of Bacterial Nitrogen Dietary Preferences: a Strategy for Nutrient Containment.', *mBio*, 7(4). doi: 10.1128/mBio.00792-16.

Wang, T. *et al.* (2019) 'An update of the suicide plasmid-mediated genome editing system in Corynebacterium glutamicum', *Microbial Biotechnology*, 12(5), pp. 907–919. doi: https://doi.org/10.1111/1751-7915.13444.

Wang, Y. *et al.* (2016) 'Perspectives on the feasibility of using microalgae for industrial wastewater treatment', *Bioresource Technology*, 222, pp. 485–497. doi: https://doi.org/10.1016/j.biortech.2016.09.106.

Wang, Y. *et al.* (2019) 'Advances in 2-phenylethanol production from engineered microorganisms.', *Biotechnology advances*, 37(3), pp. 403–409. doi: 10.1016/j.biotechadv.2019.02.005.

Wang, Y. *et al.* (2020) 'Screening of a Chlorella-bacteria consortium and research on piggery wastewater purification', *Algal Research*, 47, p. 101840. doi: https://doi.org/10.1016/j.algal.2020.101840.

Weaver, L. M. and Herrmann, K. M. (1997) 'Dynamics of the shikimate pathway in plants', *Trends in Plant Science*, 2(9), pp. 346–351. doi: https://doi.org/10.1016/S1360-1385(97)84622-5.

Wellburn, A. R. (1994) 'The Spectral Determination of Chlorophylls a and b, as well as Total Carotenoids, Using Various Solvents with Spectrophotometers of Different Resolution', *Journal of Plant Physiology*, 144(3), pp. 307–313. doi: https://doi.org/10.1016/S0176-1617(11)81192-2.

Wessel, D. and Flügge, U. I. (1984) 'A method for the quantitative recovery of protein in dilute solution in the presence of detergents and lipids', *Analytical Biochemistry*, 138(1), pp. 141–143. doi: https://doi.org/10.1016/0003-2697(84)90782-6.

Wilson, D. and Matschinsky, F. (2021) 'Metabolic Homeostasis in Life as We Know It: Its Origin and Thermodynamic Basis', *Frontiers in Physiology*, 12, p. 658997. doi: 10.3389/fphys.2021.658997.

Wilson, R. S. *et al.* (2019) 'Commentary: Achieving phosphorus reduction targets for Lake Erie', *Journal of Great Lakes Research*, 45(1), pp. 4–11. doi: https://doi.org/10.1016/j.jglr.2018.11.004.

Wobbe, L. and Remacle, C. (2015) 'Improving the sunlight-to-biomass conversion efficiency in microalgal biofactories', *Journal of Biotechnology*, 201, pp. 28–42. doi: https://doi.org/10.1016/j.jbiotec.2014.08.021.

Wollmann, F. *et al.* (2019) 'Microalgae wastewater treatment: Biological and technological approaches', *Engineering in Life Sciences*, 19(12), pp. 860–871. doi: https://doi.org/10.1002/elsc.201900071.

Wondraczek, L. *et al.* (2013) 'Solar spectral conversion for improving the photosynthetic activity in algae reactors', *Nature Communications*, 4(1), p. 2047. doi: 10.1038/ncomms3047.

Wu, S. *et al.* (2022) 'Metabolic Engineering of Shikimic Acid Biosynthesis Pathway for the Production of Shikimic Acid and Its Branched Products in Microorganisms: Advances and Prospects.', *Molecules (Basel, Switzerland)*, 27(15). doi: 10.3390/molecules27154779.

Xia, A. and Murphy, J. D. (2016) 'Microalgal Cultivation in Treating Liquid Digestate from Biogas Systems', *Trends in Biotechnology*, 34(4), pp. 264–275. doi: https://doi.org/10.1016/j.tibtech.2015.12.010.

Xu, L. *et al.* (2009) 'Microalgal bioreactors: Challenges and opportunities', *Engineering in Life Sciences*, 9(3), pp. 178–189. doi: https://doi.org/10.1002/elsc.200800111.

Xu, Q. *et al.* (2017) 'Gene modification of the acetate biosynthesis pathway in Escherichia coli and implementation of the cell recycling technology to increase L-tryptophan production', *PLOS ONE*, 12(6), p. e0179240. Available at: https://doi.org/10.1371/journal.pone.0179240.

Xu, Y. *et al.* (2019) 'Unraveling the specific regulation of the shikimate pathway for tyrosine accumulation in Bacillus licheniformis', *Journal of Industrial Microbiology and Biotechnology*, 46(8), pp. 1047–1059. doi: 10.1007/s10295-019-02213-2.

Xue, Y. and He, Q. (2018) 'Synthetic Biology Approaches to the Sustainable Production of p-Coumaric Acid and Its Derivatives in Cyanobacteria.', *Advances in experimental medicine and biology*, 1080, pp. 261–277. doi: 10.1007/978-981-13-

0854-3_11.

Yadav, G. *et al.* (2021) 'Mechanism and challenges behind algae as a wastewater treatment choice for bioenergy production and beyond', *Fuel*, 285, p. 119093. doi: https://doi.org/10.1016/j.fuel.2020.119093.

Yang, B. *et al.* (2017) 'Genetic engineering of the Calvin cycle toward enhanced photosynthetic CO2 fixation in microalgae', *Biotechnology for Biofuels*, 10(1), p. 229. doi: 10.1186/s13068-017-0916-8.

Yang, J. *et al.* (2011) 'Life-cycle analysis on biodiesel production from microalgae: Water footprint and nutrients balance', *Bioresource Technology*, 102(1), pp. 159–165. doi: https://doi.org/10.1016/j.biortech.2010.07.017.

Yangyang, Z. *et al.* (2023) 'Systematic Adaptation of Bacillus licheniformis to 2-Phenylethanol Stress', *Applied and Environmental Microbiology*, 89(2), pp. e01568-22. doi: 10.1128/aem.01568-22.

Yen, H.-W. *et al.* (2015) 'CO2, NOx and SOx removal from flue gas via microalgae cultivation: A critical review', *Biotechnology Journal*, 10(6), pp. 829–839. doi: https://doi.org/10.1002/biot.201400707.

Yu, H. *et al.* (2022) 'Effects of Different pH Control Strategies on Microalgae Cultivation and Nutrient Removal from Anaerobic Digestion Effluent.', *Microorganisms*, 10(2). doi: 10.3390/microorganisms10020357.

Zagklis, D. P. and Bampos, G. (2022) 'Tertiary Wastewater Treatment Technologies: A Review of Technical, Economic, and Life Cycle Aspects', *Processes*. doi: 10.3390/pr10112304.

ZAHN, R. K. *et al.* (1966) 'In vitro Inhibition of the Synthesis of Deoxyribonucleic Acid by 2-Phenyl-ethanol and some of its Derivatives', *Nature*, 212(5059), pp. 297–298. doi: 10.1038/212297a0.

Zakova, T. *et al.* (2019) 'Hydrodynamics as a tool to remove biofilm in tubular photobioreactor', *Chemical Engineering Transactions*, 76(2013), pp. 451–456. doi: 10.3303/CET1976076.

Zandona, E., Blažić, M. and Režek Jambrak, A. (2021) 'Whey Utilization: Sustainable Uses and Environmental Approach.', *Food technology and biotechnology*, 59(2), pp. 147–161. doi: 10.17113/ftb.59.02.21.6968.

Zapata, D. *et al.* (2021) 'Phytohormone production and morphology of Spirulina platensis grown in dairy wastewaters', *Algal Research*, 59, p. 102469. doi: https://doi.org/10.1016/j.algal.2021.102469.

Zarmi, Y. *et al.* (2020) 'Enhanced Algal Photosynthetic Photon Efficiency by Pulsed Light', *iScience*, 23(5), p. 101115. doi: https://doi.org/10.1016/j.isci.2020.101115.

Zavřel, T. *et al.* (2018) 'Spectrophotometric Determination of Phycobiliprotein Content in Cyanobacterium Synechocystis.', *Journal of visualized experiments : JoVE*, (139). doi: 10.3791/58076.

Zhang, C. *et al.* (2014) 'Construction and application of novel feedback-resistant 3-deoxy-d-arabino-heptulosonate-7-phosphate synthases by engineering the N-terminal domain for l-phenylalanine synthesis', *FEMS Microbiology Letters*, 353(1), pp. 11–18. doi: 10.1111/1574-6968.12397.

Zhang, H. *et al.* (2014) 'De-novo synthesis of 2-phenylethanol by Enterobactersp. CGMCC 5087', *BMC Biotechnology*, 14(1), p. 30. doi: 10.1186/1472-6750-14-30.

Zhang, T., Xie, X. and Huang, Z. (2014) 'Life Cycle Water Footprints of Nonfood Biomass Fuels in China', *Environmental Science & Technology*, 48(7), pp. 4137–4144. doi: 10.1021/es404458j.

Zhang, Y. *et al.* (2021) 'Efficient production of chemicals from microorganism by metabolic engineering and synthetic biology', *Chinese Journal of Chemical Engineering*, 30, pp. 14–28. doi: https://doi.org/10.1016/j.cjche.2020.12.014.

Zhao, Y. *et al.* (2020) 'Biotreatment of high-salinity wastewater: current methods and future directions', *World Journal of Microbiology and Biotechnology*, 36(3), p. 37. doi: 10.1007/s11274-020-02815-4.

Zhou, H. *et al.* (2010) 'Enhanced l-phenylalanine biosynthesis by co-expression of pheA(fbr) and aroF(wt).', *Bioresource technology*, 101(11), pp. 4151–4156. doi: 10.1016/j.biortech.2010.01.043.

Zhou, J. and Li, Y. (2010) 'Engineering cyanobacteria for fuels and chemicals production.', *Protein & cell*, 1(3), pp. 207–210. doi: 10.1007/s13238-010-0043-9.

Zhou, P. *et al.* (2022) 'CyanoOmicsDB: an integrated omics database for functional genomic analysis of cyanobacteria', *Nucleic Acids Research*, 50(D1), pp. D758–D764. doi: 10.1093/nar/gkab891.

Zhu, C. *et al.* (2016) 'Selenium-Containing Phycocyanin from Se-Enriched Spirulina platensis Reduces Inflammation in Dextran Sulfate Sodium-Induced Colitis by Inhibiting NF-κB Activation.', *Journal of agricultural and food chemistry*, 64(24), pp. 5060–5070. doi: 10.1021/acs.jafc.6b01308.

Zhu, L., Wang, J., *et al.* (2021) 'Improved aromatic alcohol production by strengthening the shikimate pathway in Saccharomyces cerevisiae', *Process Biochemistry*, 103, pp. 18–30. doi: https://doi.org/10.1016/j.procbio.2021.01.025.

Zhu, L., Xu, S., *et al.* (2021) 'Improvement of 2-phenylethanol production in Saccharomyces cerevisiae by evolutionary and rational metabolic engineering', *PLOS ONE*, 16(10), p. e0258180. Available at: https://doi.org/10.1371/journal.pone.0258180.

Zhu, Z., Jiang, J. and Fa, Y. (2020) 'Overcoming the Biological Contamination in Microalgae and Cyanobacteria Mass Cultivations for Photosynthetic Biofuel Production.', *Molecules (Basel, Switzerland)*, 25(22). doi: 10.3390/molecules25225220.

Zieliński, M. *et al.* (2023) 'Microalgal Carbon Dioxide (CO2) Capture and Utilization from the European Union Perspective', *Energies*, 16(3), pp. 1–27. doi: 10.3390/en16031446.

Zuñiga, C. *et al.* (2020) 'Synthetic microbial communities of heterotrophs and phototrophs facilitate sustainable growth', *Nature Communications*, 11(1), p. 3803. doi: 10.1038/s41467-020-17612-8.